FRIEDEL-CRAFTS POLYMERS CONTAINING THIOPHEN

A thesis submitted to the University of Glasgow for the degree of Doctor of Philosophy in the Faculty of Science.

By

John B. Colford, B.Sc. (Glas.)

Supervisor

Dr. N. Grassie

Chemistry Department

September 1969.

ProQuest LLC.
789 East Eisenhower Parkway
P.O. Box 1346
Ann Arbor, MI 48106 – 1346

SUMMARY OF THESIS FOR DEGREE OF

DOCTOR OF PHILOSOPHY

FRIEDEL-CRAFTS POLYMERS CONTAINING THIOPHEN

by JOHN B. COLFORD B.Sc.

The reaction between p-di(chloromethyl) benzene (DCMB) and thiophen, catalysed by stannic chloride, has been studied with a view to elucidating the kinetics and mechanism of the reaction. In this way it was hoped to gain a clearer insight into the structure of the resultant polymer and so to account for its reported thermal stability[1].

By studying the rate of production of involatile material it was established that the self-polymerisation of thiophen would have little or no effect on the DCMB-thiophen reaction. Analyses of these involatile materials were carried out using I.R., U-V and n.m.r. spectroscopy and molecular weight determinations. The rate of self-condensation of DCMB was also found to be negligable, by studying the rate of evolution of HCl from DCMB-$SnCl_4$ mixtures.

Products of the DCMB-thiophen reaction, with molecular weights up to 850, have been separated using both gas liquid chromatography (G.L.C.) and gel permeation chromatography (G.P.C.), and identified using mass, I.R.

and n.m.r. spectroscopy. A total of eight reaction products were separated and identified. However the techniques available did not permit separation and identification of products of molecular weight greater than 850 or an estimation of the extent of isomerism among the reaction products.

A kinetic analysis of the reaction was carried out using both G.L.C. and G.P.C. for the separation and analysis of products. Using G.L.C. the dependence of the rate of the first two reactions on the first power of the concentration of each of the reactants was established. This allowed a mechanism for the overall reaction to be proposed and rate constants and activation energies for the first two steps in the polymerisation to be calculated. From the G.P.C. results reaction curves for all the identified products were constructed. The extremely complex nature of the reaction and the resultant products prevented a complete kinetic analysis of the later stages of the reaction being made. It was possible, however, to arrive at semi-quantitative conclusions about the relative reactivity of the reaction products and hence construct a useful picture of the structure of the resultant polymer.

Polymers were also prepared by reaction of DCMB with

thiophen, 2-methyl thiophen, 3-methyl thiophen, 2.5-dimethyl thiophen and 2-chloro thiophen and an assessment was made of their relative stabilities using both thermal gravimetric analysis and thermal volatilisation analysis. I.R. spectroscopy indicated that all the polymers had the same basic structure and so it was possible to correlate the observed degradative features with the differences in the thiophen monomers.

These studies have allowed the following conclusions to be drawn concerning the reaction of DCMB with thiophen and the structure of the resultant polymer.

The overall reaction may be represented by a series of competing, consecutive reactions of the type,

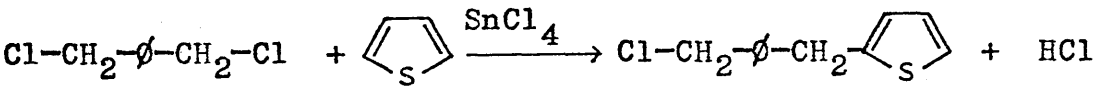

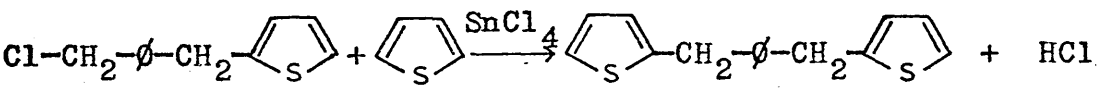

As the reaction proceeds it rapidly becomes highly complex with a proliferation of isomers at each molecular

level being brought about by the onset of branching through the disubstituted thiophen nuclei of the products. The ultimate polymer has been shown to be a highly cross-linked, insoluble material which exhibits good thermal stability in vacuum, inert atmospheres and air.

Reference

1. N. Grassie and I.G. Meldrum, Eur. Polym. J. 4, 571 (1968).

ACKNOWLEDGEMENTS

The work described in this thesis was carried out in the period October 1966 to September 1969 at the University of Glasgow, in the Department of Physical Chemistry, which is under the direction of Professor J.M. Robertson, C.B.E., F.R.S.

I wish to express my gratitude to Dr. N. Grassie for suggesting the problem and for his advice and supervision throughout this period of study.

My thanks are also due to my colleagues in the Macromolecular Chemistry Group for discussions and assistance, particularly to Dr. I.G. Meldrum. I am also grateful to the technical staff of the Chemistry Department in particular Mr. Kenneth Sheppard for carrying out many of the thermal analyses.

I would like to thank my wife for typing the manuscript.

During this period of research, I was in receipt of a grant from the Science Research Council.

John B. Colford

10th September, 1969

CONTENTS

CHAPTER 1

GENERAL INTRODUCTION

1.1 Introduction

During the last decade much of the work in polymer chemistry has been directed towards the synthesis of polymeric materials which exhibit superior thermal stability. This work has been prompted by the need for materials of good thermal stability particularly in the field of aero-space technology where they are required as adhesives, protective coatings, nose cones for missiles, ablative heat shields and electrical insulation. Although the ultimate goal of this work is the synthesis of polymers which are usable for long periods in air at 500°C, there is a need for efficient bonding resins which will have a long life between 200°C and 300°C.

Laminating materials such as the epoxy, phenolic and polyester resins are known to have excellent bonding properties below 200°C but exhibit poor thermal stability above this temperature. Attention must therefore be focused on the synthesis of polymers with chemical structures which are thermally stable and which may be readily fabricated to give useful materials. Consideration must be given, therefore,

to the chemical structural features which are known to impart thermal stability and also to the best synthetic routes to polymers with these features.

1.2 Factors Affecting Thermal Stability

The term thermal stability, when applied to a material, means the ability of the material to maintain its useful properties at a given temperature. There are two principal factors to be considered which affect the thermal stability of a polymer, one is physical and the other chemical.

The physical requirement of a thermally stable polymer is that it have high melting or softening temperatures. These temperatures can be increased by increasing interchain forces and reducing chain flexibility. Interchain attraction can be increased by the introduction of polar substituents or by hydrogen bonding. Stereoregularity in vinyl-type polymers also increases interchain attraction by allowing the polymer chains to fit more readily into a crystalline lattice, thus making it more difficult to overcome intermolecular forces. The reduction of chain flexibility can be accomplished by the replacement of hydrogen atoms by fluorine, as the side groups of the polymer backbone, the close packing of the fluorine atoms giving greater

stiffness to the polymer chain. The presence of bulky substituents, such as methyl or other alkyl groups, can reduce chain flexibility. However if the groups are too large they may lower the melting point by reducing crystallinity.

The chemical factors which affect thermal stability are more diverse. Polymers which have good heat resistance must have no bonds with low dissociation energies. Examples of bond dissociation energies are given in table 1.1[1]. High dissociation energies, however, will not impart thermal stability to a polymer if the polymer has structural features which allow degradation by low energy processes. Chain scission, followed by depolymerisation, in the degradation of some vinyl polymers, is an example of such a low energy process. (figure 1.1.).

(a) Chain Scission

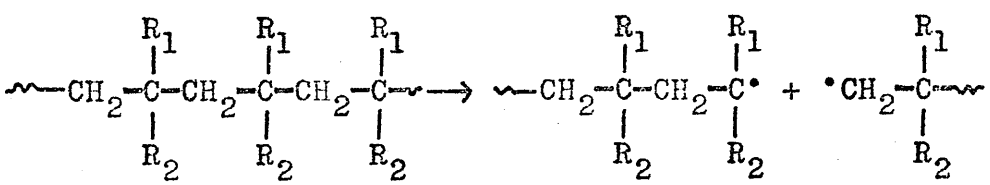

(b) Depolymerisation

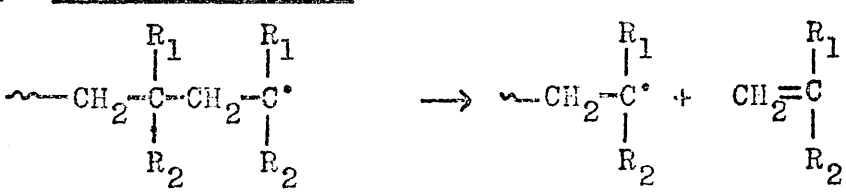

Figure 1.1

Bond (•)	Dissociation energy (K.cal./mole)
$D(HC\equiv C\overset{\bullet}{-}H)$	114
$D(H_2C=CH\overset{\bullet}{-}H)$	105
$D(C_6H_5\overset{\bullet}{-}H)$	102
$D(C_2H_5\overset{\bullet}{-}H)$	97
$D(HC\equiv CH)$	230
$D(H_2C\overset{\bullet}{=}CH_2)$	120
$D(HC\equiv CCH_2\overset{\bullet}{-}CH_3)$	67
$D(H_2C=CHCH_2\overset{\bullet}{-}CH_3)$	62
$D(C_6H_5CH_2\overset{\bullet}{-}CH_3)$	63
$D(C_6H_5\overset{\bullet}{-}F)$	115
$D(CH_3\overset{\bullet}{-}F)$	118
$D(Si\overset{\bullet}{=}O)$	193
$D(P\overset{\bullet}{=}O)$	142
$D(Al\overset{\bullet}{=}O)$	116
$D(C\overset{\bullet}{-}P)$	139
$D(C\overset{\bullet}{-}S)$	177

Table 1.1

The energy required to give chain scission is at least partially supplied through the formation of the double bonds in the monomer produced during the depolymerisation process. A second example is afforded by the degradation

of silicone rubber. Although the siloxane bond dissociation energy is very large, (Table 1.1), volatile six- and eight-membered rings are formed by the reaction shown in figure 1.2. The anionic chain ends are thought to result from traces of impurities in the polymer.

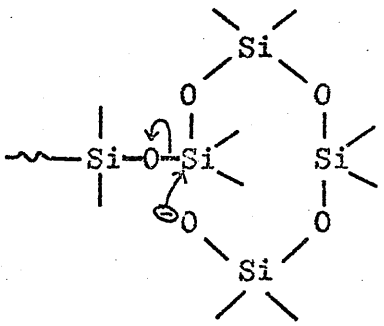

Figure 1.2

The formation of inter- or intramolecular bonds on heating is another chemical factor influencing heat resistance. The formation of these bonds can result in crosslinked structures. While these crosslinked structures, in many cases, prevent chain degradative processes occurring, the onset of crosslinking often changes the physical properties of polymers, causing embrittlement in many cases.

The third chemical factor affecting thermal stability is chemical reactivity. The low reactivity to oxygen, moisture, acids, bases, or other substances, desirable in any polymer becomes particularly important at the elevated temperatures at which thermally stable polymers

are to be used.

The features required for thermal stability in polymers can then be summarised as:

(a) high melting or softening points;

(b) high bond dissociation energies;

(c) structures which are not conducive to low energy degradation processes;

(d) structures which are not susceptible to inter- or intramolecular bond formation;

(e) low chemical reactivity.

Vigorous research and development efforts, prompted by the increasing need for high temperature materials, have led to the synthesis of a large number of new polymers which possess some or all of these features. These polymers are often highly aromatic in structure, high melting, sometimes infusible and usually insoluble in all solvents, thus making their fabrication difficult and limiting their usefulness. Nevertheless many of these polymers have reached the stage of commercial or development production in the last few years.

1.3 Fluorine Containing Polymers

The replacement of hydrogen atoms by fluorine, in a polymer, is known to increase its thermal stability, by introducing bonds of higher dissociation energy and

reducing chain flexibility. The most successful polymer of this type is poly(tetrafluoroethylene). This polymer can be used at temperatures up to 300°C, in air and is stable to most chemicals. The need for thermally stable rubbers has been partly met by fluorinated polymers such as "Viton" (figure 1.3)[2], which is a perfluoropropylene-vinylidine fluoride copolymer. This polymer is stable below 260°C but rapidly decomposes at higher temperatures.

1.4 Inorganic Polymers

As can be seen from table 1.1 the dissociation energies of bonds involving inorganic elements are generally higher than those of carbon-carbon bonds. Thus polymers containing inorganic elements would be expected to be stable in the higher temperature ranges.

The silicone polymers or the siloxanes [3] (figure 1.4 (a)) were the first representatives of systems containing inorganic elements. Although the intrinsic thermal stability of these polymers is good they tend to degrade by the low energy process described previously, and in

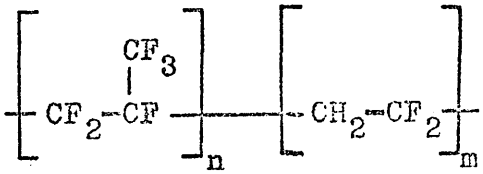

Figure 1.3

order to improve their resistance to heat other inorganic elements, such as aluminium or tin, are often included in the chain (figure 1.4 (b)).

Thermally stable boron and silicon containing polymers with carborane groups have also been prepared[3]. These have the structure shown in figure 1.4 (c) and have been found to be fusible and soluble in organic solvents.

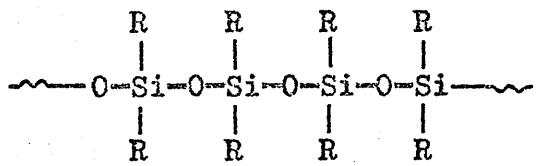

(a)

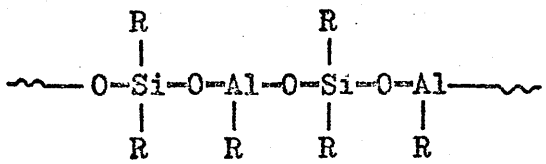

(b)

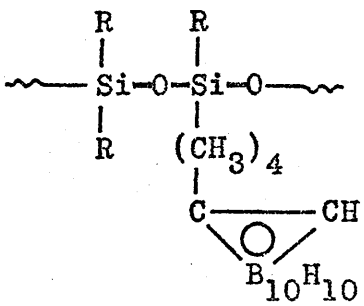

(c)

Figure 1.4

1.5 Ladder and Spiro Polymers

The strength of conventional linear polymers, which comprise single chains of atoms, is determined by the strength of the weakest link in the chain. The breaking of this link can cause drastic reductions in the molecular weight of the polymer, with corresponding deterioration of its physical properties. Polymers which consist of non-crosslinked structures in which two molecular strands are joined to each other, would require that at least two bonds must be broken before any reduction in molecular weight can occur, thus these polymers would be expected to show good thermal stability. Ladder and Spiro polymers are examples of such materials (figure 1.5).

Ladder polymers of many diverse types have been synthesised and although many have only partial ladder

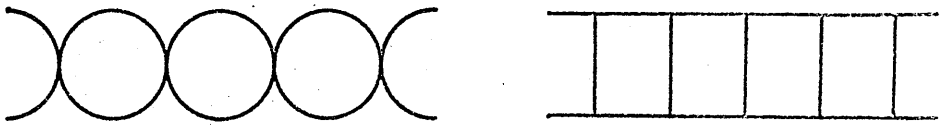

Spiro Ladder

Figure 1.5

structures most do show good thermal stability. One of the first partial ladder structures to be synthesised, and one which is practically useful, is the so-called "Black Orlon" (figure 1.6 (a))[4,5,6,7]. This material is prepared by the pyrolysis of acrylonitrile which leads to a deeply coloured polymer with a high order of thermal stability. Another early example of a ladder polymer is in the field of silicone chemistry[8]. Polyphenylsilesquioxanes of ladder structure (figure 1.6 (b)) which are stable at temperatures up to 300°C, have been prepared from phenyltrichlorosilane as a starting material.

Inorganic spiro compounds have been prepared by treating metal cations with phosphinic acids[9]. These polymers have the structure shown in figure 1.6 (c) and have been shown to exhibit good thermal stability when zinc is used as the metal cation.

1.6 Fully Aromatic Polymers

Polymers containing only aromatic units have received considerable attention in recent years. The first fully aromatic polymer was the poly-p-phenylene prepared by Marvel[10] (figure 1.7). This polymer is insoluble and infusible, however it has been shown to have good thermal stability. Most of the fully aromatic polymers which have been studied, however, have chains containing

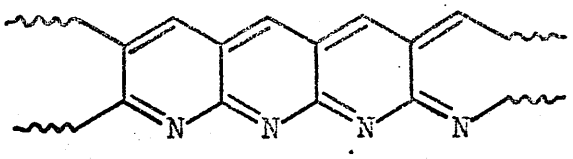

(a)

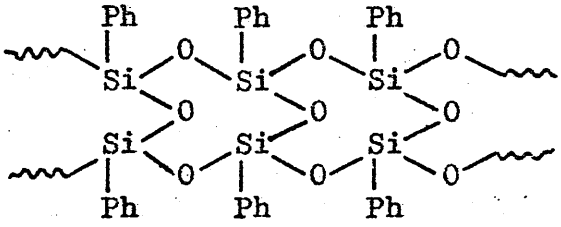

(b)

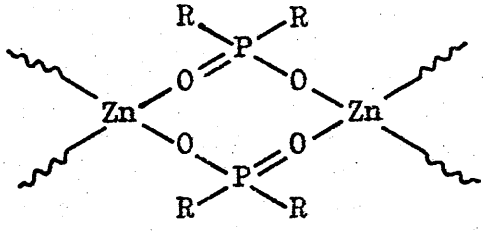

(c)

Figure 1.6

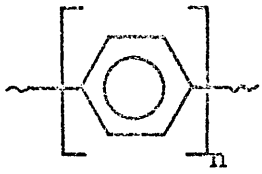

Figure 1.7

heterocyclic rings which, in most cases, are formed during the polycondensation reaction. There are a very large number of polymers which fall into this class and it is intended to mention only two, which show promise of commercial viability.

The polybenzimidizoles[11] have received limited commercial development as high temperature adhesive and laminating resins. These polymers are prepared as shown in figure 1.8 by reaction between an aromatic tetramine and the ester of an aromatic dicarboxylic acid.

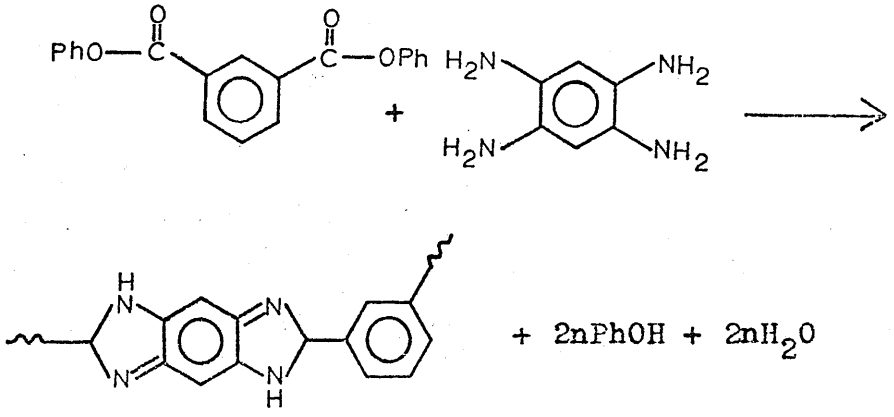

Figure 1.8

The reaction takes place in two steps, the first giving a soluble prepolymer which can be used to impregnate a reinforcement such as glass fibre, the polycondensation reaction being completed during the forming of the laminate at high temperature and pressure. The polymers thus formed exhibit excellent thermal and oxidative stability.

The polyoxadiazoles[12] (figure 1.9) show considerable promise as fibre forming materials for use at high temperatures. These polymers can be prepared by several routes and show good thermal stability in air.

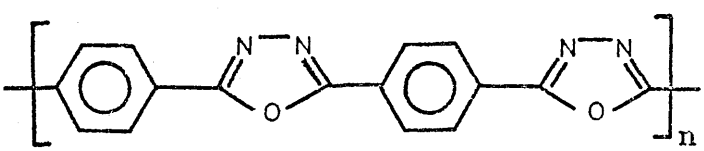

Figure 1.9

1.7 Polymers with Aromatic Units Linked to Non-Aromatic Units

The completely aromatic polymers, described in the previous section, show good thermal stability, but the high rigidity of the backbone chain, while introducing good mechanical properties, often makes them completely insoluble and brittle, thus hindering their commercial development. In order to reduce chain rigidity, while still retaining good thermal properties, many high temperature polymers are based upon aromatic rings

linked by various groupings.

Many of these polymers have reached the stage of commercial development. Polymers such as the polyphenylene oxides[13] (figure 1.10(a)) and the polysulphones[14] (figure 1.10(b)), while not exhibiting exceptional thermal stability, are distinguished by their wide range of working temperatures (-170°C to 190°C) and (-100°C to 150°C) respectively. Others, however, have been shown to have good thermal stability. The polyimide polymers[15] (figure 1.10(c)) are possibly the most successful of the new high temperature materials. These polymers have been used as films, engineering plastics, fibres, binders for reinforced plastics composites and adhesives, where high temperature stability has been required. Other polymers which have received limited commercial success are the aromatic polyamides[16] (figure 1.10(d)), which are being manufactured as fibrous yarns and papers, and poly-p-xylylene[17] (figure 1.10(e)), which has been developed as a protective coating medium and as an unsupported film. The polyarylene sulphides[18,19] (figure 1.10(f)) are an example of a group of polymers of this type which have been shown to exhibit good thermal stability but have not reached the stage of commercial development.

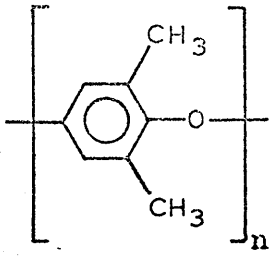

(a)

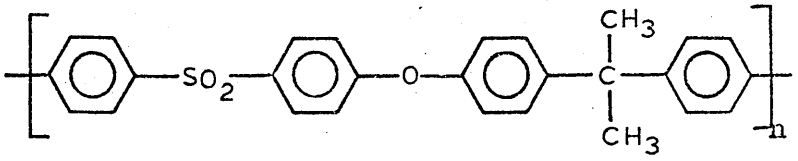

(b)

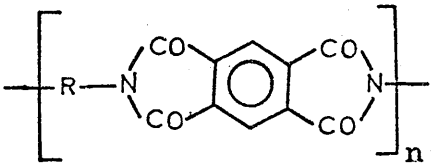

(c)

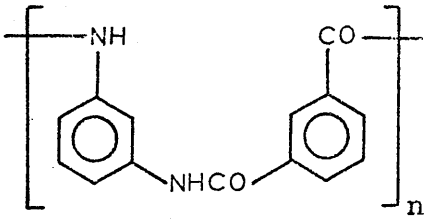

(d)

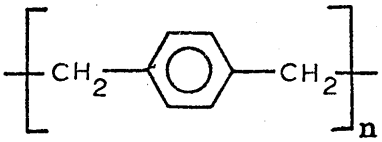

(e)

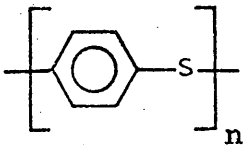

(f)

Figure 1.10

1.8 Friedel-Crafts Polycondensation

Many of the polymers mentioned in the previous section, while exhibiting good thermal stability, have progressed very slowly to the stage of practical utility because they form insoluble and infusible materials, which are extremely difficult to fabricate. There is, therefore, a need for a flexible method of formation of aromatic resins which would allow the manipulation of reaction conditions to produce polymers capable of fabrication.

An example of such a reaction is the polycondensation of benzyl compounds, in the presence of Friedel-Crafts catalysts, to yield macromolecular hydrocarbon materials. The benzyl compounds which have been used for the formation of polybenzyls are benzylhalides, alcohols, ethers[20] and aldehydes[21], but the most thoroughly investigated monomer has been benzyl chloride. Two kinds of polymer can be produced by the action of Lewis acids on benzyl compounds by varying the catalyst and reaction conditions. One is a low molecular weight material which softens about 80°C and is soluble in some solvents, while the other is a granular solid which is infusible and insoluble in any solvents.

The structure of polybenzyl has been the subject of

much discussion. Four possible structures have been proposed.

(a) Polystilbene Structure: Henne and Leicester[22] proposed this structure (figure 1.11 (a)) but little evidence has been found to support their proposal and it is generally considered to be the least likely one.

(b) Linear: This structure (figure 1.11 (b)) was first proposed by Jacobson[23] who suggested that the benzene rings were predominantly disubstituted in the p-position. Such a polymer, however, would be expected to be crystalline and high melting like the poly-p-xylylenes.

(c) Random Branching: Flory[24] has cited polybenzyl as an example of this type of polymer (figure 1.11 (c)). This type of structure would be formed if at any stage in the reaction any hydrogen atom on any benzene nucleus has the same chance of being substituted as any other, subject to the directive influences of existing substitution.

(d) "Sow and Piglet" branching: Based on infrared, oxidation and degradation studies, Haas et.al.[20] have presented evidence for a structure consisting of a core of almost completely substituted benzene rings surrounded by a periphery of pendant benzyl groups (figure 1.11 (d)). This structure is supported by spectroscopic and kinetic studies carried out by Valentine and Winter[25].

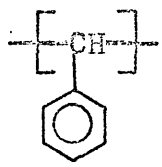

(a)

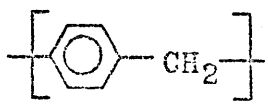

(b)

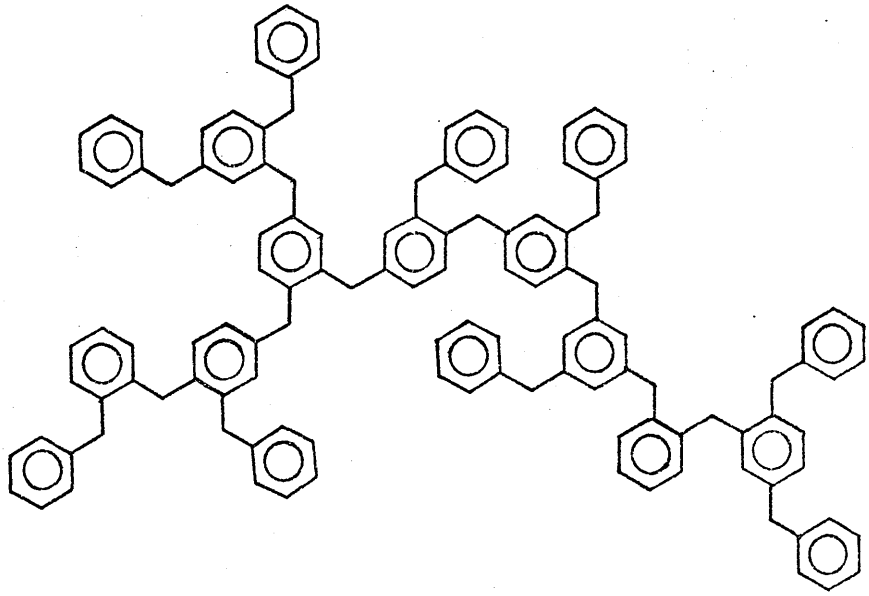

(c)

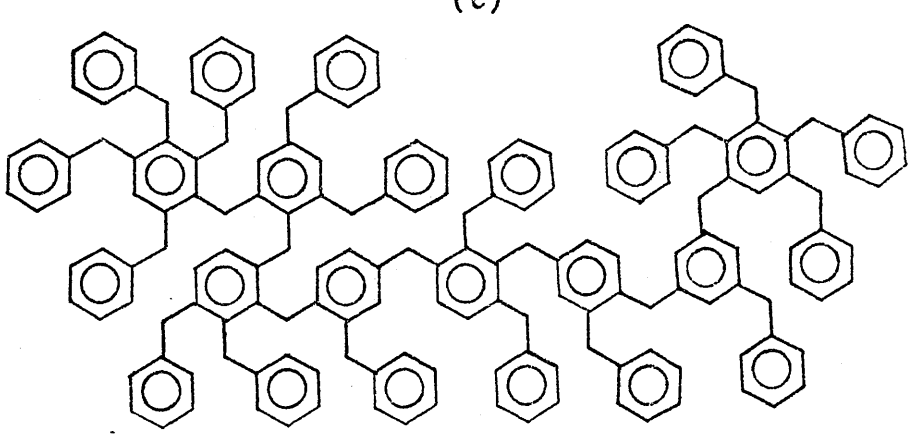

(d)

Figure 1.11

While it seems to have been established that polybenzyl predominantly contains phenyl groups linked by methylene bridges there still remains some doubt about the detailed structure. Most of the experimental evidence obtained seems to favour the structure put forward by Haas, but little account seems to have been taken of the steric crowding due to adjacent benzyl groups. A more reasonable structure would appear to be one in which the average degree of substitution, in all but the peripheral benzyl groups, is lower than that suggested by Haas. Parker[26] has suggested that a reasonable value for the average degree of substitution is three and has suggested the structure shown in figure 1.12. He also found that the analytical results for the insoluble resins are virtually identical with those of the soluble resins and proposed that the structures of both types of polymer are similar. Although this type of structure is unlikely to impart useful physical properties, at high temperature, to the polybenzyls, the versatility of the Friedel-Crafts reaction should allow the preparation of polymers with useful high temperature properties.

A very flexible method of formation of aromatic resins, which involves the use of a Friedel-Crafts reaction between an aromatic dichloromethyl compound and another

aromatic compound, has been described by Phillips[27], who suggested the use of p-(dichloromethyl) benzene (DCMB) as a crosslinking agent in the development of polybenzyl as a useful laminating resin.

Overhults and Ketley[28] used this type of reaction to study the effect of methyl substitution in the aromatic rings of the polybenzyls. They demonstrated that by varying the number and position of methyl substituents in the aromatic rings of the monomer and

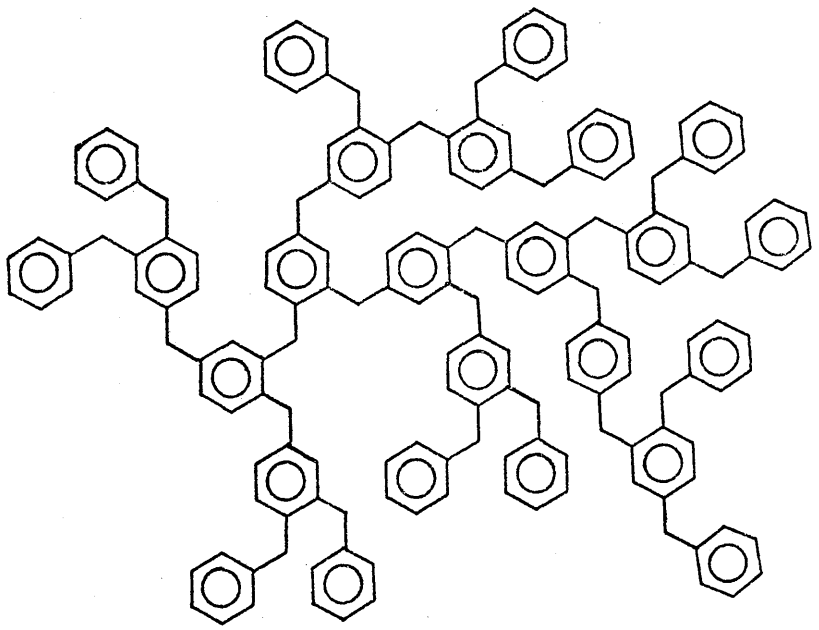

Figure 1.12

co-monomer both the melting point and crystallinity of the resulting polymer could be controlled.

Grassie and Meldrum[29,30,31] have further demonstrated the versatility of this reaction with a detailed study of the products and kinetics of the reactions of diphenylmethane, benzene and benzyl chloride with DCMB. Their work has demonstrated that the frequency of branching in the polymer and hence both its thermal and physical properties can be greatly affected by changes in the aromatic molecule. This is shown in figures 1.13, 1.14 and 1.15. All products of the reaction between DCMB and diphenylmethane up to and including products with five aromatic nuclei must be linear. Thereafter branching may occur and Grassie and Meldrum have shown that molecules become branched at the earliest possible stage. A molecule with more than five nuclei, therefore, is more likely to be branched than linear, owing to the greater rate of substitution into disubstituted nuclei than into mono-substituted nuclei. This was also shown to be true for the DCMB/Benzene system; thus branching occurs at a much earlier stage in this reaction as shown in figure 1.14. The products of the reaction between DCMB and Benzyl Chloride were found to be very complex as would have been expected for this system. This made separation and

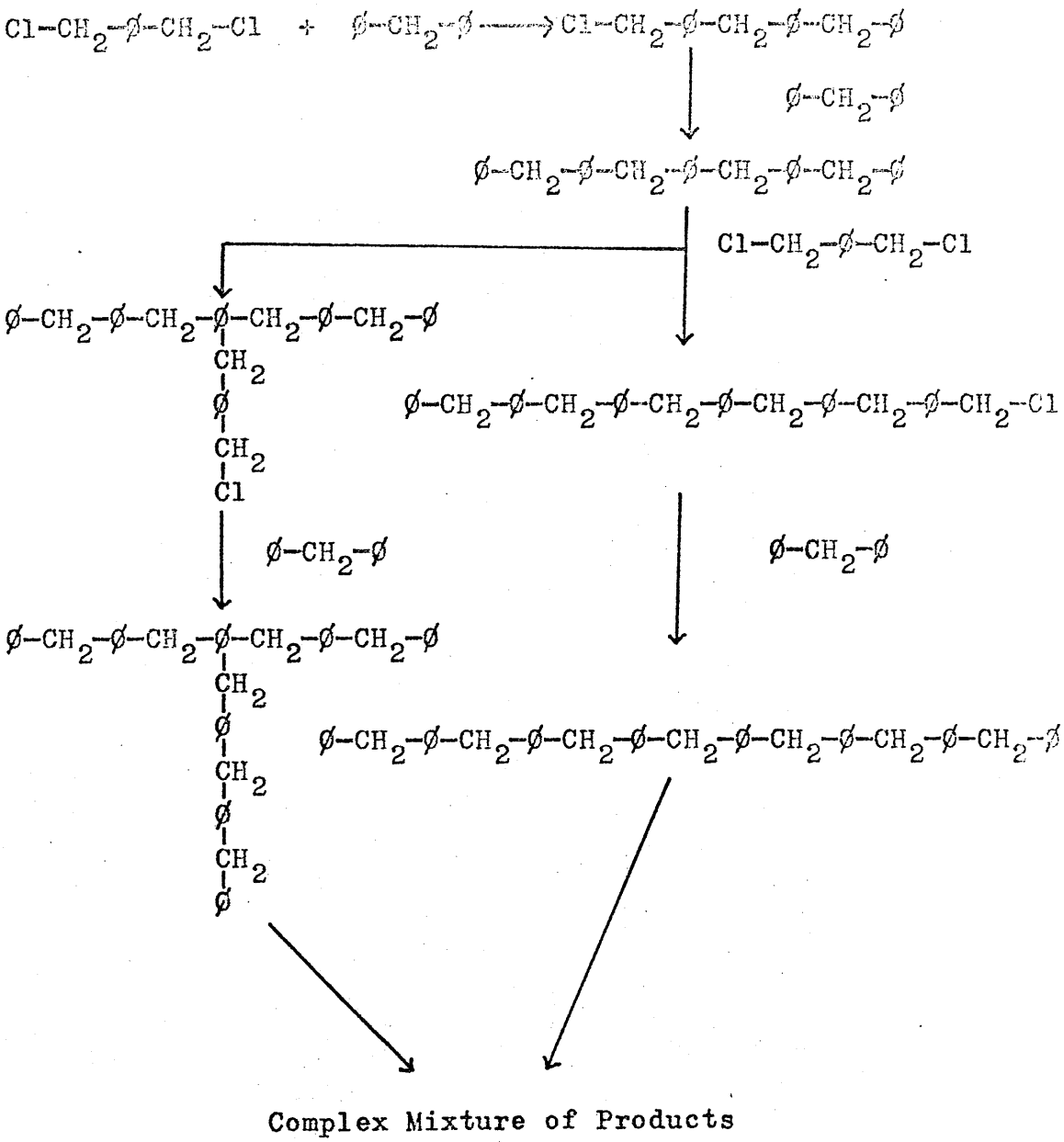

Figure 1.13 Reaction Between DCMB and Diphenylmethane

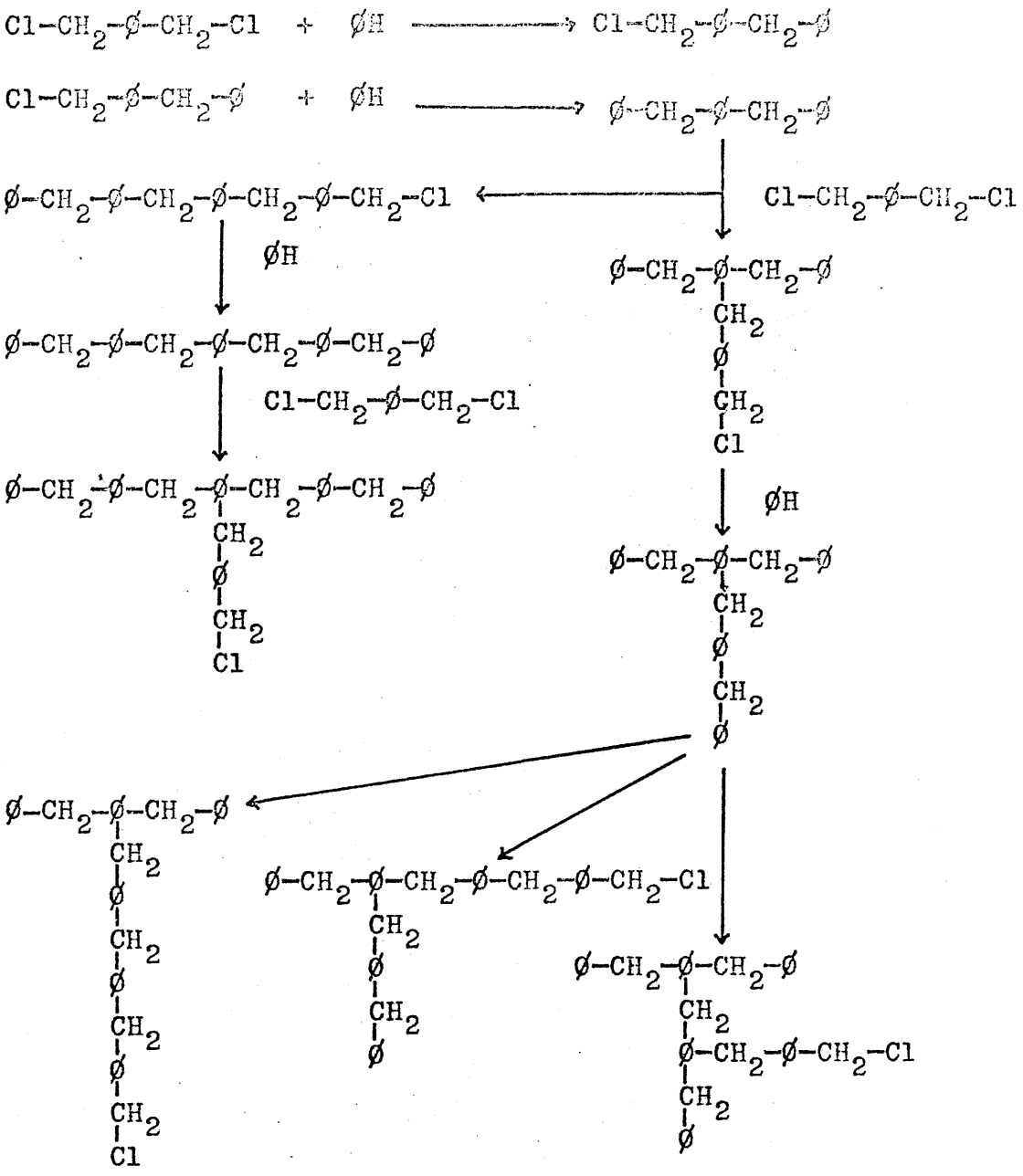

Figure 1.14 Reaction Between DCMB and Benzene

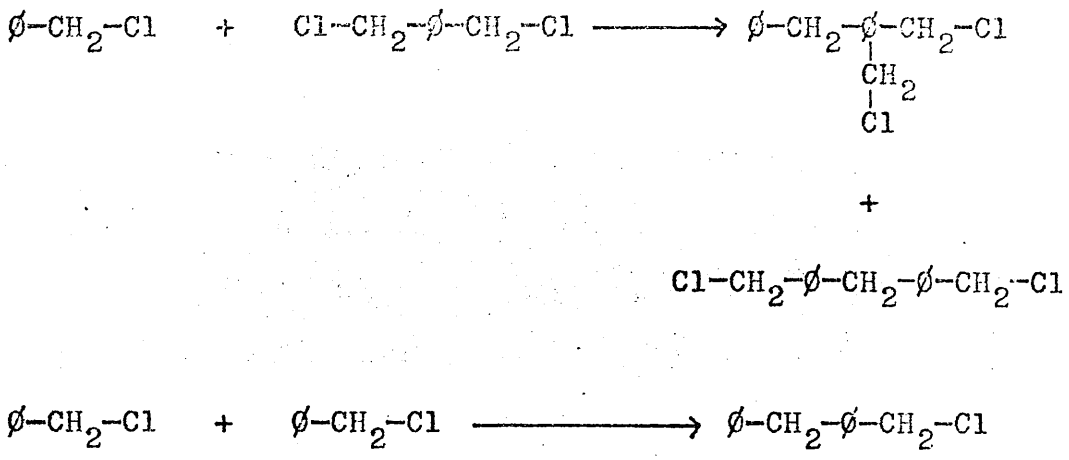

Reaction of the chloromethyl compounds presented above, with the various benzene nuclei available, will result in the formation of a large number of complex products.

Figure 1.15 Reaction Between DCMB and Benzyl Chloride

identification of products very difficult; however some of the reaction products have been tentatively identified and a possible reaction scheme is shown in figure 1.15. As can be seen there should be a rapid build up of highly branched structures in this system.

These investigations have shown that by careful separation and analysis of products the mechanism and kinetics of polymerisation of polybenzyl type structures can be determined. It should, therefore, be possible to estimate the effect of changes in the nature and initial proportions of the reactants on the polymerisation and properties of the polymers.

The preparation of polybenzyl-type polymers with heterocyclic units in the main chain has also been achieved by Grassie and Meldrum[32] using the reaction between DCMB and various aromatic heterocyclic compounds. Polymers were formed with benzene, thiophen, pyridine, indole, quinoline and pyrrole units in the chain and a rough estimate of their relative stabilities made by measuring their rates of volatilisation under conditions of continuously increasing temperature[33]. Their relative stabilities were found to be, in decreasing order, as follows:- thiophen, benzene, pyrrole and indole. Both pyridine and quinoline gave very much less stable products.

No satisfactory conclusion was drawn, however, as to whether the relative stabilities of these polymers were a function of the aromatic molecule or the extent of branching or crosslinking in the polymer.

1.9 Aim of the Present Work

In the light of the work carried out by Phillips, Overhults and Grassie it would appear that the reaction between DCMB and aromatic compounds, catalysed by Friedel-Crafts catalysts, could prove to be a valuable method for the synthesis of polymers with superior thermal stability. Grassie and Meldrum have shown that in order to determine the basic reasons for the stability of polymers of this type it will be necessary to carry out detailed investigations of the mechanism of polymerisation and structure of individual polymers and to correlate these factors with stability. As the polymer formed by the reaction between DCMB and thiophen (figure 1.16) appears to be the most stable of the polybenzyl-type

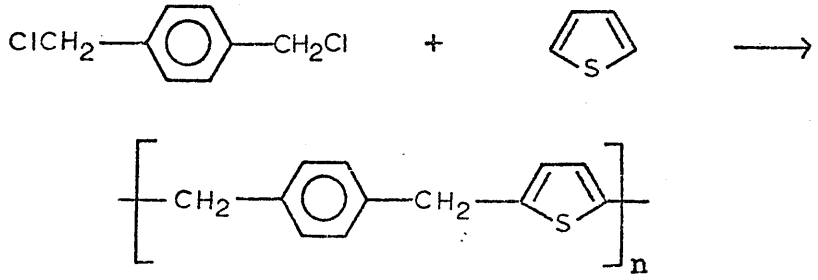

polymers, thus synthesised, it is intended to study the mechanism of formation and structure of this polymer with this ultimate end in view.

CHAPTER 2

EXPERIMENTAL TECHNIQUES AND APPARATUS

2.1 Reactions under Vacuum

(a) Purification and Drying of p-(Dichloromethyl) Benzene.

p-(Dichloromethyl) Benzene (DCMB) (Bush, Boake and Allen Ltd.) was purified by recrystallisation from warm methanol until a constant melting point was obtained (99°C). The product was dried in a vacuum oven at 60°C for 48 hours to ensure complete removal of all liquid residues.

(b) Purification and Drying of Thiophen.

Before use, Thiophen (B.D.H. Ltd. Reagent Grade) was stored over calcium hydride at atmospheric pressure. "Serious" drying was carried out under high vacuum using the following procedures. Pre-dried thiophen was filtered into a reservoir, degassed several times by the freezing and thawing method and distilled onto finely ground calcium hydride in a storage ampoule (figure 2.1 (a)). The ampoule was then sealed off, at point A, at a pressure of less than 10^{-5} torr. The thiophen was then left for a period of at least one week during which time it was intermittently agitated by shaking. Drying was completed by redistillation, under high vacuum, onto fresh finely ground calcium hydride and storage for one more week. After this time the thiophen was twice vacuum distilled

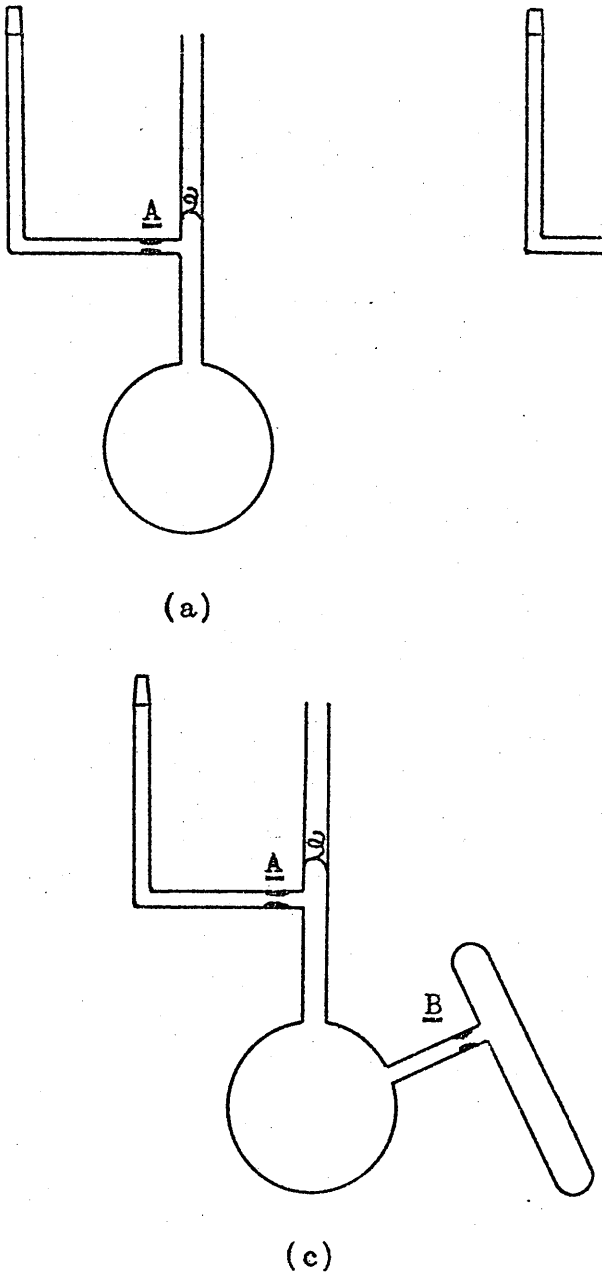

Figure 2.1 Typical All-Glass Ampoules.

and stored in a sealed ampoule until use.

(c) Purification and Drying of Stannic Chloride.

Phosphorous pentoxide was sublimed, under high vacuum, in the apparatus shown in figure 2.1 (c) to remove it from the "bottle material". After sublimation the apparatus was sealed off at point B and thereafter used as a storage ampoule.

Stannic Chloride, Anhydrous, (B.D.H. Ltd. Reagent Grade) was transferred quickly from its sealed container to a reservoir, degassed several times under vacuum and distilled onto the freshly sublimed phosphorous pentoxide. The ampoule was sealed off at a pressure of less than 10^{-5} torr and the contents stored for at least one week in the dark[34]. After redistillation onto freshly sublimed phosphorous pentoxide, followed by storage for one more week in the dark, the stannic chloride was twice vacuum distilled, in all glass apparatus, and stored in a sealed ampoule under its own vapour pressure in the dark. Before use as a catalyst, stannic chloride was subjected to two more distillations, in all glass apparatus, during the manipulation of reagents described in section (f). This ensured the removal of all traces of dissolved phosphorous pentoxide.

(d) Purification and Drying of 1,2-Dichloroethane (DCE).

The purification and drying of DCE (B.D.H. Ltd. Reagent Grade) was carried out as described in section (c) for stannic chloride. The DCE, however, was pre-dried over phosphorous pentoxide "bottle material" before degassing, distillation and drying over freshly sublimed phosphorous pentoxide. It was not considered necessary to store the DCE in the dark.

(e) Preparation of Glassware.

All glassware was made of pyrex glass and was cleaned in the following way. It was washed with cleaning solution, distilled water, acetone, chloroform and finally analar grade acetone before being evacuated on the vacuum line. The apparatus was flamed out at a pressure of less than 10^{-5} torr before use to remove all traces of moisture.

(f) Manipulation of Reagents.

Since traces of water and other impurities can have a profound effect upon catalysed reactions of the type being studied, strict precautions were taken to minimise contamination. All reagents were purified and dried, as described above, using, wherever possible, all glass apparatus with break seals instead of stopcocks. As stannic chloride is known to catalyse the self-polymerisation of thiophen strict precautions were also taken to ensure

that at no time during the manipulation of the reagents did these two liquids come into contact. The following method was devised to allow the reproducible introduction of very small amounts of stannic chloride to the reaction ampoule.

Standard solutions of thiophen in DCE and stannic chloride in DCE were made up under high vacuum in the following way. Thiophen and DCE were distilled from their storage ampoules into graduated ampoules (figure 2.1 (b)) which were then sealed off. Stannic chloride was transferred to a 1 ml. graduated ampoule using the apparatus shown in figure 2.2. The apparatus was evacuated to a pressure of less than 10^{-5} torr and sealed off at point A. After breaking the break seal, the required amount of stannic chloride was poured from storage ampoule B into the 1 ml. graduated ampoule C, which was then sealed off at point D. The remaining stannic chloride was then distilled into storage ampoule E, which was then sealed off at point F and stored in the dark. The known amounts of reagents, in the graduated ampoules, were then distilled into two storage ampoules, using an all glass apparatus similar in design to that in figure 2.4 to make up the two standard solutions.

The standard solutions were then thoroughly shaken

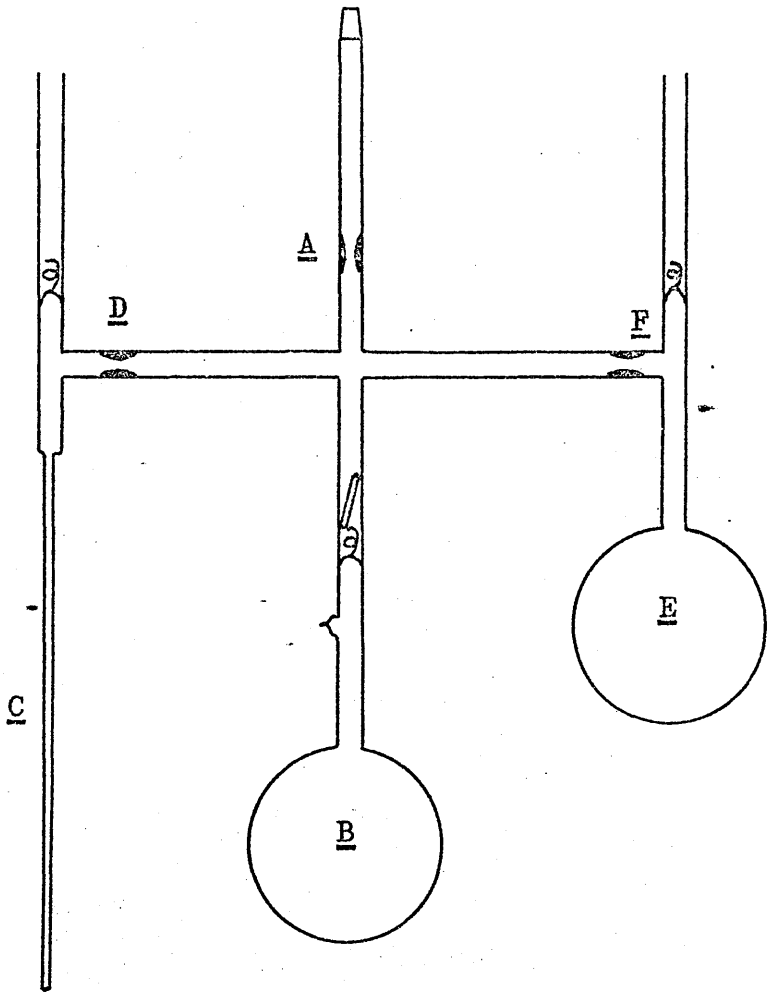

Figure 2.2 Greaseless Liquid Transfer Apparatus.

and distributed into 10 ml. calibrated ampoules using the apparatus shown in figure 2.8. The apparatus consisted of a central reservoir A surrounded by a periphery of nine 10 ml. calibrated ampoules B and one inlet tube C. The storage ampoule D, containing the standard solution, was sealed onto the inlet tube and the apparatus evacuated at point E. The apparatus was then sealed off at point F and the standard solution introduced into the central reservoir by breaking the break seal. The solution was then poured into each ampoule in turn and the ampoules sealed off at the fine constriction G.

Transfer of solutions to the reaction ampoule was then carried out using the all glass apparatus in figure 2.4. The apparatus consisted of a reaction ampoule A, into which DCMB had been introduced in the form of a crystalline solid, attached to the two calibrated ampoules B, containing the standard solutions. After evacuation and sealing off at point C, the standard solutions were distilled onto the DCMB, the thiophen solution being distilled first. The calibrated ampoules and manifold were then flamed out to ensure complete transfer of reagents and the ampoule sealed off at point D.

(g) Reaction Conditions.

Preliminary experiments were carried out at 30°C ± 0.1°C

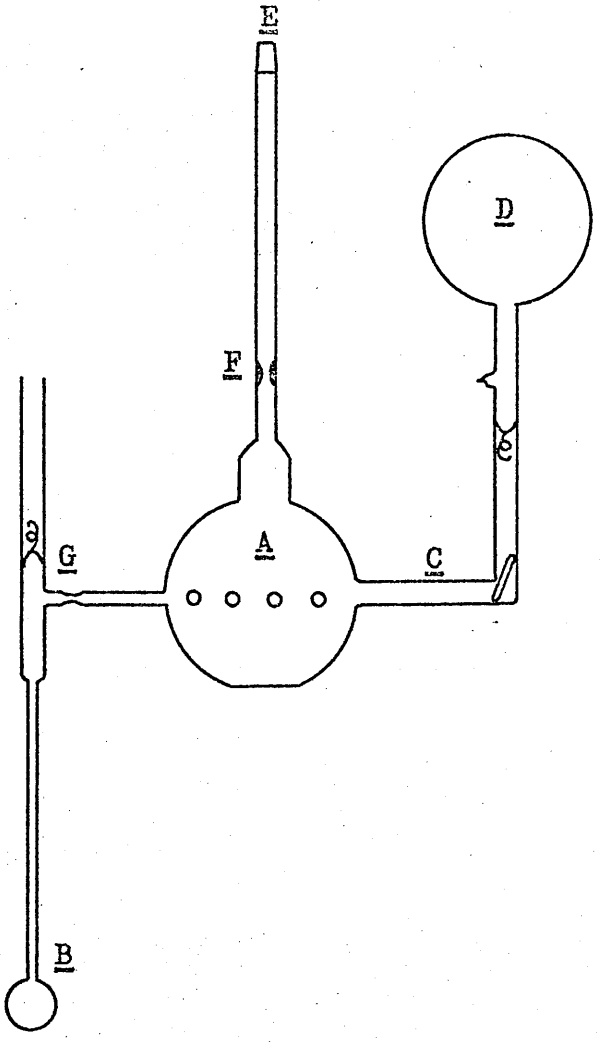

Figure 2.3 Greaseless Solution Transfer Apparatus.

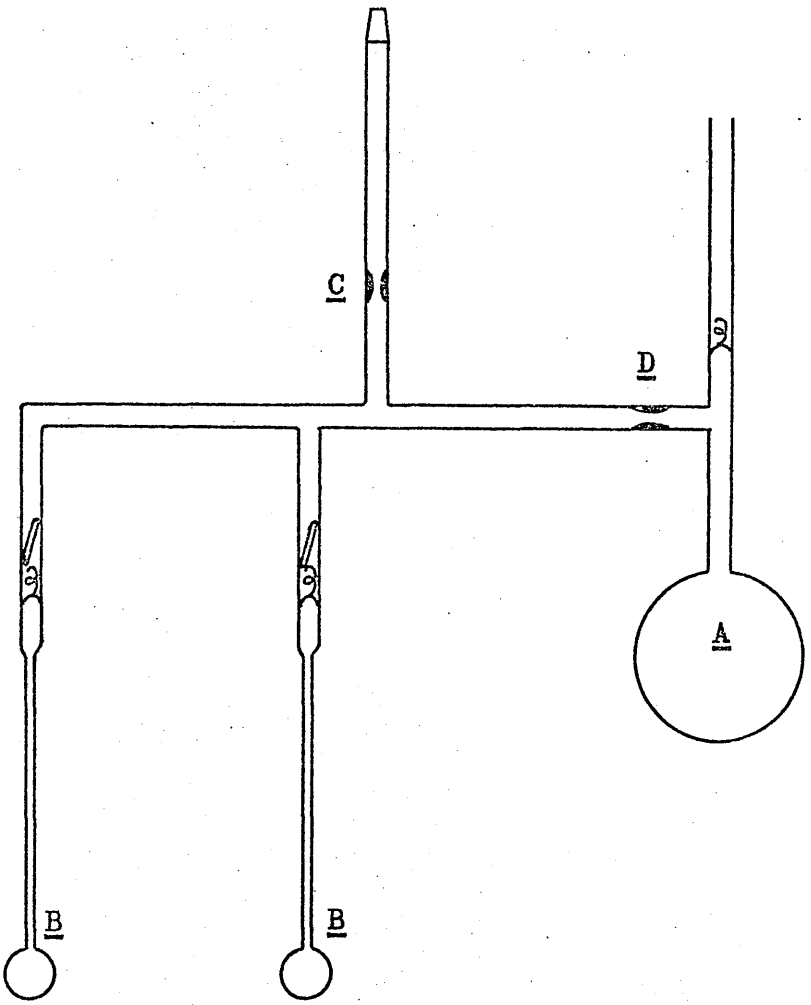

Figure 2.4 Greaseless Solution Transfer Apparatus.

in a stirred, thermostatically controlled water bath. All other experiments were carried out in a Towson and Mercer Ltd. "Minus Seventy", Bridge Control Model, Thermostat Bath. Using this equipment temperatures in the range +10°C to -20°C could be controlled to ± 0.5°C. Reactions were quenched by immersion of the reaction ampoule in liquid nitrogen.

2.2 Polymerisation under Nitrogen

(a) Purification and Drying of Reagents.

(i) Thiophen (B.D.H. Ltd. Reagent Grade), 2-Methyl-, 3-Methyl- and 2,5-Dimethylthiophen (Ralph N. Emanuel Ltd. Puriss Grade) and 2-Chlorothiophen (Koch-Light Laboratories Ltd. Puriss Grade) were distilled at atmospheric pressure and dried over finely powdered calcium hydride for 48 hours. The reagents were then filtered, redistilled and stored over finely powdered calcium hydride until use. All reagents were again filtered and redistilled, at atmospheric pressure, immediately before use.

(ii) Stannic chloride and DCE (B.D.H. Ltd. Reagent Grade) were dried as described in section 2.1. Before use stannic chloride was distilled several times under high vacuum to remove all traces of phosphorous pentoxide. DCE was distilled at atmospheric pressure immediately before use.

(iii) DCMB (Bush, Boake and Allen Ltd.) was purified as in section 2.1.

(b) Preparation of Glassware.

Pyrex glass reaction vessels were washed with cleaning fluid, distilled water, acetone, chloroform and finally analar grade acetone before being dried for 24 hours in an oven at 120°C. Washing and drying of glassware was carried out immediately before use.

(c) Polymerisation.

The apparatus was as shown in figure 2.5. Reactions were carried out in an atmosphere of pure nitrogen (British Oxygen "White Spot") which had been dried by passing through a column A, containing Molecular Sieve Type 4A, which had been activated by heating at 120°C for 24 hours.

DCMB was added to the reaction flask B in the form of a crystalline solid and the flask flushed out with nitrogen. DCE and the aromatic compound were added separately by syringe through a septum C and the apparatus again flushed out with nitrogen before addition of stannic chloride. In order to ensure the reproducible addition of small amounts of stannic chloride to the reaction flask this reagent was added in the form of a solution in DCE, by syringe. The time of addition of the stannic chloride solution was noted and was taken to be zero time for the reaction.

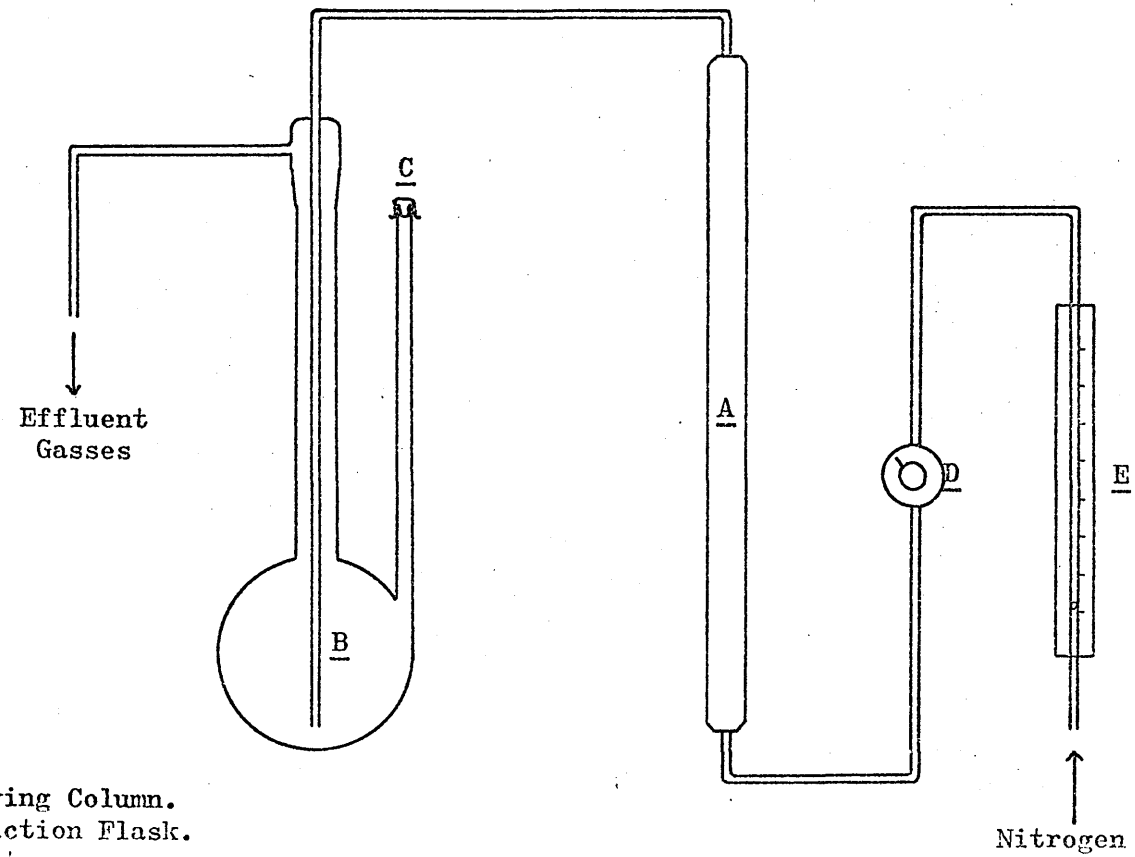

A Drying Column.
B Reaction Flask.
C Septum.
D Needle Valve.
E Nitrogen Flowmeter.

Figure 2.5 Apparatus for Polymerisations under Nitrogen.

Reactions were carried out at 30°C ± 0.1°C in a stirred, thermostatically controlled water bath and the effluent gases collected by bubbling into distilled water. The rate at which hydrogen chloride was carried from the reaction mixture was measured by titration with standard alkali. The rate of nitrogen flow was maintained at 10 ml./min. and this was shown, by means of "blank" experiments to be consistent with negligable carrying-over of stannic chloride.

(d) Polymer Recovery and Purification.

Soluble and insoluble products of reaction were separated by filtration of the reaction mixture. Recovery and purification methods for both types of product are described below.

(i) Soluble Polymers: After washing the solution with water to remove the dissolved stannic chloride the polymer was precipitated by addition of the solution to either analar methanol or n-hexane. The solution was slowly run into 3 litres of the precipitant with constant stirring. The product was filtered, dried at room temperature in a vacuum oven, and dissolved in chloroform. This procedure was repeated twice. The final product was then dried in a vacuum oven at 100°C for 48 hours.

(ii) Insoluble Polymers: The insoluble polymers were

purified by thorough washing with anolar solvents. Washing was carried out by vigorously shaking the material with distilled water, acetone, chloroform and finally diethyl ether for 24 hours. After each washing the product was dried at room temperature, in a vacuum oven. After the final washing the polymer was finely ground and dried in a vacuum oven at 100°C.

Purification of the polymers, as described above gave materials of fairly high purity. It was not possible, however, to ensure complete removal of all low molecular weight species small amounts of which may still have been present.

2.3 Analysis of Products

The separation and analysis of products of the reactions described in this thesis were carried out using the techniques described below.

(a) Analysis of HCl Produced in the Reaction under Vacuum.

Analysis of HCl was carried out in the apparatus shown in figure 2.6. A glass bulb A was sealed onto the reaction ampoule at point B. 20 ml. of distilled water was then added to bulb A and a glass rod inserted through the rubber seal C. The distilled water was added to the reaction mixture by breaking the glass seal with the rod. The mixture was then shaken vigorously for 15 minutes to

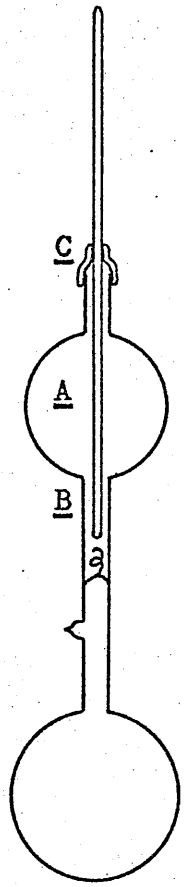

Figure 2.6 Hydrolysis Apparatus.

ensure complete dissolution of all HCl in the water. The apparatus was then opened below the break seal, the glassware washed with distilled water and the washings added to the reaction mixture. The amount of HCl was estimated by titration with standard alkali.

The organic layer was washed thoroughly with water, separated and dried over anhydrous sodium carbonate.

(b) Gas-Liquid Chromatography (G.L.C.).

(i) Quantitative Analysis: Quantitative G.L.C. analyses were carried out using a Microtek 2000R gas chromatograph equipped with dual columns, flame ionisation detector and linear temperature programmer. In order to achieve good separation of products samples were injected onto a 1% silicone gum (SE30) on 100/120 Embacel column which was then linearly programmed from 50°C to 250°C at 10°/min. After calibration of the flame ionisation detector, as described in chapter 5, quantitative analyses of DCMB and the first two products of reaction were carried out. The calibration of the detector was checked at regular intervals.

(ii) Preparative G.L.C.: Preparative G.L.C. was used for the separation of small amounts of products for calibration of the Microtek 2000R flame ionisation detector. A Pye 105 Automatic Preparative Chromatograph

was used with a 1.25% silicon gum (SE30) on 80/90 Gas Chrom column.

(c) Gel Permeation Chromatography (G.P.C.).

The separation and estimation of the concentration of reaction products with molecular weights higher than 300, for which G.L.C. was found to be inapplicable, was achieved by the use of preparative gel permeation chromatography. The apparatus used is illustrated in figure 2.7.

Outgassing of solvent (analar chloroform) was carried out by refluxing solvent from reservoir A above the inlet to the chromatographic columns in such a way that a constant amount of outgassed solvent was retained in reservoir B. This solvent then maintained a constant hydrostatic pressure on the liquid flowing through the columns.

The gel, a crosslinked dextran (Sephadex LH20, Pharmacia Ltd.) was contained in two pyrex glass columns C (4 x 75 cm. and 3 x 75 cm.) which were connected in series. In both columns the liquid flowed downward in order to oppose the tendancy for the gel to float. The solvent resistant column ends (Pharmacia Ltd.) ensured that except for the nylon sieves and a small metal ring, in the column ends, all surfaces in contact with the solvent

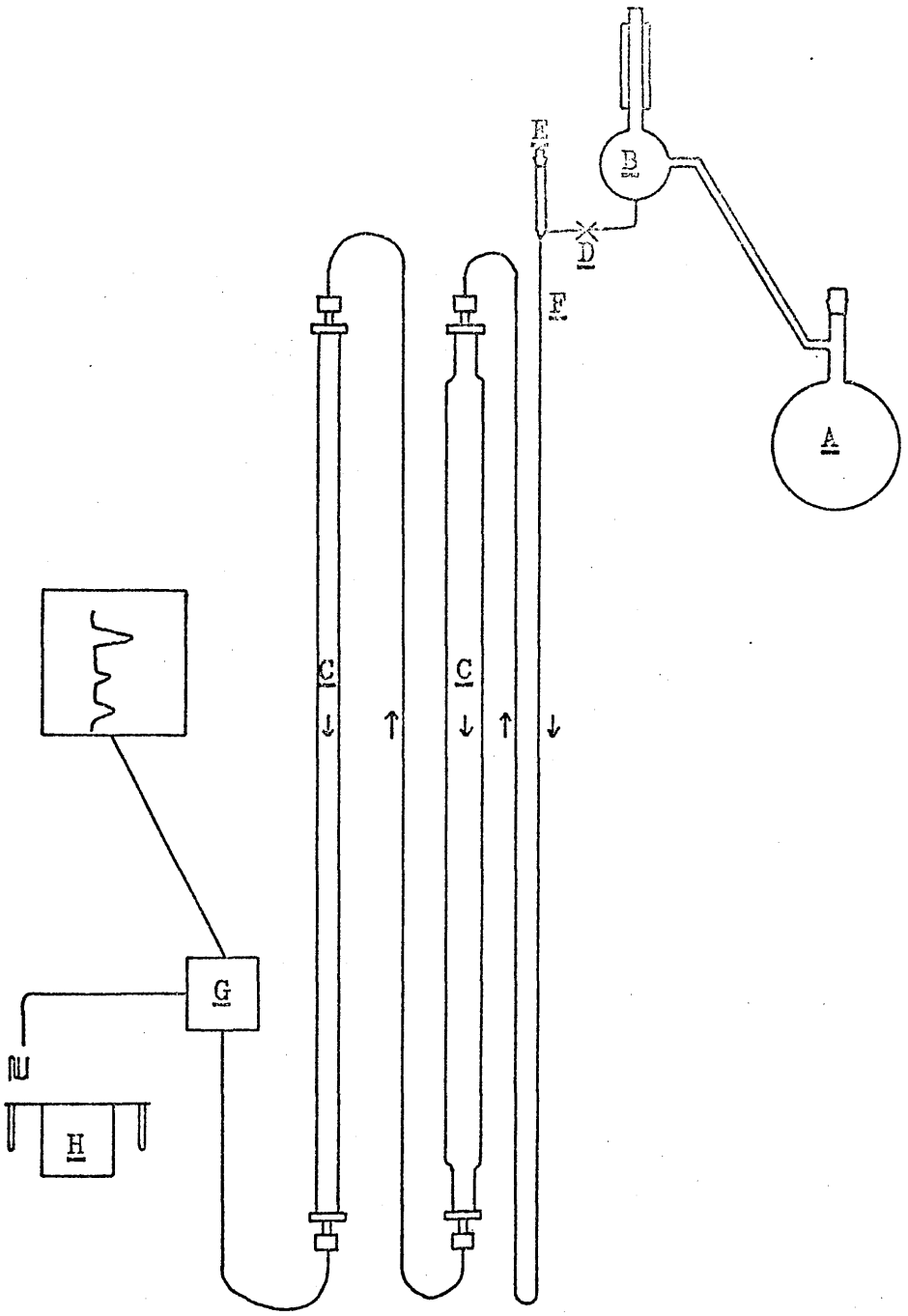

Figure 2.7 Gel Permeation Apparatus.

were of pyrex glass or polytetrafluoroethylene.

Injection of sample was achieved simply by closing the teflon stopcock D, removing stopper E and allowing the solvent to run off. When the head of solvent had passed point F the sample was added through opening E and allowed to flow into the first column. Stopcock D was then reopened, stopper E replaced and the solvent flow continued. Eluate from the second column passed through a L.K.B. Uvicord 4701A U-V detector G and was collected in 10 ml. fractions by the automatic fraction collector H. The U-V detector could not be used quantitatively so quantitative estimations of products were carried out by evaporation of solvent from the fractions, at room temperature, and weighing the residues.

Samples were prepared for injection by drying of the organic solution, as described in section 2.3 (a), removal of solvent under vacuum and dissolution of the residue in 10 ml. analar chloroform.

(d) Gas Chromatography-Mass Spectrometry (G.C.M.S.).

Reaction products which could be separated by G.L.C. were initially analysed by means of a L.K.B.900 (L.K.B.-Produkter) combined gas chromatograph - mass spectrometer, a schemetic diagram of which is shown in figure 2.8. The novel feature of this equipment is the molecule separator (Becker-Ryhage)[35] which pumps away most of the helium

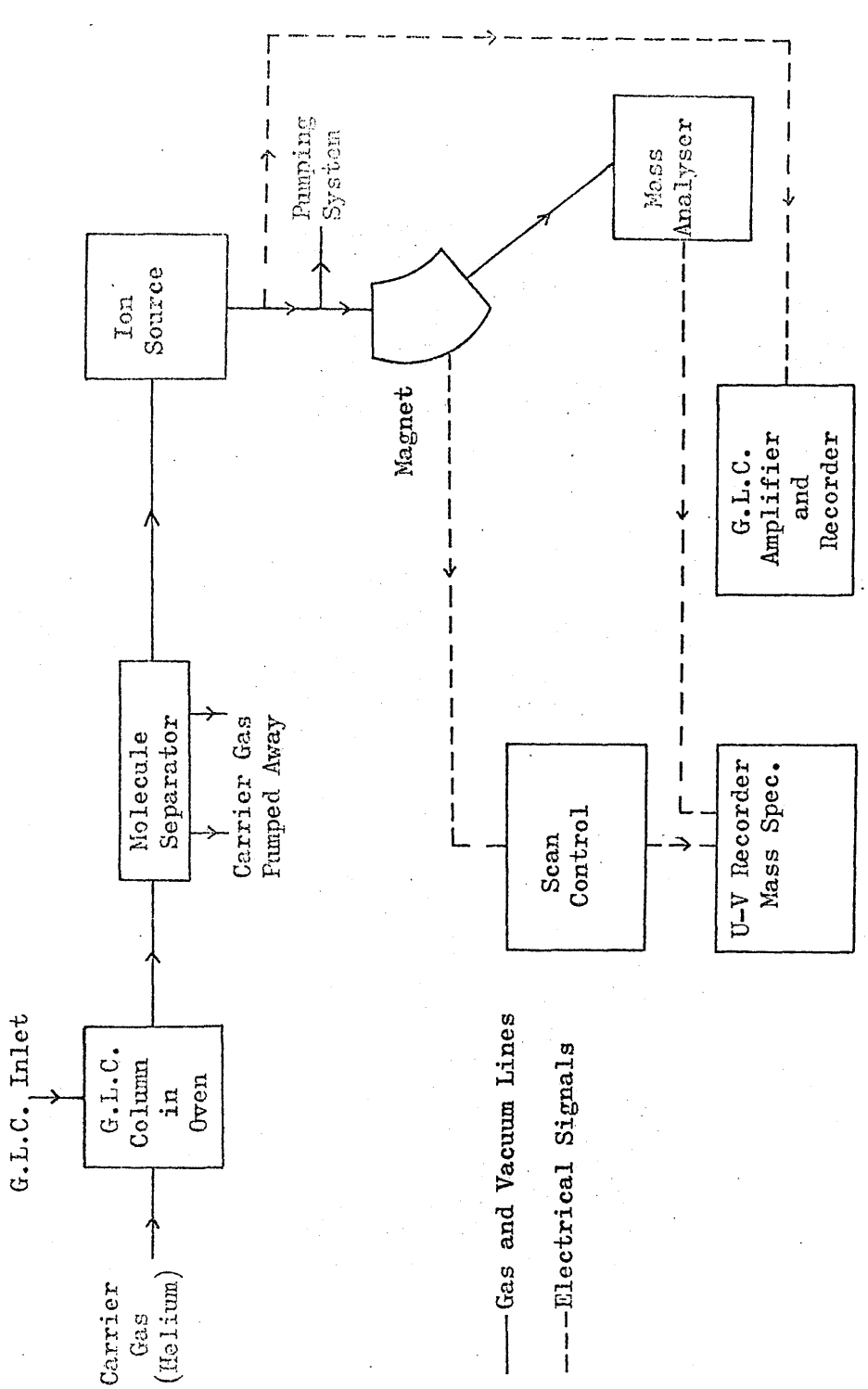

Figure 2.8 Schemetic Diagram of L.K.B.900 G.C.M.S.

carrier while allowing 50-75 per cent. of the separated component under analysis to pass into the mass spectrometer.

At all times, other than when a mass spectrum is being scanned, the instrument operates with an electron beam energy of 20ev which is below the ionisation potential of helium (24.8ev) but high enough to ionise any organic matter coming off the column. The total ion current is measured by an electrometer, in the ion source, and fed through an amplifier to the G.L.C. recorder.

The mass spectrometer is a single focusing instrument with a fast scanning speed. When a component is observed on the G.L.C. recorder pressing the scan button automatically increases the ionisation voltage to 70ev and a mass spectrum is obtained from the fast U-V recorder.

(e) Molecular Weight Measurements.

Molecular weight measurements were carried out using a Hewlett Packard 301A Vapour Pressure Osmometer. The measurements were made at 65°C in toluene solution.

(f) Miscellaneous Spectroscopic Analysis.

(i) Mass Spectrometry: Mass spectra of reaction products of molecular weight greater than 300 were obtained using an A.E.I. MS12 mass spectrometer. Spectra were obtained using ionisation voltages within the range 20ev - 70ev.

(ii) Nuclear Magnetic Resonance Spectrometry (n.m.r.):

Spectra were obtained using either a Perkin Elmer R10 60 Mc.p.s. spectrometer or a Varian HA100 100 Mc.p.s. spectrometer. In many cases, due to the small amounts of materials available, samples run on the Varian HA100 spectrometer were run in 0.15 ml. micro-cells with resulting loss of resolution.

(iii) Infrared Spectrometry (I.R.): I.R. spectra were obtained using Perkin Elmer 225 and 257 spectrometers. Samples were prepared as potassium bromide discs or run as liquid films between sodium chloride discs.

(iv) Ultra Violet Spectrometry (U-V): U-V analyses were carried out on a Unicam SP800 spectrophotometer. Solutions of the reagent in analar diethyl ether (approx. 1 mg/ml.), contained in 2mm quartz cells, were used.

2.4 Thermal Methods of Analysis

Two methods have been used to study the thermal degradation of the polymers. Both have been devised for studying continuously the changes in the nature of a substance on heating and in this work both involved linearly programming the temperature of the sample from room-temperature to 1000°C.

(i) Thermogravimetric Analysis (T.G.A.): Thermogravimetric analyses were carried out using a Dupont 950 Thermo-gravimetric Analyser. This instrument operates on the

null balance system; the beam being maintained in the reference position by an optically activated servo loop. Samples were heated at 10°C/min. in an atmosphere of either oxygen free nitrogen or air. It was not possible to obtain a high vacuum with this apparatus.

Although many theoretical methods have been devised for obtaining kinetic data from T.G.A.[36], these are generally only applicable to simple degradation processes and so no kinetic analyses of the degradation processes described in this thesis have been attempted.

(ii) Thermal Volatilisation Analysis (T.V.A.)[37]: The T.V.A. apparatus used in this work was similar in design to the Differential Condensation T.V.A. which has been described by McNeill[38]. A schematic diagram of the apparatus is shown in figure 2.9. Two cold traps at -75°C and 0°C were mounted in parallel between the silica glass reaction vessel and a cold trap at -196°C. Samples were heated at 10°C/min. as the system was continuously pumped. The pressure in the vicinity of each cold trap was continuously monitered by a Pirani Gauge (Edwards High Vacuum Ltd.).

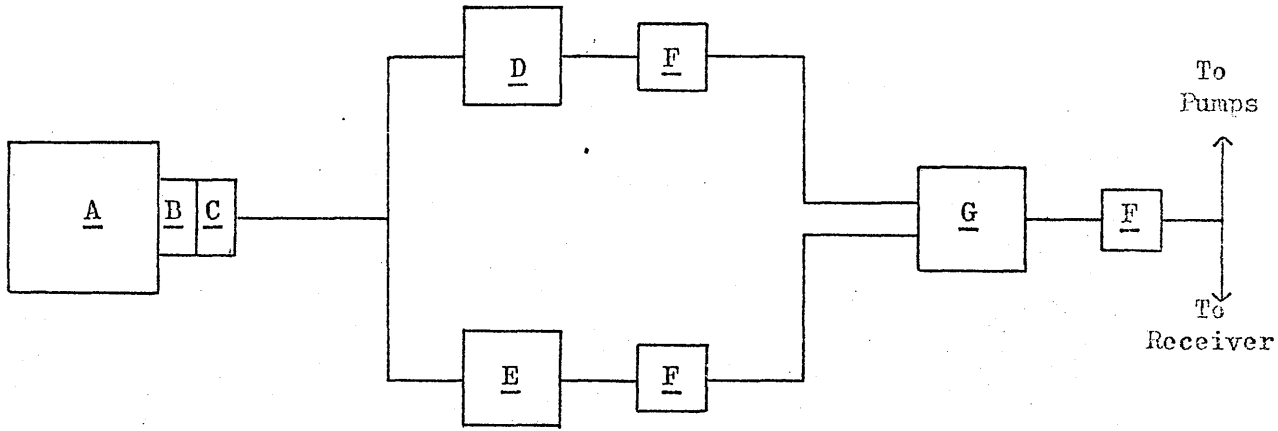

A Silica Glass Degradation Tube in Temperature Programmed Oven.
B Cold Ring at 18°C.
C Solid CO_2 Cold Ring.
D Cold Trap at 0°C.
E Cold Trap at -75°C.
F Pirani Gauges.
G Cold Trap at -196°C.

Figure 2.9 Schematic Diagram of T.V.A. Apparatus.

CHAPTER 3

PRELIMINARY OBSERVATIONS

3.1 Introduction

Before carrying out a detailed investigation of the reaction between DCMB and thiophen it was necessary to establish the effect of impurities, such as water, on the reaction and also to estimate the extent to which reactions other than that between DCMB and thiophen took place. It was also important to obtain an overall picture of the main features of the polymerisation and the resultant polymer. As a result of these preliminary experiments it was hoped that a convenient method and suitable conditions for following the course of the polymerisation could be chosen and the best experimental conditions established.

3.2 The Self-Polymerisation of Thiophen

Since Victor Meyer[39] first reported the polymerisation of thiophen catalysed by sulphuric acid, a large number of workers have polymerised thiophen in the presence of a great variety of acidic species. The polymerisation of thiophen by Friedel-Crafts catalysts was first reported by Bruce and his co-workers[40] who obtained amorphous solids from the reaction of thiophen with ferric and stannic chlorides. While in most cases the product of

the polymerisation of thiophen has been an insoluble and infusible solid, thus making a detailed analysis of the polymer difficult, several workers have prepared soluble materials by reaction of thiophen with mild acidic reagents. Analysis of these products has allowed a clearer picture of the structure of the thiophen polymer to be built up.

Using the dielectric polarisation method Gold'stein and co-workers[41,42] have established that polymerisation of thiophen in the presence of stannic chloride proceeds through the formation of π-complexes between thiophen and stannic chloride. These complexes are formed by the interaction of stannic chloride with the π-electrons of the thiophen ring and lead to the gradual polymerisation of the thiophen. Infrared spectroscopy of the thiophen - stannic chloride complex showed absorption in the region of 1440 cm^{-1} due to C-H deformation vibrations. Absorption in this region is generally indicative of the presence of C-H bonds where the hydrogen is attached to an aliphatic carbon. It would therefore appear that during the polymerisation of thiophen hydrogen migration occurs to produce completely saturated centres in the polymer.

Further studies carried out by Curtis and co-workers[43] and Armour and co-workers[44] have confirmed that while

unsaturated centres do persist in the thiophen polymer, saturated centres are produced during polymerisations catalysed by acidic reagents. A detailed analysis of the "trimer" and "pentamer" produced by the reaction of thiophen with 100%-orthophosphoric acid was carried out by Curtis and co-workers. U-V analysis indicated that these products still contain unconjugated thiophen nuclei. I.R. and n.m.r. analyses, while giving support to the U-V analysis, also showed the presence of aliphatic carbon atoms in these compounds. Dehydrogenation of the "trimer" and x-ray analysis of the "pentamer" confirmed these analyses and revealed that these compounds have the structure shown in figure 3.1.

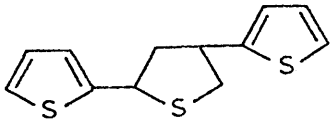

"trimer"

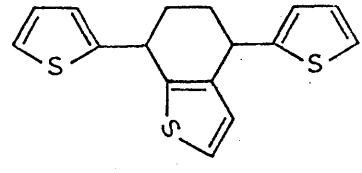

"pentamer"

Figure 3.1

It is clear, therefore, that the reactions occurring during the polymerisation of thiophen, catalysed by acidic reagents, are extremely complex and should lead to polymeric materials with complex structures. The production of such structures during the DCMB-thiophen reaction could greatly

affect the resultant polymer and also render kinetic studies meaningless. It was therefore necessary to estimate the extent to which thiophen self-polymerised under reaction conditions similar to those to be used in the study of the DCMB-thiophen reaction.

Attempts were made to polymerise thiophen at 30°C, both under vacuum and under nitrogen, using stannic chloride as the catalyst and 1,2-dichloroethane as the solvent. Reactions were terminated by addition of distilled water to the reaction mixture. The organic layer was then separated and dried over anhydrous sodium carbonate. The extent of reaction was estimated from the total weight of the involatile residue obtained by evaporation of volatile materials from 10 ml. aliquots of the reaction solution. The results were calculated as the percentage of thiophen which had been converted to involatile material and are presented as percentage polymerisation. Details of the experiments are presented in table 3.1 and are illustrated in figure 3.2.

The plots of percentage polymerisation against time of reaction show that after seven days reaction, at 30°C, the maximum amount of thiophen which has polymerised represents only 1.57% of the starting material. It would appear, therefore, that the self-polymerisation of thiophen

Table 3.1 Self-polymerisation of Thiophen

Series Number S6	Atmosphere Vacuum	Concentrations of Reactants (moles l^{-1}) $SnCl_4$ 0.020			Thiophen 2.52		
Reaction Time (Hr)	24	48	72	96	120	144	168
Wt. of Involatile Product/litre (g)	0.100	0.625	0.675	0.825	1.250	0.700	1.650
%ge Polymerisation	0.047	0.295	0.318	0.390	0.590	0.332	0.780

Series Number S7	Atmosphere Vacuum	Concentrations of Reactants (moles l^{-1}) $SnCl_4$ 0.018			Thiophen 3.43		
Reaction Time (Hr)	24	48	72	96	120	144	168
Wt. of Involatile Product/litre (g)	0.700	1.200	1.750	2.650	3.100	4.000	4.550
%ge Polymerisation	0.243	0.412	0.608	0.920	1.080	1.390	1.580

Series Number S22	Atmosphere Nitrogen	Concentrations of Reactants (moles l^{-1}) $SnCl_4$ 0.024			Thiophen 5.50		
Reaction Time (Hr)	20	50	77	103	125	155	
Wt. of Involatile Product/litre (g)	0.715	1.800	2.900	3.880	4.501	5.479	
%ge Polymerisation	0.155	0.389	0.627	0.839	0.975	1.179	

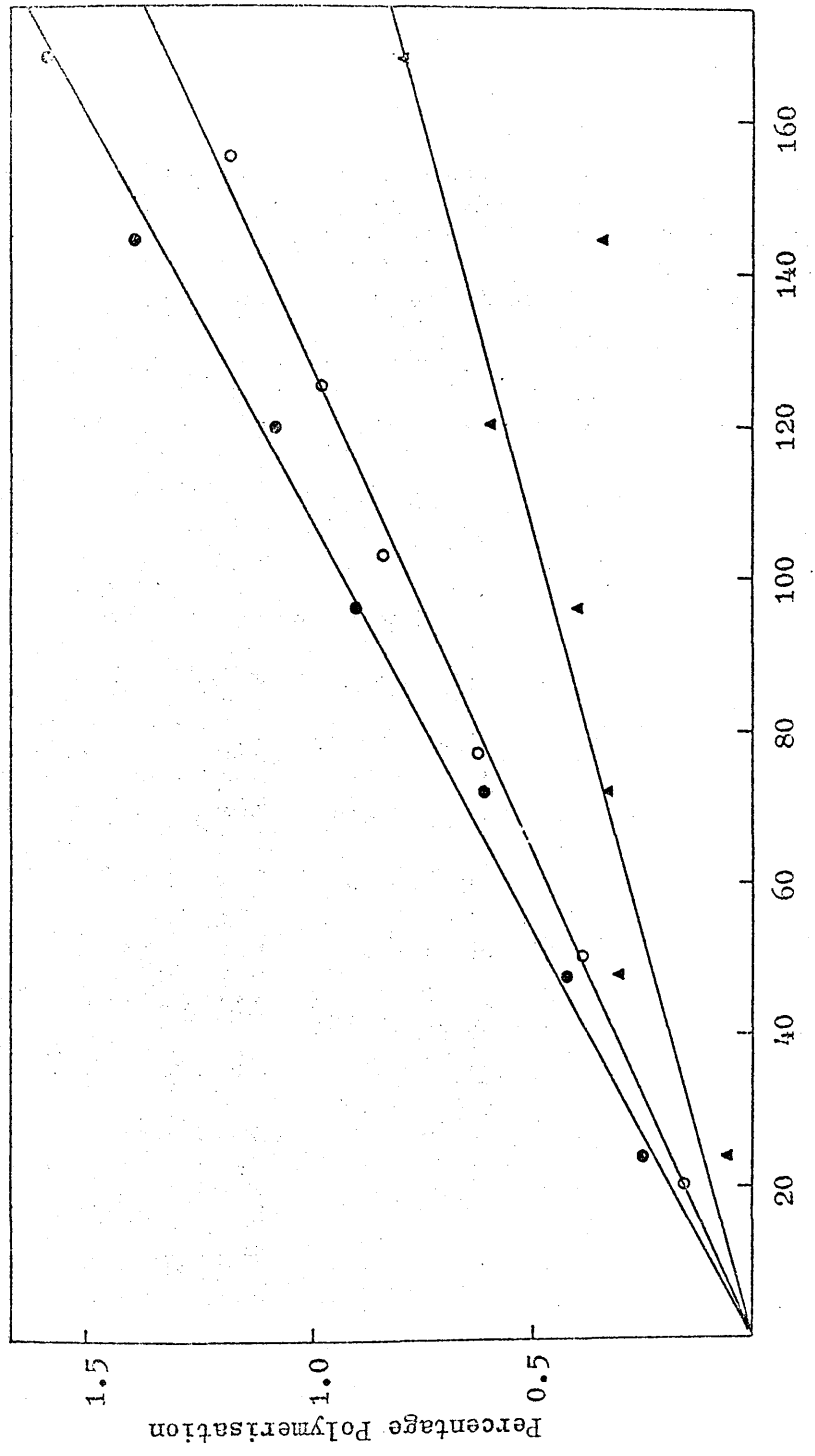

Figure 3.2 Percentage Polymerisation Against Time of Reaction

will have little effect on the DCMB-thiophen reaction if reaction times are kept low and reagent concentrations not allowed to rise above those used in this study.

Analyses of the products of the polymerisation of thiophen under nitrogen were undertaken to establish the nature of the involatile materials. Molecular weight measurements of the deep brown viscous oils, produced during polymerisation, gave a value of 343 $\pm$ 28. The U-V spectra of these oils all showed a single peak at 237 mμ. This is similar to results obtained by Curtis and co-workers from U-V analysis of the thiophen "pentamer" and is taken as evidence for the presence of unconjugated thiophen nuclei. These observations were confirmed by bands at 850, 825 and 695 cm^{-1} in the I.R. spectra (figure 3.3) of these compounds and absorption at 2.7τ-3.2τ in their n.m.r. spectra (figure 3.4). I.R. absorption at 1455 cm^{-1} and n.m.r. absorption at 5.5τ-9.2τ however, also confirmed the presence of aliphatic carbon atoms in the products. The ratio of aliphatic to aromatic protons, obtained from n.m.r. was found to be 2.1 : 1. This was considerably greater than would have been expected from structures such as those shown in figure 3.1. It would appear therefore that as polymerisation proceeds there is a decrease in the number of aromatic nuclei

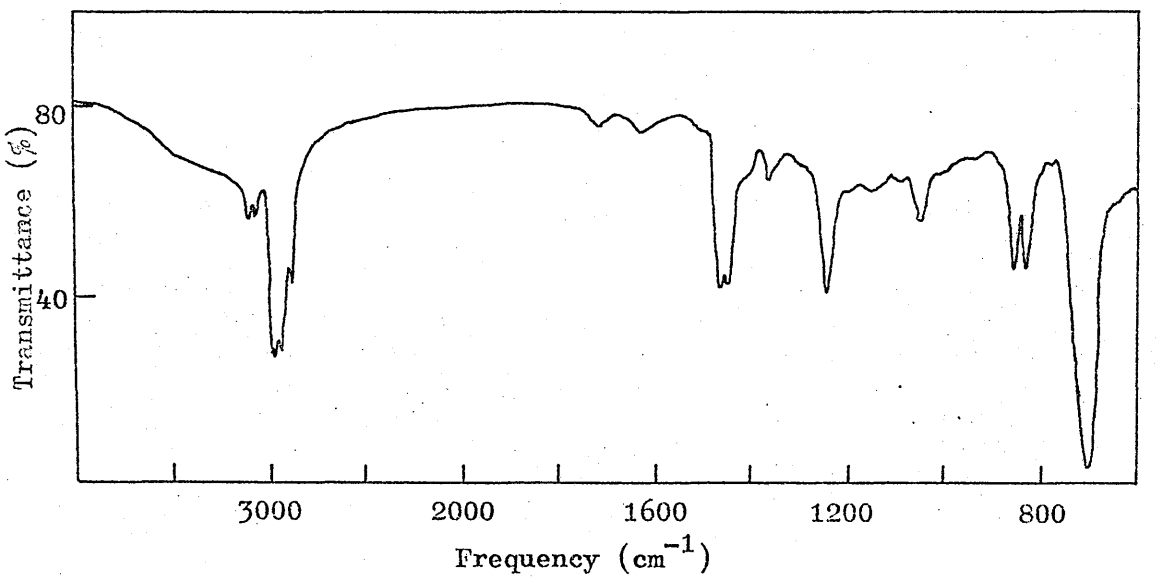

Figure 3.3 Infrared Spectrum of Involatile Product

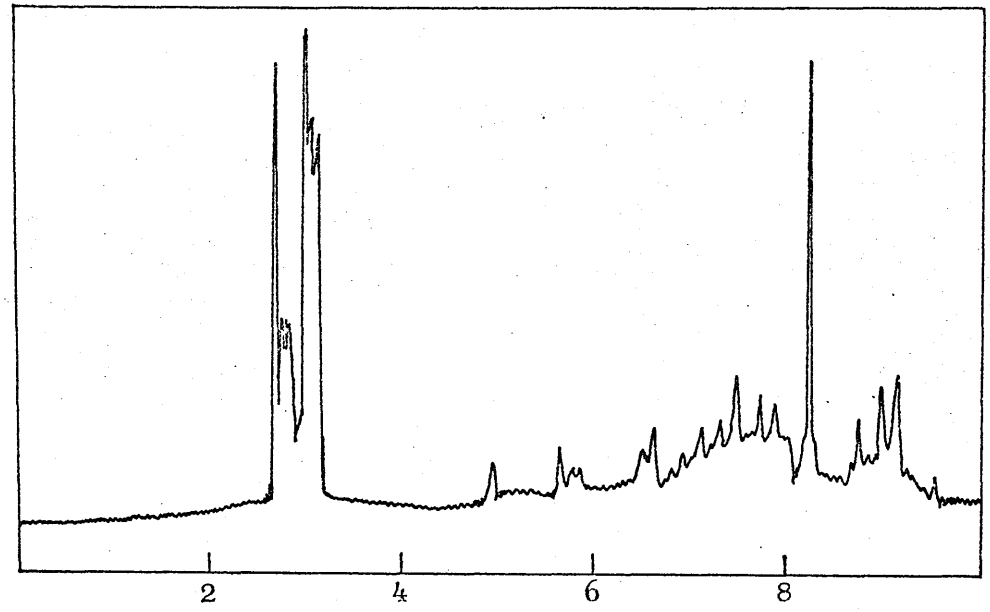

Figure 3.4 n.m.r. Spectrum of Involatile Product

accompanied by a corresponding increase in the number of aliphatic and olefinic units in the polymer. These observations are in agreement with results obtained by Armour and co-workers[44], however differences in spectral evidence indicate that as the molecular weight of the product increases the polymer becomes very complex and makes a detailed analysis very difficult.

3.3 The Self-Condensation of p-di(Chloromethyl) Benzene

It was important to determine the extent of the reaction of DCMB with itself as this represents a possible method of introducing branching at a very early stage of the polymerisation. Mixtures of DCMB, stannic chloride and DCE were allowed to react at 30°C and the amount of HCl produced estimated by titration with standard alkali. The rate of evolution of HCl from this reaction system was found to be too slow to be measured accurately as the amounts of standard alkali required to neutralise the evolved HCl fell within the experimental error. Hence it can be assumed that the self-condensation of DCMB does not make an important contribution to the structure of the polymer. These results were found to be in good agreement with those obtained by Grassie and Meldrum[29].

3.4 The Influence of Water on the Reaction

It has been shown[34] that water acts as a co-catalyst

in many polymerisation reactions catalysed by stannic chloride. Although rigorous drying of reagents before polymerisation has frequently been shown to reduce the rate of polymerisation to zero, Grassie and Meldrum[29] found that, while water acts as a co-catalyst in the reaction between DCMB and benzene catalysed by stannic chloride, the reaction does proceed at a reasonable rate in the complete absence of water. Their results demonstrated that a maximum reaction rate is observed when the $SnCl_4/H_2O$ ratio is unity. At higher water concentrations, stannic chloride is precipitated from solution in the form of a hydrate with an accompanying decrease in reaction rate due to the decrease in the $SnCl_4$-H_2O complex concentration. The decrease in rate at lower concentrations of water can be accounted for by the reduction in concentration of the $SnCl_4$-H_2O complex in favour of the less active $SnCl_4$ catalyst.

Clearly the presence of water greatly affects the rate of Friedel-Crafts reactions of this type and in order to obtain reproducible results the concentration of water in the reaction mixture must be accurately controlled. The most convenient way of doing this, and so to achieve easy reproducibility, is to exclude water completely by the rigorous drying procedures described

in chapter 2 and to carry out all rate determinations under vacuum. These procedures minimize contamination and good reproducibility was thus obtained throughout this study.

3.5 The Reaction between DCMB and Thiophen

Before embarking on a quantitative study of the reaction between DCMB and thiophen, it was necessary to carry out some preliminary observations in order to determine the best experimental conditions for polymerisation and to devise a convenient method for studying the reaction. Initially all experiments were carried out at 30°C, under high vacuum, using the techniques described in chapter 2. During the course of these experiments the following observations were made.

Initially all reaction solutions were clear and colourless. After a short time, however, a yellow colour appears, which gradually deepens, through orange, to a deep red. As the solutions darken, they also become opaque and precipitation of a solid begins. Addition of water to the reaction mixture results in the rapid discharge of the deep red colouration giving a pale green solution. After washing with organic solvents and drying a deep yellow polymer is obtained. I.R. analysis (figure 3.5) of this polymer indicated that the structure is very

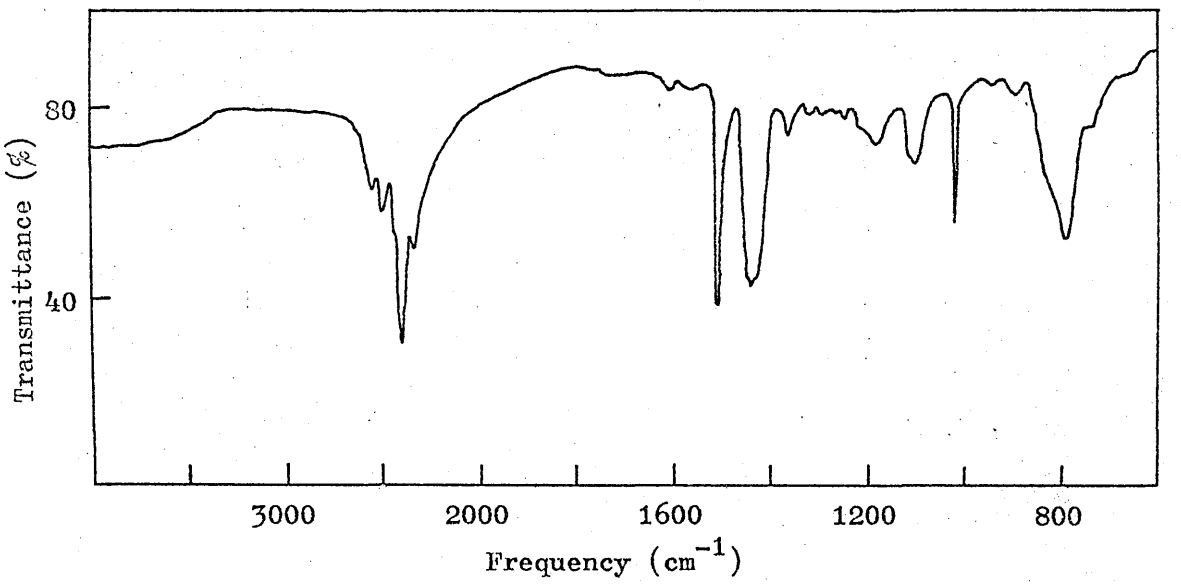

Figure 3.5 Infrared Spectrum of DCMB-Thiophen Polymer

similar to the DCMB-thiophen polymer prepared by Grassie and Meldrum[32]. The mechanical properties of the polymer are rather poor, however; it is infusible and insoluble in all common solvents. Thermal volatilisation analysis, figure 3.6 while showing certain differences from the analysis carried out by Grassie and Meldrum, indicated that the polymer is stable below 300°C.

The onset of colouration, during polymerisation probably indicates the formation of complexes involving stannic chloride and aromatic nuclei. It has already been shown in section 3.1 that such complexes can be formed between stannic chloride and thiophen. The formation of these complexes was also accompanied by gradual colouration of the reaction mixture. As addition of water causes hydrolysis of the stannic chloride it would also be expected to cause the colouration to be discharged, as was found to happen in both the self-polymerisation of thiophen and the reaction between DCMB and thiophen.

At no point during the reaction was complete gelation observed. The loss of transparency during the reaction could have been due to the formation of microgel. Thus instead of a continuous gel being formed throughout the solution discrete particles of gel are formed and are

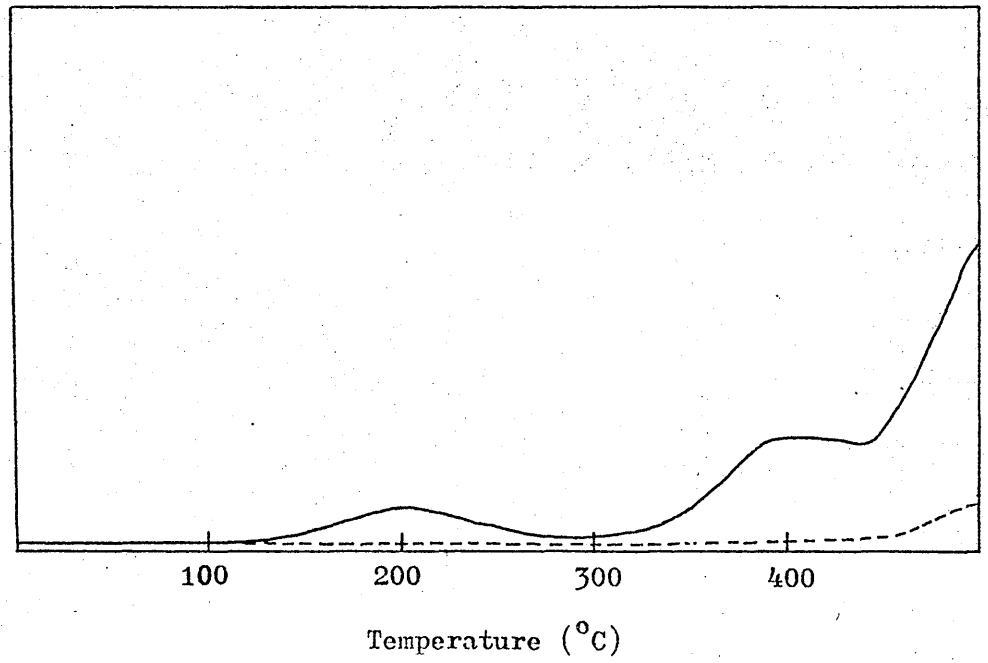

Figure 3.6 T.V.A. Thermogram of DCMB-Thiophen Polymer

suspended in the solution. This in turn would account for the poor mechanical properties of the precipitated polymer.

It is possible that the formation of complexes between stannic chloride and the aromatic nuclei could lead to depletion of the amount of active catalyst in the reaction mixture. It would be better therefore to carry out rate determinations during the initial stages of the reaction, before the onset of the deep red colouration. In this way all such determinations would also be carried out before the formation of microgel with the resulting loss of homogeneanity of the reaction mixture.

Separation of the reactants and the first two products of reaction was achieved by G.L.C. Later products of reaction were not volatile enough to be eluted from the column, however. Separation of these later products was finally achieved using the G.P.C. apparatus described in chapter 2. Preliminary experiments were carried out to estimate the rate of HCl production and to study changes in the concentrations of the reagents and the first two products of reaction using G.L.C. The rate of reaction at 30°C, however, was found to be so fast that there were large proportional errors in the estimated reaction times. In order to reduce the rate of reaction, and hence these

errors, the experiments were repeated at 0°C. At this temperature the reaction could be conveniently controlled and the reaction curves shown in figure 3.7 were obtained. These curves were obtained before the identification of the reaction products had been established and so no calibration of the G.L.C. detector had been carried out. The reaction curves did, however, suggest that two consecutive first order processes were involved.

3.6 Summary

The experiments reported in this chapter have shown that DCMB and thiophen react, in the presence of stannic chloride, to form polymeric materials. Neither thiophen nor DCMB have been found to react with themselves to any significant extent under the conditions used in this study. The ultimate product of the reaction was found to be an insoluble and infusible powder, which showed promise of good thermal stability. These properties, however, made a complete analysis of the polymer extremely difficult.

These experiments have confirmed, that in order to gain a greater insight into the structure of the ultimate polymer, a detailed investigation of the polymerisation should be carried out. Preliminary experiments have indicated that such an investigation could be carried out using both G.L.C. and G.P.C. as analytical tools. These

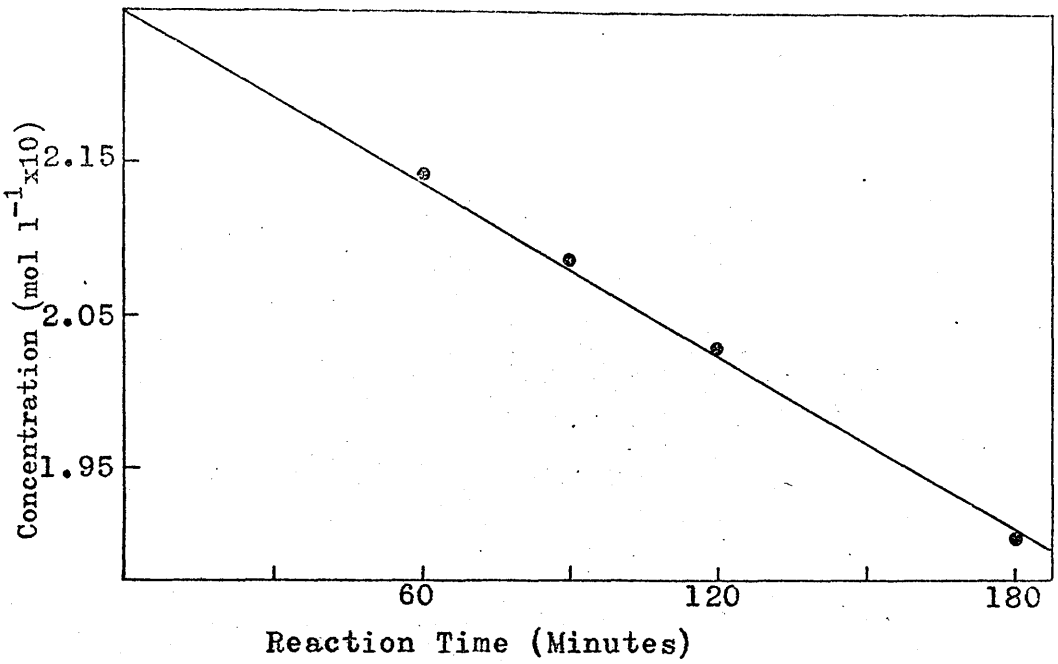

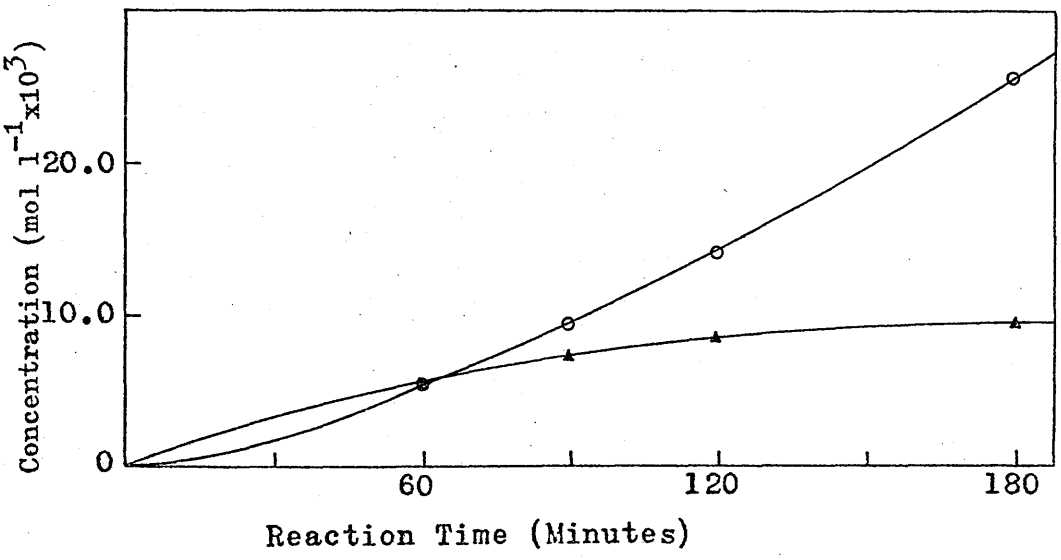

Figure 3.7 Reaction Curves for Products Separated by G.L.C.

techniques should allow both the separation of reaction products and the determination of reaction curves for these products.

The results of these investigations into the reaction between DCMB and thiophen are described in chapters 4 and 5.

CHAPTER 4

IDENTIFICATION OF PRODUCTS

4.1 Introduction

The work described in chapter 3 of this thesis indicated that before a satisfactory account can be given for the good thermal stability of the DCMB--thiophen polymer it will be necessary to determine the mechanism and kinetics of the polymerisation process. As a first step in this investigation attempts were made to separate and identify all the soluble products of reaction before carrying out a kinetic analysis of their formation. The identification of these products of reaction is described below.

4.2 Experimental

Using G.L.C. as described in chapter 2, reaction mixtures were readily resolved into three main components as illustrated in figure 4.1. Mass spectra of these components were obtained using the L.K.B.900 G.C.M.S. apparatus and small amounts of the pure materials were separated using preparative G.L.C. All other products of reaction proved to be too involatile to be eluted from the G.L.C. column, however the development of the G.P.C. apparatus allowed the separation of these products up to species with molecular weights near the limit determined

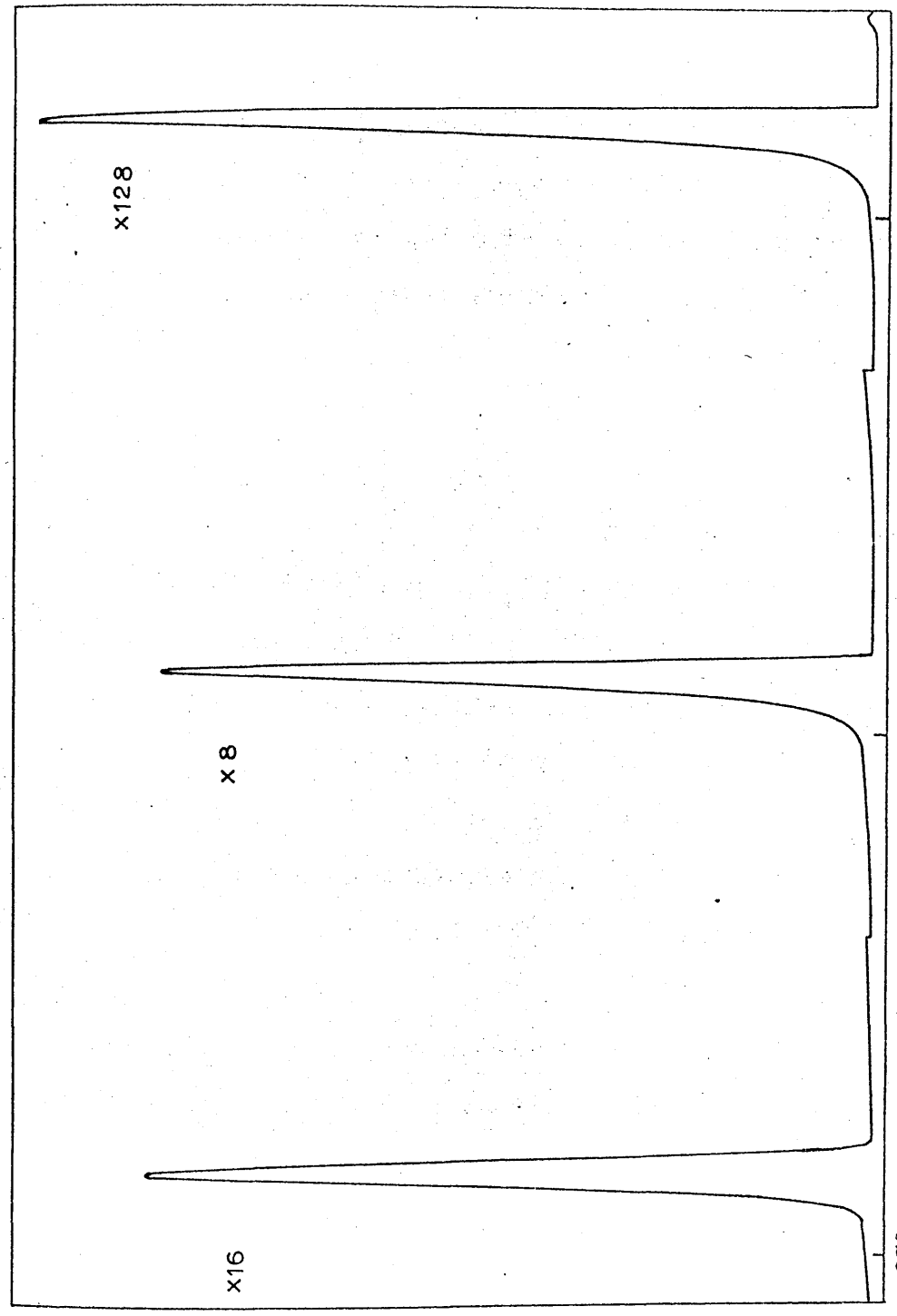

Figure 4.1 Typical Gas Liquid Chromatogram.

by the pore size of the gel. G.P.C. chromatograms and the treatment of G.P.C. results are described and illustrated in chapter 5. A total of eleven different products were separated using this technique and whenever possible mass, I.R. and n.m.r. spectra were obtained using the equipment described in chapter 2. In many cases the small amounts of materials available meant that n.m.r. analyses had to be carried out using micro-cells. This led to loss of resolution in the resultant spectra and the increased detection of impurities present in the samples. These impurities give rise to the background between 6.40 τ and 6.80 τ and the peaks around 8.80τ.

4.3 Identification of Products

The high volatility of both thiophen and DCE prevented their separation using either G.L.C. or G.P.C. In this discussion products will be denoted by their peak number in the G.P.C. (P_1, P_2 etc.) while possible products which have not been identified will be denoted by the letters of the alphabet. Comparison of the spectra obtained confirmed that the products separated by G.L.C. were identical with P_1, P_2 and P_3 separated by G.P.C. For convenience the symbols $\mathbb{T}$ and $\emptyset$ will be used throughout this text to represent thiophen

and benzene nuclei respectively.

(a) Peak Number 1 (P_1)

The mass, I.R. and n.m.r. spectra for P_1 are illustrated in figures 4.2 and 4.3. These spectra are identical to spectra obtained for pure DCMB. It can therefore be assumed that P_1 is due to unreacted DCMB. Peaks at 139, 125 and 104 in the mass spectrum are due to loss of Cl- and Cl-CH_2- while the presence of chloromethyl groups is confirmed by absorption at 675 cm^{-1} in the I.R. spectrum. The peaks at 2.65 τ and 5.49 τ in the n.m.r. spectrum are due to absorption by the aromatic and chloromethyl protons respectively.

(b) Peak Number 2 (P_2)

The mass, I.R. and n.m.r. spectra for P_2 are illustrated in figures 4.4 and 4.5. The parent ion mass number in the mass spectrum occurs at 222 which would be expected from substitution of one chloromethyl group in DCMB by thiophen to form thenyl chloromethyl benzene (TCMB). Peaks at 187, 173 and 97 suggest the loss of Cl-, Cl-CH_2- and Cl-CH_2-ϕ- from the material with the peak at 97 being due to the $(\text{T}-CH_2-)^+$ ion. This would be consistent with the structure shown for P_2.

$$\text{T}-CH_2-\phi-CH_2-Cl$$

P_2 (TCMB)

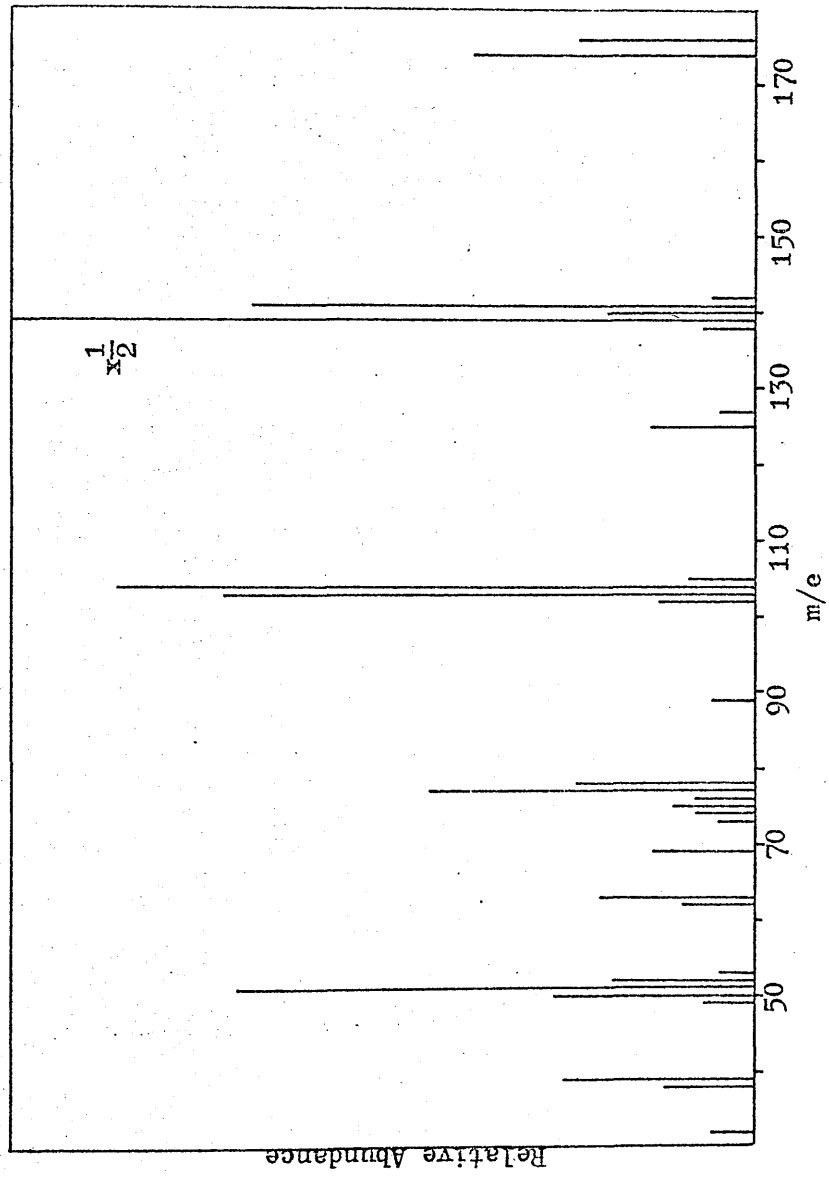

Figure 4.2 Mass Spectrum of P_1

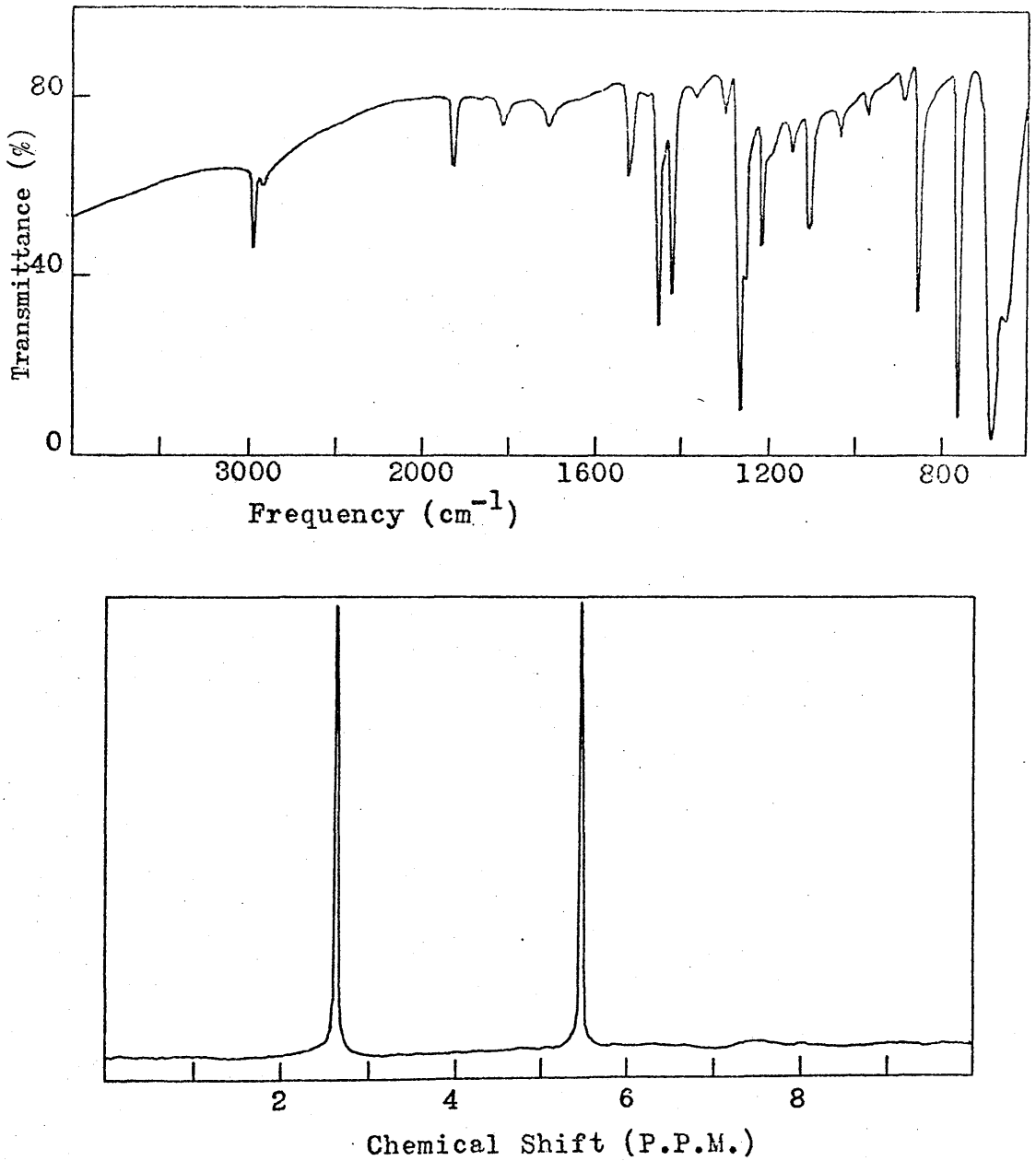

Figure 4.3 I.R. and n.m.r. Spectra of P_1.

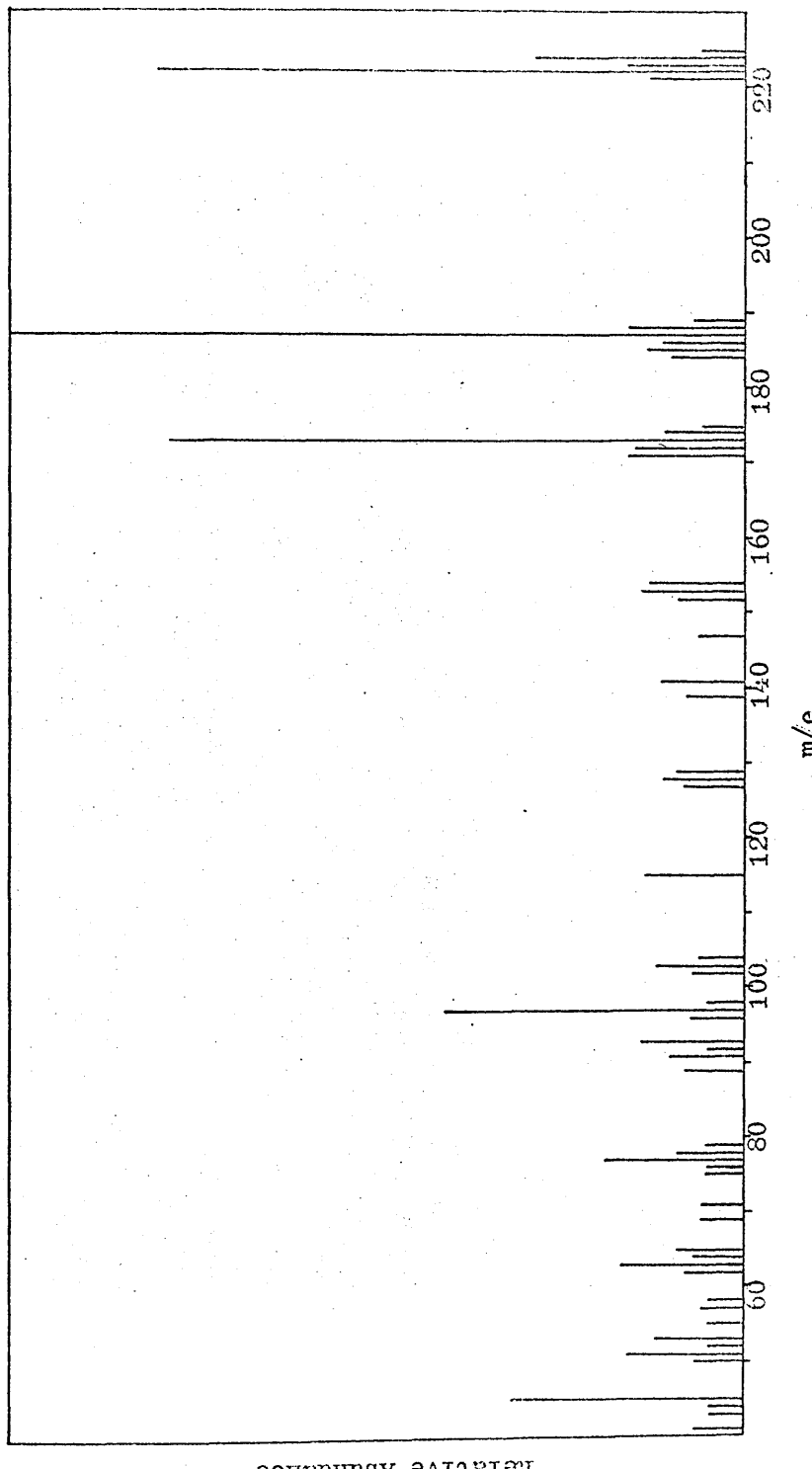

Figure 4.4 Mass Spectrum of P_2

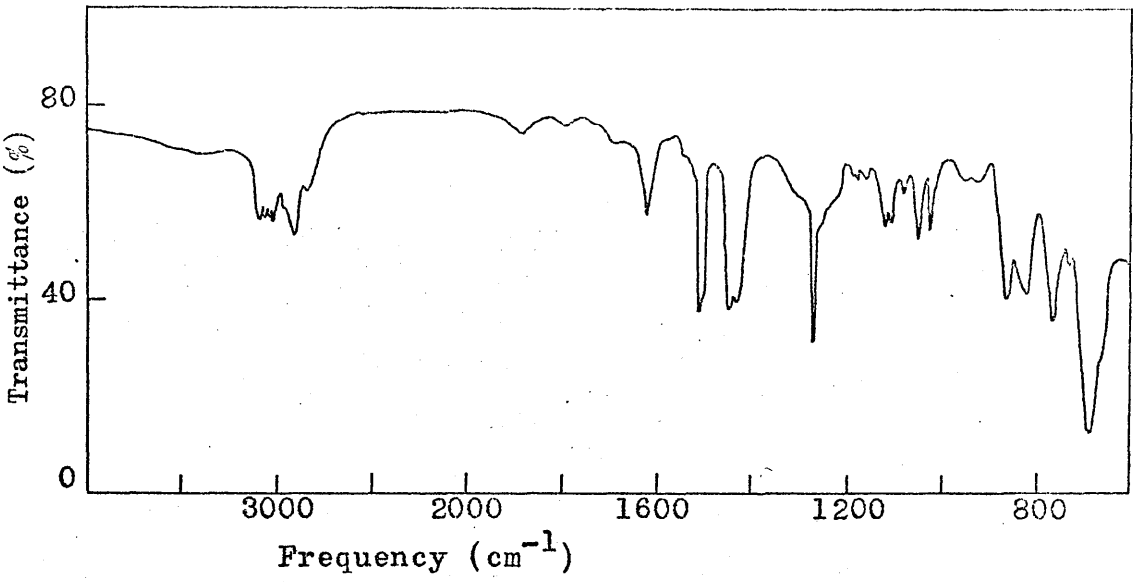

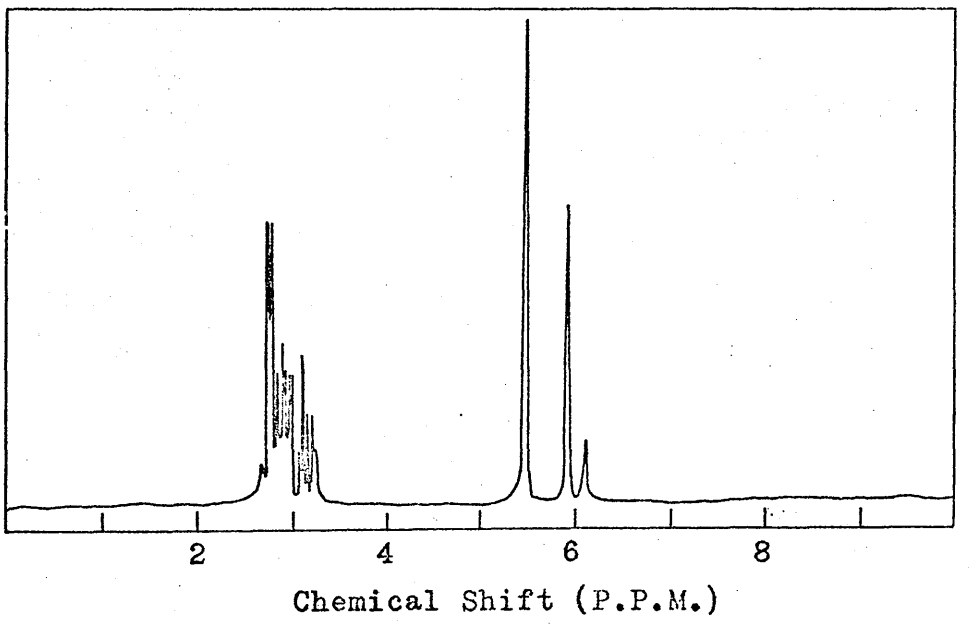

Figure 4.5 I.R. and n.m.r. Spectra of P_2.

This identification is confirmed by the I.R. and n.m.r. spectra. The complex array of peaks between 2.60 τ and 3.30 τ in the n.m.r. spectrum are due to resonance by the aromatic protons present in the molecule while resonances between 5.40 τ and 6.20 τ can be attributed to protons attached to aliphatic carbon atoms. The peak at 5.46 τ is taken to be due to absorption by the chloromethyl group, as found for DCMB, and the peaks at 5.88 τ and 6.06 τ attributed to absorption by the protons of the methylene bridge between the thiophen and benzene nuclei. This shift to higher field is caused by replacement of the strong inductive deshielding effect of the chlorine atom by the less effective anisotropic deshielding effect of the thiophen ring. The peak at 5.88 τ is attributed to the methylene groups substituted in the 2-position of thiophen and the peak at 6.06 τ is assigned to substitution in the 3-position. These assignments were confirmed by comparison of the n.m.r. spectra of 2-Me and 3-Me thiophen (figure 4.6) which indicated that the deshielding effect of the thiophen nucleus was greater on substituents in the 2-position thus making them resonate at lower field. The relative concentrations of 2- and 3- substituted thiophen nuclei were calculated from the relative intensities of the two absorptions and found to be in

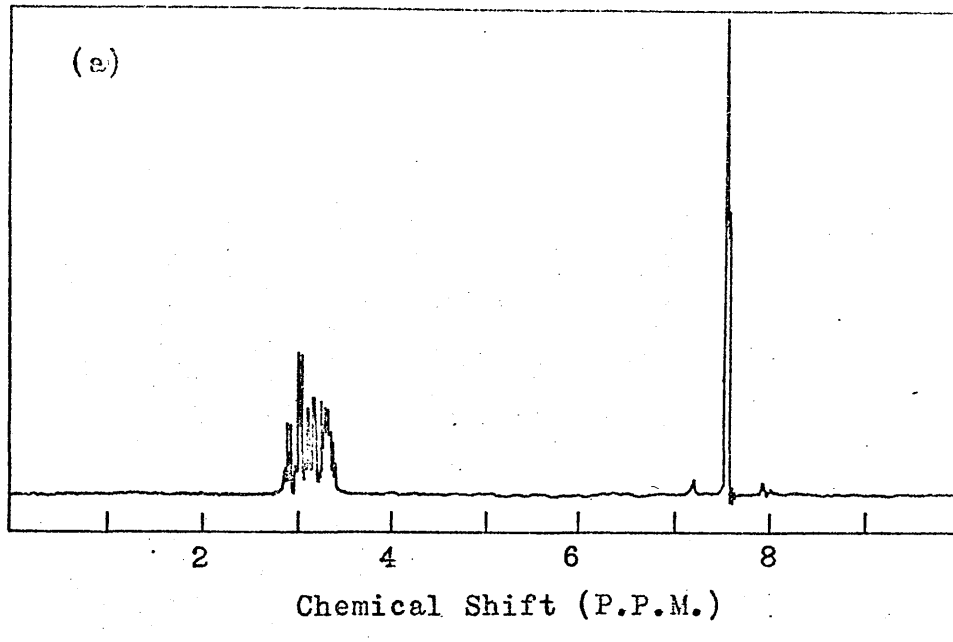

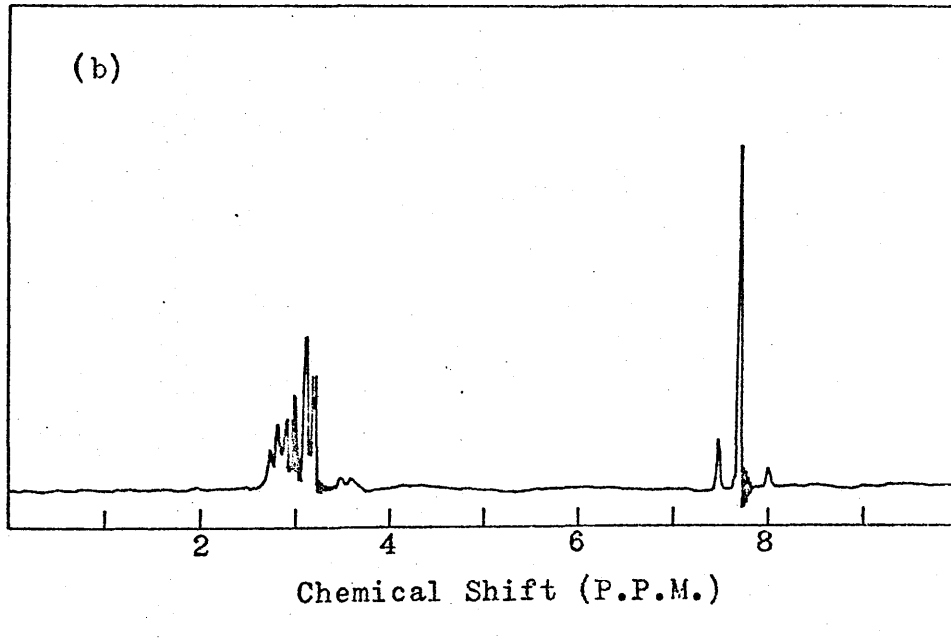

Figure 4.6 n.m.r. Spectra of (a) 2-Methyl Thiophen.
(b) 3-Methyl Thiophen.

the ratio of 3 : 1.

The presence of both 2- and 3- substituted thiophen nuclei in P_2 is confirmed by absorptions at 695 cm^{-1} and 760 cm^{-1} in the I.R. spectrum which are due to the 2- and 3- substitution respectively. The relative intensities of these peaks while not giving any quantitative information do indicate that the relative concentrations of 2- and 3- substitution were in the direction found by n.m.r. Although there is no clear absorption at 675 cm^{-1}, which would have been expected from the chloromethyl group, there is a small shoulder at 678 cm^{-1} on the broad peak at 695 cm^{-1}.

(c) Peak Number 3 (P_3)

The mass spectrum of P_3, illustrated in figure 4.7, has a parent ion mass number of 270, while the cracking pattern indicates the loss of $\text{T-CH}_2\text{-}$ and $\text{T-CH}_2\text{-}\phi\text{-}$ units to give peaks at 173 and 97 respectively. This is consistent with the identification of P_3 as dithenyl benzene which has the structure shown.

$$\text{T-CH}_2\text{-}\phi\text{-CH}_2\text{-T}$$

P_3 (DTB)

The I.R. spectrum (figure 4.8) is very similar to that of P_2 and indicates the presence of both 2- and 3-

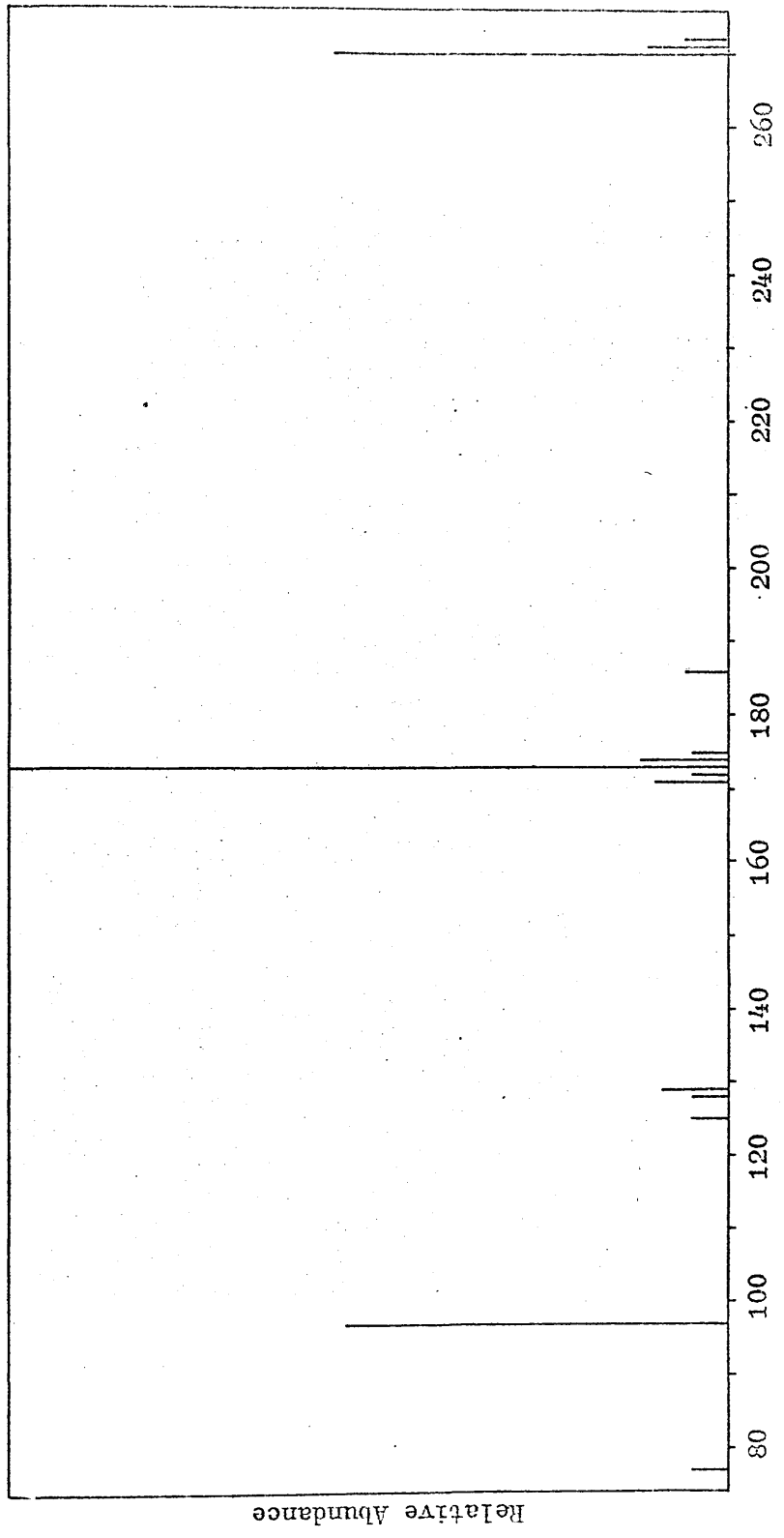

Figure 4.7 Mass Spectrum of P_3

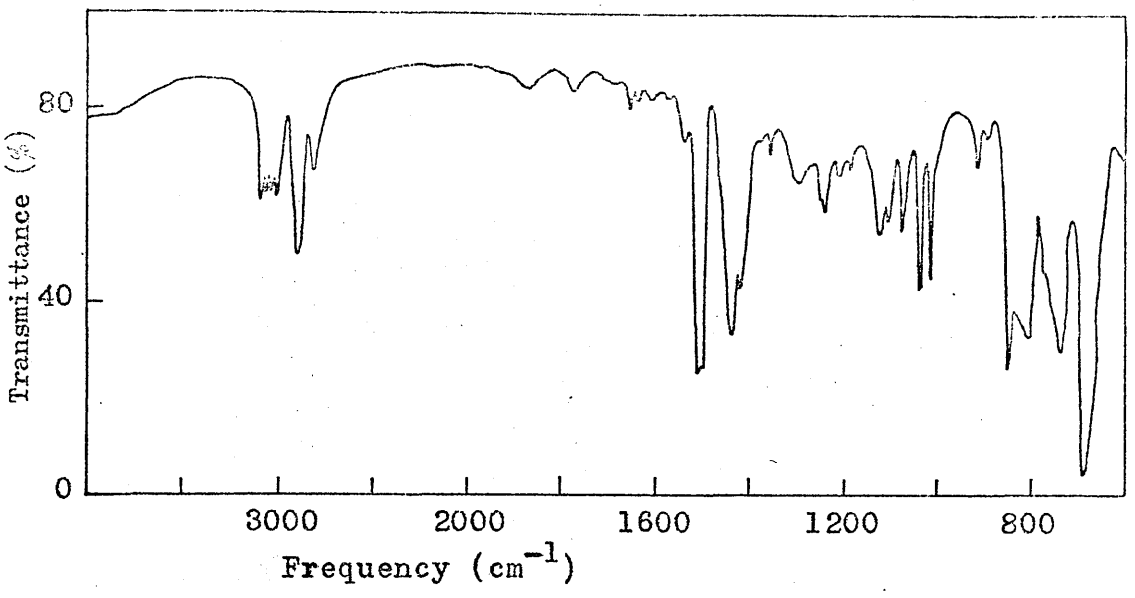

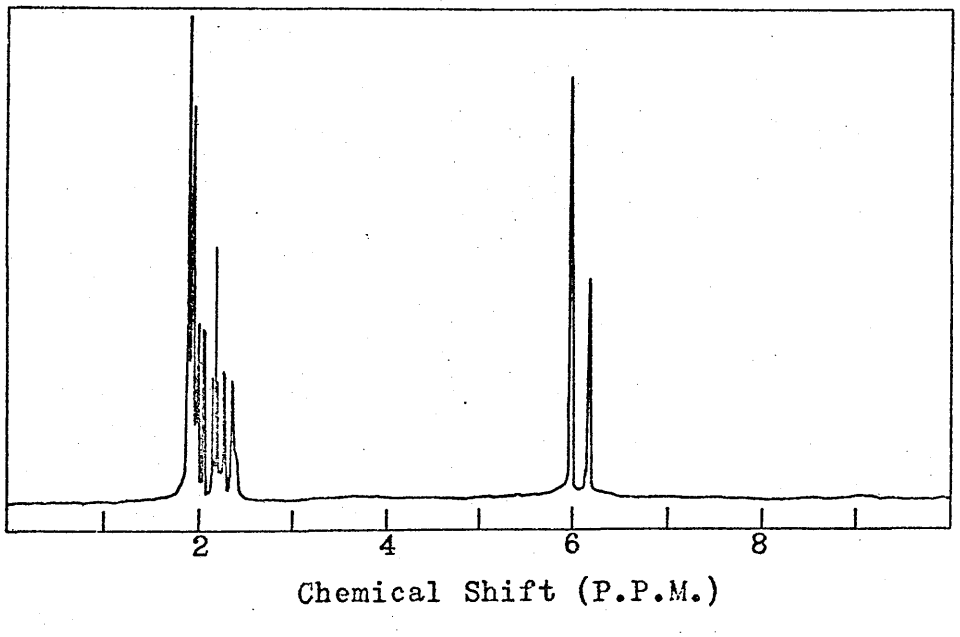

Figure 4.8 I.R. and n.m.r. Spectra of P_3.

substituted thiophen nuclei as would be expected. The peak at 695 cm^{-1}, however, is not as broad as the corresponding peak in the spectrum of P_2 and shows no shoulder at 675 cm^{-1}.

The absence of chloromethyl groups in P_3 is confirmed by the absence of resonances at 5.46 τ in the n.m.r. spectrum (figure 4.8). Absorptions in the region 2.60 τ to 3.40 τ are again taken to be due to the aromatic protons of the benzene and thiophen rings. The superimposition of the benzene and thiophen proton resonances again prevent any detailed analysis of these absorptions. However it would appear that the large absorption at 2.94 τ can be attributed to the hydrogens on the benzene nucleus. The absorptions due to the hydrogens of the methylene bridges occur at 5.94 τ and 6.11 τ for the 2- and 3- substitutions respectively. The movement of both the aromatic and methylenic absorptions to higher field can be accounted for by the complete removal of the strong inductive deshielding effect of the chlorine atoms. The relative concentrations of the 2- and 3- substituted thiophen nuclei were found to be in the ratio of 2 : 1.

(d) Peak Number 4 (P_4)

P_4 is eluted from the column immediately after P_3 and as the elution ratio should be expected to decrease

with increasing molecular weight it is reasonable to consider structures of progressively increasing complexity as possible structures for P_4 and all succeeding products. As P_4 occurs as an imperfectly resolved, small shoulder on P_3 it would seem reasonable to consider molecules with similar molar volumes to DTB as possible products.

The product A formed by the self-condensation of DCMB,

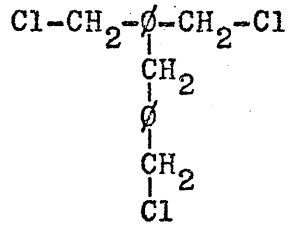

A

would probably be expected to elute from the G.P.C. column near DTB. The mass spectrum of P_4 (figure 4.9) however, gives a molecular weight of 372 for this product which is considerably higher than that of A (313). This also rules out the possibility that P_4 might have been the product B of the reaction between TCMB (P_2) and DCMB (P_1).

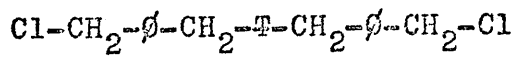

B

This compound has a molecular weight of 355 which again is lower than that given by the mass spectrum of P_4. Furthermore there are no peaks in the mass spectrum of P_4

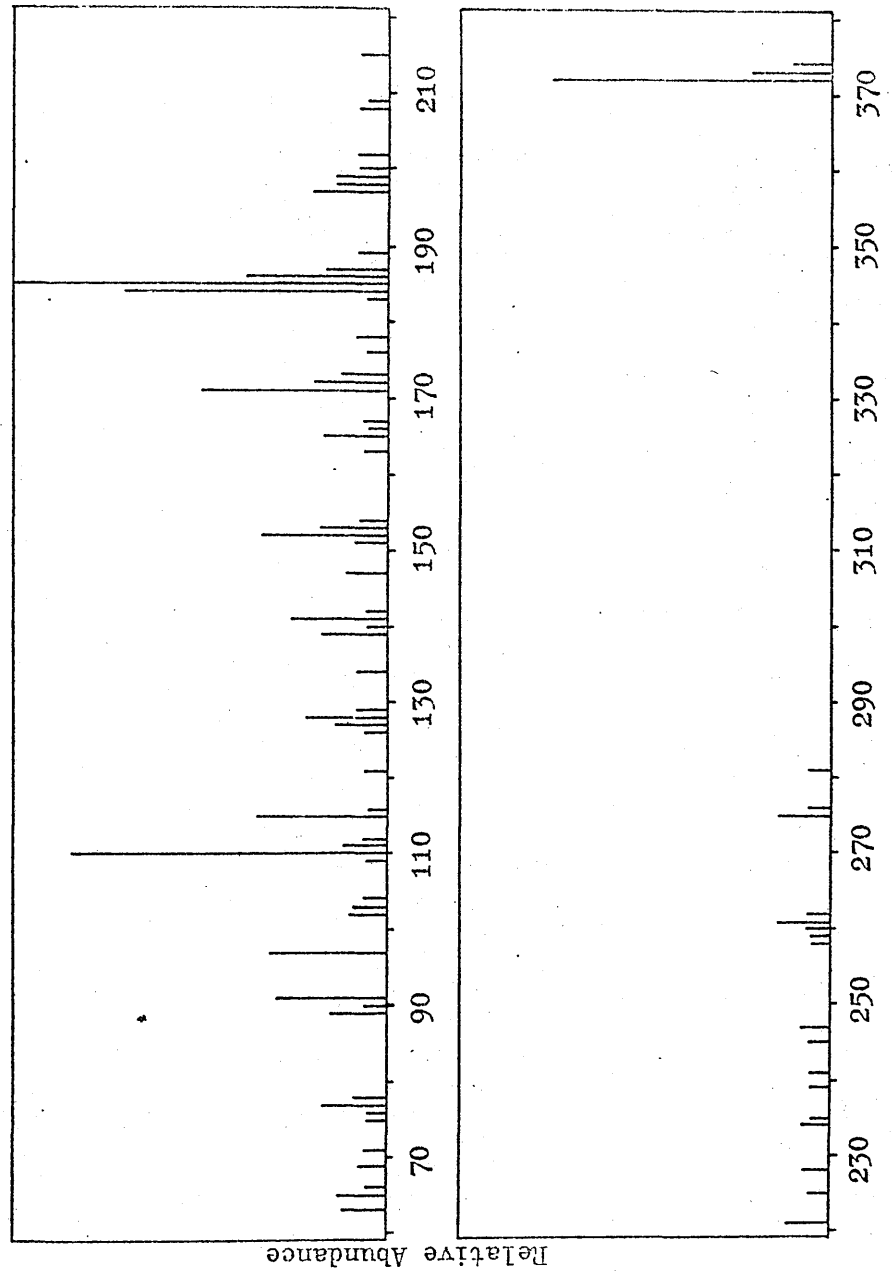

Figure 4.9 Mass Spectrum of P_4

at either 313 or 315 which might indicate that either A or B are present as impurities. In order to account for P_4 it is therefore necessary to consider molecules with four aromatic nuclei.

C and D represent possible isomeric materials which could give rise to P_4.

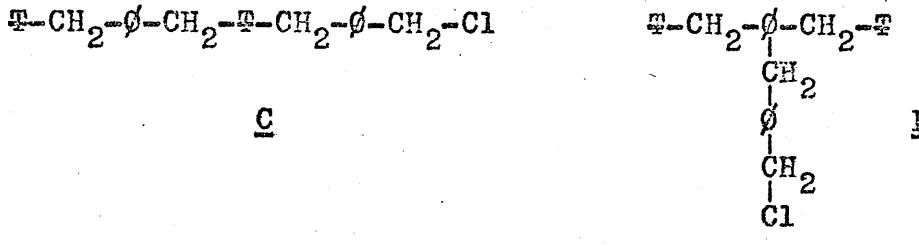

C

D

Although both of these materials have a molecular weight of 408, loss of Cl- would give rise to a peak at 373 in their mass spectra, and the complete absence of a parent ion, although unusual, could occur. These compounds would also be expected to give rise to absorption at 675 cm^{-1} in their I.R. spectra and 5.48τ in their n.m.r. spectra. Although there is no absorption at 675 cm^{-1} in the I.R. spectrum of P_4 there is a peak at 5.48τ in its n.m.r. spectrum (figure 4.10) which could be attributed to resonance by chloromethyl group protons. Comparison of the intensity of this peak with other peaks in the spectrum, however, clearly shows that this absorption is so small that it can only be accounted for as a minor

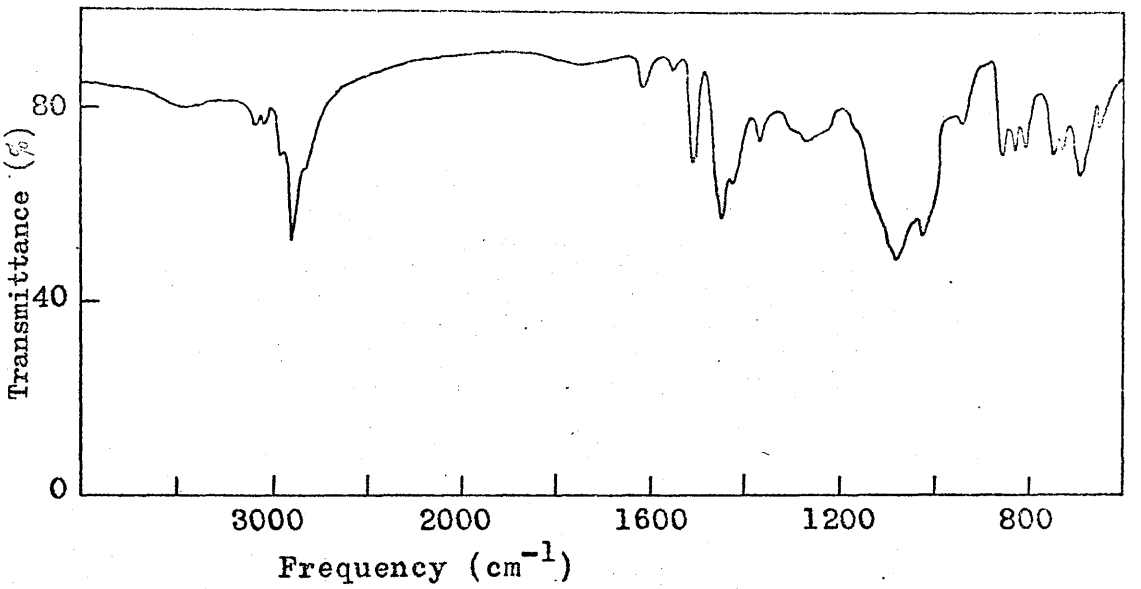

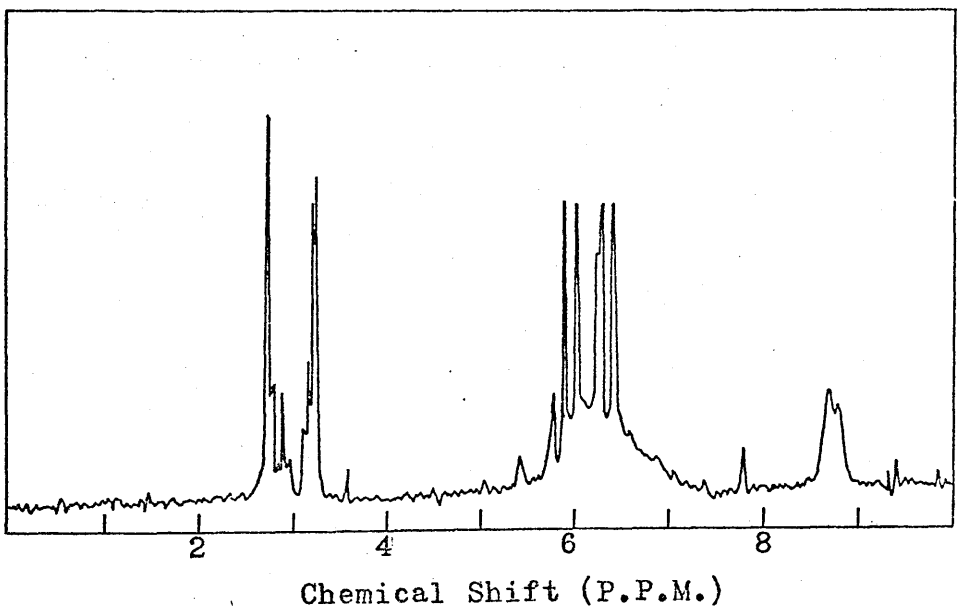

Figure 4.10 I.R. and n.m.r. Spectra of P_4.

impurity. Evidence will also be presented, in the following section, which proves that compounds C and D do give rise to a parent peak in their mass spectra which is of considerably greater intensity than any peaks in the region of 373. Furthermore the large increase in molar volume in going from P_3 to either C or D would be expected to cause a much greater decrease in elution ratio than that found for P_4.

The molecular weight of 372 found for P_4 suggests that this product could have been formed by elimination of HCl from either C or D. One possible product could be produced by an intramolecular Friedel-Crafts reaction giving rise to E.

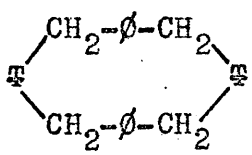

E

Studies with molecular models have revealed that this product could be formed with the thiophen rings being disubstituted in any two positions. It would not be possible to form a similar type of molecule from D.

This compound has a molecular weight of 372 which is in agreement with the mass spectral data. Peaks at 185, 171 and 110 in the mass spectrum suggest the presence

of $(\text{-}CH_2\text{-}\phi\text{-}CH_2\text{-}\phi\text{-})^+$; $(\text{-}\phi\text{-}CH_2\text{-}\phi\text{-})^+$ and $(\text{-}CH_2\text{-}\phi\text{-}CH_2\text{-})^+$ ions among the scission products. Minor differences between the masses of the ionic species and the m/e values can be accounted for by hydrogen transfer which is known to occur in aromatic systems.

Before accounting for the major features of the n.m.r. and I.R. spectra of P_4 it is necessary to consider the conformational features of E. Products of this type can exist in either of the two extreme conformational forms shown below.

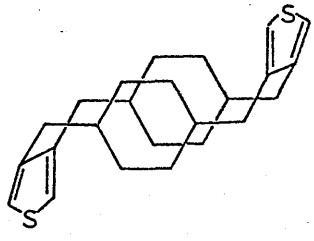

Chair Form

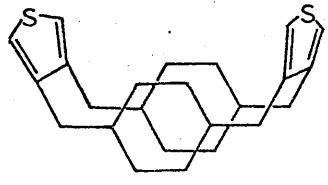

Boat Form

The equatorial and axial hydrogens of the methylene bridges would be inequivalent in both these forms. These structural features could have a considerable effect on

the spectroscopic properties of such molecules making interpretation of their spectra difficult.

Consideration of the two conformations of E suggests that the free rotation of the benzene nuclei in these compounds will be severely restricted. The effect of this is that the planes of the benzene nuclei are possibly held parallel and at right angles to the planes of the thiophen nuclei. The overall effect of this would be that in the n.m.r. spectrum of E the deshielding effect which would normally be present in a linear or branched molecule of this type, due to the induced magnetic field at right angles to the plane of the aromatic rings, would be reduced as the fields induced in the benzene and thiophen rings would tend to cancel out. Moreover the resultant induced field would be different for the chair and boat forms as the planes of the thiophen rings are held at different angles in these conformations. Thus the n.m.r. spectrum of E would be expected to be reasonably complex. A further complicating feature would also be the possibility of thiophen being substituted in different positions.

The n.m.r. spectrum obtained for P_4 does not, however, appear to be extremely complex. Although the aromatic resonances occur in the same region as found for P_3

i.e. 2.60 τ to 3.40 τ, the relative intensity of the absorptions at higher field is considerably greater than that found for other products. This is as would have been expected from the discussion above. There are however absorptions due to methylenic protons at 5.94 τ and 6.07 τ which are similar to those obtained for P_3. Absorptions at 6.28 τ and 6.39 τ are however at considerably higher field than would have been expected for a linear or branched molecule. A possible explanation for this is that four of the protons are held near to the plane of the resultant field thus experiencing a shielding effect while the other four are held at approximately right angles to the field and so experience a deshielding effect. The presence of four peaks could be accounted for by the different resultant fields produced by the two different conformations of the molecule. This however is a very simple picture of the n.m.r. spectrum and is not considered to be a complete explanation. There is evidence of other absorptions in this region of the spectrum and account must be taken of the possibility of different positions of substitution in the thiophen ring.

The I.R. spectrum of P_4 is extremely complex and gives no clear indication of the structure of this compound.

From the evidence presented above it is suggested that P_4 has the structure E. It cannot be claimed, however, that this evidence unequivocably assigns this structure to P_4 and it is clear that a more sophisticated spectral investigation would be required before a definite assignment can be made.

(e) Peak Number 5 (P_5)

P_5, like P_4, is a relatively minor product of the reaction and there is evidence to suggest that two imperfectly resolved peaks make up this product. It was not possible to separate the two components, however, and the spectral data presented was obtained from mixtures of the two peaks.

The I.R. spectrum of P_5 (figure 4.12) indicates that substitution in the aromatic rings is rather complex. The bands in the region 900 cm^{-1} to 625 cm^{-1} are not all perfectly resolved but it would appear that there is no absorption due to chloromethyl groups at 675 cm^{-1}. The presence of both 2- and 3- substituted thiophens is again confirmed by absorptions at 695 cm^{-1} and 760 cm^{-1}.

The n.m.r. spectrum of P_5 (figure 4.12), however gives strong evidence for the presence of chloromethyl groups with resonance at 5.50τ. Absorption in this region has already been shown to be due to this type

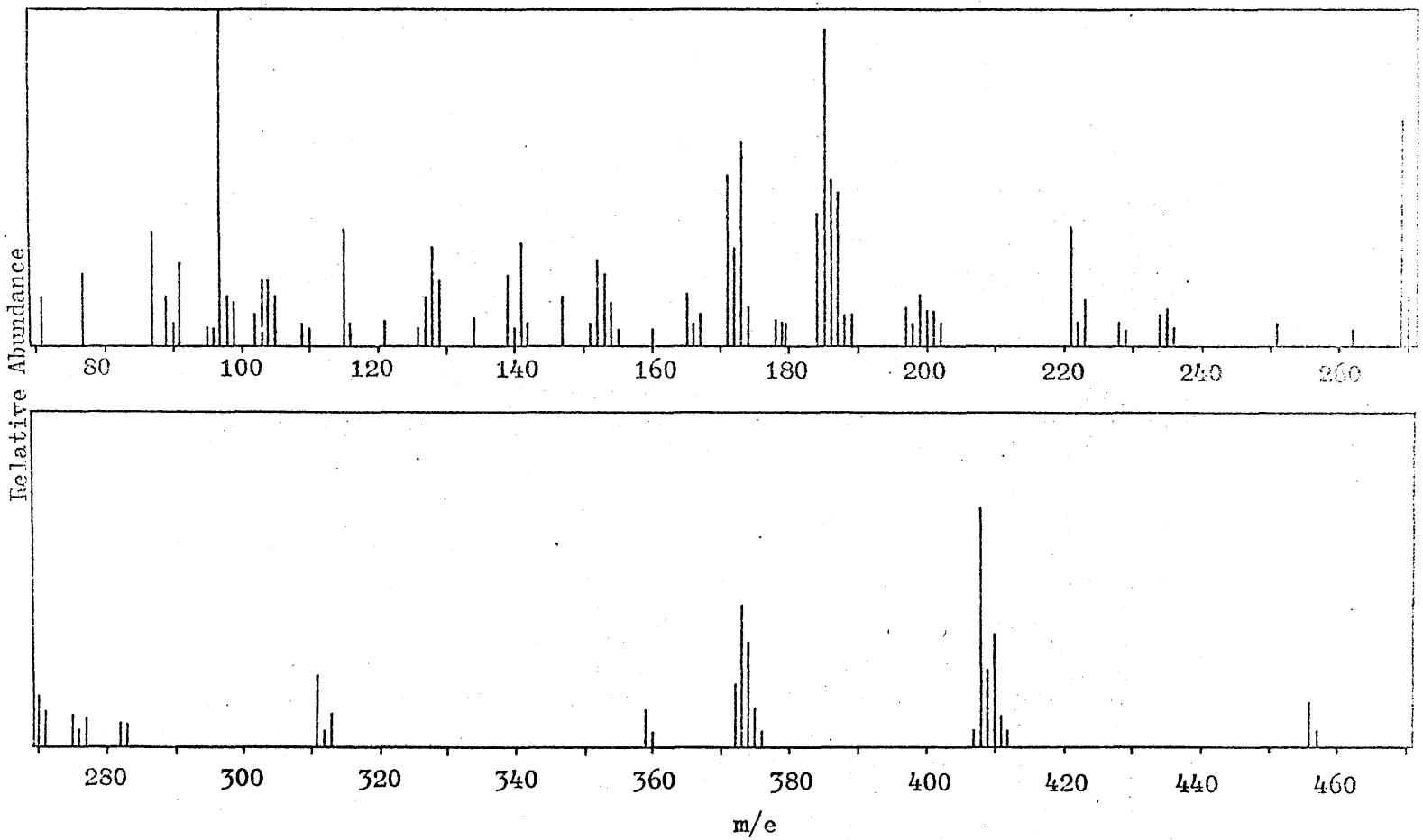

Figure 4.11 Mass Spectrum of P_5

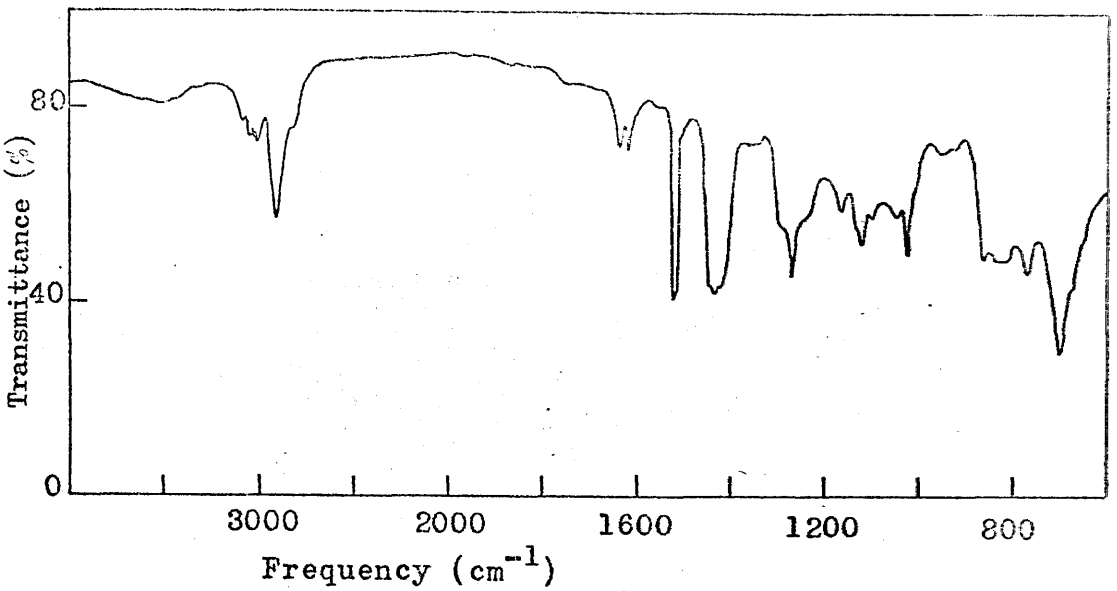

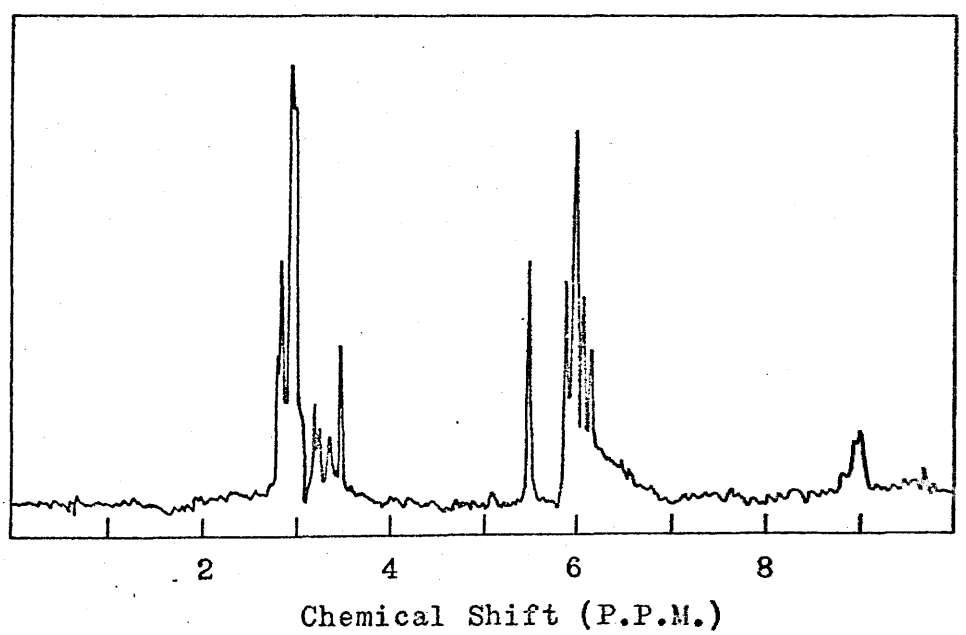

Figure 4.12 I.R. and n.m.r. Spectra of P_5.

of group. Absorptions in the region 2.70τ to 3.50τ again confirm the presence of both benzene and thiophen nuclei in the product, while absorptions in the region 5.90τ to 6.20τ can be assigned to the protons of methylene bridges between aromatic nuclei. The peak at 5.92τ is due to methylene groups substituted in the 2-position of thiophen with the peak at 6.09τ being assigned to substitution in the 3-position. The large peak at 5.99τ may be attributed to methylene groups linking two disubstituted aromatic nuclei where the thiophen ring is 2,5-disubstituted. Similarly the peak at 6.16τ could be assigned to 2,4- or 3,4-disubstitution in the thiophen ring. This latter peak, however could also be due to methylene groups linking di- to tri-substituted benzene rings.

The mass spectrum of P_5 (figure 4.11) has a large peak at 408 which is taken to be the parent ion. A small peak is observed at 456. However this is probably impurity arising from inadequate separation of P_5 from P_6. Peaks at 373, 359, 311, 269, 221, 185 and 173 suggest the loss of Cl-, Cl-CH_2-, T-CH_2-, Cl-CH_2-ϕ-CH_2-, T-CH_2-ϕ-CH_2-, Cl-CH_2-ϕ-CH_2-T-, and Cl-CH_2-ϕ-CH_2-T-CH_2- units from the molecule. This evidence would suggest the structures C and D for P_5. On the basis of molar

volume and adsorption effects the elution ratio of the linear isomer would be expected to be smaller than that of the branched isomer[45]. Thus it would appear that throughout the reaction the linear isomer predominates with the branched isomer only making a brief appearance during the earlier stages of the reaction. This would be in agreement with data presented in chapter 5 which indicates that the thiophen nuclei are much more reactive than the benzene nuclei. These conclusions would also be in agreement with the n.m.r. data presented above where only four peaks are observed for the methylene bridges between aromatic nuclei. The concentration of methylene bridges linking di- and tri-substituted benzene rings would be so small that no absorption, due to them, would be expected to be clearly resolved in the spectrum.

P_5 could be formed by reaction of P_1 with an aromatic nucleus in P_3, by reaction of thiophen with B or by reaction of pairs of P_2 molecules. The first seems to be the most likely major path in view of the complete absence of B among the reaction products and the relatively low concentration of P_2 during the reaction (see chapter 5).

(f) Peak Number 6 (P_6)

The largest peak in the high molecular weight end of the mass spectrum of P_6 (figure 4.13) occurs at mass number 456 while the cracking pattern suggests the progressive loss of Ŧ-, Ŧ-CH_2- and Ŧ-CH_2-Ø-CH_2- units from the parent. Comparison of the mass spectra of P_5 and P_6 with that of P_3 indicates that as the molecular weight of the product increases the higher mass ionic species become increasingly unstable.

The I.R. spectrum of P_6 (figure 4.14) shows the complete absence of absorption at 675 cm^{-1}, indicating that P_6 does not contain chloromethyl groups. The absence of these groups is confirmed by the absence of absorption at 5.50τ in the n.m.r. spectrum (figure 4.14).

This evidence suggests that P_6 is a five nuclei product formed by reaction of P_5 with thiophen or by reaction of P_2 with an aromatic nucleus in P_3. It would appear therefore that P_6 is a mixture of F and G which both have a molecular weight of 456.

Ŧ-CH_2-Ø-CH_2-Ŧ-CH_2-Ø-CH_2-Ŧ

F (P$_6$)

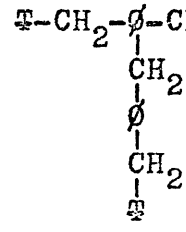

G (P$_6$)

The n.m.r. spectrum of P_6 shows a complex array of peaks in the region 5.90τ to 6.20τ. Absorptions at

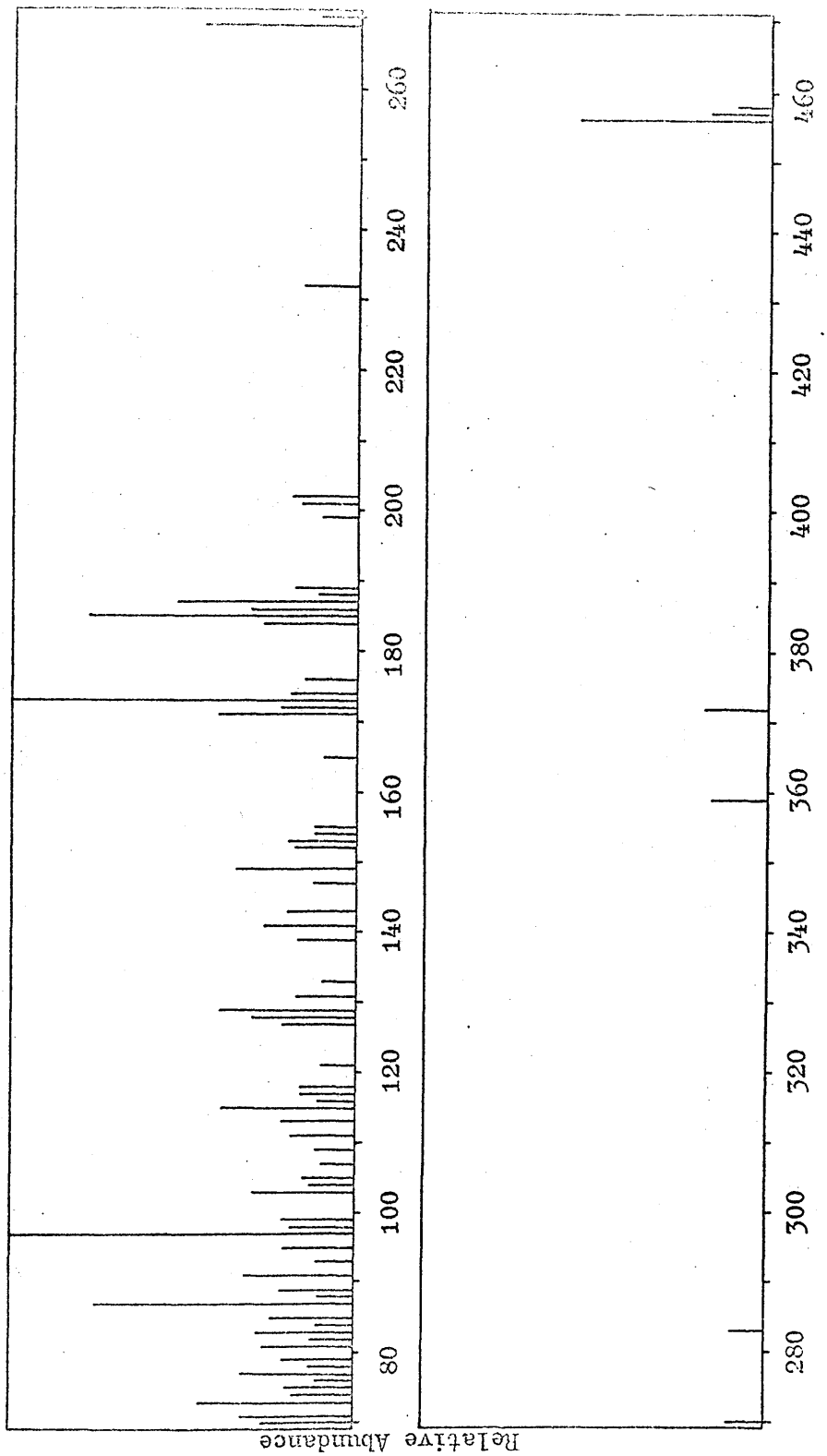

Figure 4.13 Mass Spectrum of P_6

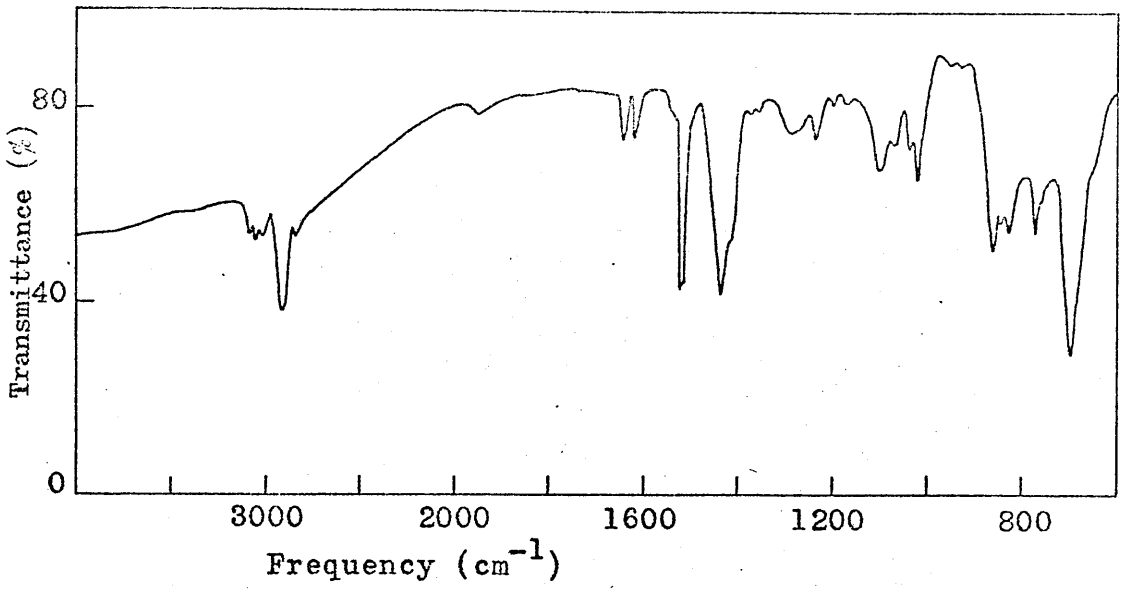

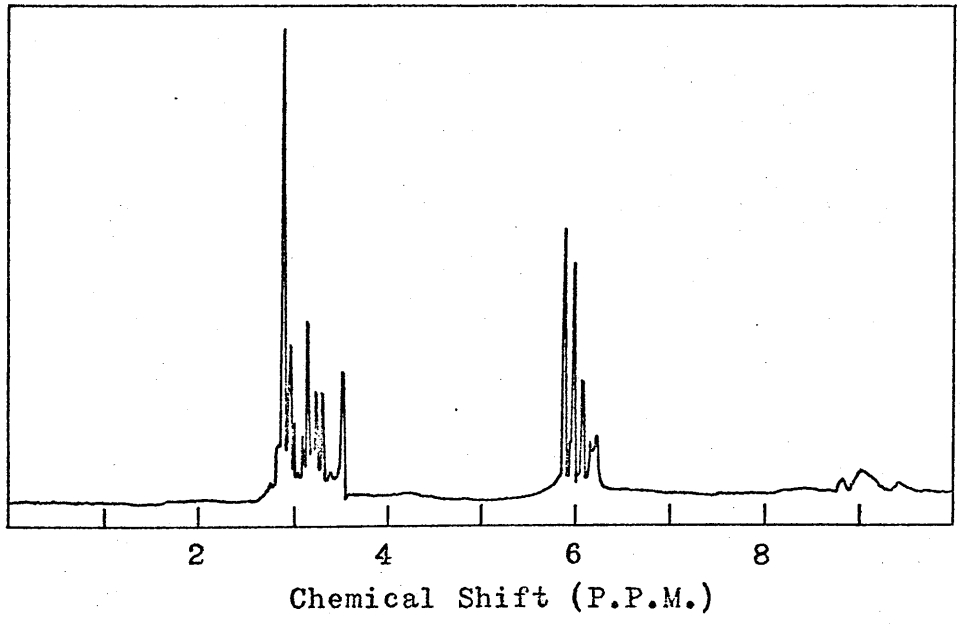

Figure 4.14 I.R. and n.m.r. Spectra of P_6.

5.90τ , 6.07τ and 5.99τ can again be assigned to protons of the methylene bridges attached to 2- and 3-mono and 2,5-disubstituted thiophen nuclei respectively. Peaks at 6.14τ and 6.17τ could be assigned to methylene groups attached to 2,4- and 3,4-disubstituted thiophen nuclei. However, it must also be considered possible that either of these peaks is due to the methylene bridge between di- and tri-substituted rings. The small absorption at 5.95τ could also be taken to account for these absorptions but work by Grassie and Meldrum[30] has indicated that the protons of methylene bridges linking substituted benzene rings resonate at higher field. The proportion of aromatic to aliphatic protons were estimated from n.m.r. absorptions and found to be 2.02 which is in very good agreement with the value 2.00 calculated for the molecular structure of P_6.

The I.R. spectrum of P_6 again indicates the presence of more complex substitution in the product. While the peaks at 700 cm^{-1} and 765 cm^{-1} confirm the presence of both 2- and 3-monosubstituted thiophen nuclei the peak at 755 cm^{-1} and the shoulders at 690 cm^{-1} and 670 cm^{-1} indicate the presence of other types of substitution.

It would appear therefore that while both linear

and branched forms of P_6 are present, the n.m.r. spectrum indicates that the linear form I predominates. This is in agreement with the data obtained for P_5.

(g) Peak Numbers 7 and 8 (P_7 and P_8)

The mass (figure 4.15), I.R. and n.m.r. (figure 4.16) spectra for P_7 and P_8 were found to be very nearly identical and it may therefore be concluded that both P_7 and P_8 are isomers.

Neither the I.R. nor n.m.r. spectra show any evidence for the presence of chloromethyl groups and it therefore seems necessary to account for this material in terms of the addition of at least one benzene and one thiophen nucleus to the five nuclei products comprising P_6. The absence of the intermediate product formed by reaction of P_1 with P_6 is perhaps surprising in view of the presence of P_5 among the products. This however can be accounted for in terms of the very much higher reactivity of the second chloromethyl group in P_1 compared with the first and is similar to evidence presented by Grassie and Meldrum[29] in a study of the benzene-DCMB system.

The largest peak in the mass spectrum of both P_7 and P_8 occurs at mass number 642 and corresponds with the molecular weight expected for seven nuclei products.

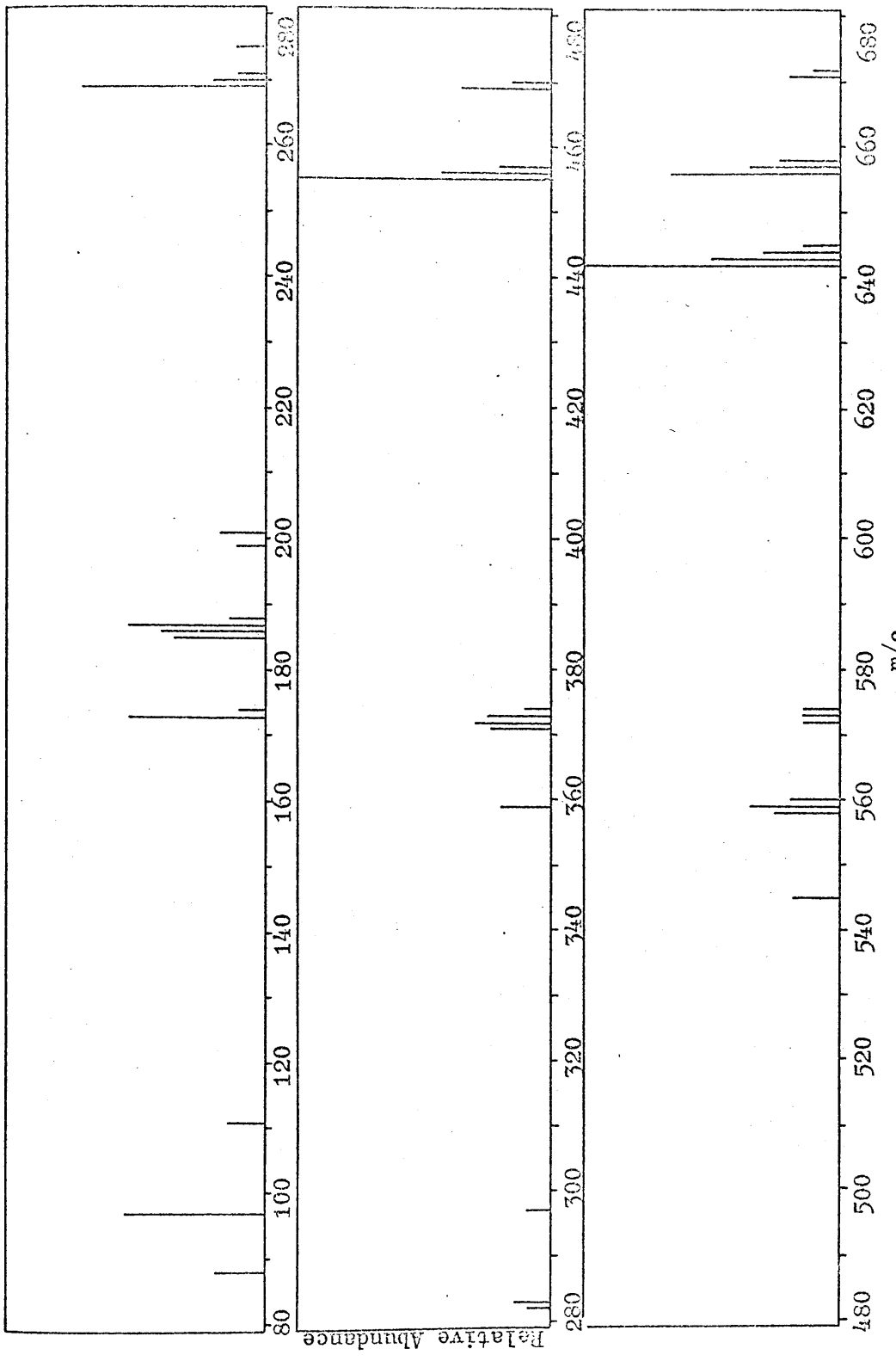

Figure 4.15 Mass Spectrum of P_8

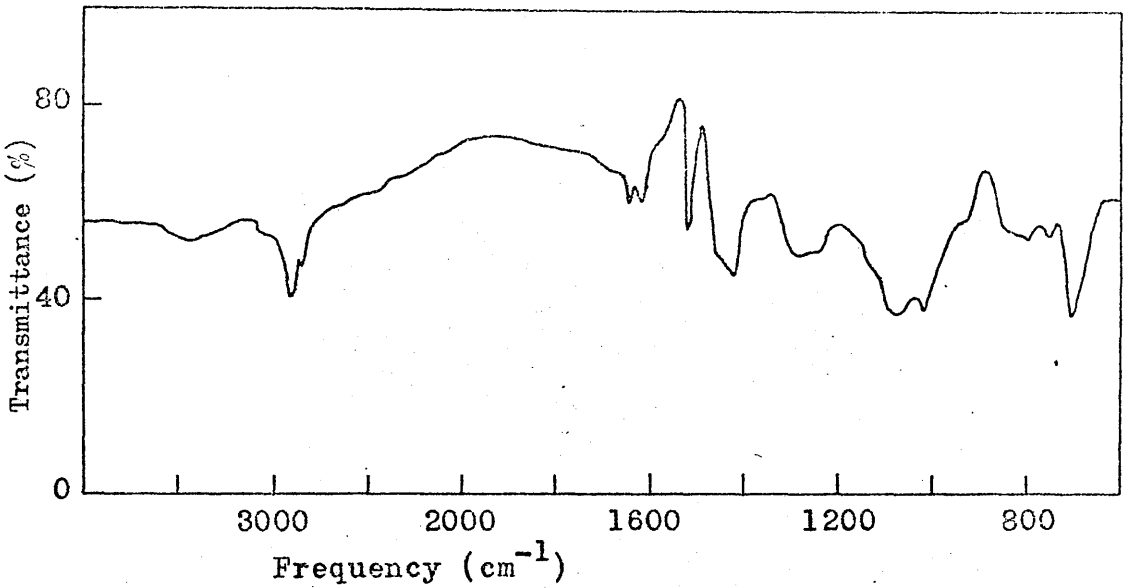

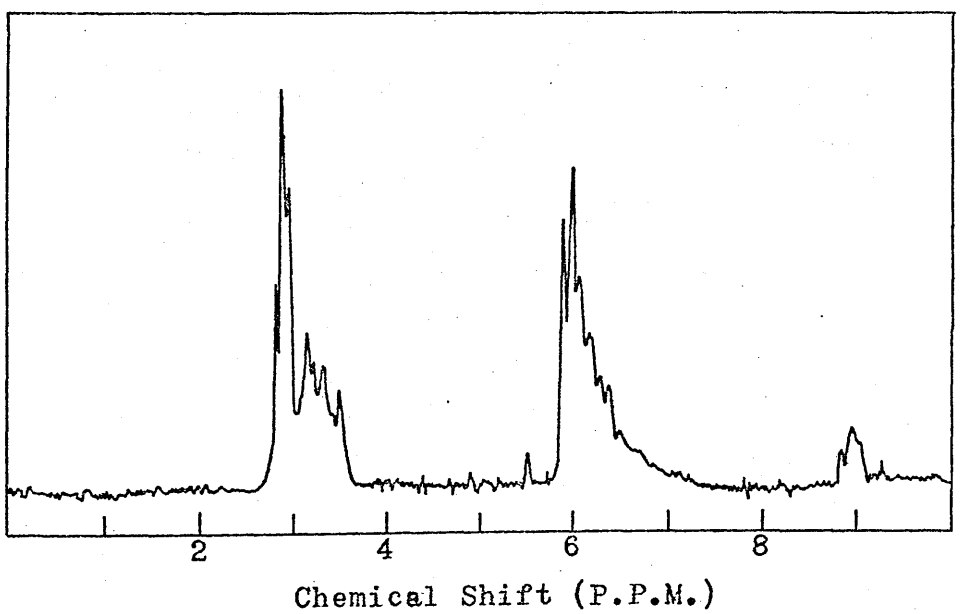

Figure 4.16 I.R. and n.m.r. Spectra of P_8.

There are also peaks of reasonably high intensity at 656 and 671 but it is believed that these arise by combination of the parent ion with methylene fragments.

A large number of 7-nuclei products are possible. However, in view of the much greater reactivity of the thiophen nuclei compared with the benzene nuclei and the small amount of tri-substituted benzene nuclei found in previous products it is reasonable to assume that the major branched isomer will be substituted in the central thiophen ring. This does not, however, exclude the possibility of branched isomers being formed by substitution into the benzene nuclei.

The I.R. and n.m.r. spectra of P_7 and P_8 are poorly resolved. However, peaks at 5.90τ , 5.98τ , 6.07τ and 6.17τ can be identified and accounted for as in section (f) for P_6. There are in addition two small peaks at 6.25τ and 6.34τ which could possibly be due to the appearance of benzene tri-substitution in the products. Both the I.R. and n.m.r. spectra confirm the absence of chloromethyl groups by lack of absorption at 675 cm^{-1} and 5.50τ respectively. The value for the ratio of aromatic to aliphatic protons (1.78) is in good agreement with the value (1.83) calculated for the molecular formula. The principal features of mass spectrum of

P_7 and P_8 can be accounted for as for P_6.

The spectral evidence presented is in good agreement with the structures H and I shown.

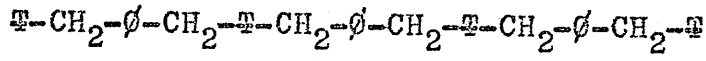

H (P_8)

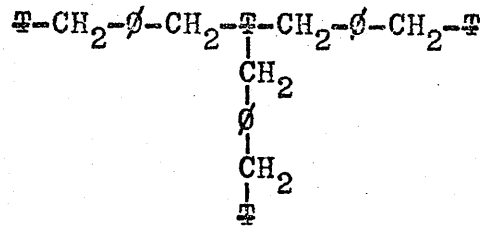

I (P_7)

As discussed for P_5 the elution ratio of branched isomer should be expected to be larger than that of the linear isomer. Thus H and I are probably P_8 and P_7 respectively. However it must also be borne in mind that a large number of branched isomers are possible and that the above assignments may be a simplification of what is really present.

(h) Peak Number 9 (P_9)

In the mass spectrum of P_9 there is a small group of peaks at mass number 828 which would suggest that this product contains eleven aromatic nuclei. The cracking pattern for P_9 can also be interpreted in the

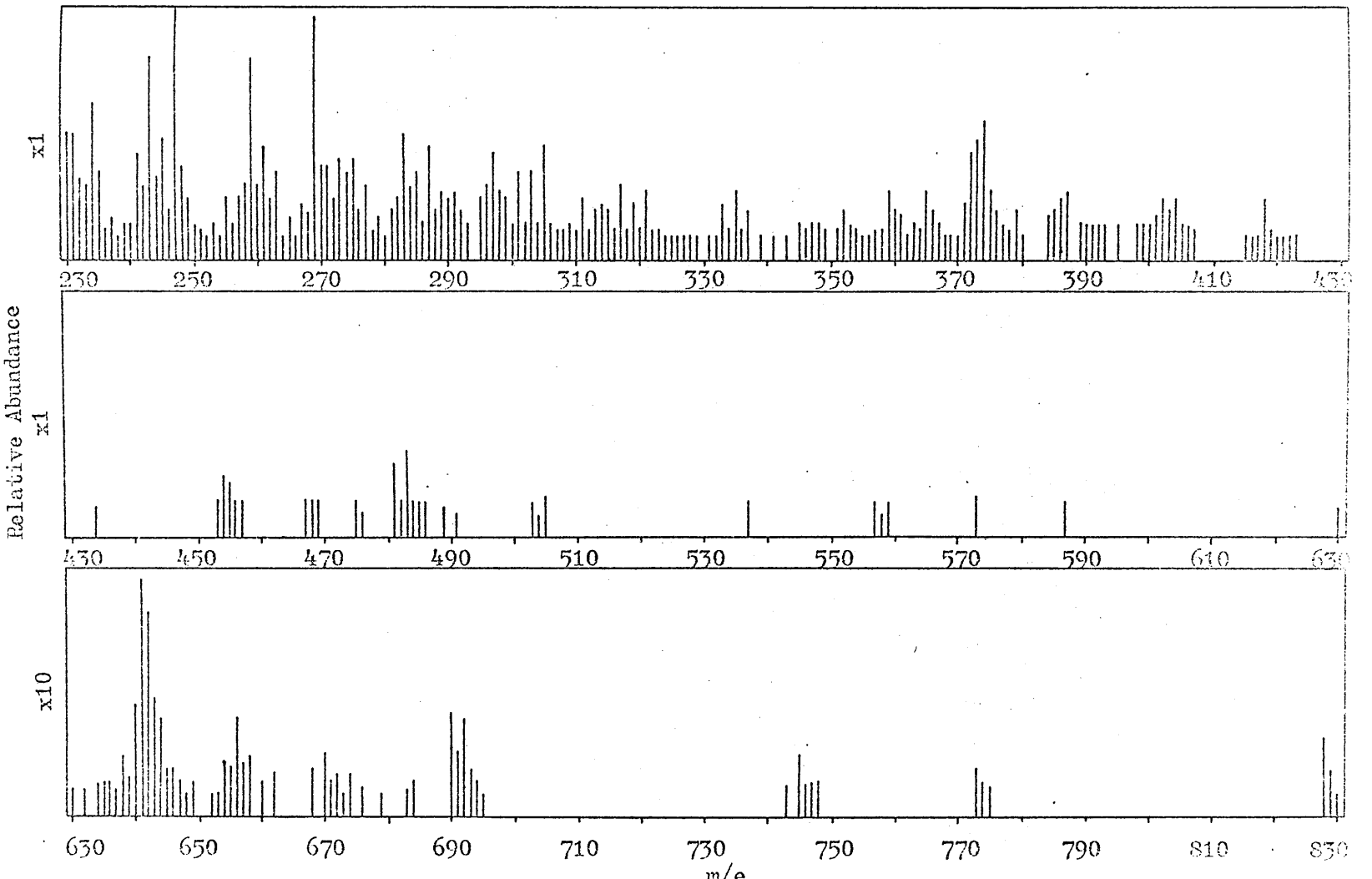

Figure 4.17 Mass Spectrum of P_9

same way as for previous products.

Both the I.R. and n.m.r. spectra of P_9 are again very poorly resolved. They are however very similar to those shown for P_8. The relative intensities of the peaks at 5.90τ and 5.99τ indicate, however, that the proportion of mono- to di- or tri-substituted thiophen nuclei is slightly lower than for P_8. Although this is, at best, only a semi-quantitative observation it does indicate that the proportion of linear molecules in P_9 is quite high. Nevertheless the very poor resolution of the spectra does suggest that more complex branched structures do occur in P_9.

(i) Peak Numbers 10 and 11 (P_{10} and P_{11})

It was not possible to obtain any peaks in the mass spectra of P_{10} or P_{11} above mass number 600. It may therefore be concluded that the parent ion and subsequent high mass number scission products were too unstable to be recorded. I.R. and n.m.r. spectra of these products were again very similar to those shown for P_8 but were so poorly resolved that it was not possible to make even qualitative conclusions about the preferred arrangements of nuclei. It may be concluded however that P_{10} and P_{11} are products with more than eleven aromatic nuclei and that they consist of complex mixtures of linear

and branched species.

4.4 Summary

The evidence presented in this chapter allows certain generalisations to be made about the course of the reaction between thiophen and DCMB. The overall reaction is represented by a series of reaction steps increasing in complexity as the size of the product molecules increases.

During the initial stages of reaction the principal events are the formation of P_2 and P_3 by replacement of the chlorine atoms of DCMB by thiophen. The second chloromethyl group in P_1 is very much more reactive than the first (chapter 5) and this leads to the very low concentrations of compounds containing chloromethyl groups during the reaction.

As the concentrations of P_2 and P_3 increase more complex products are formed. While the concentrations of P_1 and thiophen are high these products will be formed by reaction of P_1 with an earlier product followed by reaction of thiophen with the free chloromethyl group produced. As the reaction proceeds and an appreciable concentration of products accumulates in the reaction mixture, however, the pendant chloromethyl groups will tend to react increasingly with the aromatic nuclei in

the products. It is clear that the chloromethyl groups will react preferably with the thiophen nuclei and that intramolecular reactions can occur. In this way the reaction rapidly becomes highly complex with branching increasing as thiophen nuclei are increasingly absorbed into the products.

CHAPTER 5

KINETIC STUDIES OF THE DCMB - THIOPHEN REACTION

5.1 Introduction

It has already been shown that the products of the DCMB-Thiophen reaction can be separated using both G.L.C. and G.P.C. Using these techniques a study of the mechanism and kinetics of the reaction has been carried out in two stages. A study of the initial stages of the reaction was carried out using G.L.C. as an analytical tool which allowed DCMB, TCMB and DTB to be separated and their concentrations estimated. The later products of reaction were separated using the preparative G.P.C. technique. All studies were carried out under high vacuum using thoroughly dried reagents and all experimental techniques were as described in chapter 2.

5.2 The Initial Stages of the Reaction

The use of G.L.C. to separate and identify the products of the reaction between DCMB and thiophen and the resultant chromatograms have already been described in chapters 3 and 4. Three main components are resolved and have been identified as DCMB, TCMB and DTB. Preliminary experiments indicated that G.L.C. could be used to follow the course of the formation of these products and so build up a detailed picture of the reaction scheme. Such

a study has been undertaken and is described below.

As the reaction between DCMB and thiophen proceeds higher molecular weight products, which cannot be resolved by G.L.C. are increasingly produced. In order to discourage the formation of these products reactions were carried out using a large excess of thiophen. Thus the reaction between thiophen and DCMB or TCMB is promoted at the expense of the reaction between DTB and DCMB or TCMB. In addition the investigations were confined to the initial stages of the reaction such that the HCl liberated did not exceed 15% of the theoretical maximum amount. Despite these precautions very small amounts of higher molecular weight products did appear at later stages of reaction when the HCl liberated approached this value. The appearance of these products was indicated by a discrepancy between the theoretical and actual amounts of HCl found. The absolute concentrations of products were calculated, however, using the simple expression whose derivation is described below. The use of this expression has previously been described by Grassie and Meldrum[29] in the study of a similar system.

Quantitative Estimation of Products:

The flame ionisation detector of the gas chromatograph gives a response which depends on the nature of the

component being measured. It is necessary, therefore, to calibrate the detector for each component in order to estimate its absolute concentration. These calibrations were carried out using mixtures of DCMB, TCMB and DTB in known proportions. By plotting the peak areas obtained for TCMB and DTB, relative to that obtained for DCMB, against their relative molar proportions in the mixtures, graphs of the type shown in figure 5.1 were obtained. From these plots it was established that the peak areas per unit molar concentration for DCMB, TCMB and DTB were in the ratio 1 : 0.98 : 1.44. The relative molar ratio a : b : c of the three compounds in a mixture is given by,

a : b : c = area of $P_1/1$: area of $P_2/0.98$: area of $P_3/1.44$

The absolute concentrations of the three components were then determined in the following way.

If N_a, N_b and N_c are the concentrations of DCMB, TCMB and DTB at time t, then,

$$N_a : N_b : N_c = a : b : c$$

and,
$$\frac{N_a}{a} = \frac{N_b}{b} = \frac{N_c}{c} \qquad (1)$$

If N_o = the initial concentration of DCMB, then,

$$N_o = N_a + N_b + N_c + \sum x_i N_i \qquad (2)$$

where N_i is the yeild of all other products of higher

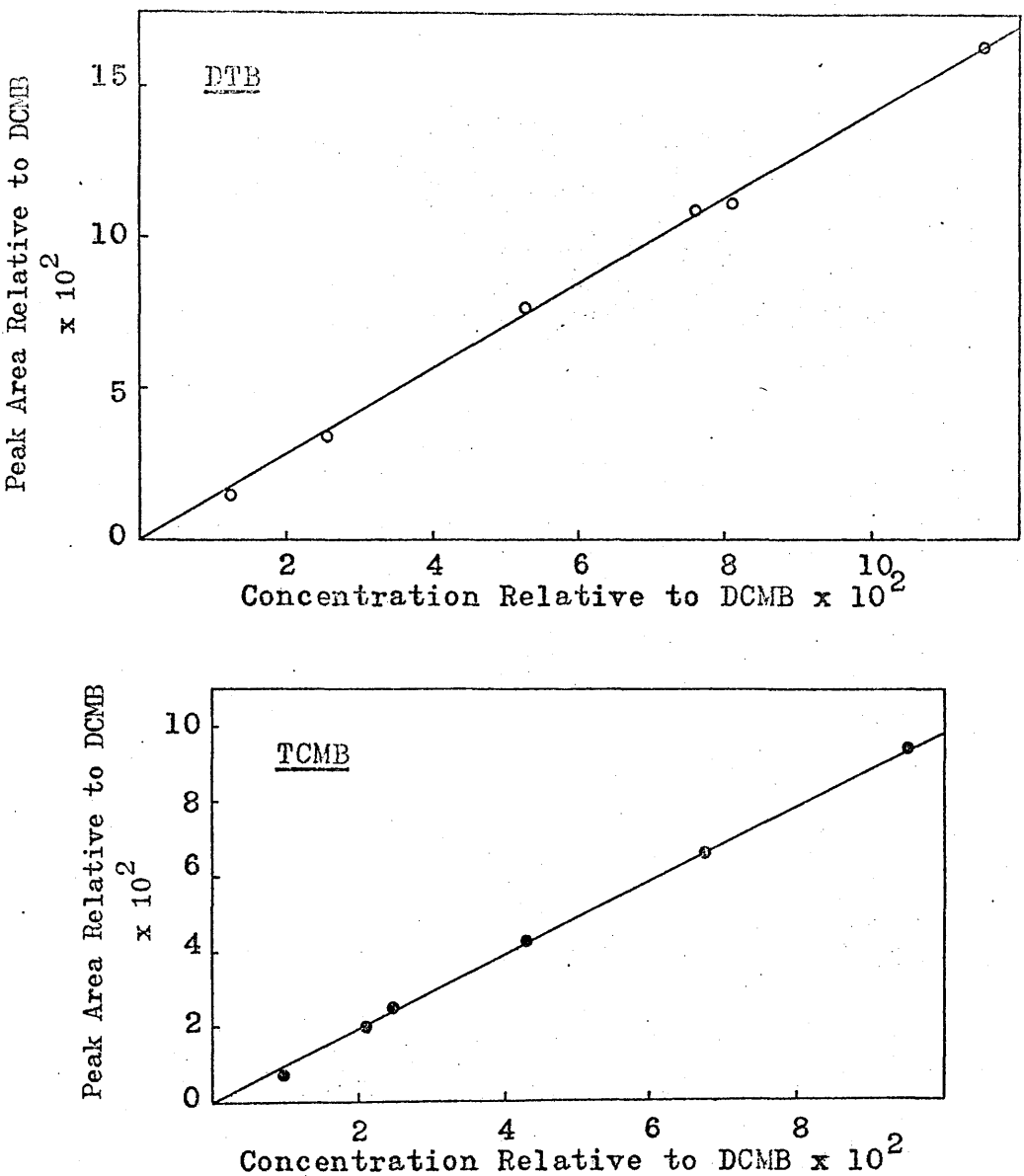

Figure 5.1 Calibration Curves for Flame-Ionisation Detector

molecular weight and x_i is the number of DCMB molecules incorporated into the ith product. The experiments described in section 5.2 have shown that the concentration of chloromethyl groups in later products is very low, therefore if N_H = the concentration of HCl at time t,

$$N_H = N_b + 2N_c + 2\Sigma x_i N_i \qquad (3)$$

Solution of equations (1), (2) and (3) leads to the following equations.

$$N_a = a(2N_o - N_H)/(2a+b)$$

$$N_b = b(2N_o - N_H)/(2a+b)$$

$$N_c = c(2N_o - N_H)/(2a+c)$$

Since all the parameters on the right hand sides of these equations are known or can be measured N_a, N_b and N_c can be found.

The errors involved in the calculation of concentrations from gas chromatographic data have been estimated from a large volume of data and found to be in the order of $\pm$ 5%. As great care was taken to minimise the errors in the handling of reagents, described in chapter 2, the errors involved in the overall determination of product concentrations should not have risen much above this value.

Characteristics of the Reaction:

The methods described above have allowed the changes

in the concentration of the three components during the reaction to be studied. The reaction curves obtained were similar to those described in chapter 3 and are shown in figures 5.2 - 5.21. As suggested in chapter 3 these curves are of the form to be expected as the result of two consecutive reactions,

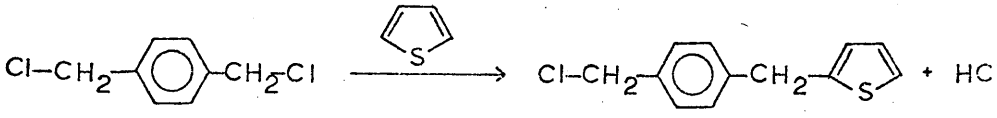

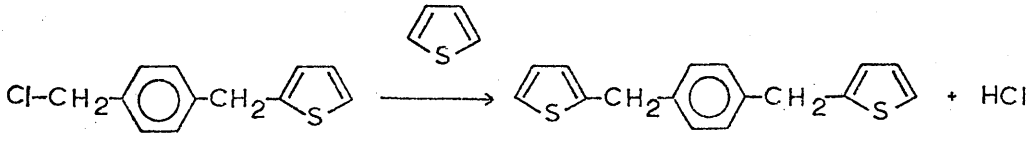

Throughout the initial stages of the reaction the decrease in the concentration of DCMB is linear with time. A decrease in the rate of reaction of DCMB would have been expected at later stages of reaction causing the conversion curve for DCMB to become concave upwards. The fact that the rate of reaction of DCMB is maintained at a constant level, throughout the reaction is an indication that the aromatic nuclei in later products of reaction are as reactive if not more reactive than thiophen. The reaction curve for TCMB shows an

Table 5.1 Kinetic Data from G.L.C. Study

Run No.	Concentration of Reactants ($mol.l^{-1}$) DCMB	Thiophen	$SnCl_4$	$\frac{-d(DCMB)}{dt}$ ($mol.l^{-1}sec^{-1}x10^6$)	$\frac{d(DTB)}{dt(TCMB)}$ ($sec^{-1}x10^4$)	k_1 ($l^2mol^{-2}sec^{-1}x10^4$)	k_2 ($l^2mol^{-2}sec^{-1}x10^3$)
S10	0.2250	2.46	0.0171	2.60	2.58	2.75	6.13
S11	0.0770	2.50	0.0171	0.85	2.67	2.58	6.25
S12	0.1530	2.48	0.0171	1.72	2.66	2.65	6.27
S13	0.2250	1.23	0.0168	1.38	1.36	2.97	6.58
S14	0.2240	1.85	0.0168	2.04	1.98	2.93	6.37
S15	0.2240	2.47	0.0088	1.45	1.37	2.97	6.30
S16	0.2240	2.46	0.0245	3.64	4.05	2.69	6.75
S18	0.0770	2.50	0.0172	1.54	4.52	4.66	10.50
S19	0.0770	2.48	0.0171	2.93	0.89	0.90	2.09
S20	0.0770	2.50	0.0172	5.42	1.71	1.64	3.98

Table 5.2 Experimental Data for S10

Reaction Time (mins.)	Concentrations of Products (moles l^{-1}) DCMB	TCMB	DTB	HCl	Data from Reaction Curves $\frac{d(DTB)}{dt}$ ($mol.l^{-1}sec^{-1}x10^{6}$)	(TCMB) ($mol.l^{-1}$)
20	0.2221	0.0024	0.0005	0.0034	0.42	0.0013
40	0.2191	0.0041	0.0018	0.0079	1.00	0.0034
60	0.2157	0.0058	0.0035	0.0133	1.33	0.0051
80	0.2121	0.0070	0.0059	0.0187	1.58	0.0065
100	0.2094	0.0078	0.0078	0.0229	1.92	0.0076
120	0.2051	0.0091	0.0108	0.0235	2.08	0.0084
140	0.2037	0.0090	0.0123	-	2.25	0.0089
160	0.1998	0.0093	0.0159	0.0428	2.50	0.0093
180	0.1965	0.0097	0.0188	0.0318	2.50	0.0096

Table 5.3 Experimental Data for S11

Reaction Time (mins.)	Concentrations of Products (moles l^{-1}) DCMB	TCMB	DTB	HCl	Data from Reaction Curves $\frac{d(DTB)}{dt}$ ($mol.l^{-1}sec^{-1}x10^{6}$)	(TCMB) ($mol.l^{-1}$)
20	0.0760	0.0009	0.0001	0.0011	0.08	0.0004
40	0.0752	0.0014	0.0004	-	0.25	0.0011
60	0.0741	0.0019	0.0010	0.0045	0.37	0.0014
80	0.0729	0.0024	0.0017	-	0.50	0.0017
100	0.0719	0.0027	0.0024	0.0077	0.58	0.0021
120	0.0707	0.0029	0.0034	0.0045	0.67	0.0026
140	0.0693	0.0032	0.0045	0.0117	0.75	0.0028
160	0.0684	0.0033	0.0053	0.0144	0.83	0.0030
180	0.0674	0.0033	0.0063	0.0150	0.83	0.0032

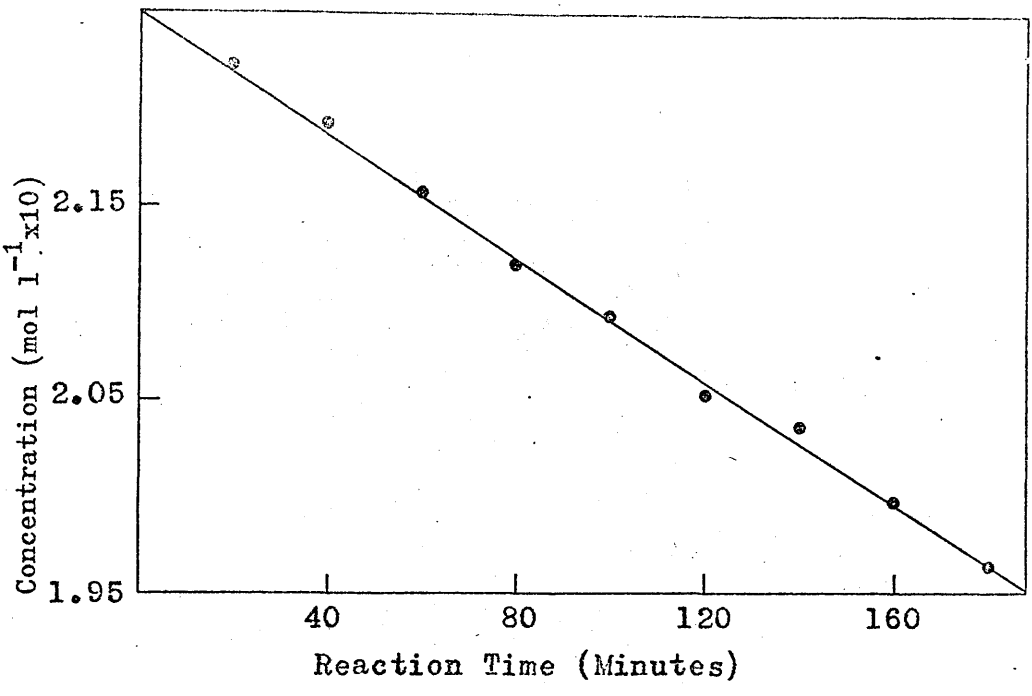

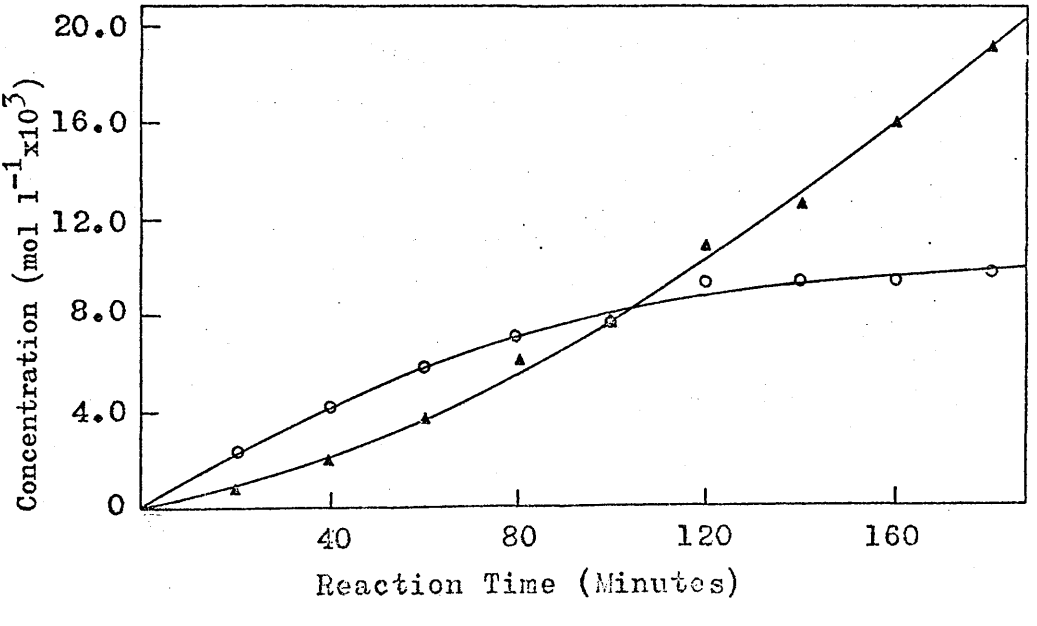

Figure 5.2 Reaction Curves for DCMB ⊙ , TCMB ○ , and DTB ▲ . Series S10.

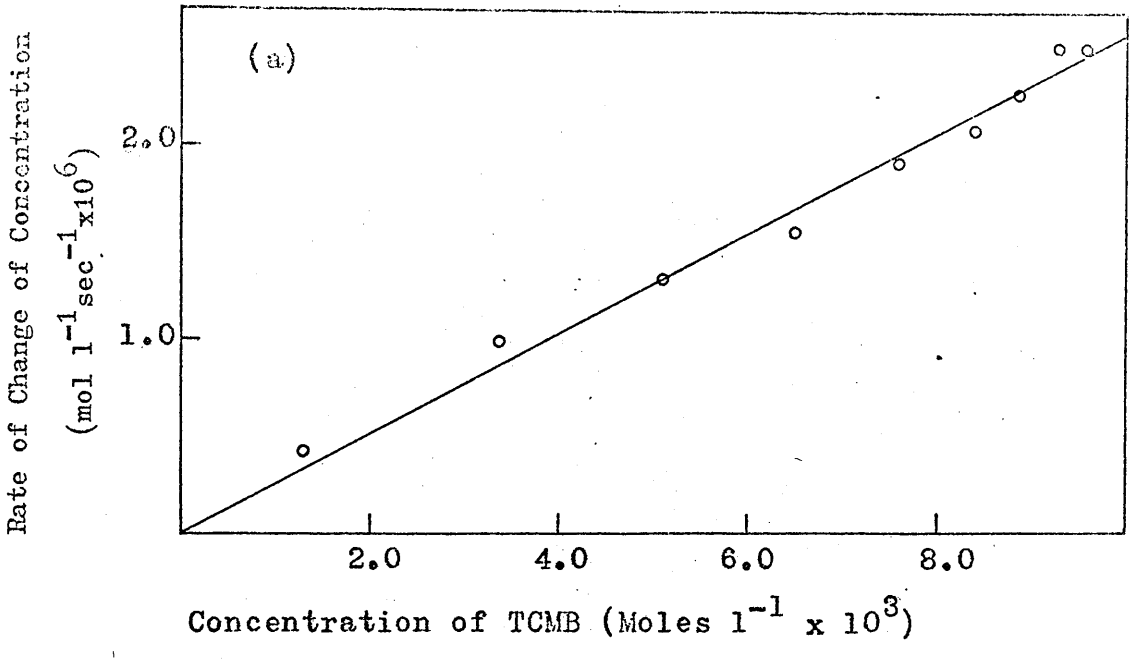

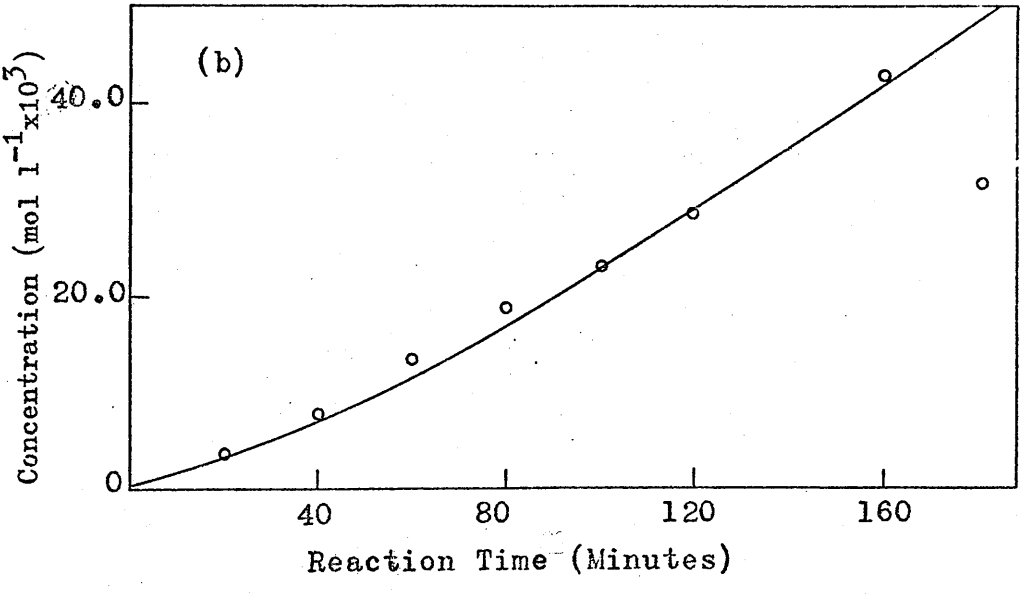

Figure 5.3 (a) Dependence of Rate of Formation of DTB on TCMB Concentration.

Series S10 (b) Reaction Curve for HCl.

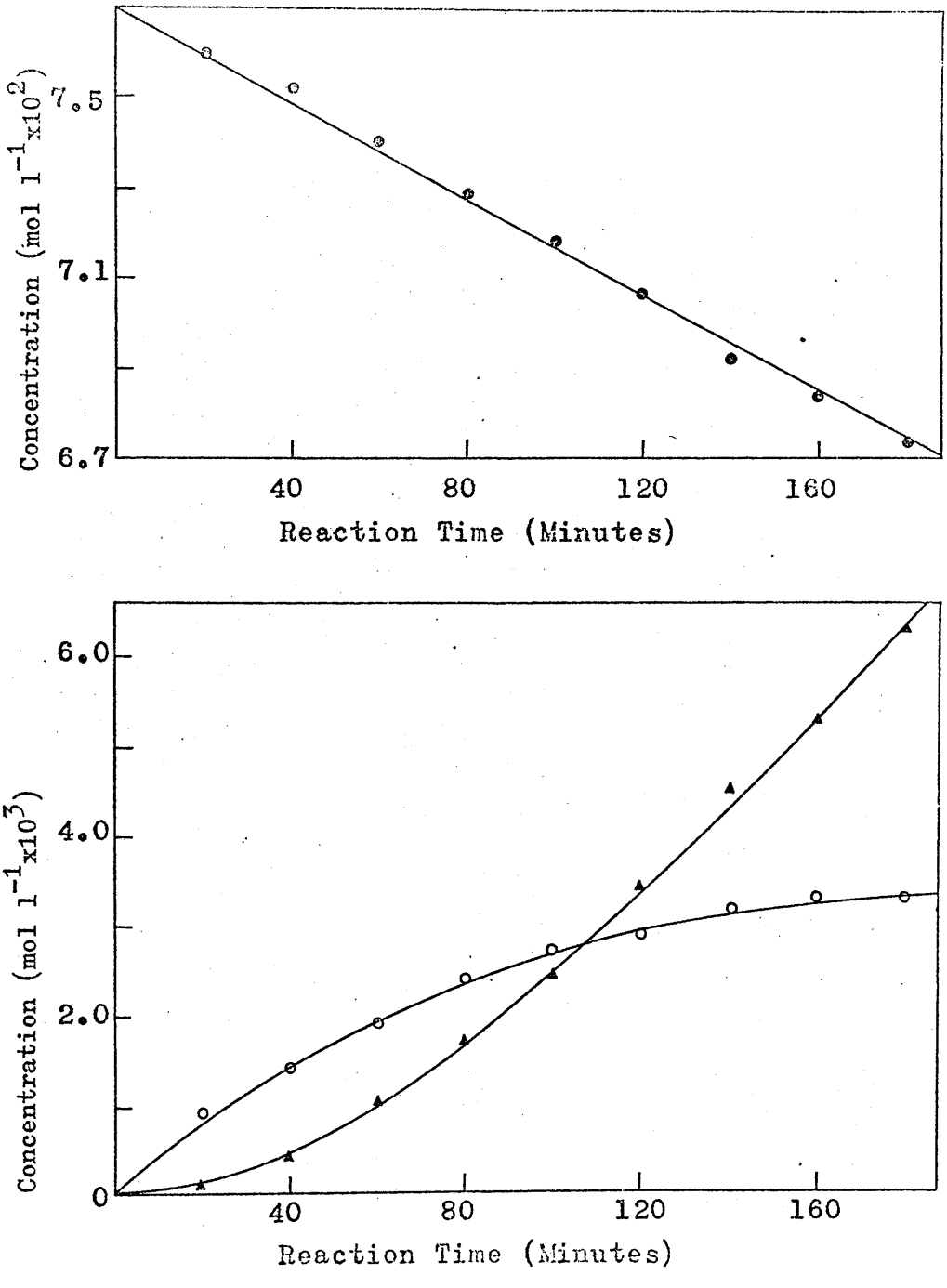

Figure 5.4 Reaction Curves for DCMB ●, TCMB ○, and DTB ▲. Series S11.

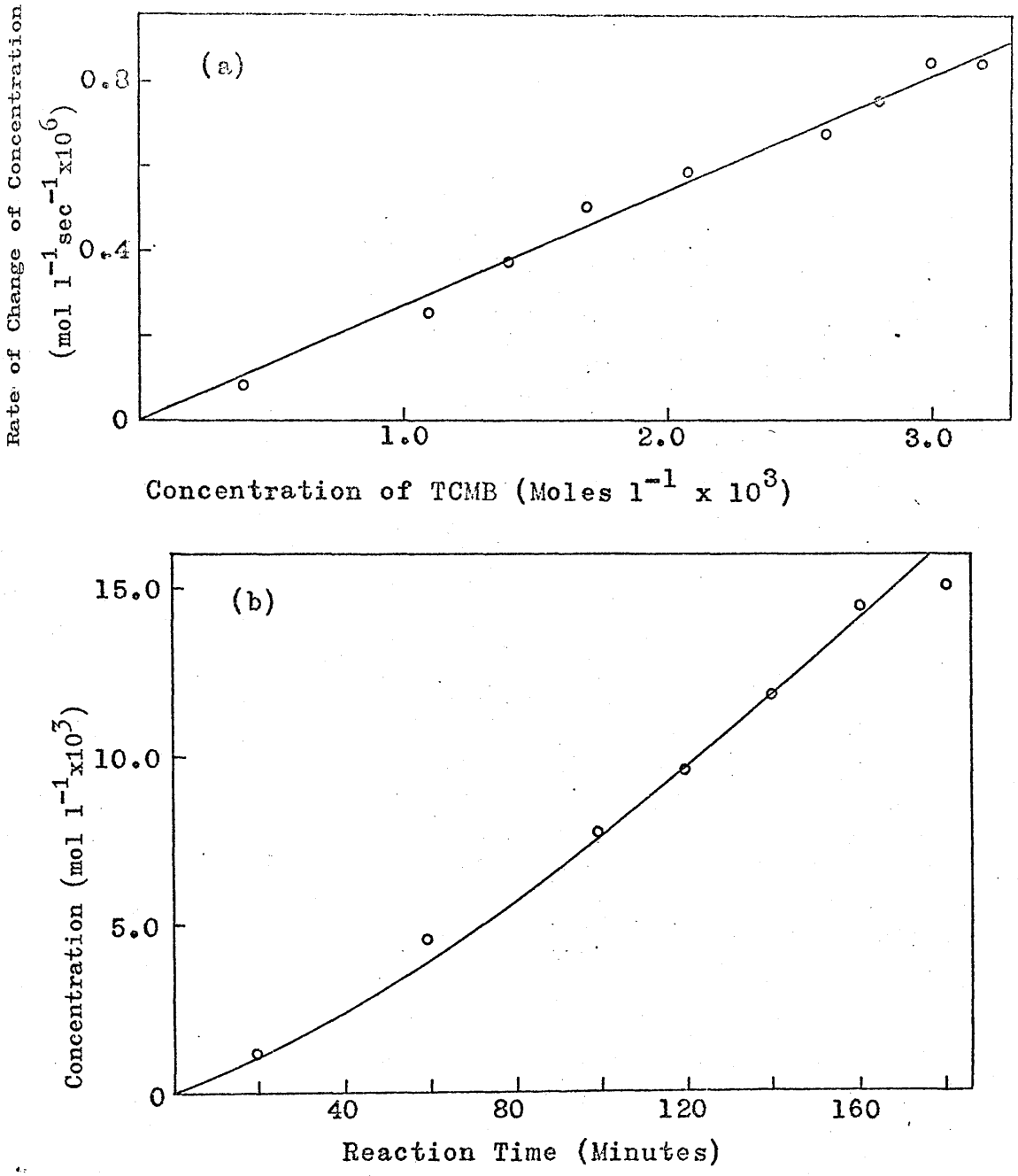

Figure 5.5 (a) Dependence of Rate of Formation of DTB on TCMB Concentration.

Series S11 (b) Reaction Curve for HCl.

Table 5.4 Experimental Data for S.12

Reaction Time (mins.)	Concentrations of Products (moles l^{-1}) DCMB	TCMB	DTB	HCl	Data from Reaction Curves $\frac{d(DTB)}{dt}$ ($mol.l^{-1}sec^{-1}x10^6$)	(TCMB) ($mol.l^{-1}$)
20	0.1510	0.0018	0.0002	0.0024	0.17	0.0009
40	0.1489	0.0033	0.0008	0.0040	0.58	0.0024
60	0.1467	0.0043	0.0020	0.0085	0.92	0.0037
80	0.1450	0.0049	0.0031	0.0124	1.08	0.0045
100	0.1432	0.0051	0.0047	0.0144	1.33	0.0051
120	0.1406	0.0058	0.0066	0.0189	1.50	0.0056
140	0.1384	0.0059	0.0087	0.0229	1.66	0.0059
160	0.1360	0.0063	0.0107	0.0279	1.75	0.0062
180	0.1339	0.0064	0.0127	0.0318	1.66	0.0063

Table 5.5 Experimental Data for S.13

Reaction Time (mins.)	Concentrations of Products (moles l^{-1}) DCMB	TCMB	DTB	HCl	Data from Reaction Curves $\frac{d(DTB)}{dt}$ ($mol.l^{-1}sec^{-1}x10^6$)	(TCMB) ($mol.l^{-1}$)
20	0.2235	0.0014	0.0001	0.0012	0.08	0.0007
40	0.2218	0.0028	0.0004	0.0042	0.25	0.0021
60	0.2204	0.0038	0.0008	0.0054	0.50	0.0033
80	0.2183	0.0050	0.0017	0.0064	0.58	0.0044
100	0.2167	0.0058	0.0025	0.0104	0.67	0.0054
120	0.2150	0.0065	0.0035	0.0143	0.83	0.0061
140	0.2136	0.0069	0.0045	0.0153	0.92	0.0068
160	0.2118	0.0074	0.0058	0.0183	1.00	0.0072
180	0.2102	0.0077	0.0071	0.0212	1.08	0.0076

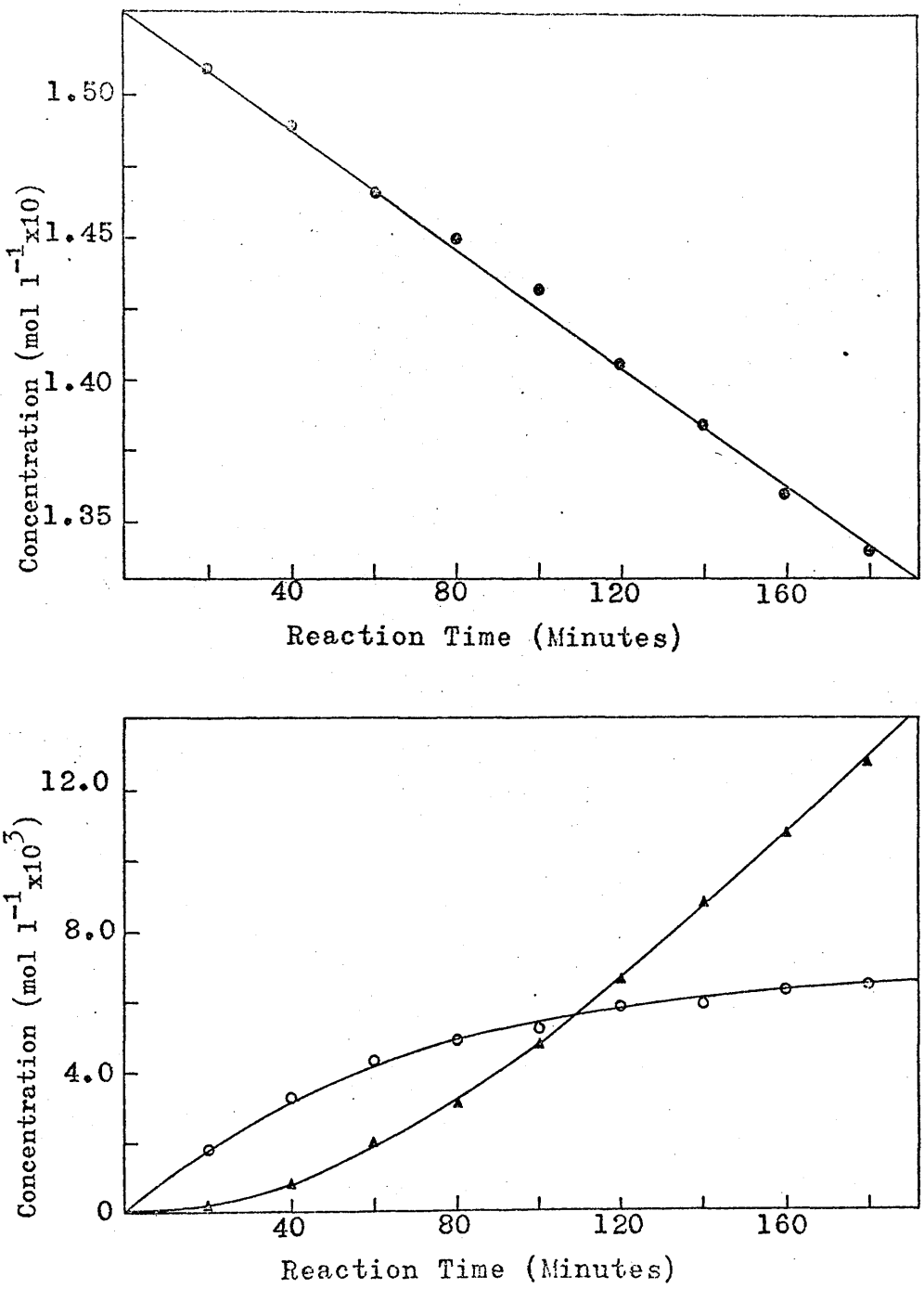

Figure 5.6 Reaction Curves for DCMB ⊙, TCMB ○, and DTB ▲. Series S12.

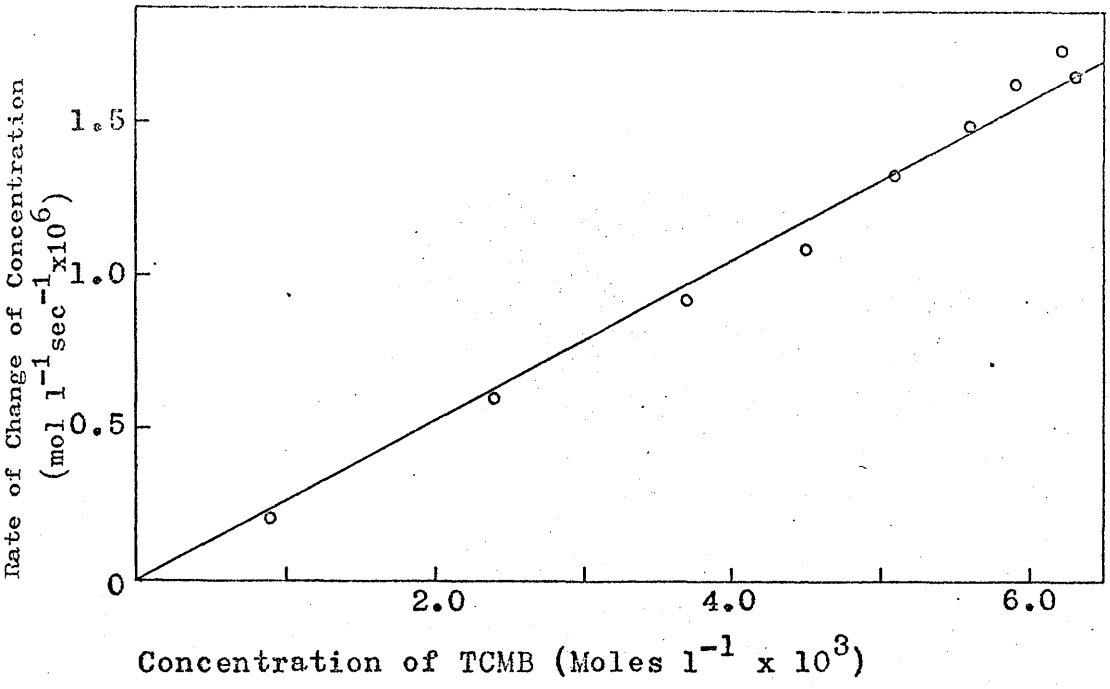

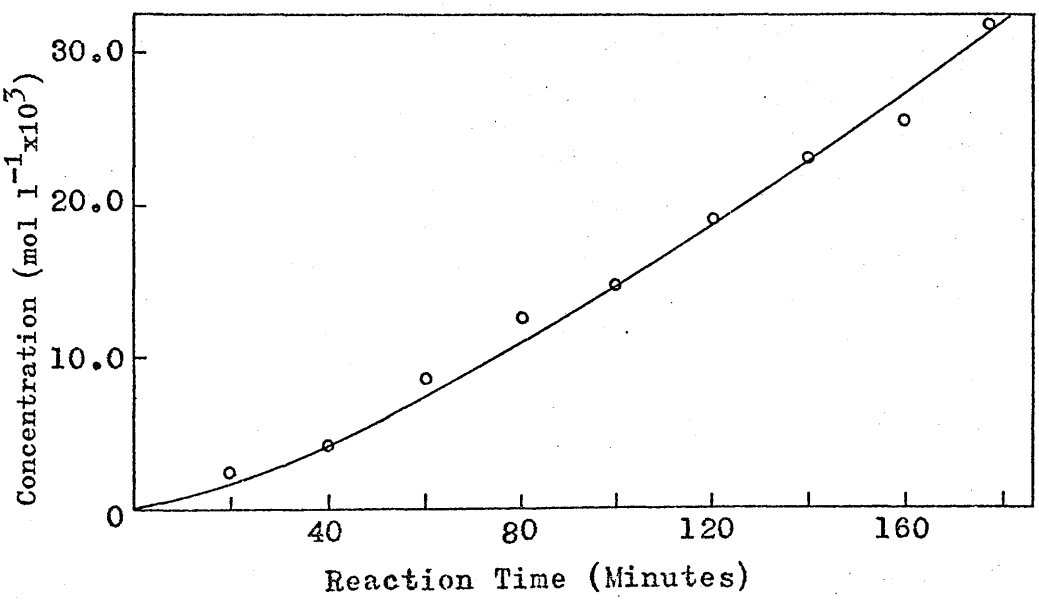

Figure 5.7 (a) Dependence of Rate of Formation of DTB on TCMB Concentration.

Series S12 (b) Reaction Curve for HCl.

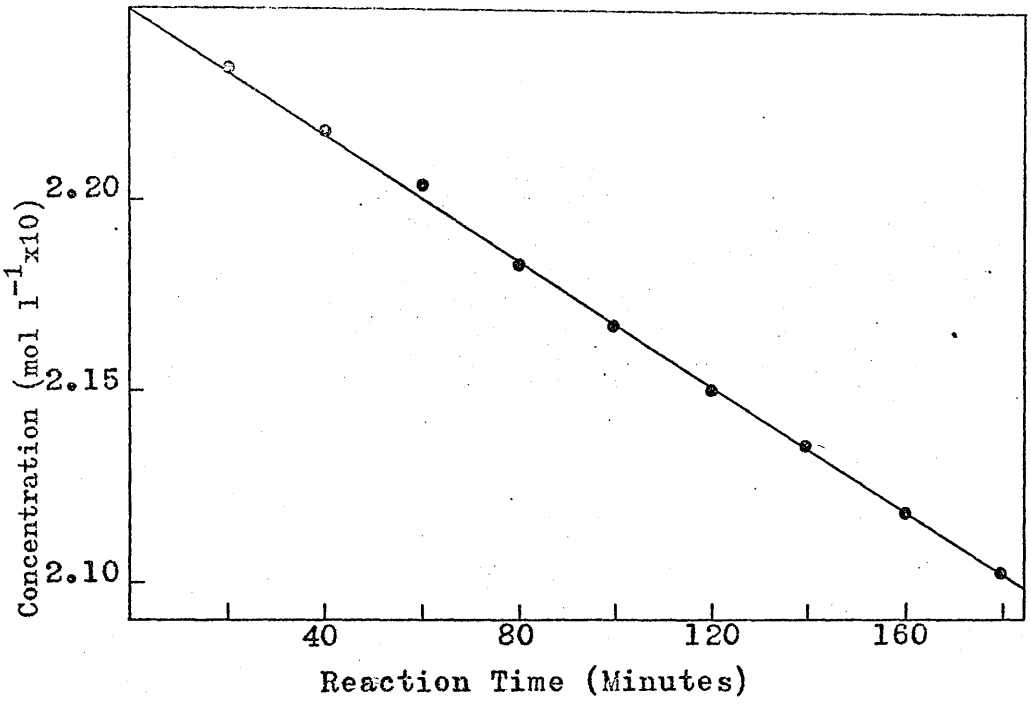

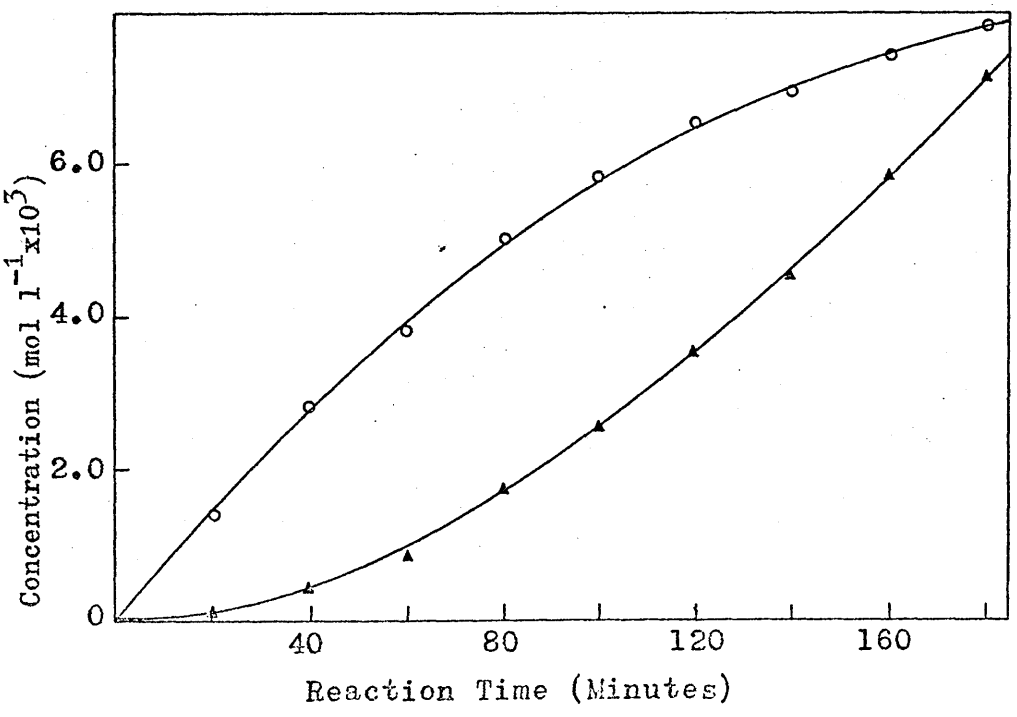

Figure 5.8 Reaction Curves for DCMB ● , TCMB ○ , and DTB ▲ . Series S13.

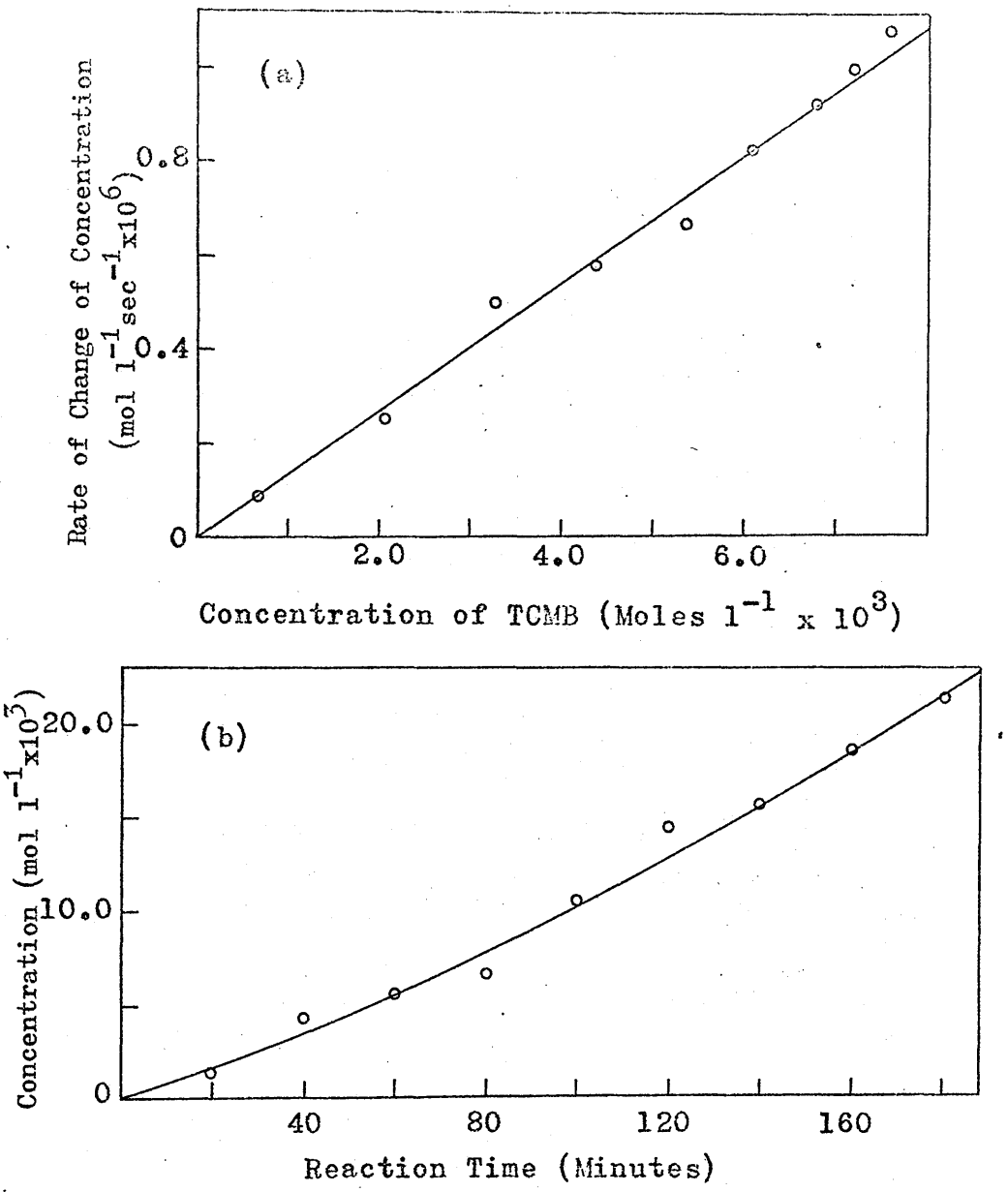

Figure 5.9 (a) Dependence of Rate of Formation of DTB on TCMB Concentration.

Series S13 (b) Reaction Curve for HCl.

Table 5.6 Experimental Data for S.14

Reaction Time (mins.)	Concentrations of Products (moles l^{-1}) DCMB	TCMB	DTB	HCl	Data from Reaction Curves $\frac{d(DTB)}{dt}$ ($mol.l^{-1}sec^{-1}x10^{6}$)	(TCMB) ($mol.l^{-1}$)
30	0.2203	0.0032	0.0005	0.0051	0.28	0.0017
60	0.2169	0.0052	0.0019	0.0117	0.78	0.0043
90	0.2133	0.0068	0.0039	0.0123	1.17	0.0061
120	0.2097	0.0077	0.0066	0.0190	1.44	0.0073
150	0.2059	0.0088	0.0093	0.0262	1.55	0.0083
180	0.2020	0.0094	0.0126	0.0336	1.78	0.0090
210	0.1985	0.0096	0.0159	0.0420	1.94	0.0095
240	0.1948	0.0098	0.0194	0.0464	2.00	0.0099
270	0.1906	0.0102	0.0232	0.0554	2.06	0.0101

Table 5.7 Experimental Data for S.15

Reaction Time (mins.)	Concentrations of Products (moles l^{-1}) DCMB	TCMB	DTB	HCl	Data from Reaction Curves $\frac{d(DTB)}{dt}$ ($mol.l^{-1}sec^{-1}x10^{6}$)	(TCMB) ($mol.l^{-1}$)
30	0.2218	0.0020	0.0002	0.0022	0.06	0.0010
60	0.2193	0.0039	0.0008	0.0060	0.39	0.0029
90	0.2167	0.0055	0.0018	0.0085	0.61	0.0047
120	0.2135	0.0069	0.0036	0.0133	0.84	0.0063
150	0.2107	0.0081	0.0052	0.0162	1.00	0.0074
180	0.2087	0.0084	0.0069	0.0224	1.11	0.0082
210	0.2056	0.0090	0.0094	0.0277	1.22	0.0087
240	0.2030	0.0092	0.0118	0.0315	1.27	0.0091
270	0.2005	0.0095	0.0140	0.0368	1.30	0.0093

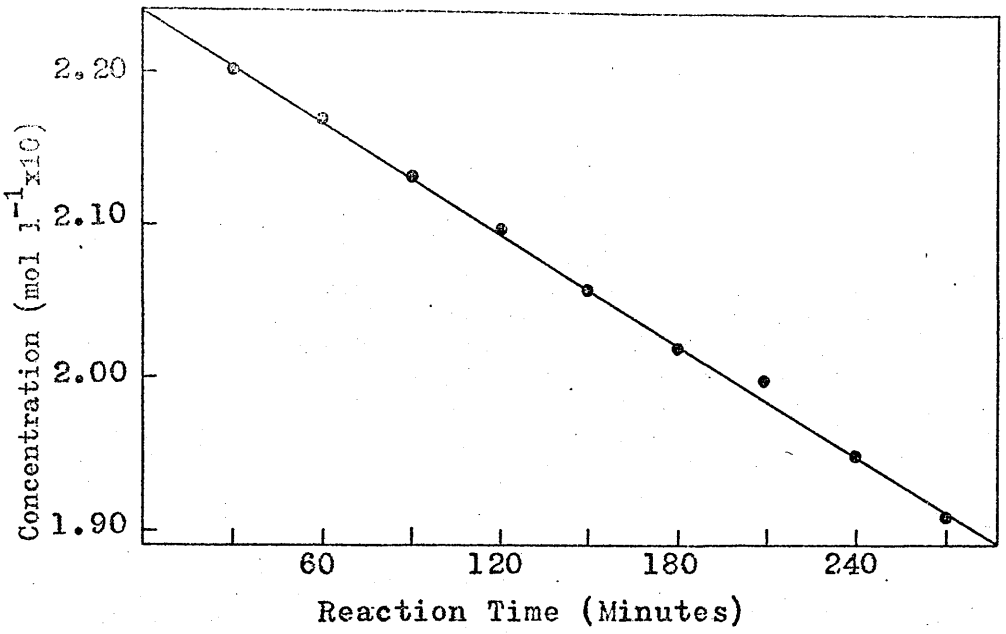

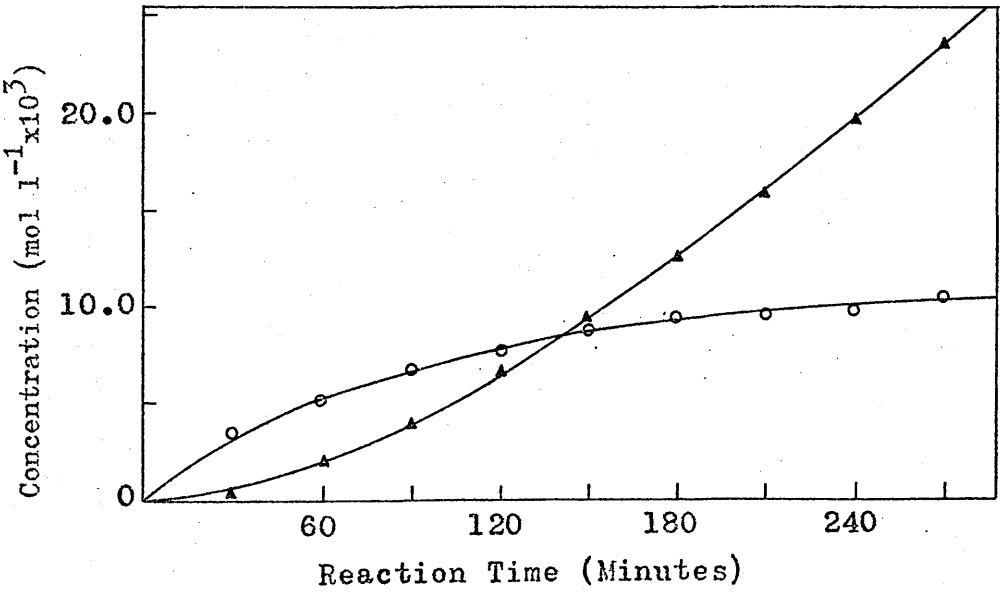

Figure 5.10 Reaction Curves for DCMB ● , TCMB ○ , and DTB ▲ . Series S14.

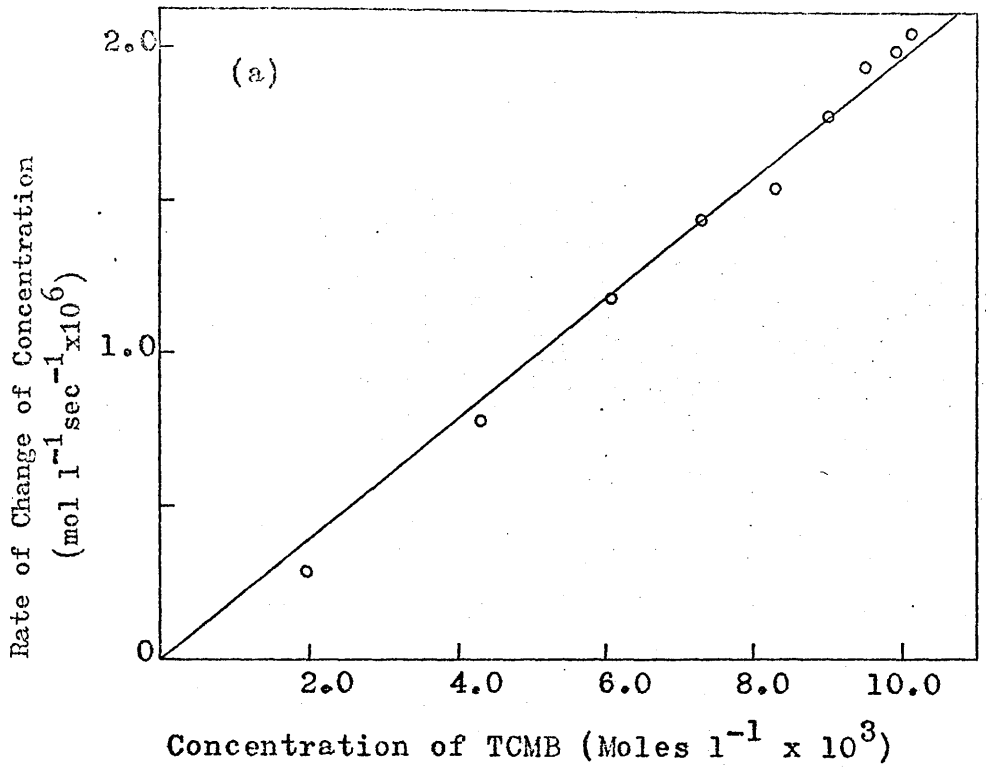

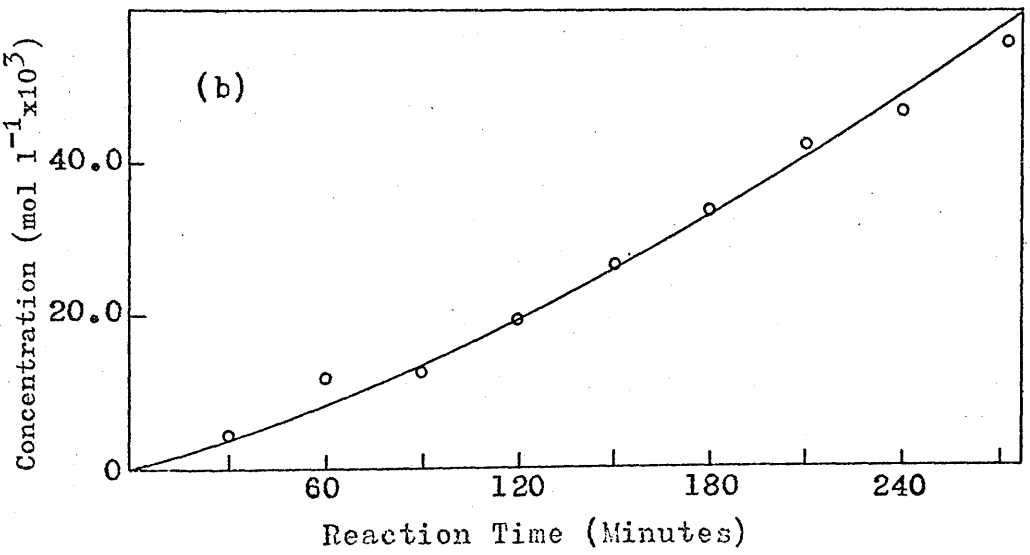

Figure 5.11 (a) Dependence of Rate of Formation of DTB on TCMB Concentration.

Series S14 (b) Reaction Curve for HCl.

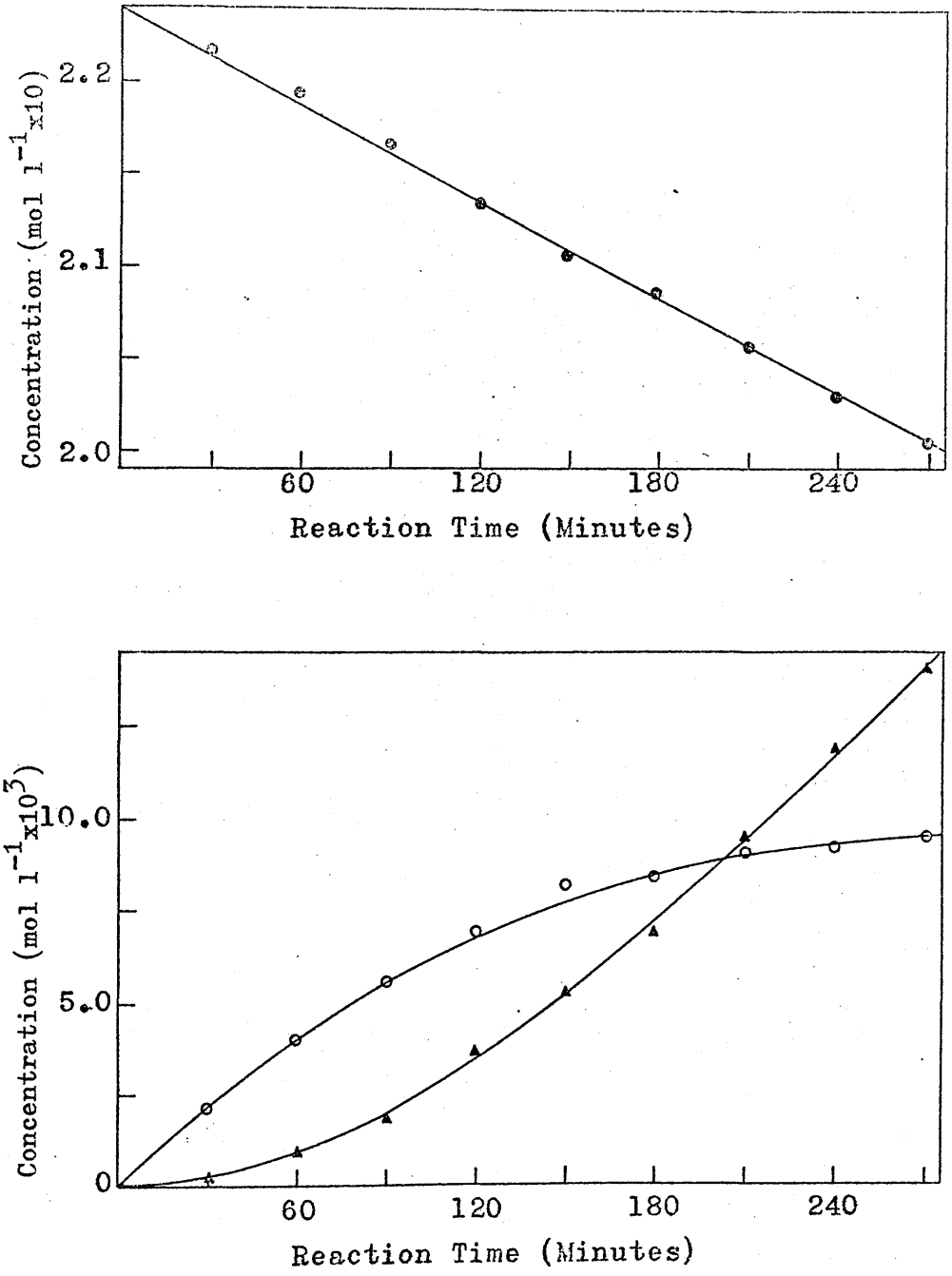

Figure 5.12 Reaction Curves for DCMB ⊙, TCMB ○ and DTB △. Series S15.

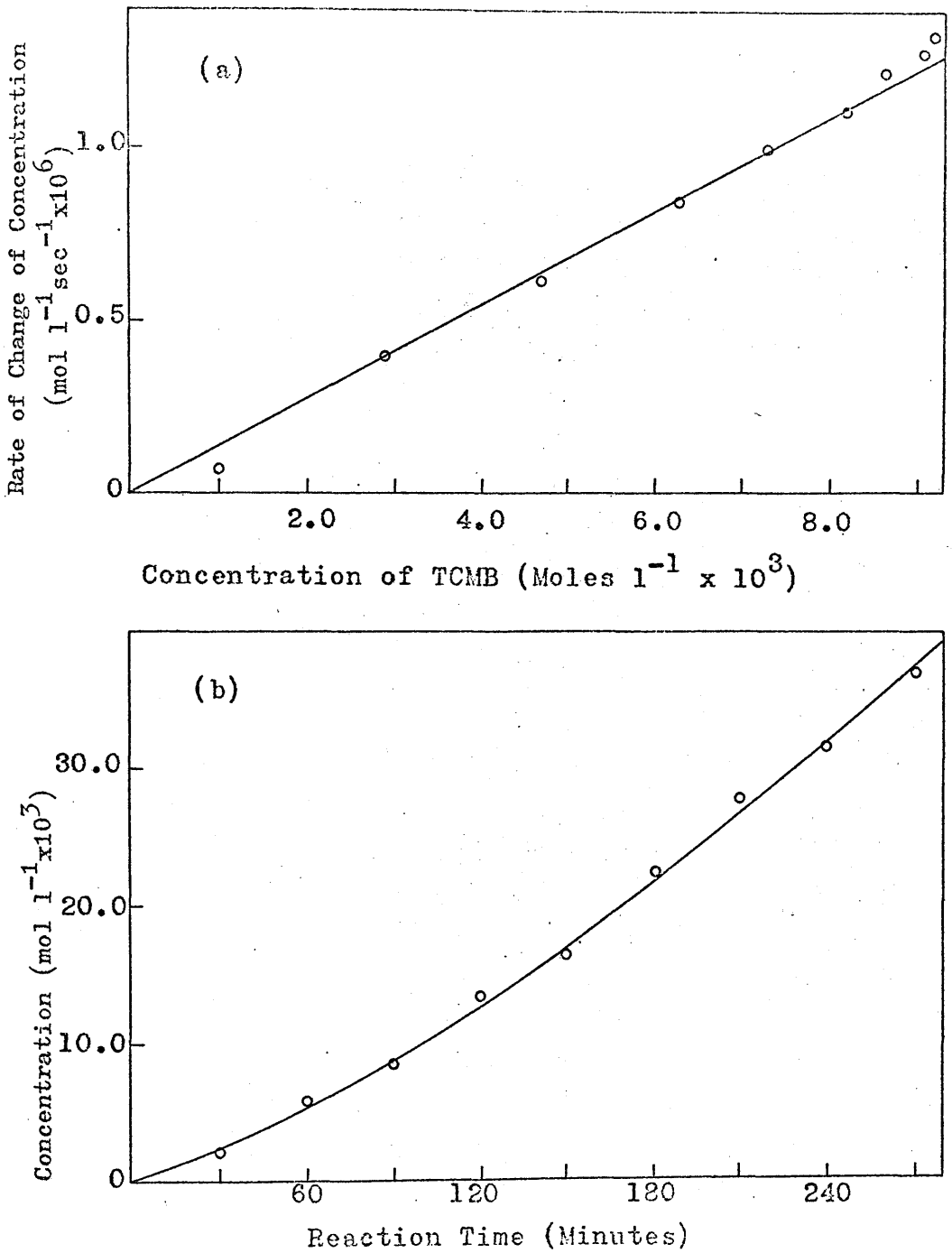

Figure 5.13 (a) Dependence of Rate of Formation of DTB on TCMB Concentration.

Series S15 (b) Reaction Curve for HCl.

Table 5.8 Experimental Data for S.16

Reaction Time (mins.)	Concentrations of Products (moles l^{-1}) DCMB	TCMB	DTB	HCl	Data from Reaction Curves $\frac{d(DTB)}{dt}$ ($mol.l^{-1}sec^{-1}x10^{6}$)	(TCMB) ($mol.l^{-1}$)
20	0.2206	0.0027	0.0007	0.0120	0.70	0.0017
40	0.2161	0.0053	0.0026	0.0180	1.16	0.0029
60	0.2113	0.0070	0.0057	0.0210	1.66	0.0041
80	0.2051	0.0086	0.0103	0.0290	2.08	0.0052
100	0.2017	0.0092	0.0131	0.0360	2.50	0.0062
120	0.1975	0.0098	0.0167	0.0450	2.91	0.0070
140	0.1938	0.0098	0.0198	0.0510	3.08	0.0077
160	0.1885	0.0090	0.0231	0.0620	3.08	0.0087
180	0.1858	0.0095	0.0265	0.0670	2.92	0.0093

Table 5.9 Experimental Data for S18

Reaction Time (mins)	Concentrations of Products (moles l^{-1}) DCMB	TCMB	DTB	HCl	Data from Reaction Curves $\frac{d(DTB)}{dt}$ ($mol.l^{-1}sec^{-1}x10^{6}$)	(TCMB) ($mol.l^{-1}$)
40	0.0740	0.0019	0.0011	0.0074	0.46	0.0010
80	0.0699	0.0031	0.0040	0.0113	0.83	0.0019
120	0.0659	0.0036	0.0075	0.0169	1.17	0.0026
160	0.0620	0.0036	0.0114	0.0179	1.46	0.0030
200	0.0585	0.0035	0.0150	0.0255	1.54	0.0034

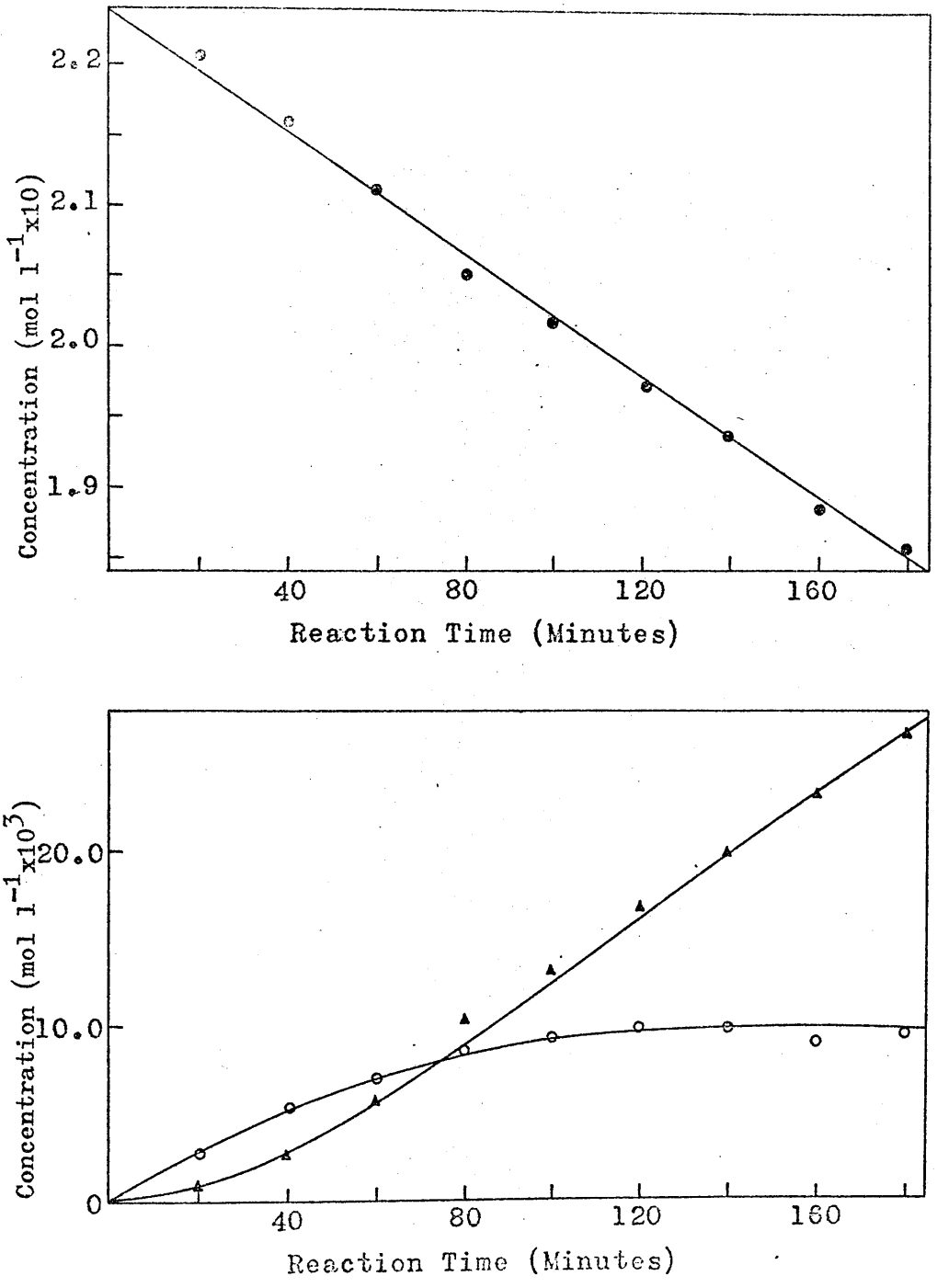

Figure 5.14 Reaction Curves for DCMB ⊙ , TCMB ○ and DTB ▲ . Series S16.

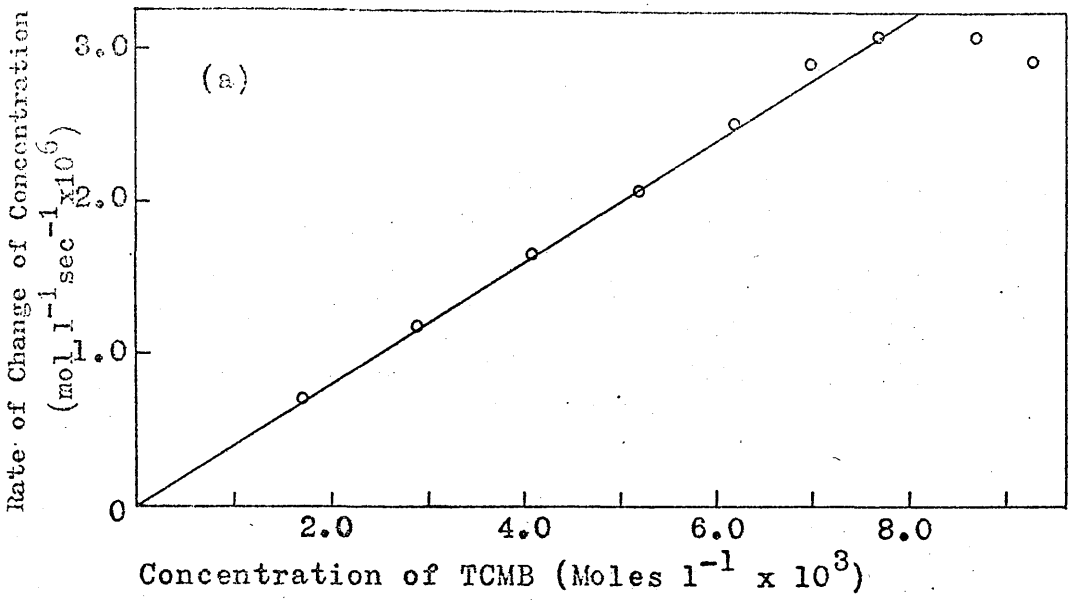

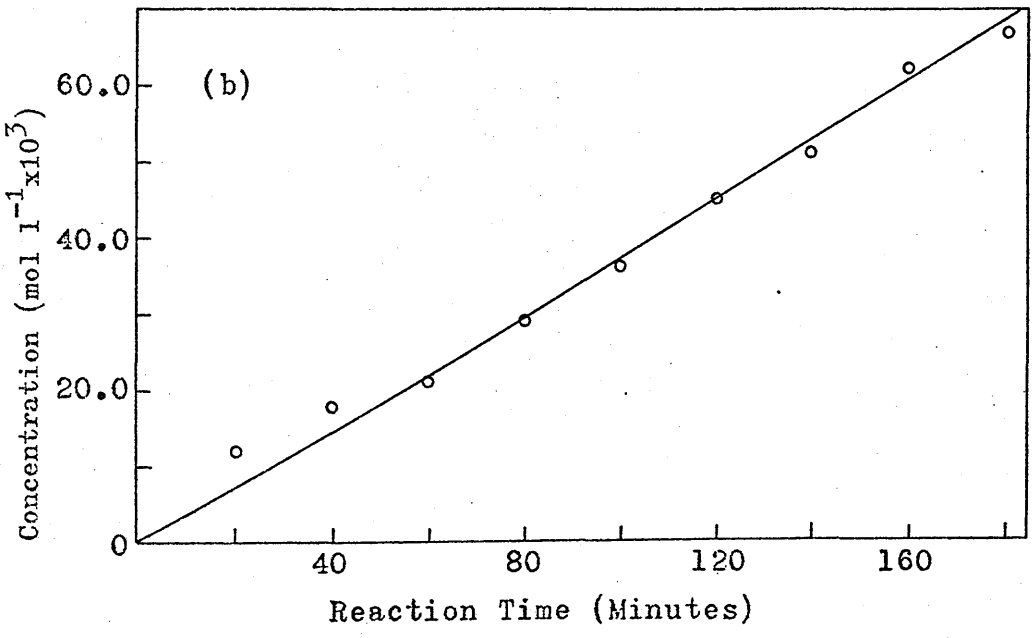

Figure 5.15 (a) Dependence of Rate of Formation of DTB on TCMB Concentration.

Series S16 (b) Reaction Curve for HCl.

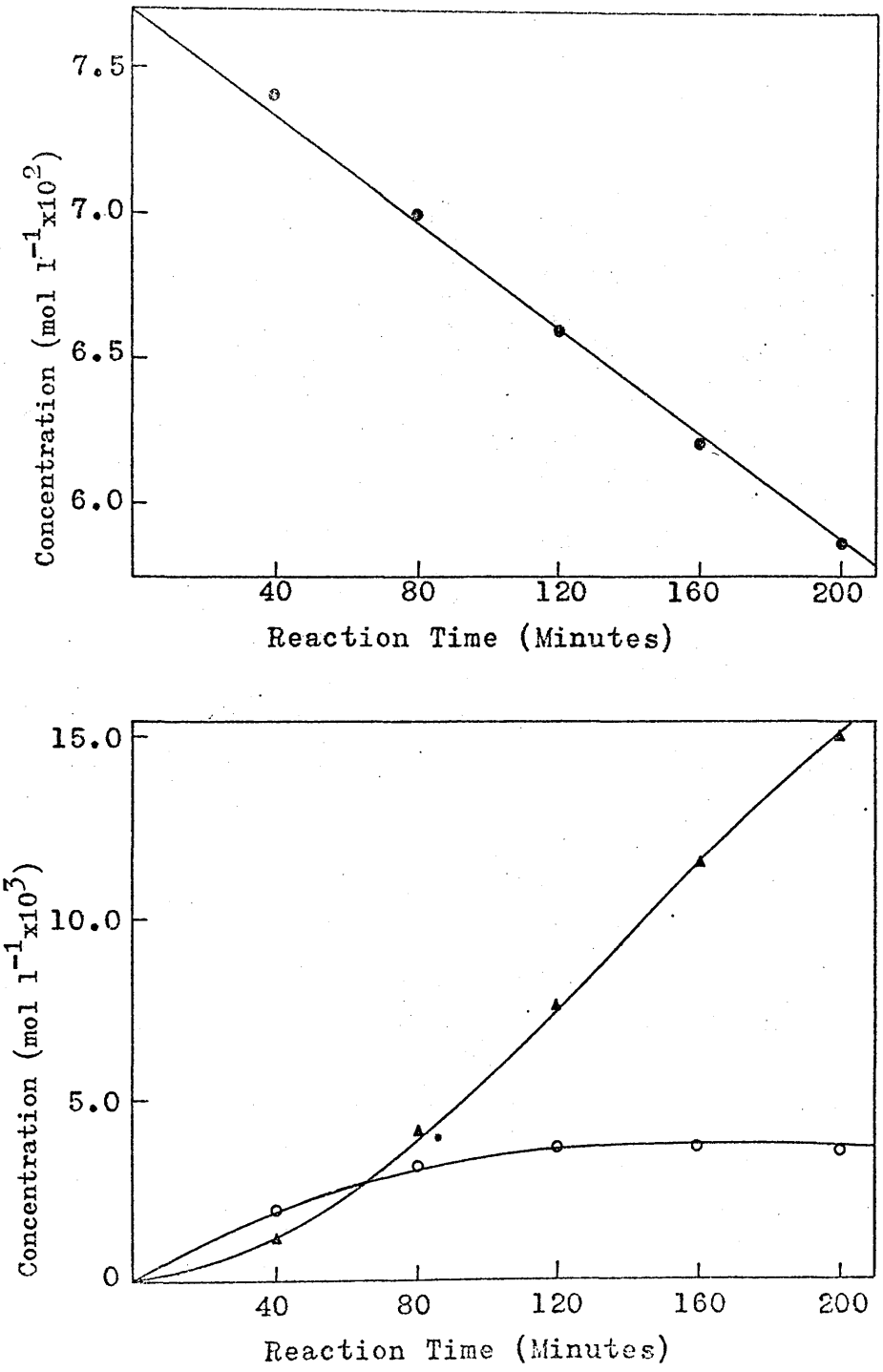

Figure 5.16 Reaction Curves for DCMB ⊙ , TCMB ○ and DTB ▲ . Series S18.

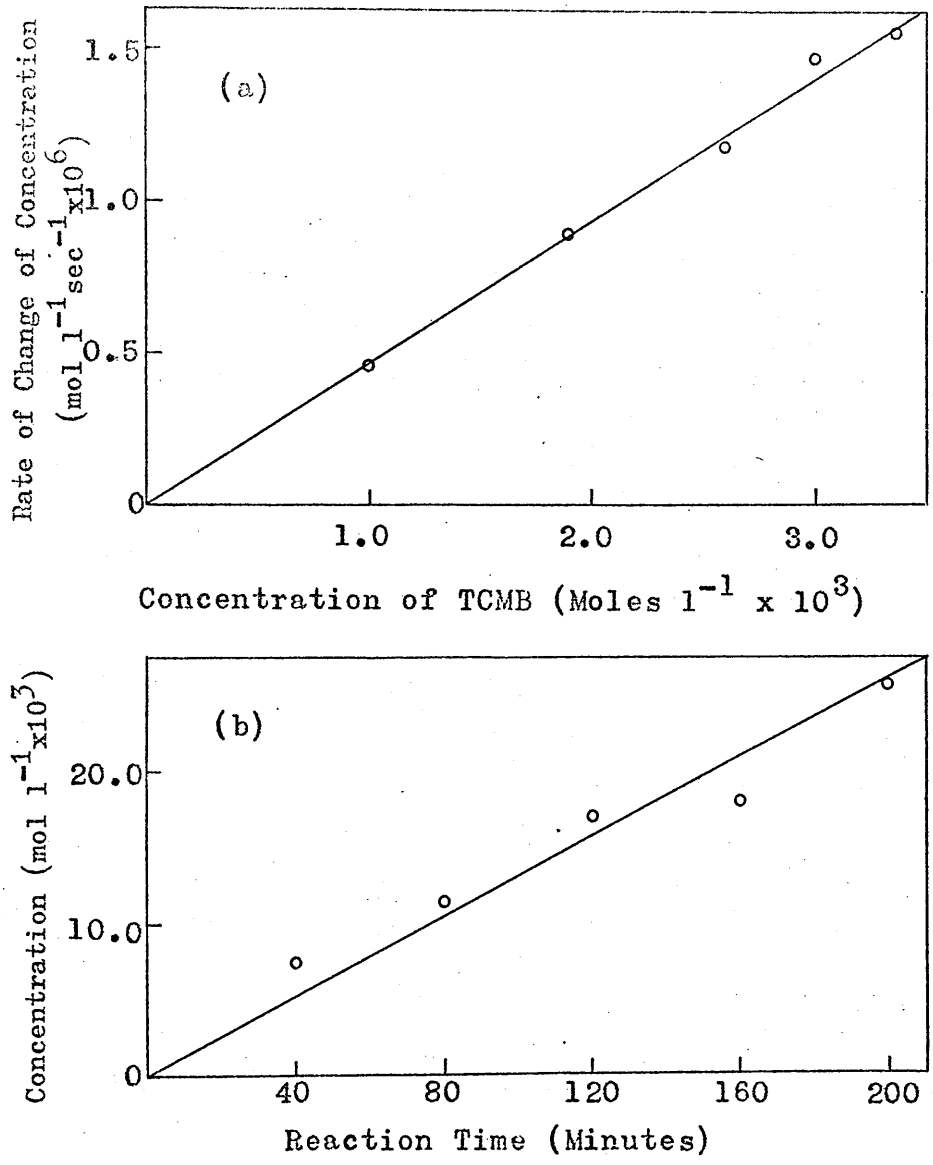

Figure 5.17 (a) Dependence of Rate of Formation of DTB on TCMB Concentration.

Series S18 (b) Reaction Curve for HCl.

Table 5.10 Experimental Data for S.19

Reaction Time (mins.)	Concentrations of Products (moles l^{-1}) DCMB	TCMB	DTB	HCl	Data from Reaction Curves $\frac{d(DTB)}{dt}$ ($mol.l^{-1}sec^{-1}x10^6$)	(TCMB) ($mol.l^{-1}$)
180	0.0742	0.0018	0.0010	0.0075	0.5	0.0006
300	0.0717	0.0025	0.0028	0.0104	0.8	0.0010
420	0.0696	0.0029	0.0045	0.0120	1.2	0.0014
600	0.0662	0.0032	0.0076	0.0164	1.5	0.0175
760	0.0636	0.0033	0.0101	0.0230	1.8	0.0200

Table 5.11 Experimental Data for S.20

Reaction Time (mins.)	Concentrations of Products (moles l^{-1}) DCMB	TCMB	DTB	HCl	Data from Reaction Curves $\frac{d(DTB)}{dt}$ ($mol.l^{-1}sec^{-1}x10^6$)	(TCMB) ($mol.l^{-1}$)
120	0.0738	0.0019	0.0013	0.0077	0.21	0.0012
240	0.0695	0.0030	0.0045	0.0102	0.32	0.0019
360	0.0653	0.0034	0.0083	0.0187	0.42	0.0024
480	0.0611	0.0033	0.0126	0.0266	0.49	0.0028
600	0.0578	0.0032	0.0160	0.0308	0.51	0.0031

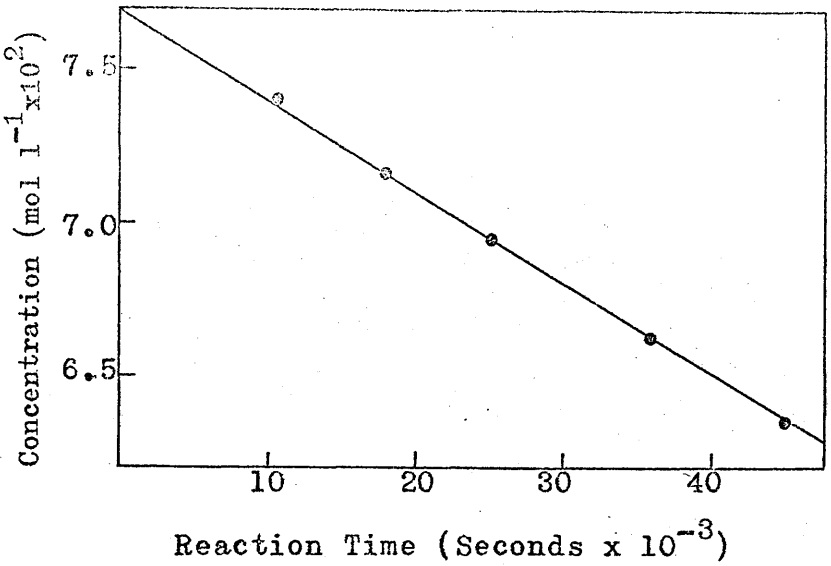

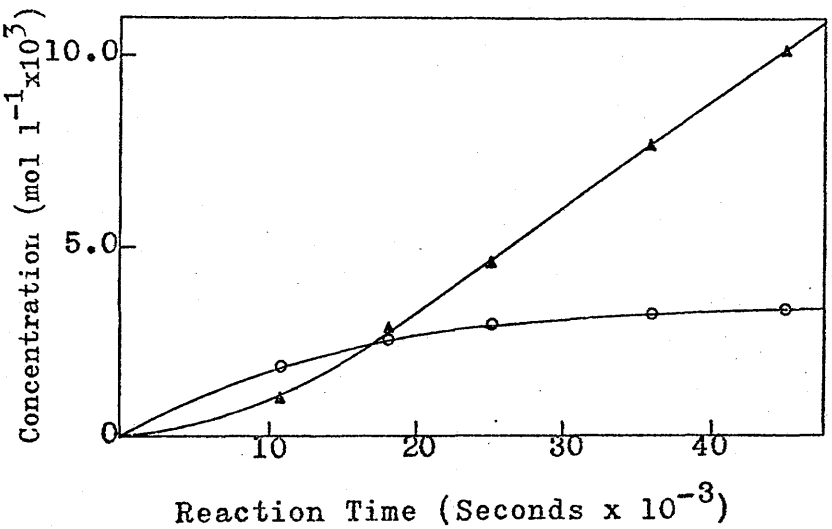

Figure 5.18 Reaction Curves for DCMB ⊙ , TCMB ○ and DTB ▲ . Series S19

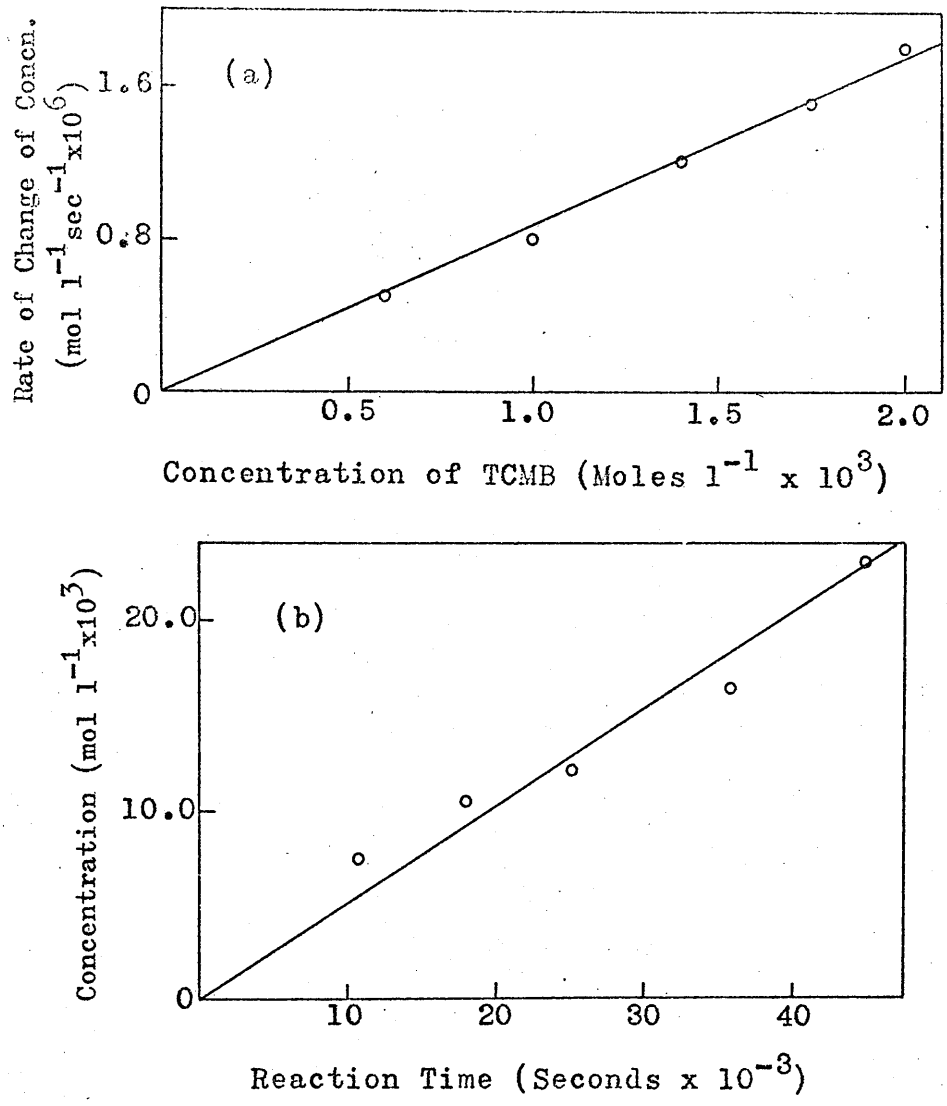

Figure 5.19 (a) Dependence of Rate of Formation of DTB on TCMB Concentration.

Series S19 (b) Reaction Curve for HCl.

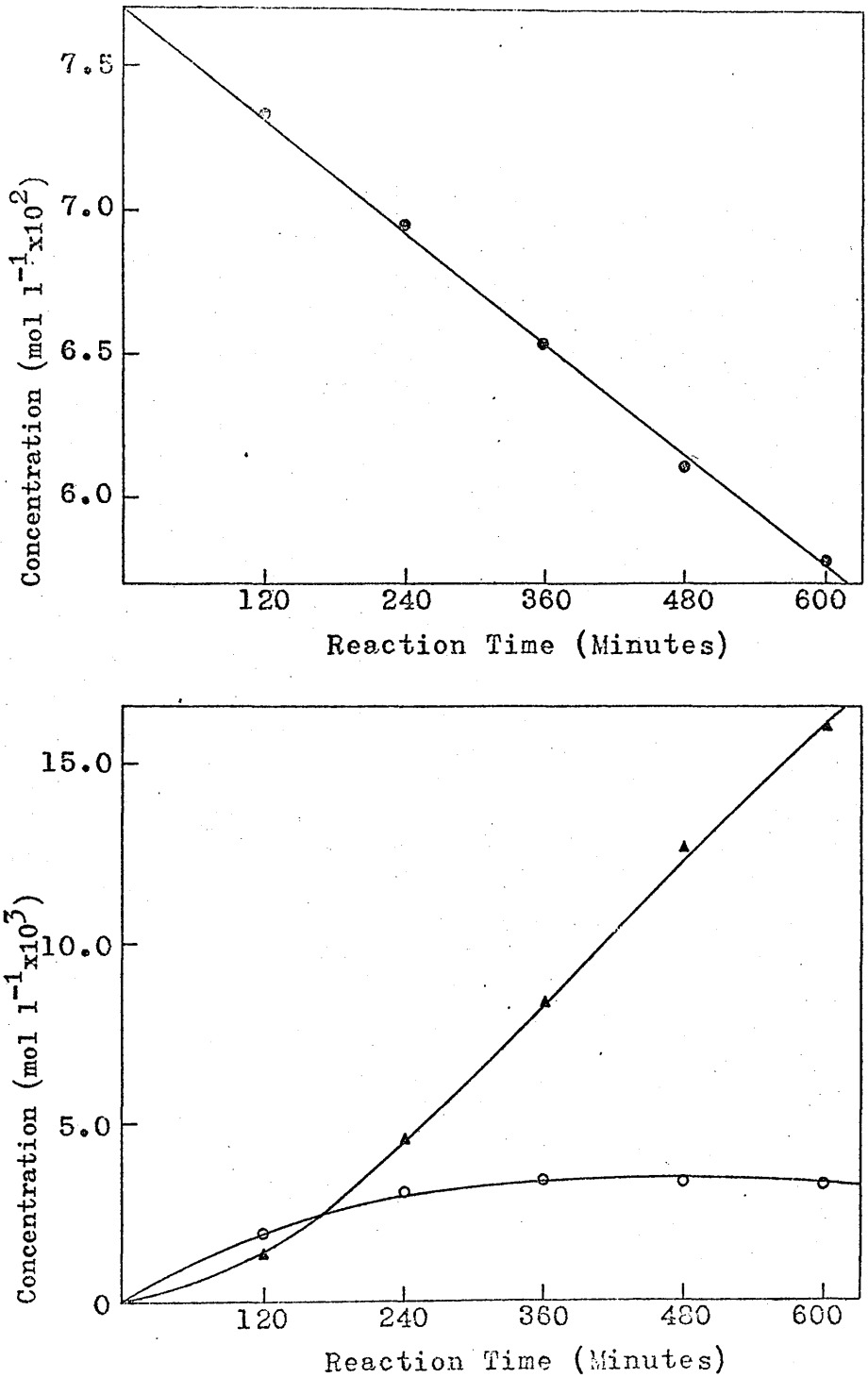

Figure 5.20 Reaction Curves for DCMB ⊙ , TCMB ○ and DTB ▲ . Series S20.

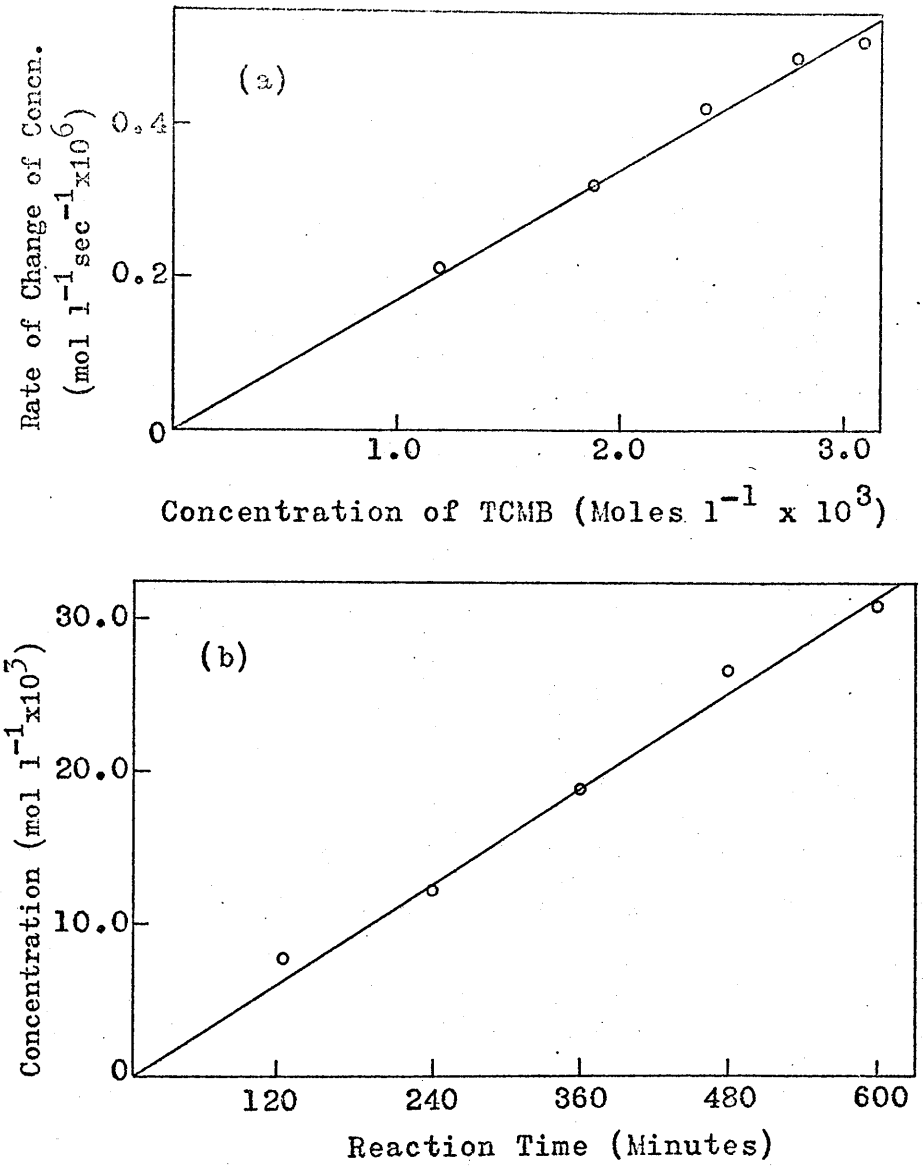

Figure 5.21 (a) Dependence of Rate of Formation of DTB on TCMB Concentration.

Series S20 (b) Reaction Curve for HCl.

initial rapid increase in concentration which levels off as the rate of formation of DTB increases continuously to high conversions. The reaction curves for HCl are not all well defined as the errors involved in measuring small amounts of HCl were large. They do suggest however that the rate of production of HCl is initially slow, increasing rapidly as the concentration of DTB increases and finally levelling off at later stages of the reaction.

Kinetics of Reaction:

The kind of experiments described above have allowed information about the kinetics of these reactions to be obtained. This information is presented in table 5.1 and details of the experiments are presented in tables 5.2 - 5.11 and figures 5.2 - 5.21.

The rate of the reaction between DCMB and thiophen to give TCMB can be estimated from the slope of the DCMB curve, as initially the decrease in concentration of DCMB will be due entirely to this reaction. By varying the initial concentrations of DCMB, thiophen and stannic chloride in turn, while keeping the concentrations of the other two constant, and plotting the rate of change of concentration of DCMB against initial concentrations of reagents, it has been shown that this reaction is first order with respect to DCMB, thiophen and stannic

chloride. The appropriate data is presented in figures 5.22 - 5.24.

As the thiophen concentration in all of these experiments was high compared with the DCMB concentration it may be assumed that this concentration does not change significantly during the initial stages of reaction. As stannic chloride is not consumed in the reaction its concentration will also remain constant. Thus plots of the changing slopes of the DTB curves against the corresponding values of the TCMB concentration illustrate directly the dependence of the rate of the second reaction on the concentration of TCMB. These plots are presented in figures 5.3 - 5.21 and it can be seen that there is a linear relationship indicating first order dependence. The slopes of these graphs plotted against varying initial concentrations of thiophen and stannic chloride again show first order dependence on both these reagents. The appropriate data is presented in figures 5.23 and 5.24.

The overall reaction may then be represented by,

$$DCMB + \text{Th} + SnCl_4 \xrightarrow{k_1} TCMB + HCl + SnCl_4$$

$$TCMB + \text{Th} + SnCl_4 \xrightarrow{k_2} DTB + HCl + SnCl_4$$

$$-\frac{-d(DCMB)}{dt} = k_1(DCMB)(\text{Th})(SnCl_4)$$

$$-\frac{-d(\text{Th})}{dt} = k_1(DCMB)(\text{Th})(SnCl_4) + k_2(TCMB)(\text{Th})(SnCl_4)$$

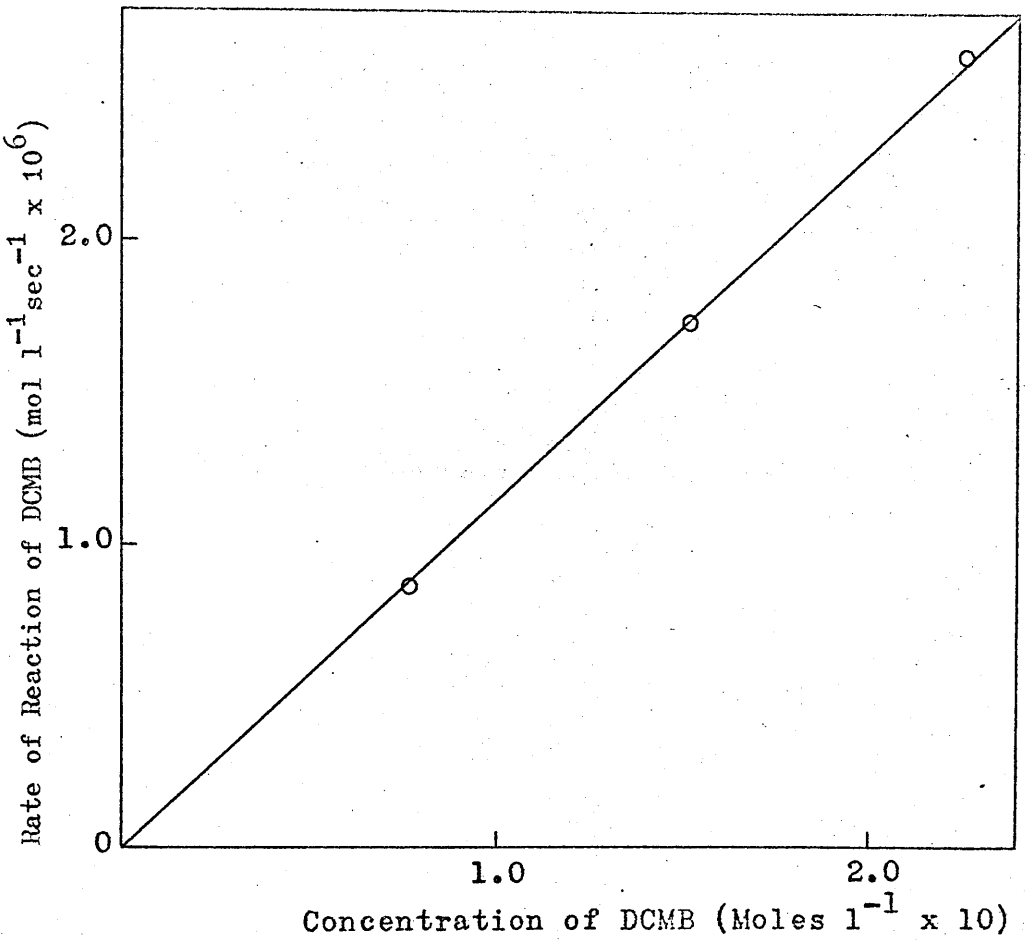

Figure 5.22 Dependence of Rate of Reaction of DCMB on DCMB Concentration.

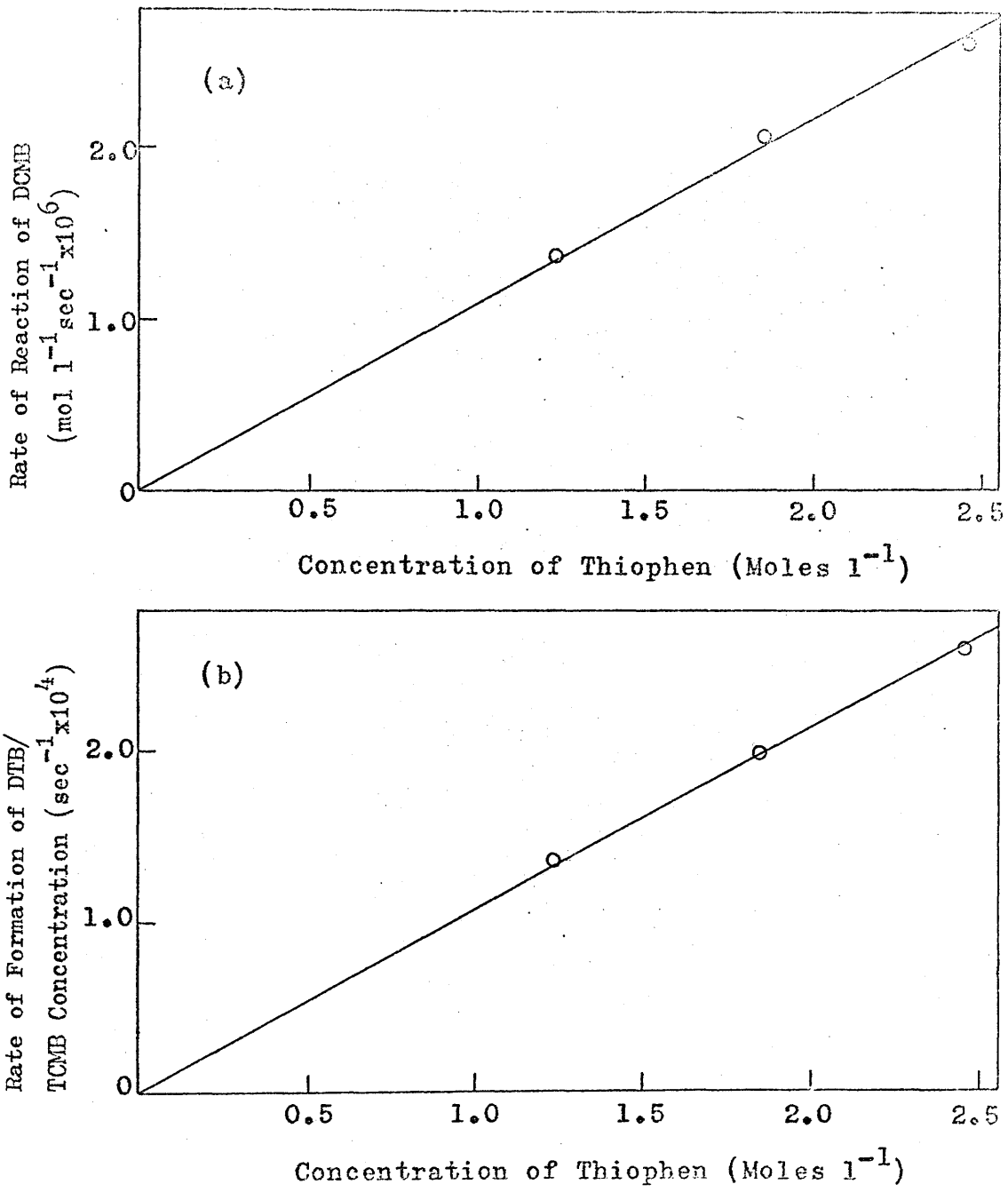

Figure 5.23 (a) Dependence of Rate of Reaction of DCMB on Thiophen Concentration.

(b) Dependence of Rate of Formation of DTB/ Concentration of TCMB on Thiophen Concentration.

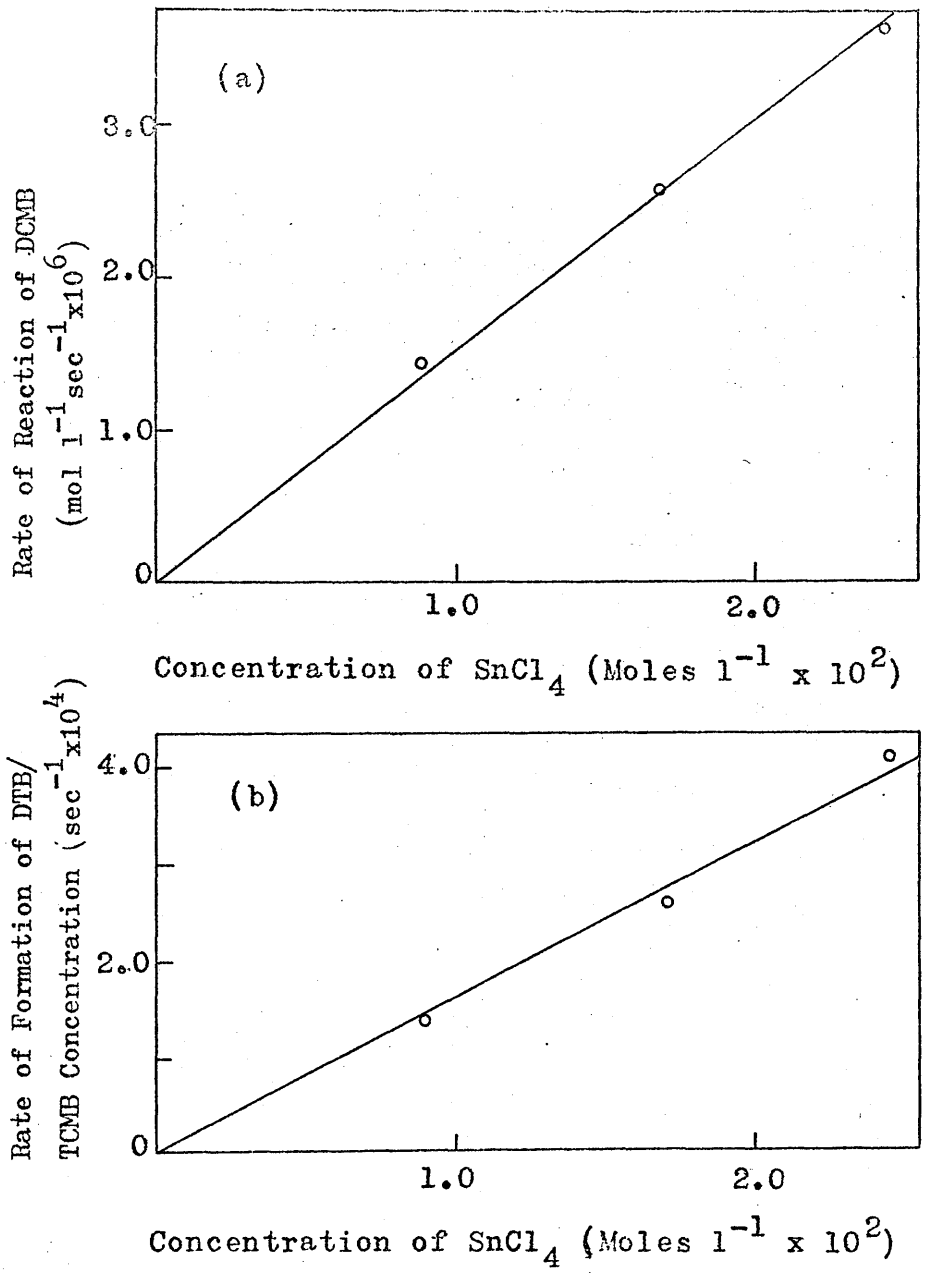

Figure 5.24 (a) Dependence of Rate of Reaction of DCMB on $SnCl_4$ Concentration.

(b) Dependence of Rate of Formation of DTB/ Concentration of TCMB on $SnCl_4$ Concentration.

$$\frac{d(TCMB)}{dt} = k_1(DCMB)(\text{⊙})(SnCl_4) - k_2(TCMB)(\text{⊙})(SnCl_4)$$

$$\frac{d(DTB)}{dt} = k_2(TCMB)(\text{⊙})(SnCl_4)$$

Average values of k_1 and k_2 have been calculated, using the above equations, from a large amount of data, and were found to be,

$$k_1 = 2.79 \times 10^{-4}\ l^2 mol^{-2} sec^{-1}$$

$$k_2 = 6.37 \times 10^{-3}\ l^2 mol^{-2} sec^{-1}$$

Reactions of this type are generally accepted as occurring in two steps[46], namely, complex formation between stannic chloride and a chloromethyl group followed by reaction of the complex with thiophen. Thus it seems probable that these rate constants are composite. They do however give a direct measure of the relative reactivity demonstrating that replacement of a chloromethyl group of DCMB by a thenyl group increases the reactivity of the other chloromethyl group by a factor of about forty. Grassie and Meldrum[29] in a similar investigation, using benzene as the aromatic molecule found that replacement of one chloromethyl group of DCMB by benzene caused an increase in reactivity of the second one by a factor of twenty, while the rate constants k_1 and k_2 were found to be $1.10 \times 10^{-4}\ l^2 mol^{-2} sec^{-1}$ and $1.30 \times 10^{-3}\ l^2 mol^{-2} sec^{-1}$ respectively. Thus replacement of the

benzene by the thiophen nucleus leads to greater reactivity in both stages of the reaction.

Energies of Activation E_1 and E_2 for these reactions were calculated from Arrhenius plots of data obtained over the temperature range $-20^{\circ}C$ to $+10^{\circ}C$. These plots are presented in figure 5.25 and the values obtained were,

$$E_1 = 7.93 \text{ k.cal/mole}$$

$$E_2 = 7.67 \text{ k.cal/mole}$$

The similarity of these values suggests that the structure of the polymer should not change significantly with the temperature of polymerisation.

5.3 Later Stages of the Reaction

Gel Permeation Chromatography has been used in this study to separate reaction products of higher molecular weight. Typical chromatograms are presented in figures 5.26 and 5.27. These chromatograms were obtained by plotting the weight of the residue from each fraction against its elution ratio, which may be defined as the ratio of the elution volume of the fraction to the elution volume of a reference material. The elution behaviour of samples are often described in terms of the ratio of elution volume to interstitial volume[45], however this method is sensitive to changes in external conditions,

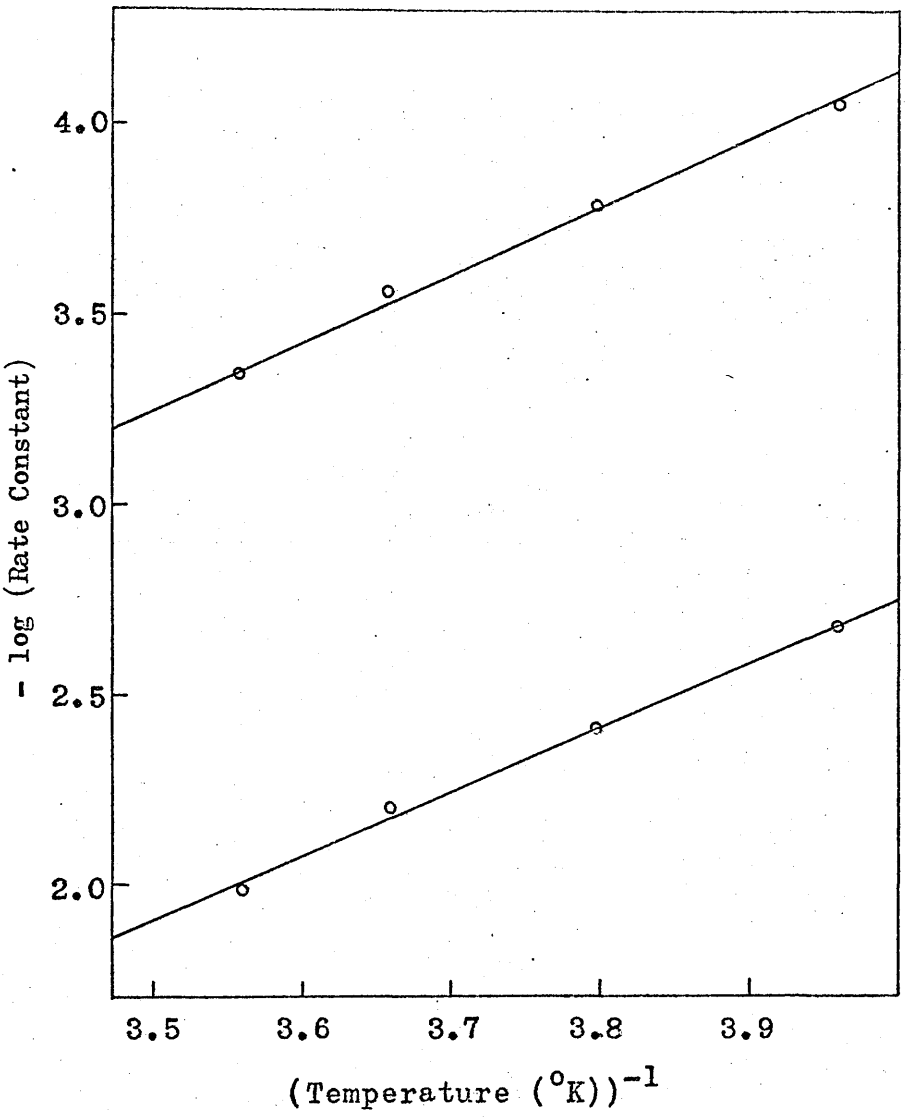

Figure 5.25 Arrhenius Plots of Rate Constants k_1 and k_2.

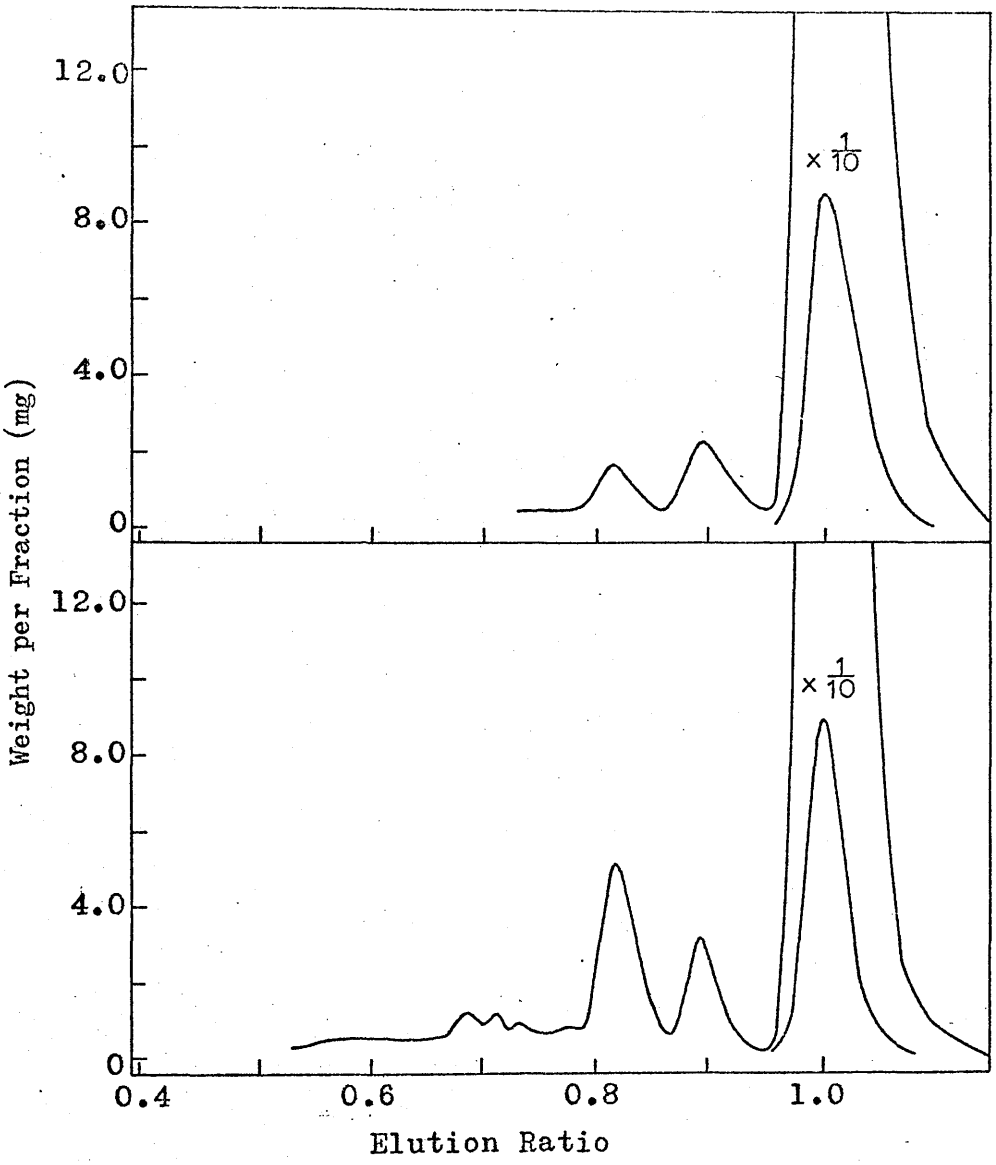

Figure 5.26 Typical Gel Permeation Chromatograms.

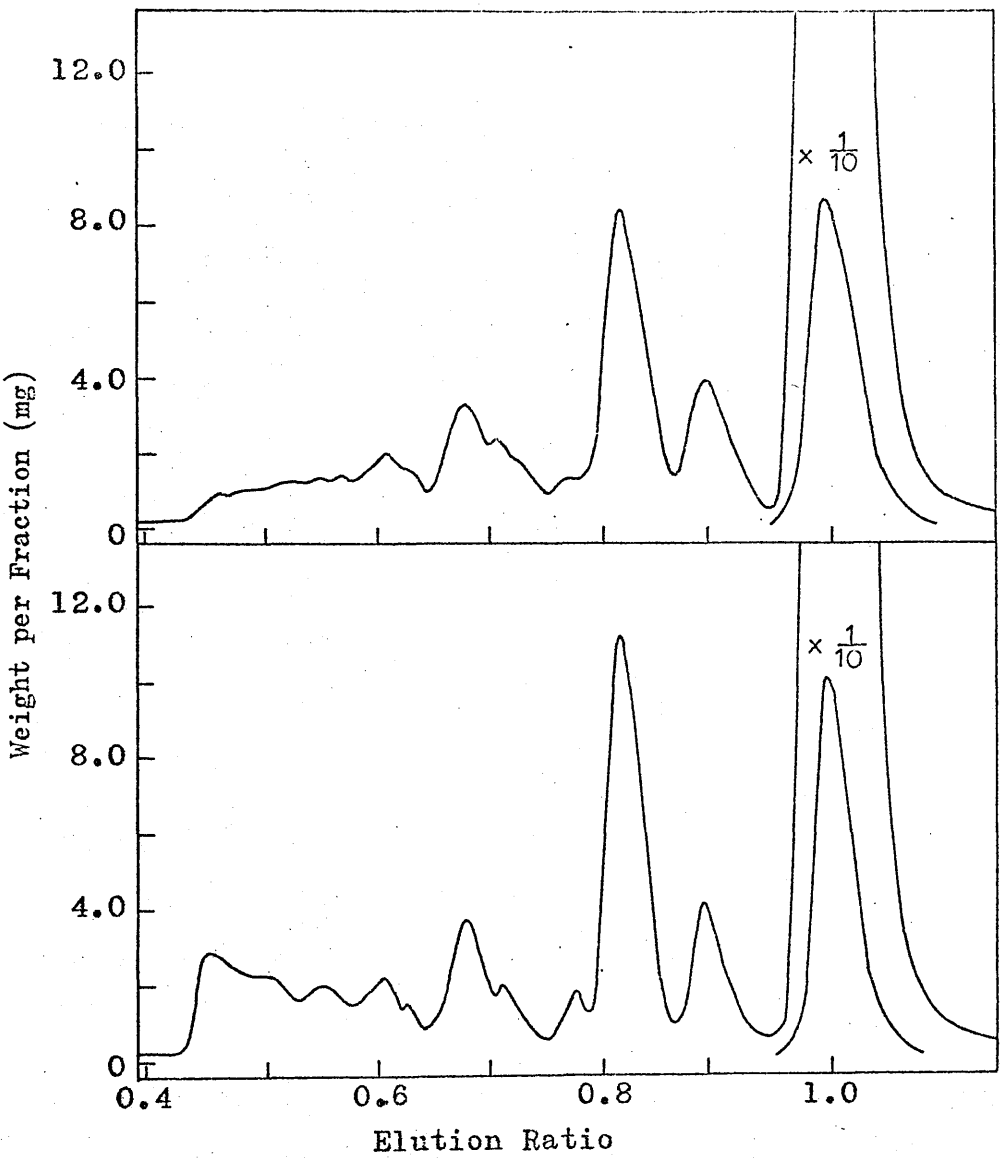

Figure 5.27 Typical Gel Permeation Chromatograms.

such as room temperature, which could not be readily controlled during this study. It was found convenient to use the maximum of the DCMB peak as the reference elution volume. This peak was common to all chromatograms and the elution ratio, thus defined, is less sensitive to changes in experimental conditions as the resulting changes in elution volumes tend to cancel each other.

It was not possible to subject every peak in every chromatogram to spectroscopic analysis, however it was found possible to identify the peaks by their elution ratios which are presented in table 5.12. It is clear that the elution ratios may be arranged in columns which do not overlap in value. The accuracy with which the peaks are defined is demonstrated in table 5.13 which provides justification for the use of elution ratios for the identification of peaks.

The typical chromatograms presented in figures 5.26 and 5.27 show that early in the reaction there is evidence of only the first two products, TCMB and DTB. As the reaction proceeds new peaks appear and increase in intensity until after long reaction times species with molecular weights near or above the limit determined by the pore size of the gel are present in high

Table 5.12 Product Elution Ratios

Reaction Time (hours)	ELUTION RATIO									
	P_2	P_3	P_4	P_5	P_6	P_7	P_8	P_9	P_{10}	P_{11}
6	0.896	0.817								
13	0.889	0.817	0.770	0.705	0.685					
18	0.889	0.816	0.770	0.710	0.685		0.612			
24	0.888	0.815	0.770	0.705	0.678	0.645	0.612			
30	0.890	0.819	0.774	0.715	0.680	0.637	0.610			
36	0.896	0.818	0.778	0.713	0.680	0.635	0.608	0.554	0.523	0.457
41	0.890	0.817	0.778	0.714	0.681	0.630	0.610	0.552	0.513	0.454
48	0.889	0.817	0.771	0.713	0.681	0.641	0.615	0.550	0.523	0.445

Table 5.13

Peak No.	Mean Elution Ratio	Maximum Deveation from Mean Elution Ratio
1	1.000	0
2	0.891	+ 0.005 - 0.003
3	0.817	+ 0.002 - 0.002
4	0.773	+ 0.005 - 0.003
5	0.711	+ 0.004 - 0.006
6	0.681	+ 0.004 - 0.003
7	0.638	+ 0.007 - 0.003
8	0.611	+ 0.003 - 0.003
9	0.552	+ 0.002 - 0.002
10	0.520	+ 0.003 - 0.007
11	0.452	+ 0.005 - 0.007

concentration. These species account for peaks P_{10} and P_{11} in the chromatograms and indicate that in this system the molecular weight limit determined by the gel is of the order of 1300.

Quantitative Estimation of Products:

Although good separation of DCMB, TCMB and DTB was achieved all other peaks in the chromatograms, except P_4 and P_5, overlapped considerably. Thus the total amount of material represented by each peak had to be obtained by extrapolating its resolved parts. Because of the very small amounts of materials present and the necessity for the extrapolation of peaks, there were considerable errors in estimated amounts of the products. It was not

possible to estimate these errors precisely. However they were not so large as to prevent useful delineation of the changes in concentration of the products during reaction.

The overlapping of peaks P_7 and P_8 and peaks P_{10} and P_{11} was so great in some chromatograms that separation by extrapolation into their resolved parts was not feasible. It has already been shown, however, that P_7 and P_8 are isomers and no identification of P_{10} and P_{11} has been achieved. It seemed reasonable therefore to calculate the total amounts of P_7 and P_8 and P_{10} and P_{11} together and to treat them as one product in the construction of reaction curves.

Analysis of Reaction Curves:

Experimental data and the concentrations of products obtained using the techniques described above are presented in table 5.14. The reaction curves obtained by delineation of the changes in concentration of the products during reaction are represented in figures 5.28 and 5.29.

Again, as found in the G.L.C. study of the initial stages of reaction, the reaction curve for DCMB is linear, thus confirming that substitution of DCMB into the aromatic nuclei of the products occurs at a rate which is comparable, if not higher, than the rate of

Table 5.14 Gel Permeation Data

Concentrations of Starting Materials (moles l^{-1})

DCMB 0.2239 Thiophen 0.2229 $SnCl_4$ 0.0170

Concentrations of Products (moles l^{-1})

Run No.	Reaction Time (hours)	P_1	P_2	P_3	P_4	P_5	P_6	$P_{7,8}$	P_9	$P_{10,11}$
S21/1	41	0.1914	0.0069	0.0130	0.0016	0.0020	0.0034	0.0020	0.0014	0.0021
S21/2	48	0.1825	0.0081	0.0144	0.0020	0.0027	0.0045	0.0040	0.0018	0.0030
S21/3	30	0.1979	0.0071	0.0108	0.0008	0.0019	0.0027	0.0014	0.0004	0.0007
S21/4	36	0.1927	0.0073	0.0121	0.0015	0.0024	0.0034	0.0023	0.0008	0.0014
S21/5	24	0.2025	0.0064	0.0096	0.0008	0.0015	0.0018	0.0009	-	-
S21/6	18	0.2079	0.0057	0.0076	0.0006	0.0013	0.0008	0.0002	-	-
S21/7	13	0.2118	0.0056	0.0055	0.0002	0.0005	0.0002	-	-	-
S21/8	6	0.2190	0.0031	0.0017	-	-	-	-	-	-

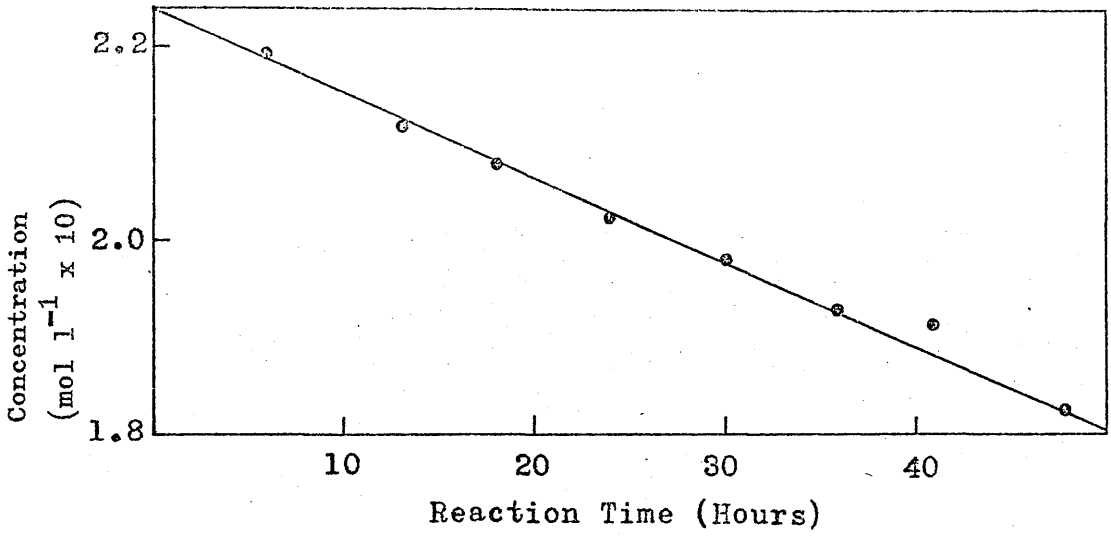

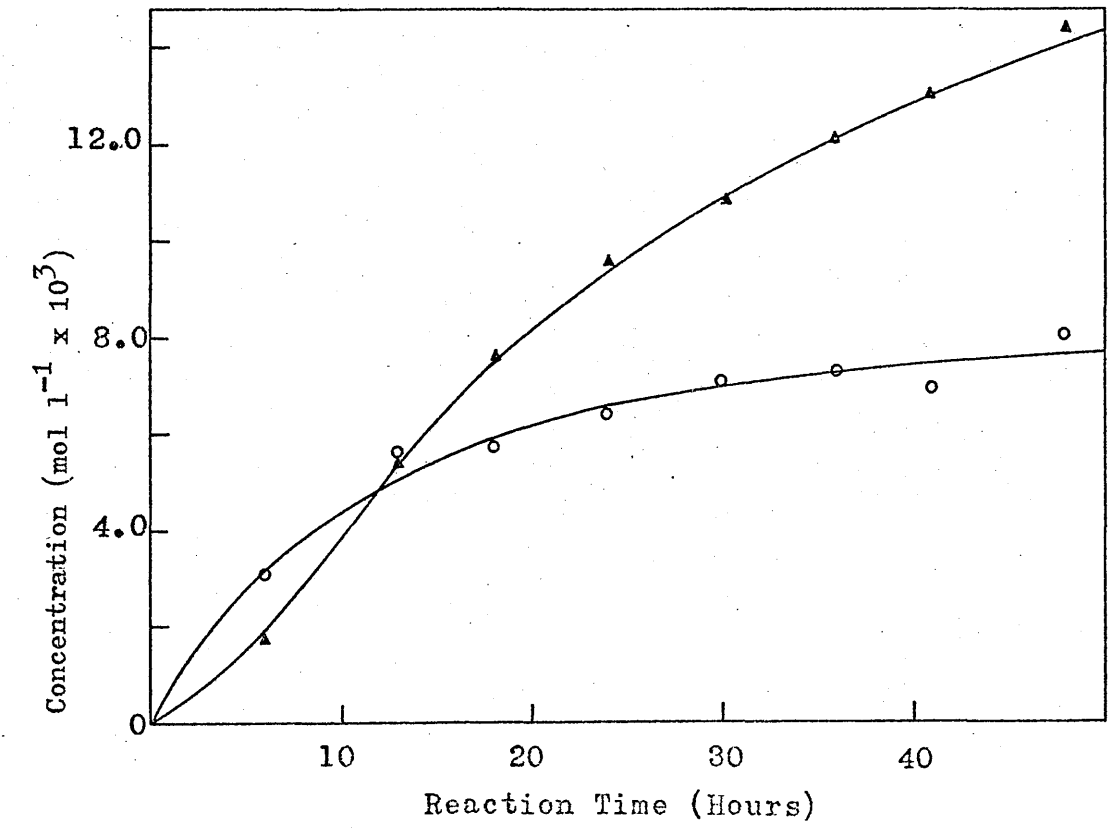

Figure 5.28 Reaction Curves for P_1 ○ , P_2 ○ and P_3 ▲ from G.P.C. Data.

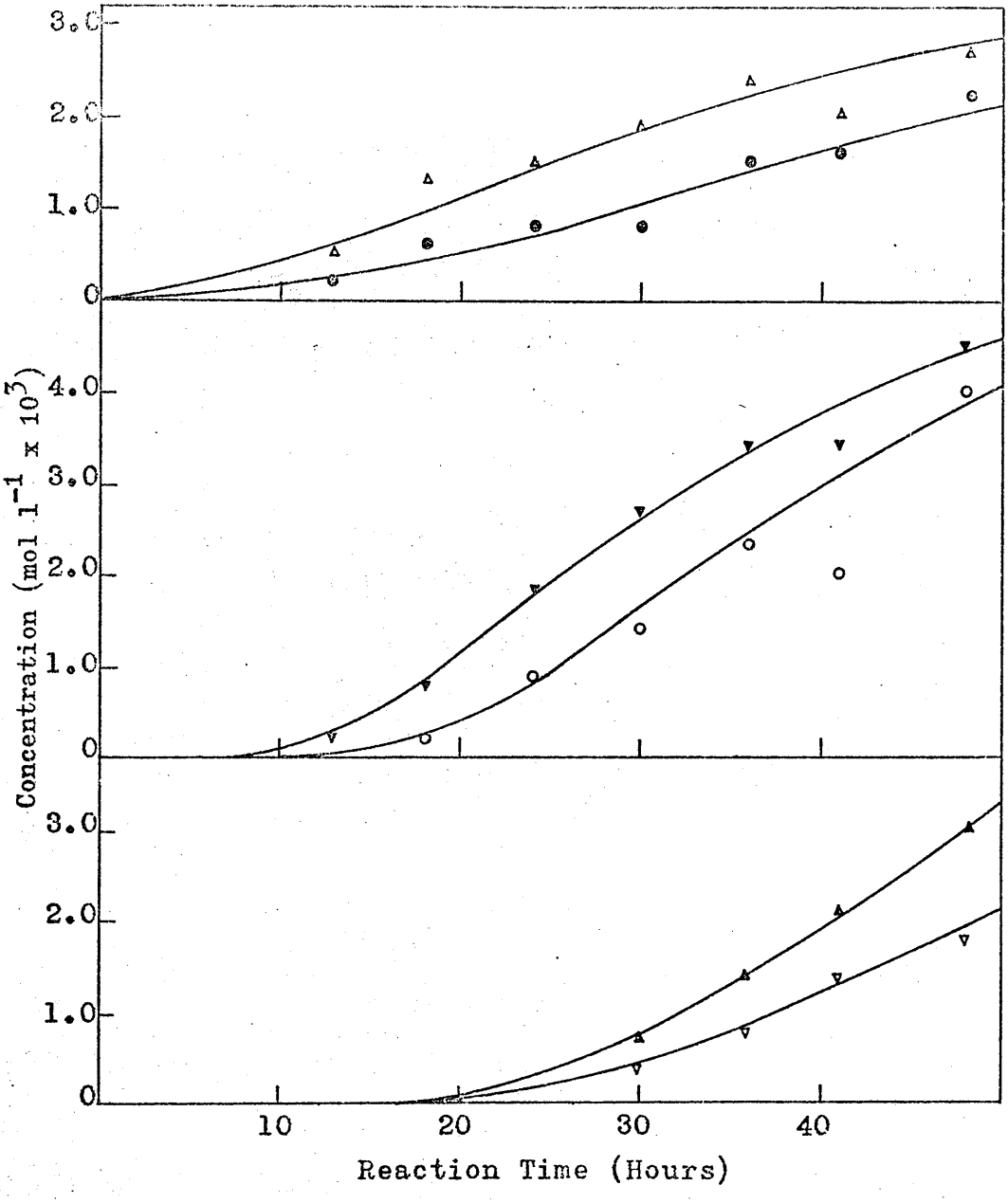

Figure 5.29 Reaction Curves for P_4 ▵ , P_5 ⊙ , P_6 ▽ , $P_{7,8}$ ○ , P_9 ▽ and $P_{10,11}$ ▲ from G.P.C. Data.

substitution into thiophen.

The reaction curves for TCMB and DTB are also similar to those obtained from G.L.C. data. It can be seen, however, that the rate of increase of DTB concentration falls off in a similar manner to that of TCMB, thus showing that the rate of reaction of DTB with chloromethyl compounds is comparable with its rate of formation. The shape of the DTB curve also confirms that the use of high concentrations of thiophen in the G.L.C. study of the initial stages of reaction was successful in hindering further reaction of DTB. Only a very slight falling off in the rate of increase in DTB concentration, at later stages of reaction, was noted during the G.L.C. study while the curves obtained from G.P.C. show reaction of DTB at very early stages of the reaction.

One surprising feature of the reaction curves obtained for P_4 and P_5 is the relatively large amounts of P_4 produced early in the reaction. If it is assumed that P_4 is produced exclusively by self-condensation of P_5, then the relative proportions of P_4 and P_5 early in the reaction would suggest that this self-condensation is a very facile reaction. This would seem to suggest that account must be taken of the self-condensation of

all chloromethyl compounds of high molecular weight in any analyses of this reaction. The reaction curves for P_4 and P_5 are very similar and both show only a very gradual increase in concentration as the reaction proceeds. This would seem to indicate that both are very reactive. The curve obtained for P_5 does confirm that the second chloromethyl group of the DCMB molecule, incorporated into a higher molecular weight products, is extremely reactive. Further evidence for the reactivity of this group is given by the complete absence of chloromethyl compounds of higher molecular weight than P_5 in all chromatograms. While it is true that conditions for separation of these compounds are not very good, due to the overlapping of peaks, if they had been present some evidence would have been expected of their presence as impurities in the spectroscopic studies of the other materials.

The reaction curves for all other products are similar in form to that obtained for DTB. These curves, however, were not well enough delineated or carried to high enough conversion to determine relationships between the various components. Thus it was not possible to determine whether the maximum rates of formation of fully aromatic products coincide with the concentration

maximum of the preceeding fully aromatic compound. The reaction curves for all products do however indicate that the products are produced by a series of consecutive reactions which are similar to those described for the formation of the first two products.

Although rate constants for some of the reaction steps involving molecules of molecular weight higher than DTB could very approximately be determined from the data presented above, using the same methods as were applied to the G.L.C. data, such calculations would involve very large approximations. It would not be possible to take account satisfactorily of the many different paths to some products, and the large extent to which self-condensation of chloromethyl compounds takes place would be another factor which would be difficult to take into account. The values of rate constants, thus obtained, would therefore be extremely doubtful and it was not considered that such calculations were justified.

5.4 Summary

The work described in this chapter represents a further step towards the precise characterisation of the polymer produced by the DCMB-thiophen reaction.

The overall reaction may be summarised as a series

of competing, consecutive reactions of the type,

$$A + B \longrightarrow C + D .$$

However account must also be taken of the self-condensation of chloromethyl compounds of higher molecular weight than TCMB.

Products containing only one chloromethyl group have been shown to be much more reactive than DCMB. Thus these products are present in small amounts throughout the reaction. The thiophen nucleus has been shown to be much more reactive than the benzene nucleus in similar reactions[29]. This should lead to higher molecular weight products which are preferentially substituted in the thiophen rings. However there is no reason to suppose that as the number of reactive sites on thiophen nuclei decreases the extent of branching through benzene nuclei will not increase.

Thus it can be seen that the overall reaction is extremely complex. The complexity of the reaction defies the complete kinetic analysis of the reaction by conventional techniques. It should, however, be possible to carry out such an analysis using computer based methods and so to gain greater insight into the structure of the polymer.

CHAPTER 6

THERMAL ANALYTICAL STUDIES OF RELATED POLYMERS

6.1 Introduction

As a further step in the study of Friedel-Crafts polymers containing heterocycles, attempts were made to synthesise polymers by reaction of DCMB with various substituted thiophens and to make a simple thermal analytical study of the resultant products. The presence of substitution on the thiophen ring would be expected to have a marked effect on the properties of the polymers by reducing the extent of branching through the thiophen ring. Thus it was hoped that a comparison of the thermal stabilities of the resultant polymers with that of the thiophen polymer would give some insight into the reasons for the known stability of polymers of this type.

6.2 Preparation of Polymers

Polymers were prepared by reaction of thiophen, 2-methyl thiophen, 3-methyl thiophen, 2.5-dimethyl thiophen and 2-chloro thiophen with DCMB, catalysed by stannic chloride. The reactions were carried out in DCE solution under an atmosphere of dry nitrogen using the techniques described in chapter 2. The course of the reaction was followed by estimating the HCl formed which was

continuously swept from the reaction vessel by the nitrogen stream. Typical reaction curves are illustrated in figure 6.1, the yields of HCl being presented as a percentage of the theoretical possible yield. These curves were obtained from a large volume of experimental data and so no experimental points are shown. The reaction curves obtained for the DCMB-thiophen (T_1), DCMB-2-methyl thiophen (T_2), DCMB-3-methyl thiophen (T_5) and DCMB-2.5-dimethyl thiophen (T_3) polymers (figure 6.2) were all very similar and are represented by curve A. The curve obtained for the DCMB-2-chloro thiophen (T_4) polymer, curve B, does not have the same characteristics, however, showing a much slower initial rate of reaction but proceeding to higher conversions.

The reaction characteristics for polymers T_1, T_2 T_3 and T_5 were also very similar. Reaction solutions became pale yellow on the addition of stannic chloride. As the reactions proceeded the yellow colouration darkened, through orange, to give deep red solutions at high conversions, except in the case of T_3 where the solution remained orange coloured throughout the reaction. As the solutions darkened they became opaque and polymer was precipitated. The insoluble material was washed with water and organic solvents and dried under vacuum

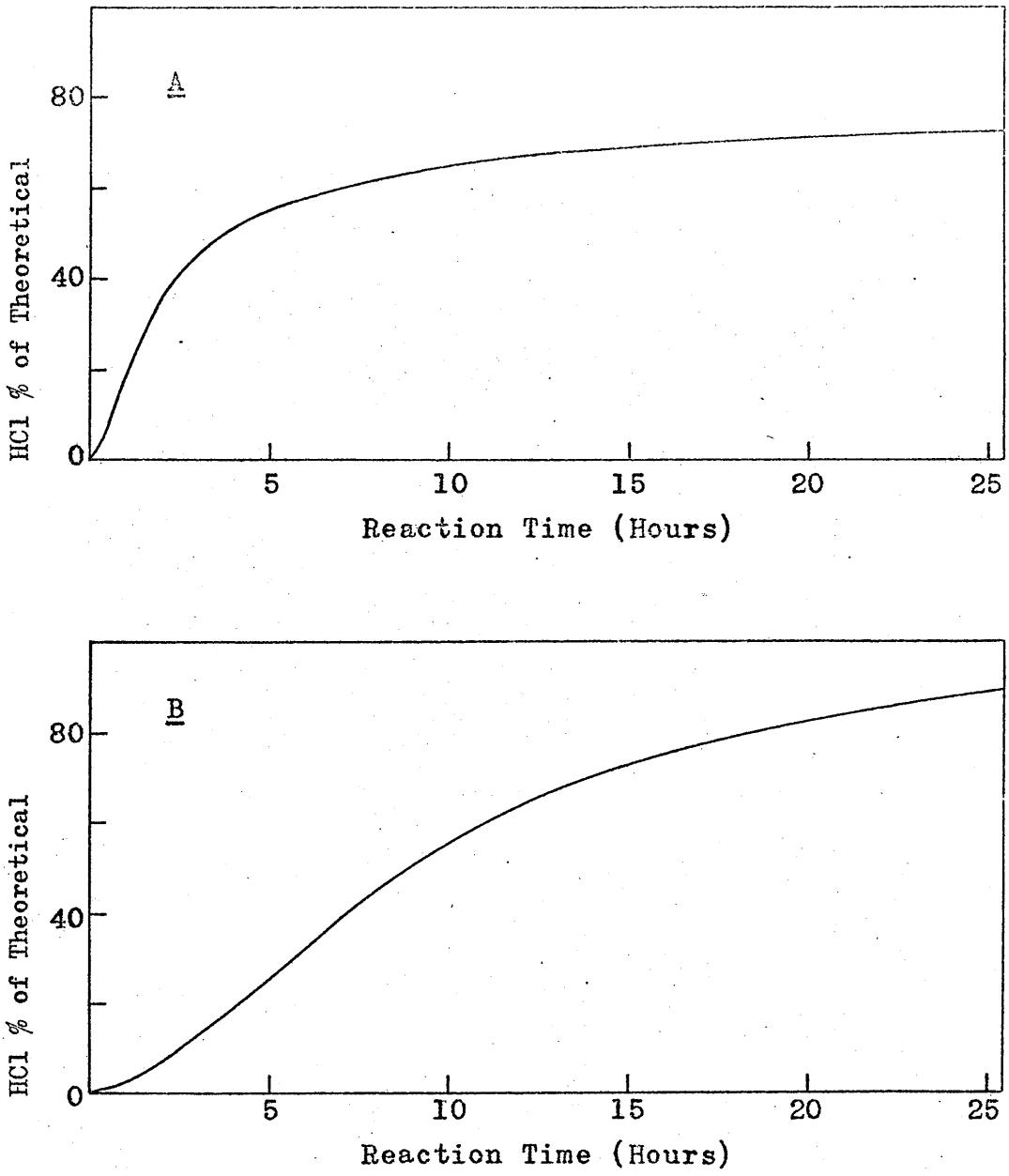

Figure 6.1 Evolution of HCl During Polymerisation.

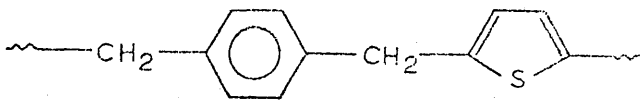

T_1

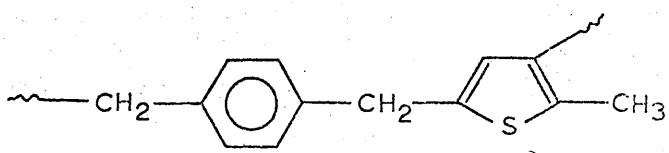

T_2

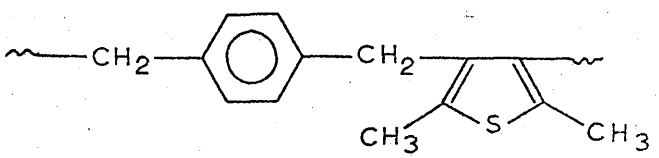

T_3

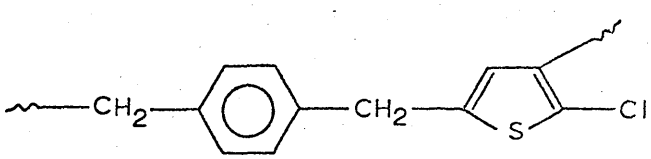

T_4

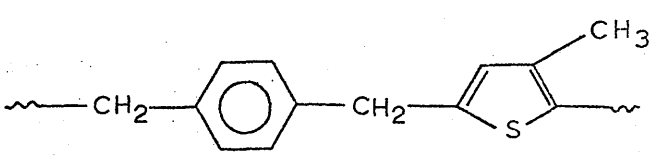

T_5

Figure 6.2 Polymer Repeat Units.

at 100°C. Soluble polymers were precipitated into either methanol or n-hexane and dried at 100°C. After drying the soluble products showed a marked decrease in solubility, in most cases becoming almost completely insoluble in all common organic solvents. All products were fine powders ranging in colour from very pale yellow T_3 to dark brown T_1 ("soluble" product).

The characteristics of the T_4 reaction were in many ways different from those described above. The initially colourless solution rapidly darkened to give an extremely dark reaction mixture. No insoluble products were obtained but a black soluble gum was obtained by precipitation by methanol and drying at 60°C under vacuum. The solubility of this material allowed a molecular weight determination to be carried out which gave a value of 4,600 ± 400.

6.3 Spectroscopic Analysis

Because of the insolubility of all polymers except T_4 spectroscopic analyses were limited to the I.R. spectra presented in figure 6.3. The spectra obtained for both the "insoluble" and "soluble" products were found to be very similar in every case and only one spectrum is presented for both types of product. The spectrum shown for T_1 is very similar to that presented for the thiophen

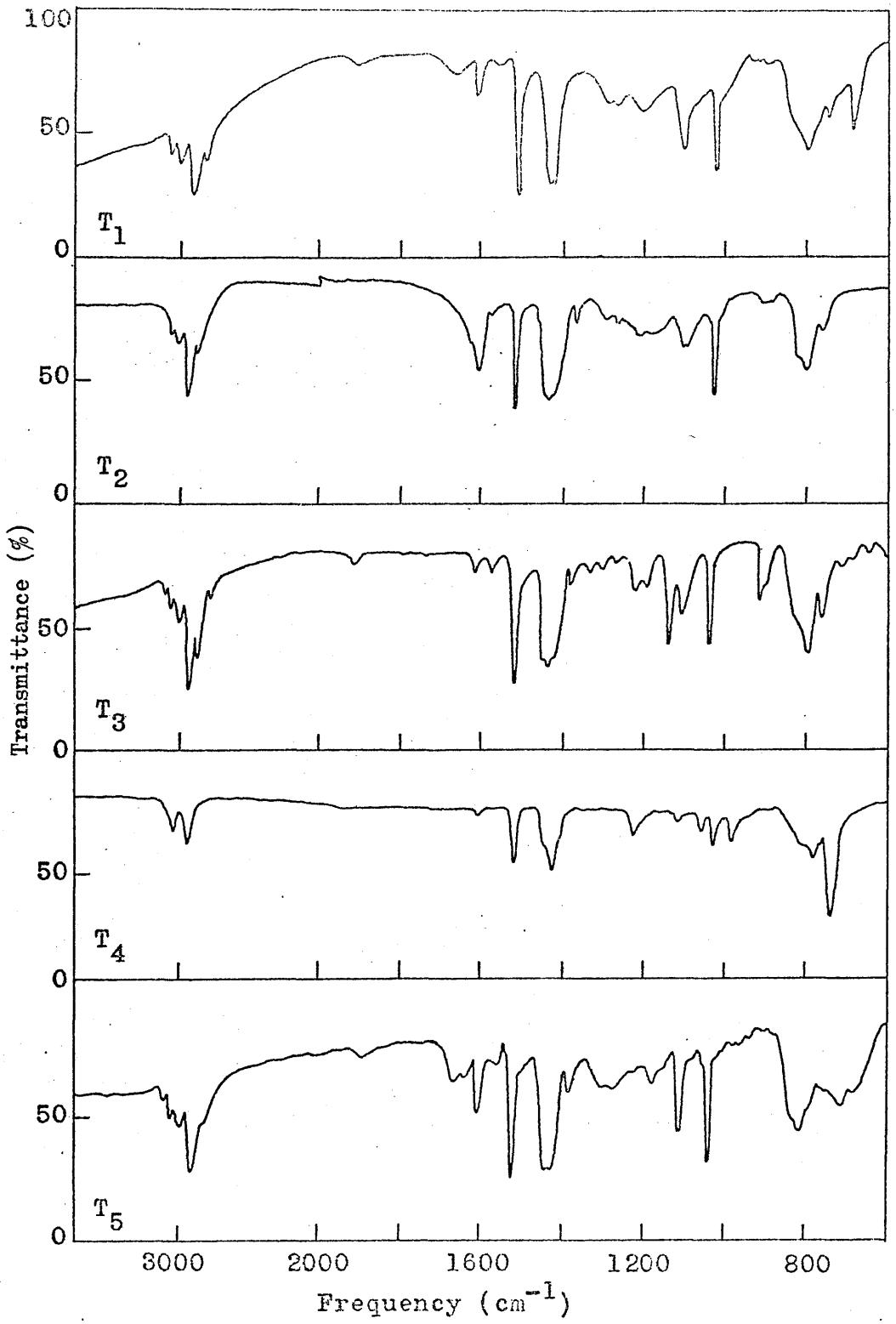

Figure 6.8 Infrared Spectra of Polymers.

polymer in chapter 3. It is better resolved, however, and shows more clearly the presence of peaks at 800, 755 and 692 cm^{-1}. The spectrum obtained for T_4 is very poorly resolved due to the great difficulty encountered in obtaining either a good salt disc or thin film of this product.

The spectra show that the general structure of all the polymers is very similar, with the only major differences occurring in the region 900 cm^{-1} - 625 cm^{-1}. These differences are undoubtably due to the different substitution patterns in the products, but the spectra are not resolved well enough to allow an analysis of these patterns to be carried out.

6.4 Thermal Analysis

Thermal analyses were carried out using both the T.G.A. and T.V.A. techniques described in chapter 2. Degradations were carried out under nitrogen and air in the T.G.A. apparatus and under vacuum in the T.V.A. apparatus. In both types of analyses samples were linearly programmed from 50°C to 1000°C at 10°/min. In the labelling of thermograms pirani gauges will be denoted by the temperature of the cold trap which they immediately follow.

The thermograms obtained for the polymers are

represented in figures 6.4 to 6.8. The "insoluble" products are designated by the symbol (I) and the "soluble" products with the symbol (S). Attempts to obtain reproducible thermograms by degrading the "insoluble" polymers in air were unsuccessful, due to the onset of combustion during degradation, and only the thermograms obtained for the "soluble" polymers are shown. The T.V.A. Thermograms obtained for both the "soluble" and "insoluble" products T_1, T_2 and T_3 were very similar and only one trace is presented. T_5(I) and T_5(S) gave very similar T.G.A. traces and again only one is shown.

The T.G.A. thermograms obtained for T_1, under nitrogen (figure 6.4), show that after an initial small weight loss at 200°C true degradation begins above 300°C. Weight loss above this temperature is a gradual process with the "insoluble" polymer exhibiting greater stability than the "soluble" material. The T.V.A. thermogram is similar to that presented in chapter 2 and supports the conclusion that true degradation begins above 300°C. The T.V.A. thermogram suggests that four separate reactions are occurring during degradation with materials which are not condensable at -196°C being given off throughout the decomposition. Degradations

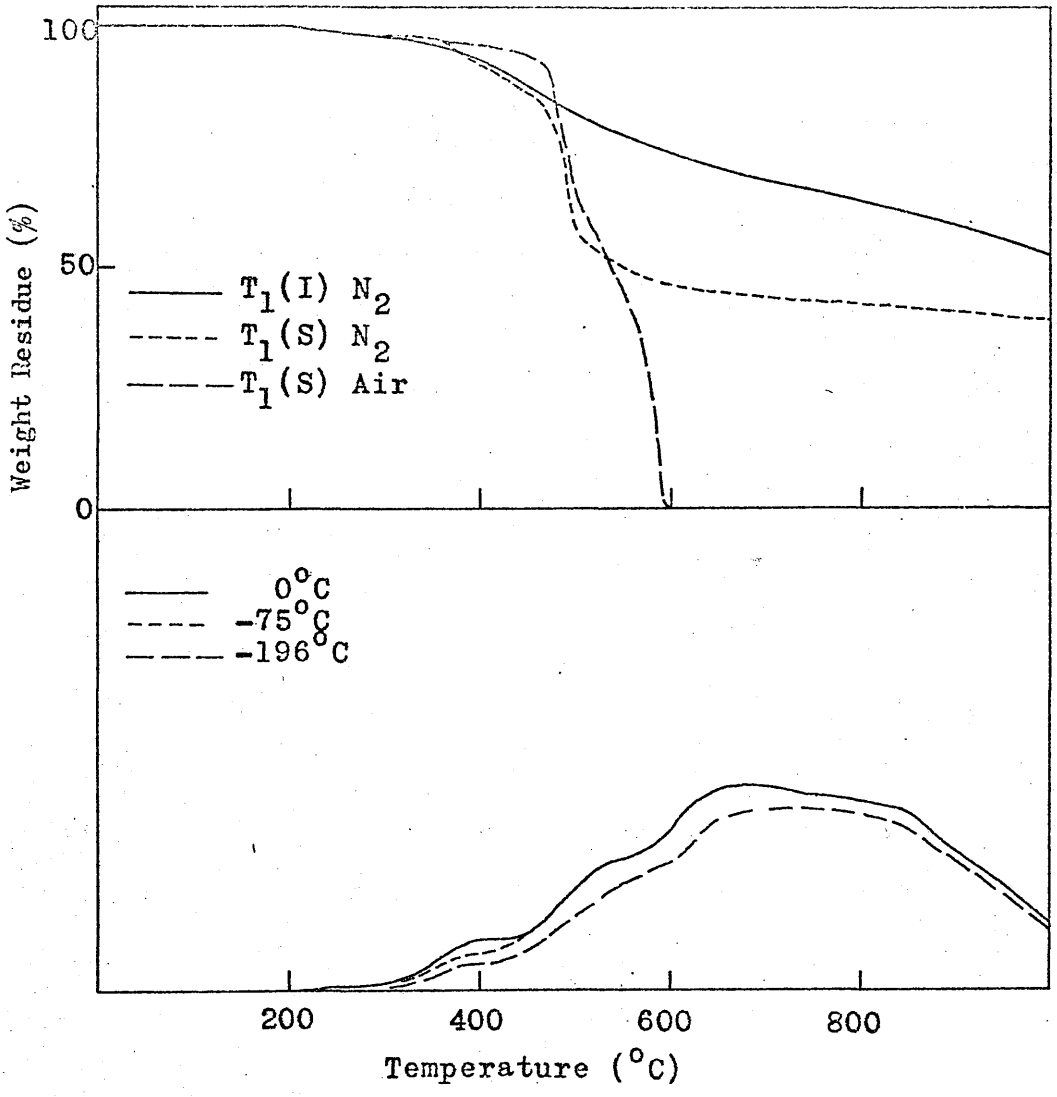

Figure 6.4 T.G.A. and T.V.A. Thermograms for T_1.

in air indicated that the polymer exhibits improved stability, under these conditions, up to 450°C. Thereafter rapid weight loss occurs until all the material has been consumed by 600°C.

When degraded under nitrogen the thermogram for $T_2(I)$ (figure 6.5) shows weight loss beginning at 100°C. This is probably due however to the presence of low molecular weight species in the polymer. This conclusion is supported by the T.V.A. analysis which indicates that degradation begins about 300°C. The thermograms, under nitrogen, for $T_2(I)$ and $T_2(S)$ are similar in shape but again weight loss is more rapid and occurs at lower temperatures with the "soluble" polymer. Analysis of these thermograms is complicated however by the initial weight loss at lower temperatures. The thermogram for degradation in air again indicates greater stability of the polymer before rapid weight loss occurs above 400°C. The T.V.A. thermogram has a large peak at 500°C coinciding with the point of most rapid weight loss in the T.G.A. thermograms. Thereafter two more reactions take place which do not appear to involve much weight loss.

The thermograms obtained for $T_3(I)$ and $T_3(S)$ (figure 6.6) are different from those obtained from

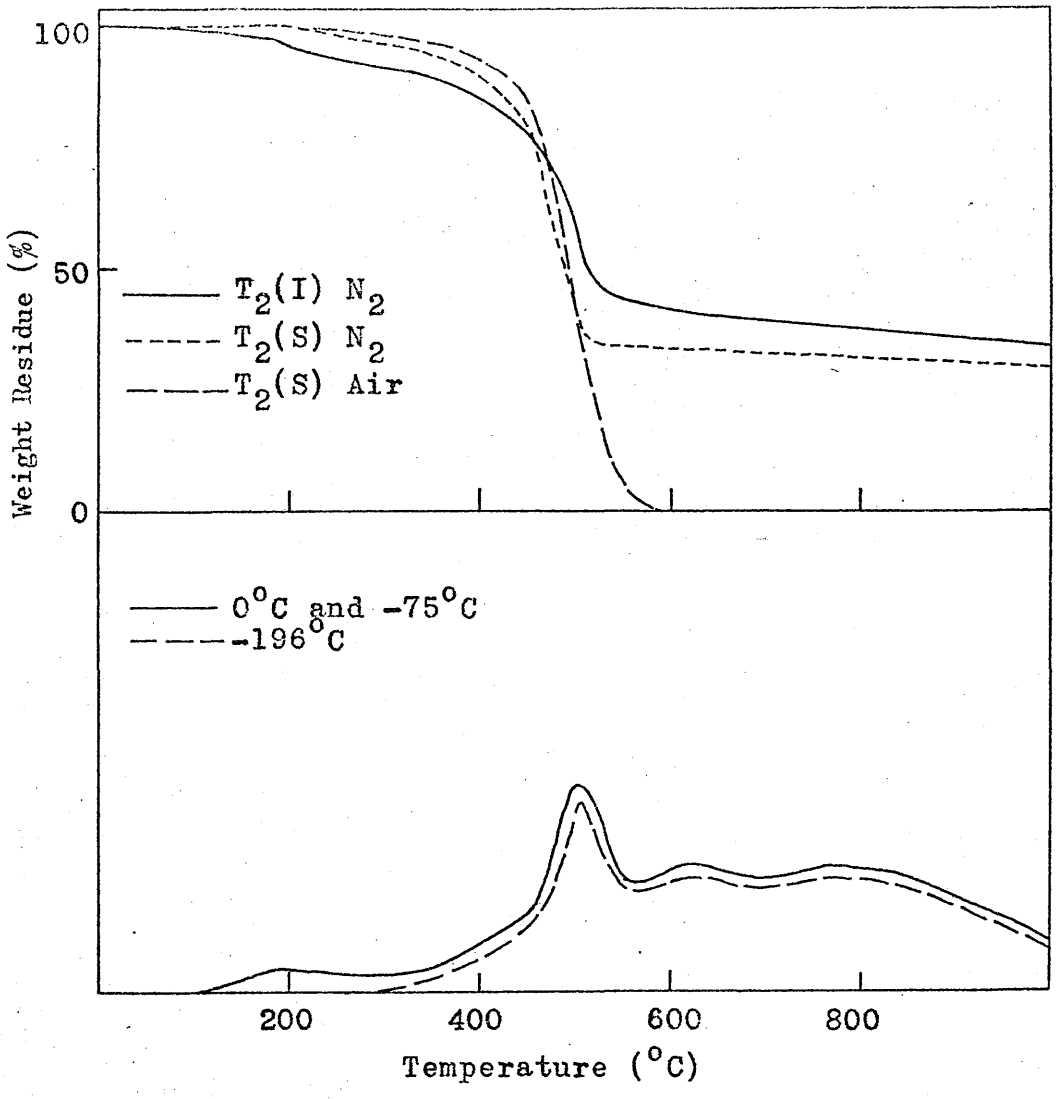

Figure 6.5. T.G.A. and T.V.A. Thermograms for T_2.

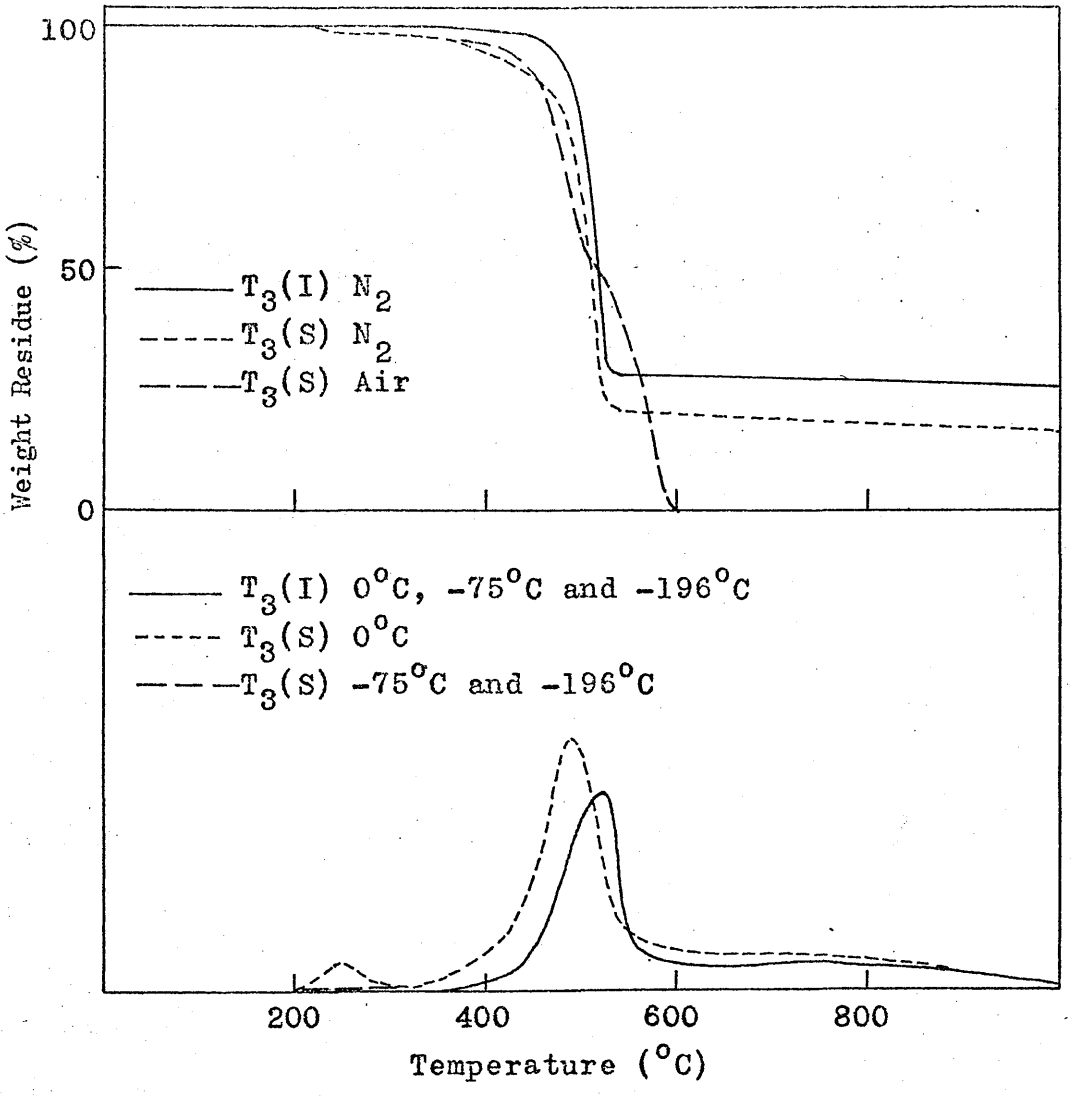

Figure 6.6 T.G.A. and T.V.A. Thermograms for T_3.

either T_1 or T_2. These thermograms indicate that the polymers have excellent stability below 400°C with rapid weight loss beginning at this temperature for the "soluble" product and at 450°C for the "insoluble" product. Both polymers show very little weight loss above 540°C. These observations were confirmed by the T.V.A. thermograms. The initial weight loss at 250°C for T_3(S) is probably again due to low molecular weight material being given off. Both T.V.A. thermograms show only one peak which coincides with the weight loss maxima in the T.G.A. thermograms. Degradation of T_3(S) in air indicated that the stability of this polymer under these conditions is comparable to that under nitrogen, below 400°C. Above this temperature rapid weight loss occurs until no material remains at 600°C.

T_4 again shows completely different degradation characteristics (figure 6.7) from those of the other polymers. The most surprising feature of the thermograms is the weight loss at 100°C, accompanied by evolution of materials which are only partially condensable at -75°C. It seems most unlikely that true degradation will begin at such a low temperature and it is therefore concluded that some process such as crosslinking is occurring with the evolution of volatile products. If it is assumed

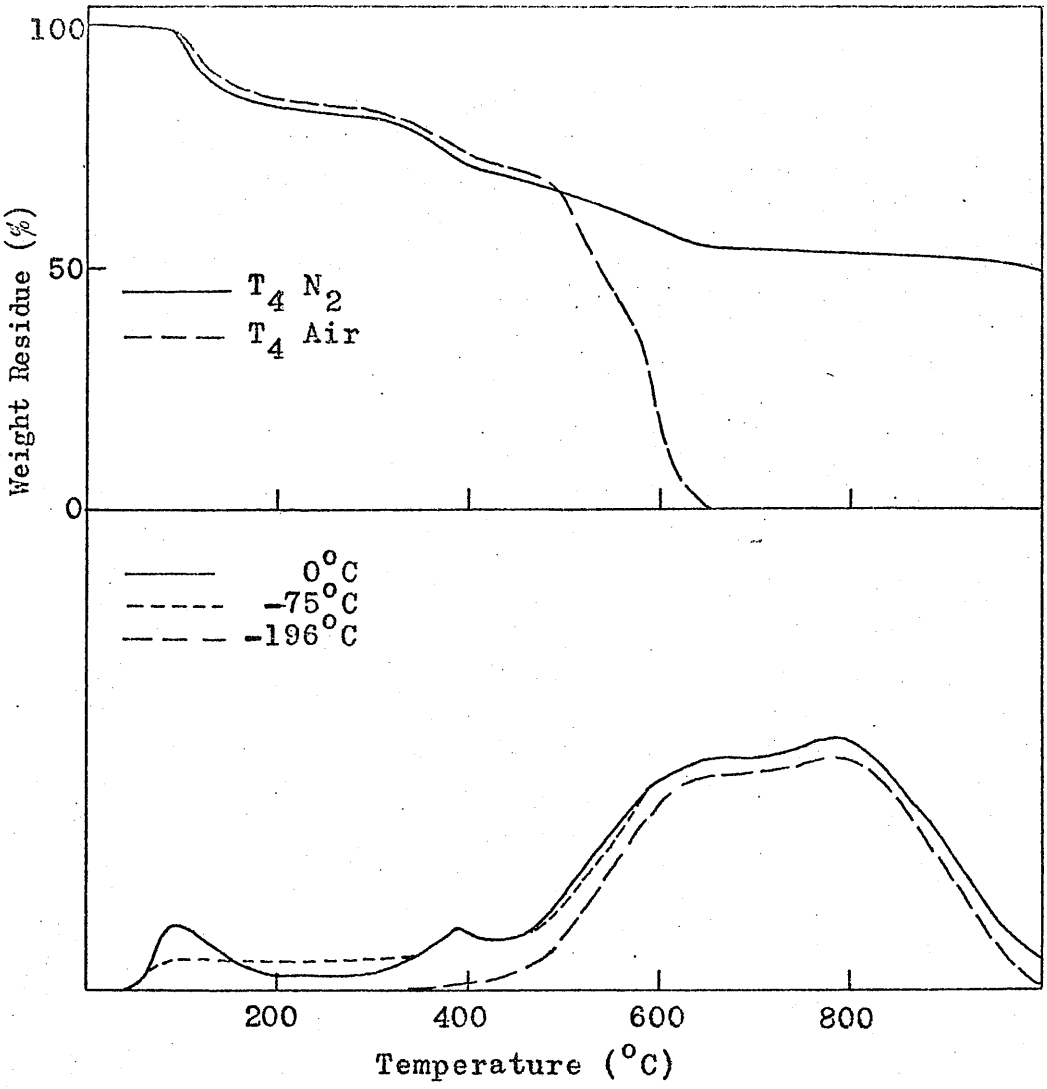

Figure 6.7 T.G.A. and T.V.A. Thermograms for T_4.

that this is true, then degradation of the polymer is seen to begin at 300°C. Like T_1, weight loss is a gradual process involving several different steps. Degradations carried out in air show that the stability of the polymer, in this medium, is comparable with that under nitrogen, up to 500°C. Thereafter rapid weight loss occurs.

The degradative behaviour of T_5 (figure 6.8) is very similar to that of T_2. Both $T_5(I)$ and $T_5(S)$ do however exhibit slightly superior stability with rapid weight loss beginning at slightly higher temperatures. Again degradations in air show comparable stability with catastrophic breakdown occurring above 400°C. The T.V.A. thermogram is also very similar to that of T_2, however the amounts of materials which are condensable at -75°C and -196°C during the earlier stages of reaction are considerably less than was found for T_2.

All the products examined gave appreciable amounts of residue when degraded in an atmosphere of nitrogen or under vacuum. Before making any comparison of the thermal stabilities of the polymers consideration must be given to the factors which will affect such assessments. The most simple criterion of thermal stability is the temperature at which true degradation occurs, however

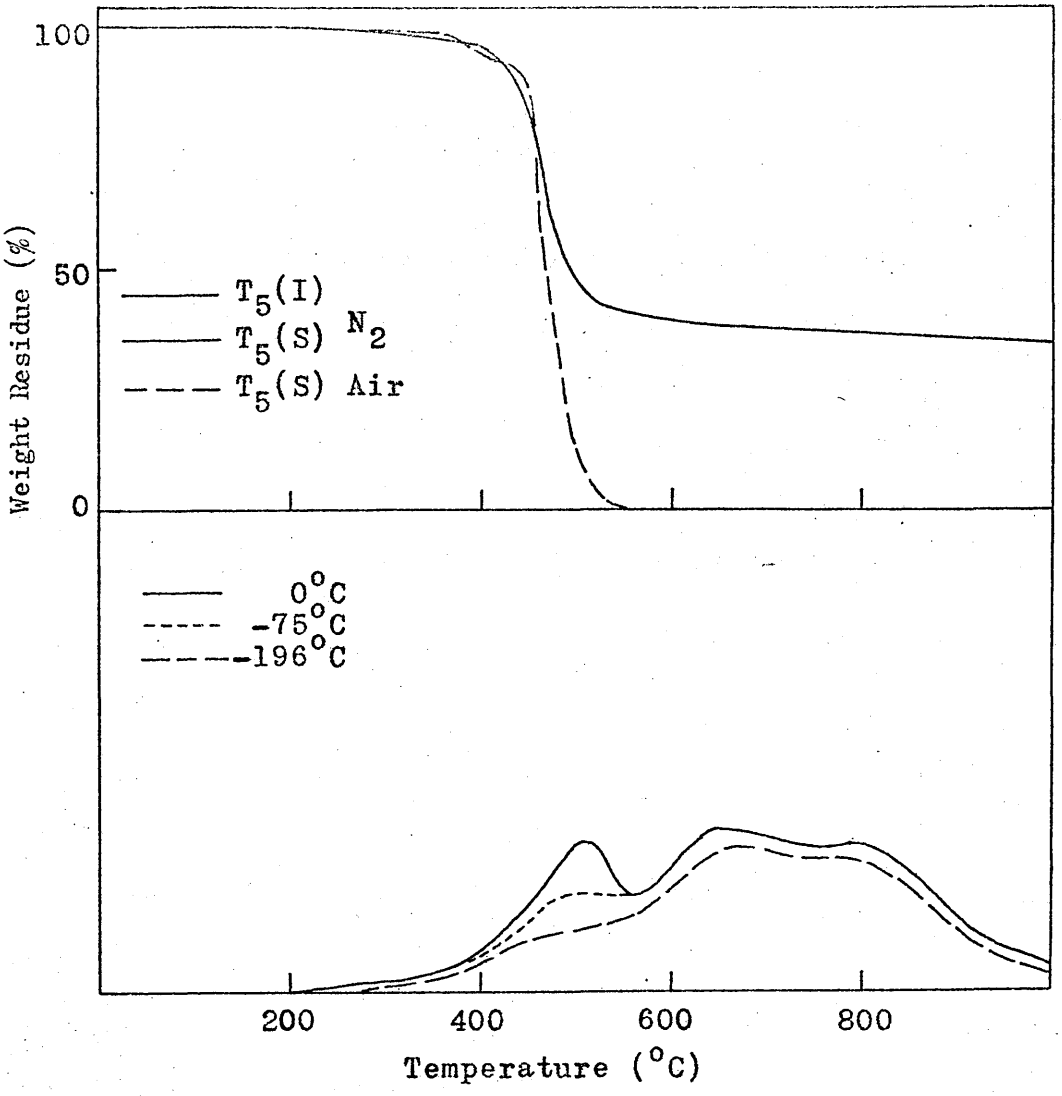

Figure 6.8 T.G.A. and T.V.A. Thermograms for T_5.

account must also be taken of the rate of degradation if a true comparison is to be made. Thus a polymer which suffers catastrophic breakdown cannot necessarily be considered more stable than one which degrades by a gradual process, even though the latter polymer begins to degrade at a lower temperature. The need to take account of both these factors makes a comparison of the thermal stabilities of the polymers considered in this chapter difficult. However some general conclusions can be drawn.

It may be concluded that the thiophen polymer T_1 shows greater stability than both T_2 and T_5 in an inert atmosphere. While in all three of these polymers true degradation appears to begin within the temperature range 350°C - 400°C, the rate of weight loss shown by the thiophen polymer is considerably lower than that found for the other two. It is however more difficult to make a comparison between T_1 and T_3. Although the temperature at which true degradation begins for T_3 is above 400°C, this polymer suffers catastrophic breakdown in the region of 500°C. Thus it can be seen that although this polymer undoubtably shows greater thermal stability than T_1 within the range 50°C - 450°C above this temperature the thiophen polymer is undoubtably the more stable of

the two. It is very difficult to make any assessment of the stability of T_4 due to the large weight loss at low temperatures. If however the involatile material remaining after this weight loss is considered to be the true polymer it can be concluded that the stability shown is of a similar order to that of T_1.

Comparisons of the relative stabilities of the polymers in air can be made much more readily as they all exhibit catastrophic decomposition soon after degradation begins. Thus it would appear that the relative stabilities are in decreasing order T_1, T_3, T_5 and T_2. Again there is very little difference between the stabilities of T_5 and T_2. The degradation characteristics of T_4, discussed above, again make any comparisons with the other products difficult.

The T.G.A. thermograms of the products also give some insight into the extent of branching or crosslinking in the polymers. The sudden, drastic weight loss, typical of many vinyl polymers, is often caused by chain processes, such as depolymerisation, which lead to a great weight loss over a small temperature range. A high degree of branching or crosslinking in a polymer would prevent such processes occurring and lead to more gradual weight loss over a much larger temperature range. The T.G.A.

thermogram obtained for T_1 is a typical example of the latter type of curve while that of T_3 is more typical of the former. Thus it may be concluded that T_1 has a highly branched or crosslinked structure while the structure of T_3 is basically linear. Both T_2 and T_5 would then be seen to have structures intermediate between these two extremes as their thermograms show features of both types of degradation. Such conclusions would also suggest that the reaction occurring at low temperatures in the degradation of T_4 involves crosslinking as the resultant product shows the typical degradative features of a crosslinked polymer.

The high order of stability shown by the 2.5-dimethyl thiophen polymer would seem to suggest that the basic stability of this type of polymer is not solely a function of the extent of crosslinking in the polymer. If however the stability were some function of the thiophen ring, T_3 would not have been expected to exhibit greater stability than T_1 in the temperature range 300°C - 450°C. The thiophen nuclei in T_3, however, would be expected to be completely substituted and it is possible that degradation at lower temperatures is initiated at the hydrogen atoms remaining on the thiophen rings in the other polymers. There is little doubt however that a much more extensive investigation would be required

before any definite conclusions can be drawn.

6.5 Summary

The work described in this chapter has shown that the extent of branching or crosslinking in Friedel-Crafts polymers containing thiophen nuclei can be altered by the presence of substituents on the thiophen monomers. The temperature at which true degradation begins has been shown to be independent of the degree of crosslinking in the polymers. However there is little doubt that the presence of crosslinked structures does give a degree of stability to the polymers at higher temperatures by preventing chain processes occurring. It has also been shown that the stability of this type of polymer is increased by increasing the degree of substitution on the thiophen nuclei in the polymer.

CHAPTER 7

DISCUSSION

In this chapter the results presented in the foregoing sections are discussed with a view to establishing the mechanism of the DCMB-thiophen reaction and the nature of the resultant products.

The reaction between DCMB and thiophen, catalysed by stannic chloride has been shown to be first order with respect to each of the reactants and to the catalyst. This first order dependance can be accounted for by the following mechanism.

The first step in reactions of this type is generally considered to be the formation of a complex between the catalyst and halocompound by interaction of the electropositive tin atoms of the catalyst with the electronegative halogen atoms[46]. Such a complex may be represented by,

$$Cl\text{-}CH_2\text{-}\phi\text{-}\overset{\delta+}{C}H_2 \cdots\cdots \overset{\delta-}{S}nCl_5$$

Reaction of the aromatic compound with this complex will then give

$$Cl\text{-}CH_2\text{-}\phi\text{-}CH_2\text{-}\mathbb{T} + \underbrace{H^+ + SnCl_5^-}_{HCl + SnCl_4}$$

Grassie and Meldrum[29] have shown that, in reactions

of this type, an equilibrium concentration of active complex is rapidly established compared with the rate of the reaction of the complex with the aromatic molecule. The absence of an induction period in the reaction curves for TCMB confirm that this is true in the case of the DCMB-thiophen reaction. The reaction may then be represented by,

$$\text{DCMB} + \text{SnCl}_4 \underset{k_{-i}}{\overset{k_i}{\rightleftharpoons}} \text{complex}$$

$$\text{complex} + \text{thiophen} \xrightarrow{k_{ii}} \text{products}$$

In the stationary state,

$$d(\text{complex})/dt = 0 = k_i(\text{DCMB})(\text{SnCl}_4) - k_{-i}(\text{complex}) - k_{ii}(\text{complex})(\text{thiophen})$$

$$(\text{complex}) = \frac{k_i(\text{DCMB})(\text{SnCl}_4)}{k_{-i} + k_{ii}(\text{thiophen})}$$

$$\text{Rate of Reaction} = k_{ii}(\text{complex})(\text{thiophen})$$

$$= \frac{k_i k_{ii}(\text{DCMB})(\text{thiophen})(\text{SnCl}_4)}{k_{-i} + k_{ii}(\text{thiophen})}$$

Now, if it can be assumed that $k_{-i} \gg k_{ii}(\text{thiophen})$

$$\text{Rate of Reaction} = \frac{k_i k_{ii}}{k_{-i}} (\text{DCMB})(\text{thiophen})(\text{SnCl}_4)$$

This accounts for the dependence of the rate of reaction on the first power of the concentration of each

of the reactants, which was reported in chapter 5. The rate of the second reaction was also found to be dependent on the first power of the concentrations of each of the reactants involved and this suggests that the polymerisation proceeds through reaction steps which are all of the type described above.

The much greater reactivity of the chloromethyl group in TCMB, observed in chapter 5, can be accounted for by the absence of a second strongly electronegative centre in this compound. Thus the formation of an active complex and so the breaking of the C-Cl bond is greatly facilitated by the greater electron density on the remaining chlorine atom.

The shape of the HCl reaction curves can be accounted for by this greater reactivity exhibited by TCMB, compared with DCMB. Although these curves do not show the induction period observed by Grassie and Meldrum, in the study of the DCMB-benzene reaction, they do show that the rate of increase in HCl concentration rises with increasing TCMB concentration. The complete absence of a true induction period can be accounted for by the greater reactivity of DCMB and TCMB with thiophen compared with the corresponding reactions in the DCMB-benzene system.

A feature of the reaction which is perhaps surprising

is the constancy of the rate of disappearance of DCMB over the full range of reaction studied. It would have been expected that as the concentrations of DCMB and thiophen decreased the rate of consumption of DCMB would also have decreased. It must therefore be concluded that the aromatic nuclei of the reaction products exhibit high reactivity and that this high reactivity offsets the decrease in concentration of the starting materials and so maintains the rate of reaction of DCMB at a nearly constant level. Olah and his co-workers[46] have shown that the reactivity of benzene nuclei, in Friedel-Crafts alkylations, increases with the number of alkyl substituents on the benzene nuclei. Thus, from these observations, it is reasonable to assume that such an effect is also to be found with thiophen nuclei.

The overall reaction may then be represented as a series of competing, consecutive reactions leading to products of increasing complexity as the reaction proceeds. The competitive nature of these reactions makes it extremely difficult to carry out a kinetic analysis of the later stages of reaction since it is very difficult to account quantitatively, from the data available, for the various paths by which a product may be formed.

Such a kinetic analysis has been shown to be possible by the application of computer based methods[47]. However in the case of the DCMB-thiophen reaction, self-condensation of the higher molecular weight chloromethyl compounds, which has been shown to be an important aspect of this reaction, has so far prevented such a study being carried out. Nevertheless it is possible to make certain generalisations about the reaction and hence the ultimate product.

The studies described in chapters 4 and 5 of this thesis have demonstrated the very high reactivity of both the chloromethyl groups and the thiophen nuclei of the reaction products. It has also been established that the reactivity of the thiophen nucleus, in this type of reaction is much higher than that of the benzene nucleus[29]. Thus the polymer would be expected to propogate preferentially through the thiophen nuclei, leading to a product in which the frequency of branching is less than that found for the DCMB-benzene polymers prepared by Grassie and Meldrum[30]. Although the DCMB-thiophen polymer would not be expected to exhibit an extremely high degree of branching, the high reactivity of the pendant chloromethyl groups coupled with that of the substituted thiophen nuclei should lead to a polymer which is highly crosslinked and which has an extremely low concentration of chloromethyl groups.

It has already been shown that the reactivity of the reaction products is sufficiently high to allow the formation of cyclic products by intramolecular reactions. It must be concluded therefore that intermolecular reactions will also occur to a great extent leading to highly crosslinked and ultimately insoluble products. The presence of cyclic structures, such as P_4, will also lead to a rapid build up of compact crosslinked structures, thus hastening the onset of insolubility. Account must also be taken of substitution into the benzene nuclei although this would be expected to be a relatively minor source of branching in the polymer.

The overall highly crosslinked nature of the thiophen polymer has also been demonstrated by the thermal analytical studies described in chapter 6. The extent to which branching or crosslinking could occur through the thiophen nuclei was controlled by altering the number of substituents on the thiophen monomer. The decrease in the density of crosslinking, indicated by T.G.A. analysis, on going from thiophen to 2- and 3-methyl thiophen and finally to 2.5-dimethyl thiophen gives support to the suggestion that crosslinking takes place mainly through thiophen nuclei.

These degradative studies also indicated that the

onset of true degradation occurs at higher temperatures when the thiophen nuclei, in the polymer, are, as far as possible, completely substituted. Thus it would appear that while Friedel-Crafts polymers containing thiophen exhibit good thermal stability, this stability is more a function of the highly crosslinked nature of the polymer than some inherent property associated with the thiophen nuclei.

It was stated in chapter 1 of this thesis that the purpose of this work was to gain information about the DCMB-thiophen polymerisation process with a view to gaining a greater insight into the stability of the ultimate polymer. The foregoing discussion has demonstrated that, although it was not possible to carry out a complete analysis of the polymerisation reaction, the work which has been carried out has permitted clarification of certain features of the reaction and a reasonable assessment of the reasons for the stability of the polymer to be made. Thus it would appear that the thermal stability of the polymer can best be accounted for in terms of the highly crosslinked structure of the product. The presence of thiophen nuclei which are not completely substituted, in the polymer, would in fact seem to be a source of thermal weakness. Increasing the stability of polymers of this

type would appear, therefore, to rely on the inclusion of fully substituted thiophen nuclei while retaining some degree of crosslinking in the polymer.

REFERENCES

1. V.I. Vedeneyev, L.V. Gurvich, V.N. Kondrat'yev, V.A. Medvedev and Ye. L. Frankevich, Bond Energies, Ionisation Potentials and Electron Affinities, Edward Arnold (Publishers) Ltd., London (1966).

2. C.S. Marvel, Pure Appl. Chem. 16, 351 (1968).

3. S.D. Bruck, J. Chem. Educ. 42, 18 (1965).

4. W.J. Barlant and J.L. Parsons, J. Polym. Sci. 22, 249 (1956).

5. N. Grassie and I.C. McNeill, J. Polym. Sci. 39, 211 (1959).

6. M. Becher and H.F. Mark, Angew. Chem. 73, 641 (1961).

7. N. Grassie and J.N. Hay, J. Polym. Sci. 56, 189 (1962).

8. J.F. Brown, L.H. Vogt and P.I. Prescott, J. Am. Chem. Soc. 86, 1120 (1964).

9. S.H. Rose and B.P. Block, J. Polym. Sci.
   A 4, 573 (1966).
   A 4, 583 (1966).

10. C.S. Marvel and G.F. Hartzell, J. Am. Chem. Soc. 81, 448 (1959).

11. R.T. Foster and C.S. Marvel, J. Polym. Sci. A 3, 417 (1965).

12. A.H. Frazer and F.T. Wallenberger, J. Polym. Sci.
A 2, 1147 (1964).
A 2, 1157 (1964).
A 2, 1171 (1964).
A 2, 1181 (1964).
A 2, 1825 (1964).

13. H. Finkbeiner, A.S. Hay, H.S. Blanchard and G.F. Endres, J. Org. Chem. 31, 549 (1966).

14. M.E.A. Cudby, R.G. Feasey, B.E. Jennings, M.E.B. Jones and J.B. Rose, Polymer 6, 589 (1965).

15. S.D. Bruck, Polymer 5, 435 (1964).

16. J. Preston, R.W. Smith and C.J. Stehman, J. Polym. Sci. C 19, 7 (1967).

17. W.F. Gorham, J. Polym. Sci. A 4, 3027 (1966).

18. R.W. Lenz, C.E. Handlovits and H.A. Smith, J. Polym. Sci. 58, 351 (1962).

19. E. Jones and I.M. Moodie, J. Polym. Sci. C 16, 2881 (1967).

20. H.C. Haas, D.I. Livingstone and M. Saunders, J. Polym. Sci. 15, 503 (1955).

21. R. Ruff, J.L. Cook and B.V. Ettling, J. Polym. Sci. A 3, 3511 (1965).

22. A.L. Henne and H.M. Leicester, J. Am. Chem. Soc. 60, 864 (1938).

23. R.A. Jacobson, J. Am. Chem. Soc. 54, 1513 (1932).

24. P.J. Flory, J. Am. Chem. Soc. 74, 2718 (1952).

25. L. Valentine and R.W. Winter, J. Chem. Soc. 4768 (1956).

26. D.B.V. Parker, Eur. Polym. J. 5, 93 (1969).

27. L.N. Phillips, Trans. Plast. Inst. Lond. 32, 298 (1964).

28. W.C. Overhults and A.D. Ketley, Makromol. Chem. 95, 143 (1966).

29. N. Grassie and I.G. Meldrum, Eur. Polym. J. 5, 195 (1969).

30. N. Grassie and I.G. Meldrum, In Press.

31. N. Grassie and I.G. Meldrum, Unpublished Data.

32. N. Grassie and I.G. Meldrum, Eur. Polym. J. 4, 571 (1968).

33. I.C. McNeill, J. Polym. Sci. A 4, 2479 (1966).

34. P.H. Plesch, The Chemistry of Cationic Polymerisation, Pergamon Press, N.Y. (1963).

35. R. Ryhage, Arkiv. Kemi. 26, 305 (1966).

36. J.H. Flynn and L.A. Wall, J. Res. Nat. Bur. Stand. 70A, 487 (1966).

37. I.C. McNeill, J. Polym. Sci. A1 4, 2479 (1966). European Polym. J. 3, 409 (1967).

38. I.C. McNeill, Second International Conference on Thermal Analysis, Worcester, Massachusetts (1968).

39. V. Meyer, Ber. 16, 1468 (1883).

40. J. Bruce, F. Challenger, H.B. Gibson and W.E. Allenby, J. Inst. Petroleum Technol. 34, 226 (1948).

41. I.P. Gold'stein, E.N. Gur'yanova and K.A. Kocheshkov, Proc. Acad. of Sciences U.S.S.R. 144, 456 (1962).

42. I.P. Gold'stein, Z.F. Il'ichera, N.A. Slovokhotova, E.N. Gur'yanova and K.A. Kocheshkov, Proc. Acad. of Sciences U.S.S.R. 144, 490 (1962).

43. R.F. Curtis, D.M. Jones, G. Ferguson, D.M. Hawley, J.G. Sime, K.K. Cheung and G. Germain, Chem. Comm. 165 (1969).

44. M. Armour, A.G. Davies, J. Upadhyay and A. Wassermann, J. Polym. Sci. A1 5, 1527 (1967).

45. W. Heitz and W. Kern, Die Angewandte Makromol. Chem. 1, 150 (1967).

46. G.A. Olah, S.J. Kuhn and S.H. Flood, J. Am. Chem. Soc. 84, 1688 (1962).

47. I.G. Meldrum, Unpublished Data.

THE PHOTODEGRADATION OF COPOLYMERS OF METHYL METHACRYLATE AND METHYL ACRYLATE AT ELEVATED TEMPERATURES

N. Grassie, B.J.D. Torrance and J.B. Colford

SUMMARY

Four methyl methacrylate/ methyl acrylate copolymers with molar ratios, MMA/MA, of 112/1, 26/1, 7·7/1 and 2/1 have been photodegraded at 170°C by 2537 Å radiation. The changes which occur in the molecular weight of the copolymers are typical of a random scission process and from these and volatilisation data the extent of chain scission during the course of the reaction has been calculated. The pattern of volatile products is the same as that previously obtained in the thermal reaction at 300° although there are a number of differences in detail. For example, only one in ten of the methyl acrylate units is liberated as monomer compared with one in four in the thermal reaction and the ratio CO_2/ chain scissions is considerably greater than the strict 1/1 ratio observed in the thermal reaction. Zip lengths are also very much greater in the photo reaction. These minor differences between the two reactions have been accounted for in terms of the mechanism previously presented to account for the thermal reaction, bearing in mind the differences in the temperature (170° and 300°) at which the two investigations were carried out.

THE PHOTODEGRADATION OF COPOLYMERS OF METHYL METHACRYLATE AND METHYL ACRYLATE AT ELEVATED TEMPERATURES

N. Grassie, B.J.D. Torrance* and J.B. Colford,
Chemistry Department, The University of Glasgow, Glasgow, W.2, Scotland.

Recent publications[1-3] have demonstrated how the presence of the comonomers, acrylonitrile and methyl acrylate influence the thermal degradation of poly(methyl methacrylate). In both systems the depolymerisation reaction is initiated by random scission in the methyl methacrylate segments of the polymer chains. Like pure poly(methyl methacrylate) these copolymers also depolymerise at elevated temperatures under the influence of 2537 Å radiation. In the acrylonitrile polymer[4], however, the initiation process consists of chain scission specifically at acrylonitrile units and the principal differences between the thermal and photo reaction have been accounted for in terms of the different sites of initiation and the influence of the temperature (280°C and 160°C for the thermal and photo reactions respectively) and viscosity of the medium upon the relative rates of the subsequent constituent processes comprising the total reaction. In the present paper the principal features of the photodegradation of the methyl methacrylate/methyl acrylate copolymer system are described and differences from the thermal reaction discussed.

*Present address: Research Department, Courtaulds Ltd., Coventry, England.

EXPERIMENTAL

Copolymers

The four copolymers studied were those whose preparations have previously been described[2]. Their molar compositions are (MMA/MA) 112/1, 26/1, 7·7/1, 2/1.

Molecular Weights

Number average molecular weights were measured using a Mechrolab high speed membrane osmometer.

The amounts of material available for the measurement of molecular weights were of the order of only a few milligrams. Molecular weight measurements are therefore subject to considerable error and this accounts for the scatter of points in figures 4 and 5.

Photodegradation Techniques

Photodegradations, except those involving the measurement of CO_2 produced, were carried out as previously described[4], the polymer (20–40 mg.), in the form of a thin transparent film, being irradiated in vacuum, through silica, by a source of 2537 Å radiation.

Because of the very small amounts of CO_2 involved it was found more convenient to make the CO_2 evolution measurements in the apparatus used for thermal studies[2] with a suitably modified reaction vessel. The exit tube was situated at the side of the reaction vessel, being replaced at the top of the

reaction vessel by a silica window through which the polymer was irradiated.

All product analyses were carried out exactly as described for the thermal reaction[2].

RESULTS

Influence of Temperature on Rate of Volatilisation

The primary influence of u.v. radiation on poly(methyl methacrylate) is to cause chain scission, the radicals, $\sim CH_2-\overset{CH_3}{\underset{COOCH_3}{\overset{|}{\underset{|}{C\cdot}}}}$, ultimately appearing in the system[5]. The overall characteristics of the photolysis depends upon the subsequent reactions of these radicals which in turn depends upon the temperature. At high temperatures, at which the polymer is in the liquid state, monomer produced in the equilibrium,

$$\sim CH_2-\overset{CH_3}{\underset{COOCH_3}{\overset{|}{\underset{|}{C}}}}-CH_2-\overset{CH_3}{\underset{COOCH_3}{\overset{|}{\underset{|}{C\cdot}}}} \rightleftharpoons \sim CH_2-\overset{CH_3}{\underset{COOCH_3}{\overset{|}{\underset{|}{C\cdot}}}} + CH_2=\overset{CH_3}{\underset{COOCH_3}{\overset{|}{\underset{|}{C}}}}$$

can easily escape so that the reaction tends to the right and quantitative conversion to monomer occurs. On the other hand, at low temperatures when the polymer is in the form of a rigid solid, monomer can not readily escape, appreciable depolymerisation does not occur and the polymer radicals subsequently mutually destroy each other. At low temperatures, therefore,

the photolysis is characterised by chain scission and at high temperatures by monomer production. It is the high temperature reaction with which this paper is concerned. Unfortunately, however, the range of temperature in which this reaction can be studied is restricted, the lower limit ($\simeq$150°C) being governed by the softening point of the polymer and the upper limit ($\simeq$200°C) by the onset of thermal degradation. Clearly in this temperature range the viscosity of the polymer is changing rapidly with temperature and since the viscosity could have a profound influence on the above equilibrium it is important to obtain some assessment of the influence of the viscosity on the overall reaction. The data in figure 1 demonstrate that there is no significant change in the rate of photodegradation of PMMA in the temperature range 150-170°C. Since the reaction consists of photoinitiation followed by complete unzipping of the polymer chains the rate of the reaction should be governed by the rate of initiation and since photoinitiation should be associated with an activation energy close to zero the constant rate is accounted for and in turn implies that there is no significant viscosity effect which should be expected to cause an increase in rate with temperature. In turn it may be concluded that the increase in the rate of photodepolymerisation of the two copolymers with temperature, illustrated in figure 1, is not

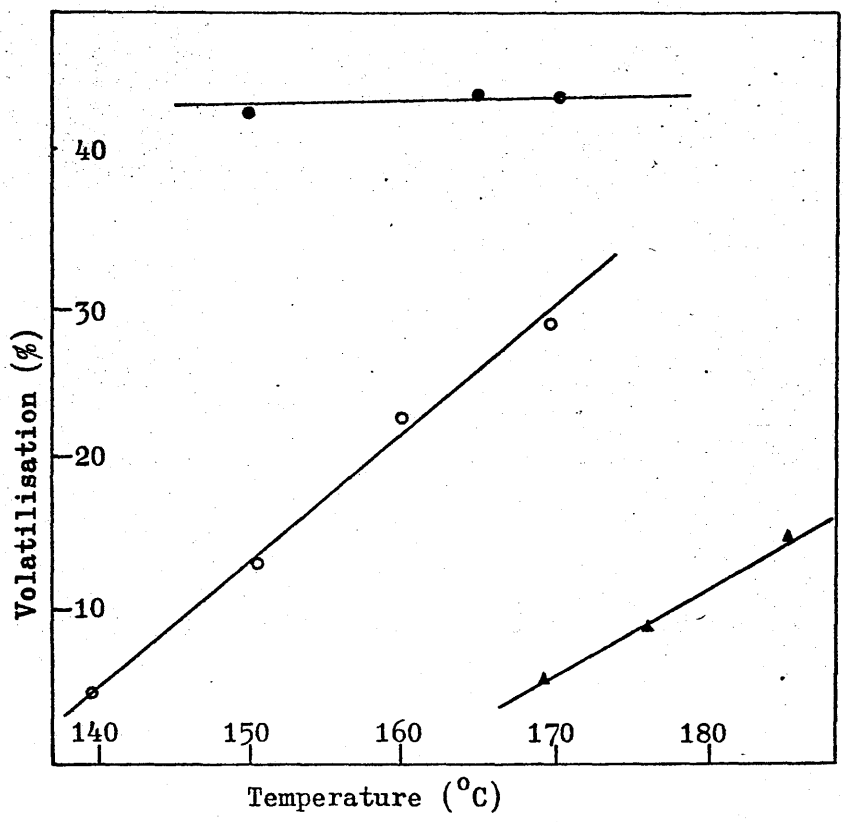

Figure 1 Extent of volatilistion in 30 mins. at various temperatures of poly(methyl methacrylate) (●) and methyl methacrylate/ methyl acrylate copolymers (○ , 26/1; ▲ , 7.7/1).

TABLE 1

Photodegradation Data obtained at 170°C

Copolymer	Time (min)	Volatilisation (%)	M.W. of Residue	Chain Length of Copolymer (CL_o)	Scissions per molecule (N)	Scissions per chain unit ($n=N/CL_o \times 10^4$)
112/1	0	0	600,000	6000	0	0
	10	5.4	250,000		1.27	2.11
	30	20.7	-		-	-
	60	41.4	237,000		0.47	0.78
	90	53.6	-		-	-
	120	60.8	-		-	-
26/1	0	0	600,000	6030	0	0
	5	1.7	376,000		0.12	0.19
	15	4.0	248,000		1.32	2.19
	23	13.4	229,000		1.27	2.11
	30	30.4	172,000		1.50	2.49
	45	34.2	180,000		1.19	1.98
	60	36.2	145,000		1.65	2.73
	90	46.2	118,000		1.68	2.79
	120	54.0	125,000		1.21	2.01
7.7/1	0	0	425,000	4370	0	0
	5	1.5	411,000		0.02	0.05
	15	2.9	321,000		0.27	0.62
	23	4.4	181,000		1.25	2.86
	30	5.2	263,000		0.53	1.21
	45	16.2	168,000		1.12	2.56
	65	20.3	144,000		1.35	3.09
	75	22.3	157,000		1.10	2.52
	90	27.8	150,000		1.05	2.40
	120	29.8	140,000		1.13	2.58
	300	40.0	81,000		1.96	4.47
2/1	0	0	370,000	3880	0	0
	30	1.75	149,000		1.46	3.76
	60	5.8	78,000		3.08	7.95
	150	13.9	49,000		5.52	14.22
	300	28.2	45,000		4.91	12.65
	600	39.6	47,000		3.75	9.65

associated with a viscosity effect but is a direct manifestation of the modification of the overall reaction by the presence of the comonomer.

As a result of these experiments 170°C was chosen as a suitable temperature for a general study of the reaction since an appreciable rate of reaction was obtained over the whole copolymer composition range without interference from thermal degradation. All subsequent data were obtained at this temperature and are summarised in table 1. Chain scissions per molecule of polymer were calculated using the formula[3],

$$N = \frac{CL_o(1-x)}{CL} - 1$$

in which CL_o and CL are the original chain length and the chain length at an extent of volatilisation x respectively. The number of chain scissions per unit length of chain, n, given by

$$n = \frac{N}{CL_o} = \frac{1-x}{CL} - \frac{1}{CL_o}$$

must be used as a comparative measure of the extent of chain scission, however, since the copolymers have substantially different molecular weights.

Molecular Weight Changes

The changes in molecular weight which occur during photodegradation are related to the extent of volatilisation in figure 2. Like the results of thermal degradation[2,3] they

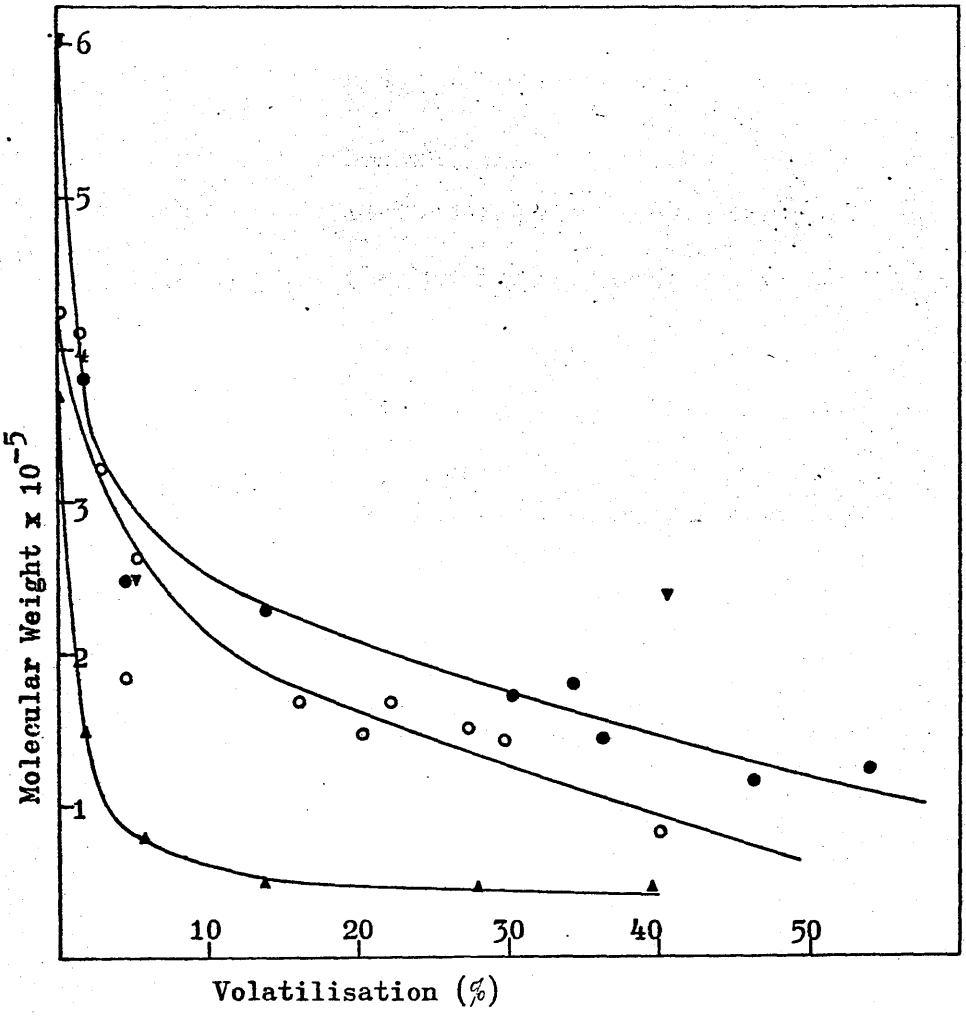

Figure 2 Change in molecular weight with volatilisation for photodegradation of methyl methacrylate/methyl acrylate copolymers at 170°C. (▼ , 112/1; ● , 26/1; ○ , 7.7/1; ▲ , 2/1).

are characteristic of a random scission reaction. Even in the 2/1 copolymers there is no direct evidence of the cross-linking which is typical of poly(methyl acrylate), the residual material being completely soluble in all cases.

Volatile Products of Degradation

The pattern of volatile products is closely comparable with that produced in the thermal reaction. The only significant difference concerns the ratio of the monomers. The g.l.c. analysis of the monomer fractions are presented in table 2, from which it is clear that approximately one in ten of the MA units is liberated as monomer compared with one in four in the thermal reaction.

TABLE 2

Molar Composition of Monomeric Products (MMA/MA)

Copolymer	Products
112/1	>1000/1
26/1	320/1
7·7/1	80/1

Rates of Volatilisation

Volatilisation vs time curves for the four copolymers and PMMA are compared in figure 3. It is obvious that, as in the thermal reaction, increasing concentrations of MA increasingly stabilise the copolymers.

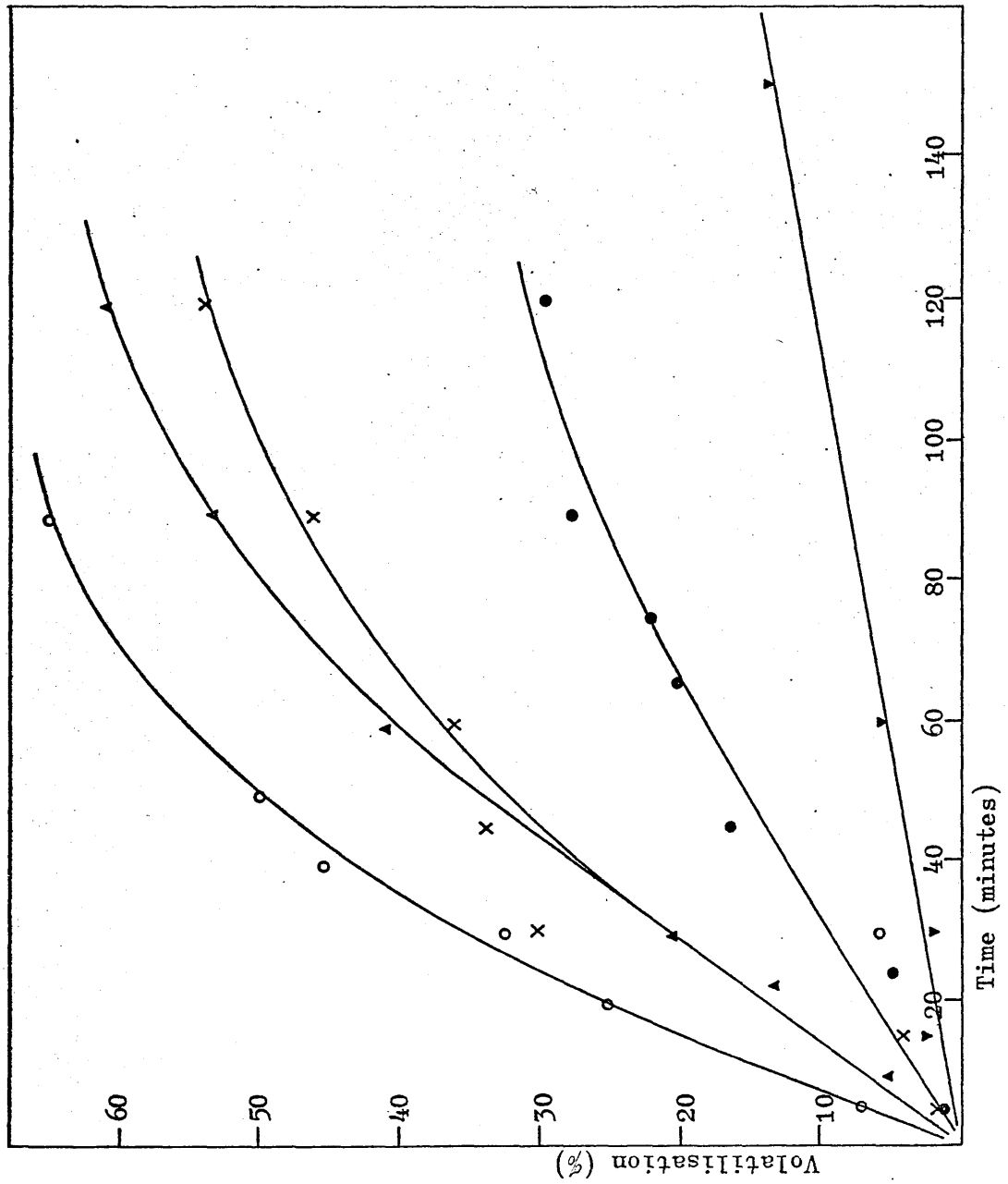

Figure 3 Volatilisation/time curves for the photodegradation of poly(methyl methacrylate) and methyl methacrylate/methyl acrylate copolymers at 170°C. (○, PMMA; ▲, 112/1; ×, 26/1; ●, 7.7/1; ▼, 2/1).

Chain Scission and the Production of Carbon Dioxide

The data in table 3 summarise the results of experiments designed to determine the relationship between chain scissions and CO_2 production.

TABLE 3

Chain Scission and the Production of Carbon Dioxide

Copolymer	Temp. (°C)	Volatilisation(%)	M.W. of Residue	Scissions/ Molecule	CO_2/ Molecule	CO_2/ Scission
26/1	160	11·6	244,000	1·062	4·84	4·5
	170	11·5	292,000	0·82	4·46	5·4
7·7/1	170	24·8	118,000	1·71	5·15	3·0
	170	46·2	70,000	2·26	10·6	4·7
2/1	170	7·4	75,000	3·57	7·47	2·1

In the thermal reaction a strict 1/1 ratio was found throughout the polymer composition range which made it possible to use CO_2 production as a direct measure of chain scission. A mechanism for chain scission was proposed which accounted for these experimental observations. From the data in table 3 it is clear that the CO_2/ chain scission ratio is considerably greater than unity in the photo reaction. There appears to be some tendency for the ratio to fall as the MA content of the copolymer is increased but the very small amounts of material available make it difficult to

obtain values of molecular weight of sufficient accuracy to study the effect with high precision.

Chain Scission and Volatilisation

The relationship between chain scission and volatilisation is illustrated in figure 4, using the data in table 1. Once again the scatter of the experimental points can be attributed to the difficulty of obtaining accurate values of molecular weight but taken as a whole the results are best interpreted as demonstrating a linear relationship as represented in the figure. Thus it may be concluded that, as in the thermal reaction, radicals are formed as a direct result of chain scission and that volatilisation occurs by depolymerisation of these radicals. Zip lengths may be calculated as in table 4 and the values are seen to be very much greater than those observed in the thermal reaction which are presented in the last column of table 4. However, as before, blockage of the depropagation reaction by the MA units is clearly occurring since zip lengths decrease with increasing MA content.

TABLE 4

Zip Lengths for Depolymerisation

Co-polymer	Slope (fig.4) A (% volat./scission/molecule)	M.W.	M.W. lost/scission (MW x A)	Average wt. of monomer unit (B)	Zip length MWxA/B	Zip length Thermal
26/1	22	600,000	132,000	99·5	1327	74
7·7/1	17	425,000	72,000	97·2	741	74
2/1	5·5	370,000	20,300	95·3	214	34

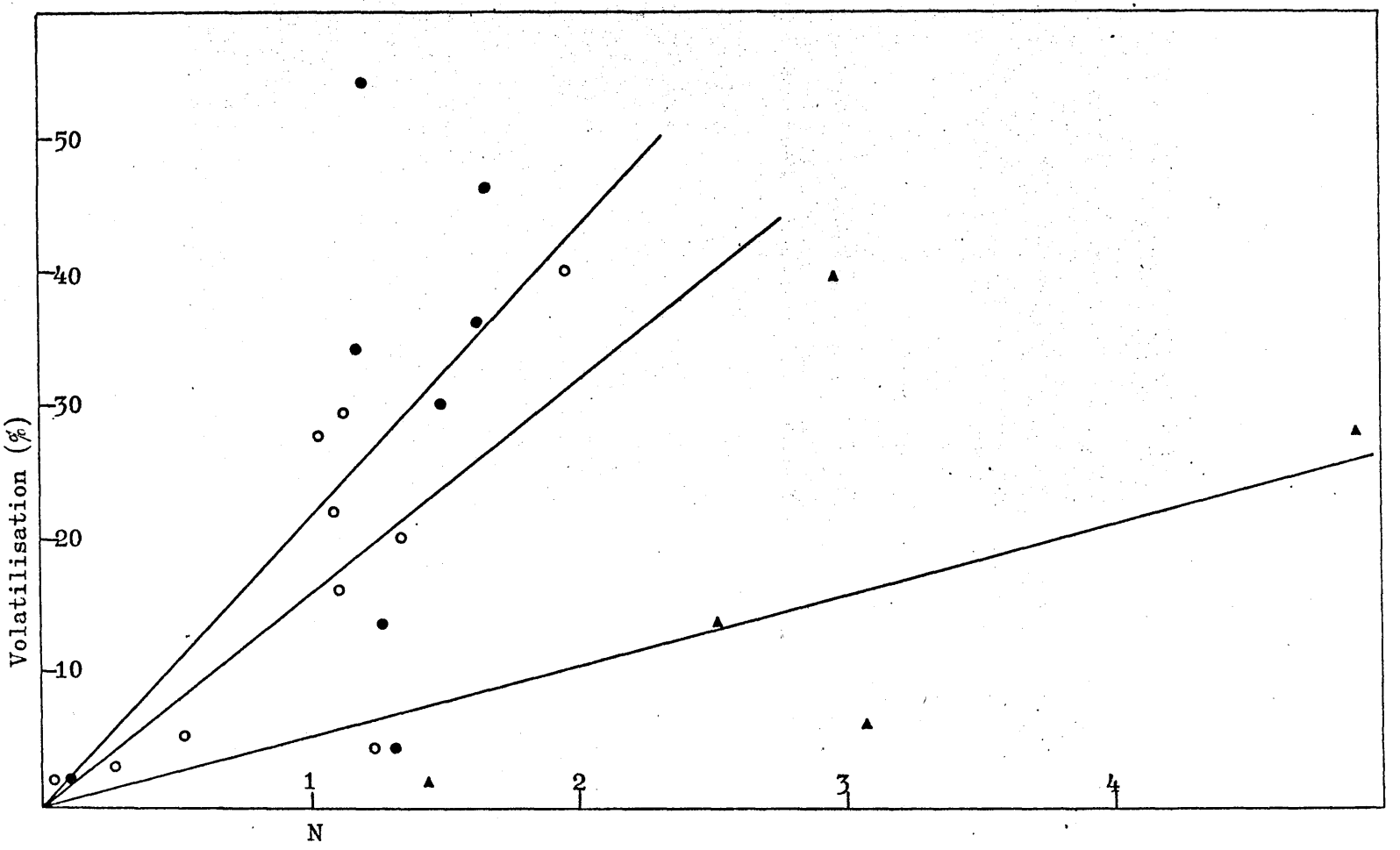

Figure 4 Relationship between chain scissions and volatilisation in the photodegradation of methyl methacrylate/methyl acrylate copolymers at 170°C. (● , 26/1; ○ , 7.7/1; ▲ , 2/1).

Chain Scission and Copolymer Composition

The time dependence of chain scission for the four copolymers is represented in figure 5. There is no clear trend with copolymer composition and all the experimental points may be reasonably represented by a single straight line. Thus the rate of chain scission is independent of the MA content of the polymer.

DISCUSSION

Figure 2 demonstrates that the photolysis of MMA/MA copolymers at elevated temperatures involves the successive scissioning of the chain. Although the data in figure 5 are of limited reliability it is clear that the rate of chain scission is not strongly dependent upon MA content and thus that the scission reaction does not occur preferentially at MA units but rather at random. Since the rate of volatilisation is progressively retarded by increasing MA content it may be deduced that MA units block the monomer producing depropagation process. This blocking action is not complete, however, since small amounts of monomer MA do appear among the volatile products. In all these aspects the photo reaction is identical with the thermal reaction[2,3].

There are, however, some well defined differences between the two processes and the following are probably the

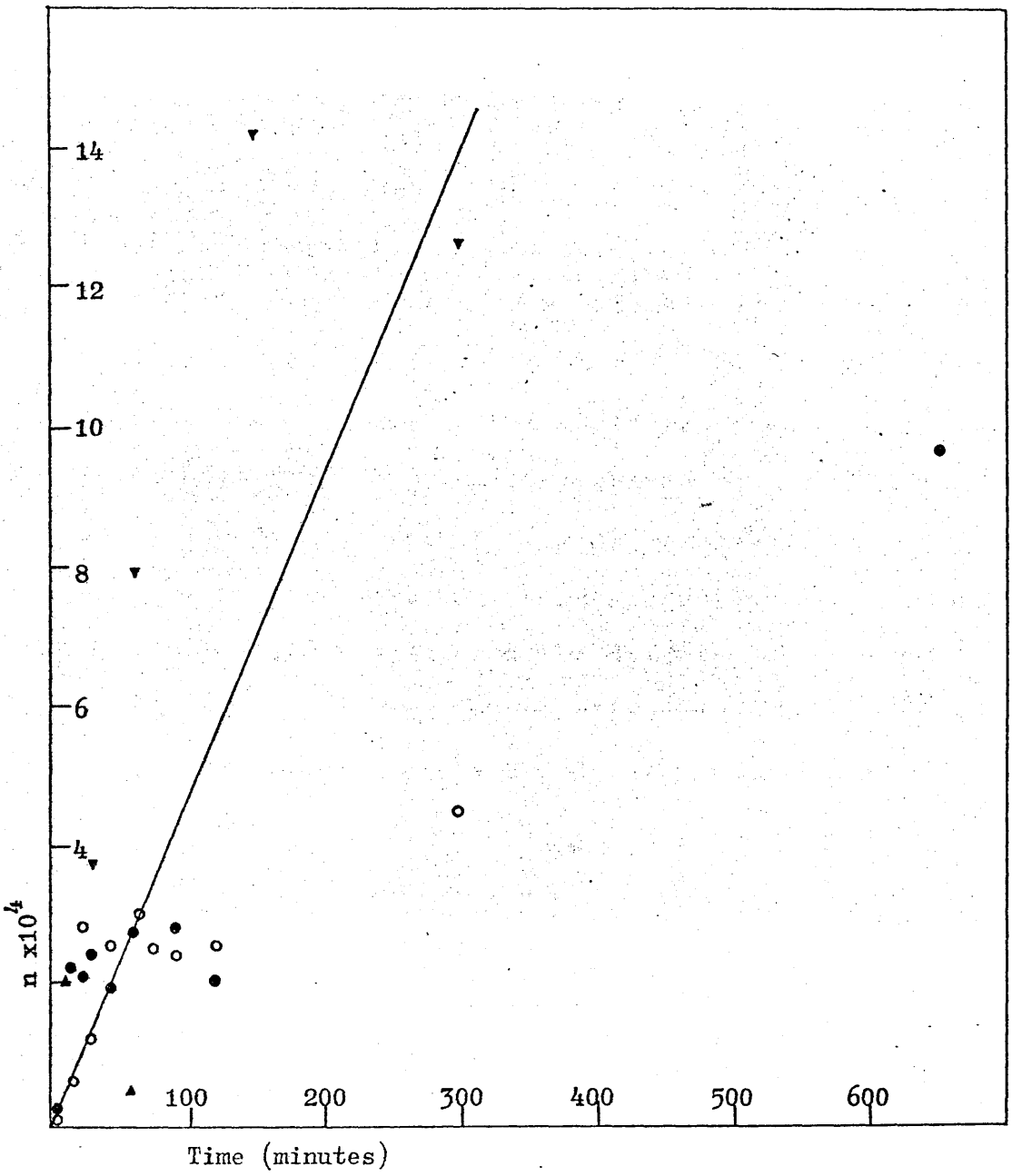

Figure 5 Time dependence of chain scissions in the photodegradation of methyl methacrylate/methyl acrylate copolymers at 170°C. (▲, 112/1; ●, 26/1; ○, 7.7/1; ▼, 2/1).

most significant. Firstly, the zip length in the photo reaction is very much greater than in the thermal reaction. Secondly, the strict 1/1 ratio between CO_2 molecules produced and chain scissions in the thermal reaction does not apply to the photo reaction. In this case a very much higher proportion of CO_2 appears. Thirdly, a very much smaller proportion of the MA is liberated as monomer in the photo reaction $\simeq$ 1 in 10 units compared with 1 in 4 in the thermal reaction.

The following reaction mechanism was presented previously[3] to account for the principal features of the thermal reaction. The minor differences mentioned above between the thermal and photo reactions can be accounted for in terms of this mechanism bearing in mind the differences in the temperatures at which the two reactions were studied. These were 170°C and approximately 300°C for the photo and thermal reactions respectively. In the present instance this difference in temperature may manifest itself through the direct influence of temperature on the relative rates of constituent reactions or these relative rates may be even more strongly influenced by the very great difference in the viscosity of the medium at the two temperatures. At 170°C the polymer is in the form of a highly viscous mass while at 300°C it is a relatively mobile liquid.

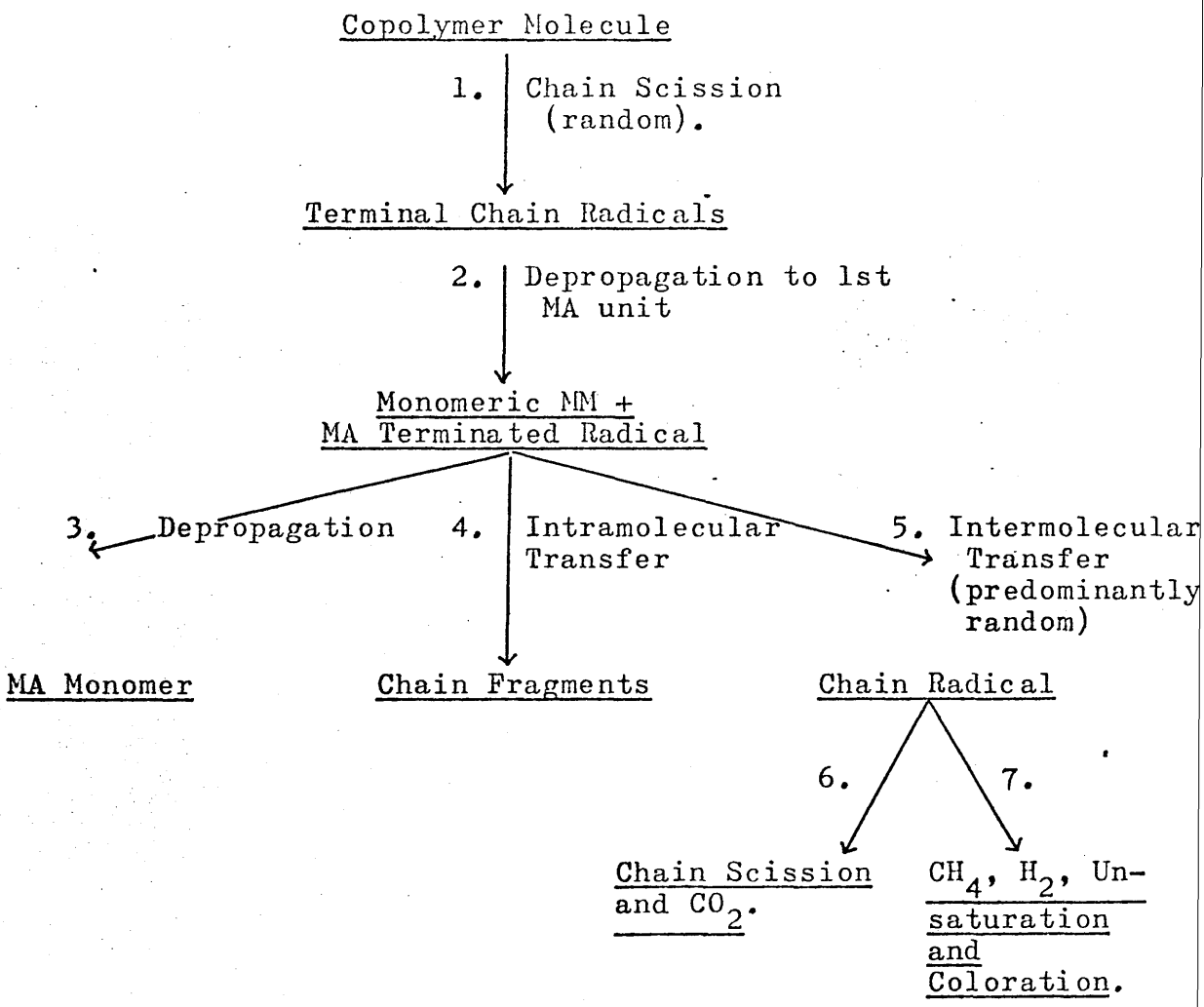

Thus the greater zip length in the photo reaction can be accounted for by the fact that the more viscous medium, by suppressing thermal motion, should be expected to favour intramolecular trensfer (reaction 4) at the expense of intermolecular transfer (reaction 5). On the other hand, the greater CO_2/chain scission ratio in the photo reaction may result from the higher viscosity favouring reaction 7 at the

expense of reaction 6. These may be represented in more detail as follows,

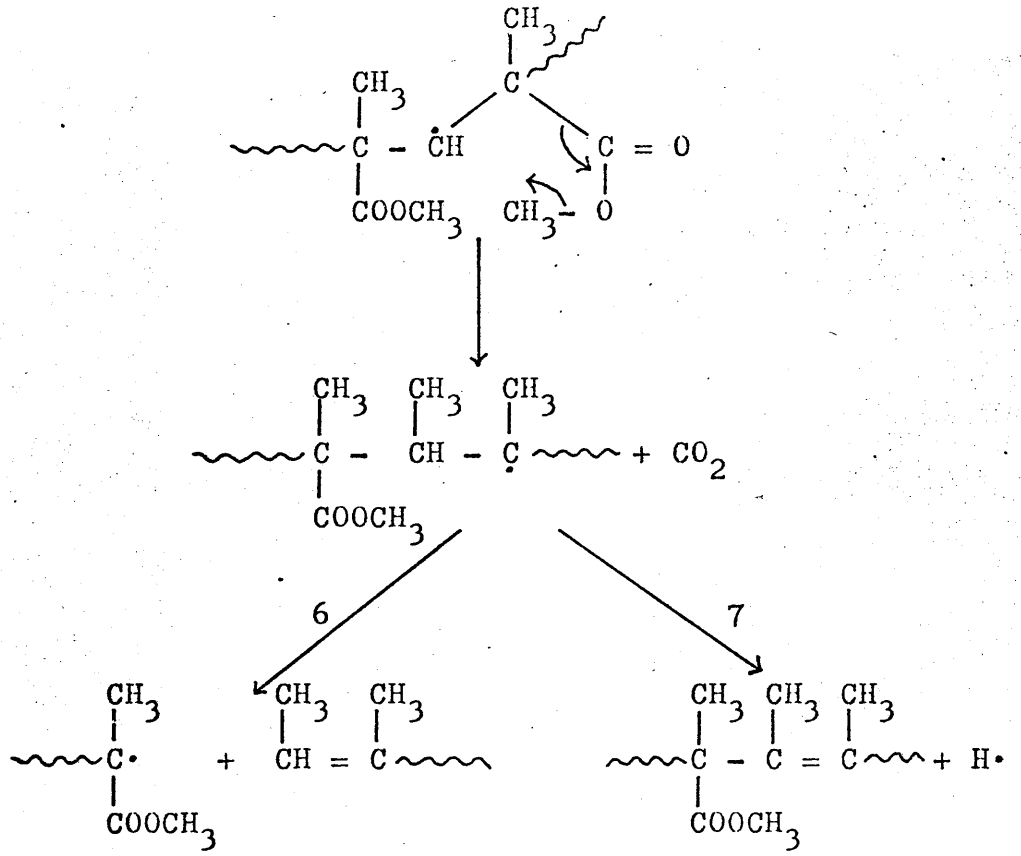

and the lower molecular mobility at the temperature of the photo reaction should be expected to favour separation of a mobile hydrogen atom at the expense of the diffusion apart of two long chain species. Finally the smaller relative amount of monomeric MA produced at the lower temperature may be a measure of the direct relative influence of temperature on reactions 3 and 4. Alternatively it may result from the

greater viscosity of the medium inhibiting diffusion from the site of the reaction of monomer produced in depropagation. This would favour the back reaction in the equilibrium,

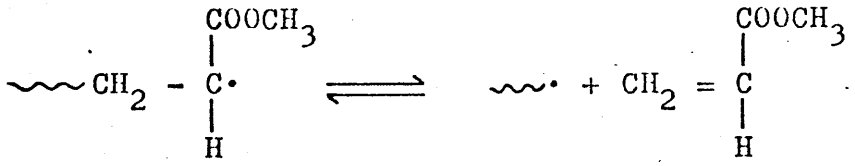

and thus in turn favour reaction 4 at the expense of reaction 3.

This research work has been sponsored by the United States Air Force under Contract AF 61 (052) - 883 through the European Office of Aerospace Research, OAR, United States Air Force.

We also record our thanks to Messrs. R. Smith and G. Perrit who carried out molecular weight measurements and gave general technical assistance.

REFERENCES

1. N. Grassie and E. Farish, European Polymer J., 3, 619 (1967).

2. N. Grassie and B.J.D. Torrance, J. Polymer Sci., In the Press.

3. N. Grassie and B.J.D. Torrance, J. Polymer Sci., In the Press.

4. N. Grassie and E. Farish, European Polymer J., 3, 627 (1967).

5. R.B. Fox, Progress in Polymer Science, Vol. 1, (Ed. A.D. Jenkins) Pergamon, London, 1967, p. 45.